HYDROGENATION OF ACETYLENES OVER SUPPORTED METAL CATALYSTS

A Thesis Presented to
the University of Glasgow
for the Degree of
Doctor of Philosophy

by

David Rankin Kennedy

November 1997

To

Rose and Katie

SUMMARY

The hydrogenation reactions of propyne, 2-butyne and phenylacetylene have been studied using a series of silica- and alumina-supported palladium and platinum catalysts, each containing a nominal metal loading of 1%. All catalysts have been the subject of numerous characterisation techniques including temperature programmed reduction, selective chemisorption, UV-Vis diffuse reflectance spectroscopy, thermal gravimetric analysis, BET measurements, atomic absorption spectroscopy and transmission electron microscopy.

The reaction of hydrogen and propyne was performed in a pulse-flow microcatalytic reactor using reaction mixtures of varying hydrogen concentration; (1:1 :: C_3H_4 : H_2) and (1:3 :: C_3H_4 : H_2). All propyne hydrogenation reactions were performed at ambient temperature.

Using low concentrations of hydrogen, both Pd/SiO_2 and $Pt/\gamma\text{-}Al_2O_3$ were completely selective for the formation of propene; $Pd/\gamma\text{-}Al_2O_3$ and Pt/SiO_2 exhibiting lower selectivities. This behaviour is believed to be the result of a particle size effect, with the former catalysts containing large metal particles which act less electrophilically towards the acetylenic bond of the reactant, and thus permit desorption of the olefin before complete saturation occurs. With higher coverages of hydrogen, the formation of the alkane was favoured over all catalysts, with an "induction period" being observed before the production of propene was evident. This behaviour has been attributed to the initial dissociative adsorption of propyne to produce surface hydrocarbonaceous overlayers and alkane precursors simultaneously. The associative adsorption of propyne on this hydrocarbonaceous overlayer, with the latter acting as a hydrogen transfer medium, is proposed as the route to

propene. The formation of either the alkane or the surface hydrocarbonaceous residues is therefore postulated as being a function of the rate of hydrogen supply to the relevant surface sites. All catalysts were prone to deactivation which is believed to occur through a site-blocking mechanism.

The gas phase hydrogenation of 2-butyne favoured the formation of the *cis*-olefin isomer when low concentrations of hydrogen were used. Stereospecific reduction of an associatively adsorbed acetylenic species (2,3-di-σ/π-butyne) is proposed as the main route to this olefin. At high reaction temperatures, trace amounts of the *trans*-olefin isomer were observed. This reaction is believed to occur by either (i) adsorption on surface defect sites or (ii) by isomerisation of the *cis* isomer via a radical intermediate.

With higher coverages of hydrogen, all catalysts displayed complete conversion of 2-butyne over a series of thirty pulses. Formation of the alkane was the predominant reaction using all catalysts except highly dispersed Pt/SiO_2, which was selective for *cis*-2-butene formation. A direct mechanism for the hydrogenation of 2-butyne via an associatively adsorbed surface species is proposed as the route to *n*-butane. The propensity of 2-butyne to undergo dissociative adsorption is evident from the production of methane. Similar to the reactions of propyne, the formation of surface hydrocarbonaceous residues and the hydrogenation products is believed to be governed by the availability of surface hydrogen.

Reaction of phenylacetylene and hydrogen in the liquid phase proceeds to yield both styrene and ethylbenzene, with the adsorption and hydrogenation of styrene predominating after the removal of all of the acetylene from the system. Co-hydrogenation experiments performed using an equimolar mixture of styrene/phenylacetylene indicates that the adsorption of both the olefin and acetylene occurs at different surface sites, with the hydrogenation of each

adsorbate occurring independently of the other. It is believed that olefin chemisorption in the presence of the acetylene has the effect of reducing the amount of available hydrogen for phenylacetylene hydrogenation.

The hydrogenation of phenylacetylene in the gas phase produces only ethylbenzene, the formation of which is proposed to occur via (i) a di-π-adsorbed species analogous to that involved in propyne hydrogenation to propene or (ii) from dissociative adsorption to yield a surface alkylidyne.

In conclusion, we can state that the surface hydrogen concentration plays a crucial role in determining the selectivity and activity of the catalysts during the hydrogenation reactions. In the presence of high coverages of hydrogen, all catalysts favoured the production of the alkane, except highly dispersed Pt/SiO_2 in 2-butyne hydrogenation. The observed deactivation phenomenon during propyne hydrogenation has been attributed to the possible formation of surface oligomers which reduce the number of exposed active sites. Since the reactions between 2-butyne and excess hydrogen exhibited no signs of catalyst deactivation, it is proposed that the formation of surface oligomers from this acetylene would be less probable due to the steric effects experienced by the substituent methyl groups. Therefore, the likelihood of extensive oligomerisation and hence, deactivation occurring is reduced.

ACKNOWLEDGEMENTS

Grateful acknowledgement is made to both Prof. G. Webb and Dr S.D. Jackson for their guidance throughout the course of this project. It has proved an invaluable and informative experience.

I am indebted to my dear wife, Rose (previously Rose - the catalysis technician) for all her assistance and good humour during my time in the Catalysis Research Group (and at home).

Thanks are also due to the numerous members of the Chemistry Departments academic and technical staff, with particular thanks to Dr. John Cole for helping me with many of my analytical queries, and also Dr. R.J. Cross for pointing me in the direction of some excellent homogeneous systems for further reading.

I am grateful to Dr. Dave Lennon for the many interesting conversations we shared over the last couple of years (many were over my head), and for suggesting the application of infra-red spectroscopy to this project. I must also thank John McNamara for his help in performing the DRIFTS study, and for carrying out the Transmission Infra-Red work (it got you away from TETRIS).

Last but not least, I would like to express my thanks to the occupants of the Inorganic Research laboratories (most are to be found in the office). There have been many through the last three years, most of whom have now flown the nest; you know who you are - Cheers.

CONTENTS

Chapter Three **EXPERIMENTAL** PAGE

Chapter One

INTRODUCTION

1. Introduction

In heterogeneous catalysis, the initial, and most important step of any surface reaction is the adsorption of the reactant(s).
Adsorption is a process in which molecules of a particular material become attached or concentrated at an interface, with an interface describing the area between two distinct phases. Typical examples of interfaces are gas-solid, liquid-solid and gas-liquid, to name but a few. Adsorption is normally classified into two areas, namely *chemisorption* and *physisorption.*

1.1 Physisorption (Physical Adsorption)

Physical adsorption or van der Waals adsorption involves weak and associative bonds between reactant and substrate. This adsorption is accompanied by only small heat changes which are often of the same order of magnitude as the heat of liquefaction of the adsorbing gas. Unlike chemisorption, the physical adsorption of a molecule at an interface is not directly associated with any distinct surface atom, and may indeed occupy an area independent of the nature of the adsorbate. Physisorption is also prone to multi-layer adsorption, since the forces involved between the adsorbate and adsorbent are similar in magnitude to those involved between molecules in a liquid. A typical example of physisorption is oxygen adsorption on titania, which involves a binding energy of approximately 5kJ mol^{-1}, not markedly different from the latent heat of condensation of oxygen (6.80kJ mol^{-1}).

Typical applications of physical adsorption include the determination of catalyst surface areas and pore structure characteristics through low temperature nitrogen adsorption; the temperature at which this adsorption occurs being close to the boiling point of the adsorbate. Such procedures

allow correlations to be drawn between catalyst structure and behaviour, under reaction conditions.

1.2 Chemisorption (Chemical Adsorption)

In chemical adsorption the adsorbate molecules are held at the surface by valence forces similar to those present between atoms in a molecule. This phenomenon can be observed between an adsorbing gas at a metal surface, where the metal possesses unoccupied orbitals, providing sites for co-ordination. The chemical bonds formed are much stronger than those formed during physical adsorption, and the heats involved are similar to those liberated during chemical reactions. Considering the energy changes observed in chemisorption processes, the reactivities of molecules may be altered upon surface adsorption, and may even be greatly enhanced. This is indeed the case when chemisorption is accompanied by dissociation of the adsorbate.
An example of this would be the adsorption of hydrogen on tungsten, where the (H-H) bonds are broken, with the resulting dissociated hydrogen atoms being more reactive than the free hydrogen molecules.

Clearly, for the purposes of catalytic reactions, chemisorption of at least one of the reactants is a prerequisite to further reaction, and a number of special features of chemisorption are detailed below;

i) surface coverage never exceeds a monolayer of adsorbate
ii) chemisorption processes may often have appreciable activation energies
iii) considerable variation in the adsorptive capacities of various surface sites observed
iv) chemisorption can occur over a wide range of temperatures

The distinction between chemical and physical adsorption can best be shown in Figure 1.1.1. Consider the diatomic molecule X_2. Physisorption of this molecule is represented by curve (a). As the molecule approaches the surface the potential energy falls to a minimum, represented by ΔH_1. This value will typically be low since the heat of physisorption can be presumed to be small. Chemisorption of the molecule at the surface is represented by curve (b). When the adsorbate molecules are separated by an infinite space from the surface, they still possess energy D, which, in the case of molecules that are prone to dissociation on adsorption, represents the molecular dissociation energy. As the molecule approaches the surface, the potential energy is observed to decreases to a low minimum. At this point the molecule is much closer to the surface than in physisorption. With chemisorption involving the formation of new chemical bonds between both adsorbate and surface, a term defining the heat of chemisorption ($-\Delta H_2$) will be applicable.

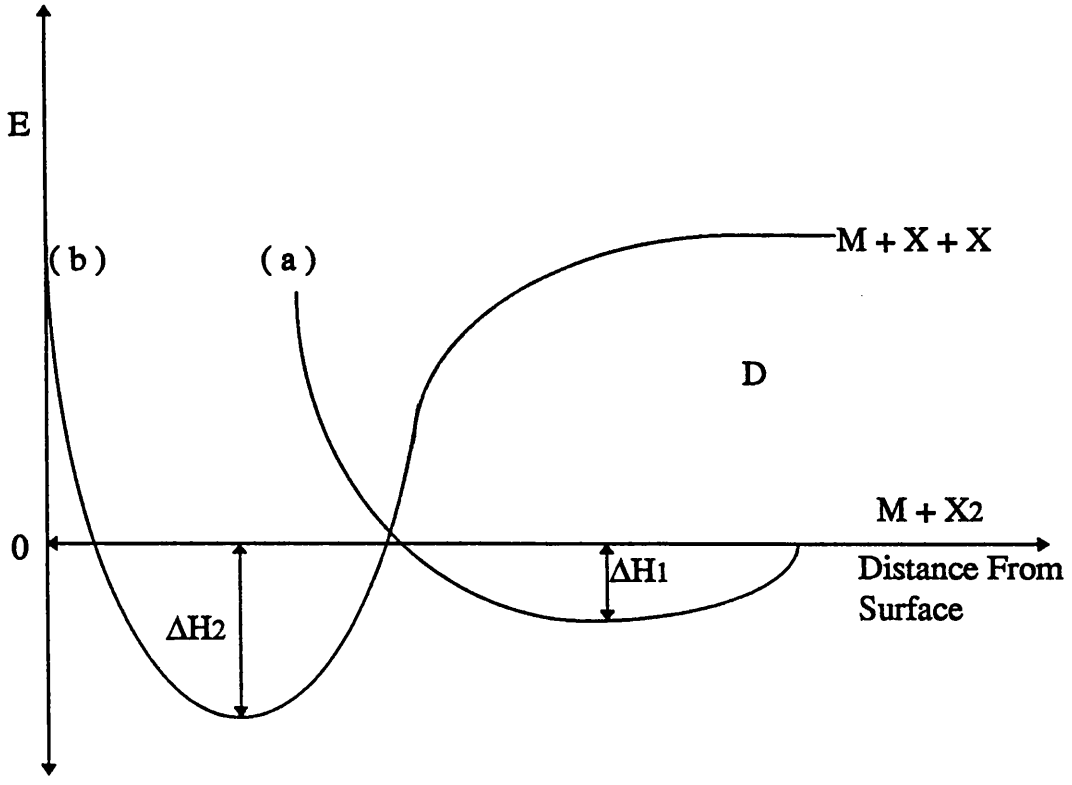

Figure 1.1.1 : *Potential Energy Diagram of Adsorption*

1.3 Thermodynamic Aspects of Adsorption

For an adsorption process to be thermodynamically feasible, the Gibbs free energy change (ΔG) must be a negative quantity, specified by the equation shown below :

$$\Delta G = \Delta H - T\Delta S \qquad \textbf{Equation 1}$$

Since the adsorption of any molecule at a surface is invariably an exothermic process, the enthalpy change (ΔH) for the process will be negative. Also, since the adsorption step converts a free molecule into a surface bound entity, there is an accompanying loss in entropy; therefore, the change in free entropy of the system (ΔS) will also be negative. Therefore, since adsorption is a spontaneous process, proceeding with the decrease of the free energy of the system, it would follow that surface adsorption was itself an exothermic reaction.

The largest contribution to the observance of this exothermic behaviour will be the enthalpy change in the system. This factor will be governed by the relative strengths of the chemical bonds involved, and hence, will be dependent upon the nature of both the adsorbate and the adsorbent.

Less influential will be the change in the entropy of the system, since ΔS values might not be expected to vary markedly on altering the identity of either the adsorbate or adsorbent once chemisorption had occurred.

1.4 Hydrogen Adsorption on Metals

For the purposes of hydrogenation reactions over metal catalysts, maximum catalytic activity is associated with rapid, but not too strong, chemisorption of the adsorbates. The most active metals for such reactions are the group VIII metals. For example, the strength of reactant adsorption over group VB and VIB metals is too great, while that observed over group IB metals is either too weak or non-existent. Therefore, for the purposes of this study, the application of supported palladium and platinum catalysts was examined.

Fundamental aspects of hydrogen chemisorption on the noble metals have been well reviewed[1,2], with particular reference given to the strength and electronic nature of the (M-H) bonds and the location and configuration of adsorbed hydrogen. Some of the key points regarding the adsorption of hydrogen on metals are detailed below :

i) The adsorption of hydrogen on metals involves four processes
   a) initial physical adsorption of molecular hydrogen
   b) formation of hydrogen atoms via molecular hydrogen dissociation
   c) hydrogen atom migration into bulk and surface layers
   d) possible formation of surface and/or bulk hydrides

ii) bonds between hydrogen and metal are generally covalent type bonds

iii) hydrogen atoms will preferentially bond to high co-ordination sites - usually three or four fold hollow sites on metal surface.

iv) hydrogen generally chemisorbs dissociatively on catalytic metals with heats of adsorption of approximately 60 to 120kJmol^{-1}. These heats of adsorption are not usually influenced by carriers or surface structure.

1.4.1 Hydrogen Adsorption on Platinum

A face centred cubic metal, platinum is one of the most versatile metals used in heterogeneous catalysis. The highest density, lowest free energy surfaces are the (111) and (100) crystal faces respectively. However, for the purposes of hydrogen adsorption and activation, the existence of atomic steps on the surface are essential in dissociating the hydrogen molecules. At these atomic steps, hydrogen readily dissociates through a low activation energy route, with the surface retaining a large concentration of the adsorbed hydrogen atoms.

The adsorption of hydrogen on platinum surfaces has been shown to exist in several different geometries. An example of this was presented by Tsuchiya[3] who studied hydrogen chemisorption on Pt-black over a wide temperature range. Analysis by TPD showed that four distinct Pt-H species existed at the surface. These species were observed at -103°C, -23°C, 77°C and 297°C. These entities were classed by Tsuchiya as α (I), β (II), γ (III) and δ (IV) hydrogen adsorbed states, and are shown in Figure 1.1.2.

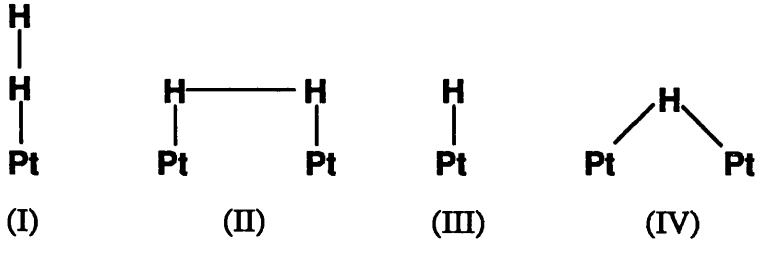

Figure 1.1.2 : *Chemisorbed Hydrogen on Platinum*

Lang *et al*[4] showed that hydrogen readily formed sub-surface layers on Pt (111) single crystals, which disappeared as the crystal temperature was elevated under vacuum. However, the re-emergence of this species was

observed upon treating the surface with oxygen; a cycle that was reproduced successfully several times.

The kinetics of hydrogen adsorption on platinum single crystals has been the subject of numerous reviews[2,5]. TPD studies on Pt/H systems reveal the existence of atomic hydrogen states of low binding energies at platinum surfaces, which are readily desorbed at temperatures of 200-300K. This therefore means that a fraction of the hydrogen adsorbed is held "reversibly" at ambient temperature. This statement should not however be taken literally. In practical terms the rate of desorption of hydrogen at room temperature is essentially negligible. However, at 300K, the β_1 state of hydrogen, which is formed at high coverages is reversibly adsorbed on platinum surfaces, while the β_2 state, which predominates at low surface coverages is mostly irreversible, since its rates of desorption are very small at these temperatures. These observations have important implications in regard to the use of hydrogen chemisorption for measuring monolayer capacities.

The ability of platinum to chemisorb hydrogen is also dependent upon the reduction temperature. On difficult to reduce support materials, the capacity of platinum for hydrogen adsorption is significantly reduced, a phenomenon which can be reversed by oxygen treatment, and subsequent reduction at lower temperatures.

The observation of decreasing hydrogen adsorption following reduction at high temperatures has also been studied over an alumina-supported platinum catalyst by Den Otter *et al*[6]. A reduction in the Pt/H ratio was observed after reduction at temperatures of 500°C or greater. Den Otter suggested that this observed behaviour was the result of alloy formation between metal and support, assuming that the Al sites did not contribute to the uptake of hydrogen, and the adsorption over Pt is both dissociative and bridged between two distinct metal sites. This behaviour was observed for both low and highly

dispersed catalysts, and is, therefore, not a strong function of platinum dispersion.

Application of hydrogen chemisorption methods to the study of EUROPT-1 was performed by Wells *et al*[7]. The exact stoichiometry of hydrogen to platinum over this silica-supported platinum catalyst was unknown, although normally it is assumed to be 1:1. EXAFS experiments performed by Joyner and Meehan[8] showed that by altering the catalyst temperature under vacuum, to simulate the evacuation process, the nature of the surface bonding was dramatically altered. An associated change in the platinum particle character occurred, with a new feature characteristic of (Pt-O) now observed. Therefore, hydrogen chemisorption on this catalyst would proceed initially by hydrogenolysis of the (Pt-O) bond, as shown.

$$(1)\quad 2\,(\text{Si-O-Pt}) + H_2 \Rightarrow 2\,(\text{Si-OH}) + (\text{-Pt-Pt-})$$

$$(2)\quad (\text{Si-O-Pt}) + H_2 \Rightarrow (\text{Si-OH}) + (\text{-H-Pt-})$$

The adsorption of hydrogen on a 16% Pt/SiO_2 catalyst was studied quantitatively by *in situ* NMR spectroscopy by Chesters *et al*[9] over a wide coverage range to produce an NMR adsorption isotherm. These workers observed not only the hydrogen atoms associated with the silica support and metal atoms, but also a signal at -20ppm assigned to hydrogen present at the interface between the metal and the support. The existence of strongly bound, bridged-bonded hydrogen resonates at -48ppm, with the weakly held "on-top" hydrogen found at 37ppm. These two species are in rapid exchange, with the "on-top" hydrogen also in exchange with gas phase hydrogen (δ = 8ppm). In summation, these three species give rise to one peak in the NMR spectrum, and it is believed that it is the weakly held "on-top" hydrogen which is active in hydrogenation reactions. The model proposed by this group is shown in Figure 1.1.3.

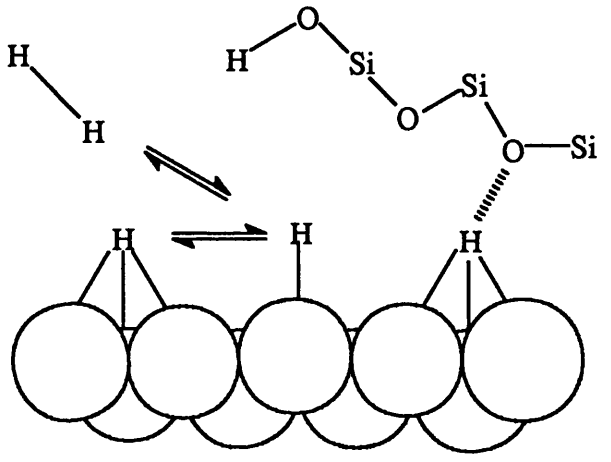

Figure 1.1.3 : *Hydrogen on Pt/silica*

1.4.2 Hydrogen Adsorption on Palladium

Palladium crystallises in a cubic close packed lattice similar to platinum but, unlike platinum, behaves very differently when exposed to hydrogen. One property palladium exhibits is its ability to absorb hydrogen up to a point represented by the stoichiometry Pd_2H[10]. At higher temperatures, the metal becomes permeable to hydrogen, a property which is employed in the separation of hydrogen from other gases.

The heats of adsorption of palladium and platinum were calculated to be 63± 4kJmol^{-1} and 56±12kJmol^{-1} respectively for hydrogen chemisorption on unsupported powders[11,12,13]. These values compare well with the calculated heats of adsorption for Pd (111) and Pt (111) estimated to be approximately 71±10kJmol^{-1} and 42±5kJmol^{-1}. Therefore, it would appear that the heat of hydrogen adsorption on palladium and platinum is independent of both crystallite size and support, over a wide range.

The above results, for hydrogen adsorption on palladium, were corroborated by Guerrero[14] using both low and highly dispersed 0.5% Pd/alumina catalysts. The observed change in heats of adsorption was attributed to changes in the electronic properties of small palladium crystallites. Results published by Chou and Vannice[12] showed observable increases in the heats of hydrogen adsorption on particles of less than 3nm in size.

The ability of palladium to dissolve hydrogen atoms into the metal bulk results in the formation of Pd-H phases which have different hydrogen concentrations. Two types of Pd-H phases predominate and are classed as the β-Pd-H and α-Pd-H systems. The former of these two is believed to exist and predominate at room temperature. The stability of this phase is believed to diminish at elevated temperatures in favour of the α-Pd-H phase. The transition between the two phases is not believed to be dependent on metal particle size, although evidence for the existence of the β-Pd-H phase on very small particles is sparse.

When palladium is found in its bulk metallic form it is still subject to surface and bulk rearrangement processes in the presence of hydrogen[15], suggesting that the metal particles are morphologically unstable under such conditions.

Static and MAS NMR spectroscopy studies on hydrogen and deuterium phases present in Pd/SiO_2 catalysts presented by Benesi *et al*[16], were performed over a series of metal particle sizes. Resolution of peaks attributed to gas phase D_2, β-phase deuteride, mobile, weakly chemisorbed deuterium on palladium, and less mobile OD groups associated with the silica support surface were detailed. Boudart and Hwang[17] showed that the pressure required for hydride formation increases with decreasing crystallite size, and

Aben[18] has reported a drop in total hydrogen uptake in the β-Pd-hydride phase with decreasing particle size.

1.5 Hydrocarbon Adsorption at Surfaces

1.5.1 Adsorption of Olefins

The hydrogenation of olefins at catalytic surfaces is undoubtedly the result of the initial chemisorption of the hydrocarbon. Clearly, the nature of this adsorbed olefinic species will have a significant effect on both the activity and selectivity of the catalyst during the course of the reaction. Therefore, it is necessary to detail some of the work performed in this area, with a view to explaining the nature and role of the adsorbed olefin complex.

There are two predominating types of adsorbed olefin species classed as :

i) di-σ-olefin species

ii) di-π-olefin species

The di-σ-species is believed to be formed by rehybridisation of the olefinic carbon atoms to sp^3 hybridisation, followed by the formation of two σ-bonds between these atoms and two metal atoms at the surface, forming an alkane structure. This species can best be represented by the model shown in Figure 1.1.4. The geometrical implications of this structure have been reported by Bond[19].

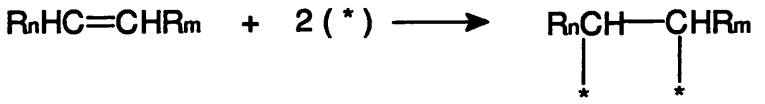

Figure 1.1.4 : σ-*Bonded Olefin State*

The di-π-olefin species is formed by the donation of electron density from the olefinic bond to a vacant d-type orbital on the metal, producing a π-donor bond. A schematic representation of this species is given in Figure 1.1.5 below.

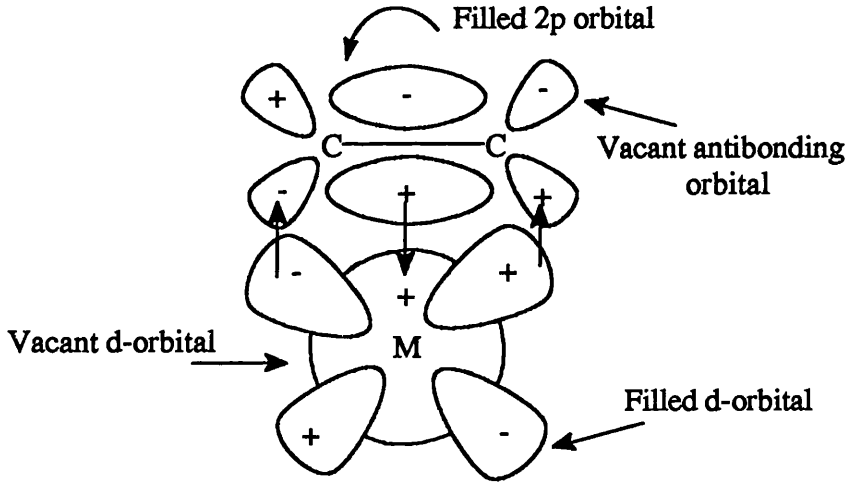

Figure 1.1.5 :π-*Bonded Olefin State*

The hybridisation of the olefinic carbon atoms is unaltered in this complex, and for this reason the atoms and any attached substituent groups, are near coplanar in a plane parallel to the surface. Unlike the di-σ-species, this entity may involve only one surface metal atom.

Infra-red studies revealed that the adsorption of ethene on a bare Pt/SiO_2 catalyst at ambient temperature produces spectra in which the di-σ-species predominates[20,21]. Using extremely sensitive interferometry techniques[22,23], Sheppard and co-workers have reported the existence of both the π-bonded species and a 1,2-di-σ-species when ethene is chemisorbed on

hydrogen precovered Pd/SiO_2 and Pt/SiO_2 catalysts. However, the observance of dissociatively adsorbed olefin complexes has also been reported[20,21]. Both the π-bonded and di-σ-species were observed from magnetic studies of ethene chemisorption on a Ni/SiO_2 catalyst at 0°C. However, at elevated temperatures molecular dissociation occurred, resulting in self-hydrogenation producing ethane. This can be explained by either the reaction of chemisorbed ethene with hydrogen atoms released by the dissociation of an associatively adsorbed ethene molecule, or by disproportionation of two associatively adsorbed ethene molecules. The existence of dissociatively adsorbed ethene on Pd/SiO_2 has been reported by Little *et al*[24].

The decomposition of ethene on transition metal surfaces has been an area of ongoing interest for many years, a phenomenon which has been shown to occur at elevated temperatures. Generally, ethene adsorbs molecularly at low to ambient temperatures. Upon heating, the ethene sequentially loses hydrogens to form a series of molecular species. Eventually at high enough temperatures the ethene completely dissociates to form carbon and hydrogen. The rates of ethene decomposition processes are believed to change with surface structure. A model for this process is shown in Figure 1.1.6.

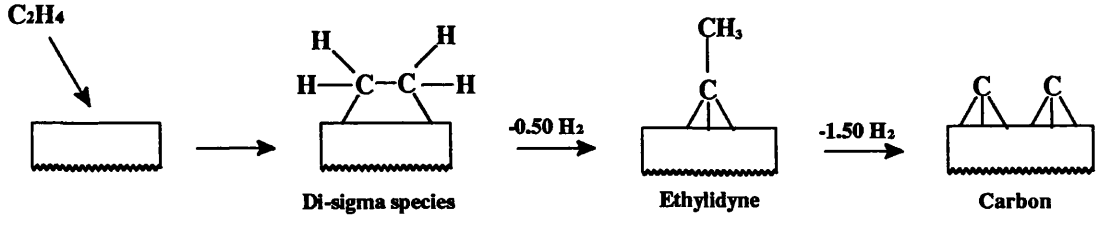

Figure 1.1.6 : *Ethene Decomposition Mechanism*

With higher hydrocarbons, similar results are obtained. The chemisorption of propene on a Pt/SiO_2 catalyst was examined by Sheppard *et al*[25] using infra-red spectroscopy. The existence of associatively adsorbed di-σ-species and smaller amounts of the π-bonded species was reported. With

the chemisorbed propene, heating under vacuum above 130°C lead to the dissociation of the initially adsorbed species to yield ethylidyne, which could only be produced through (C-C) bond scission.

The C-3 counterpart of ethylidyne called propylidyne is itself well documented[25,26,27]. Sheppard and co-workers[26] reported RAIRS results consistent with the formation of propylidyne, a di-σ-species and traces of the π-bonded species on Pt/SiO_2. The presence of the latter two complexes was accounted for by the adsorption of propene on crystal planes other than the (111) face.

In the case of C-4 hydrocarbons, the observance of the saturated butylidyne species on a Pt (111) surface, was observed by Sheppard[28]. This species however, was only observed from the direct chemisorption of 1-butene, with both 2-butene isomers producing a π-adsorbed complex at temperatures in excess of 250K.

1.5.2. Adsorption of Acetylenes

Similar to olefin hydrogenation, the initial step in the hydrogenation of an acetylenic hydrocarbon is its chemisorption at the surface. There are essentially two forms adopted by the acetylene upon surface chemisorption, which are termed :

i) di-σ-species

ii) di-π-species

The first of these two is formed by the initial rupture of the acetylenic bond to produce two σ-bonds between the unsaturated carbon atoms and two distinct surface metal atoms. This structure was first observed by Little[24] for

ethyne adsorption on palladium, nickel and copper supported on silica glass, and by Sheppard *et al*[29] over silica-supported platinum and nickel catalysts. This species was not removable by evacuation, but formed a new saturated molecule when exposed to hydrogen. The geometry of this associatively adsorbed state has been investigated[30,31], and the optimum metal-metal distances required are available on the commonly exposed crystal planes. Figure 1.1.7 displays both adsorbed states schematically.

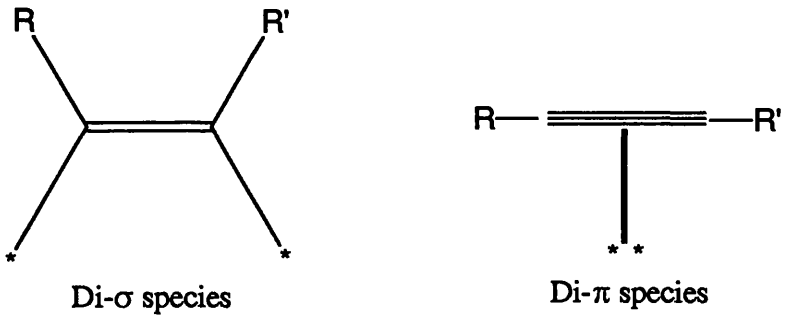

Figure 1.1.7 : *Adsorbed States of Acetylenes*

The second of the two modes of adsorption is termed the di-π-species. This is produced by the donation of electron density from the triple bond to vacant orbitals on the surface metal atoms. In this case, two metal atoms constitute an adsorption site. Of the two possible adsorption modes described, the di-σ-species is expected to be the more strongly adsorbed to the surface, since the first π-bond in acetylene is weaker than the second[19,32]. Also, for the π-adsorbed mode of acetylene adsorption, the acetylene can bond with two metal sites, whereas the olefin may only bind through one.

The existence of an associatively adsorbed di-σ-species has been proposed from volumetric studies[33,34]. Infra-red experiments on Ni/SiO_2 revealed a band at approximately $3020cm^{-1}$, which was assigned to this species. Admission of hydrogen resulted in an increase in the intensity of this

band, which was attributed to surface alkyl groups of average form, H_3C-(CH_2)$_n$, where n = 3 on nickel, and n > 4 on platinum.

The effects of hydrogen on the IR spectra of adsorbed acetylenes combined with mechanistic studies of ethyne hydrogenation reactions has led to the conclusion that the acetylenic species active in hydrogenation reactions are associatively bound to the surface. It was assumed that these species could be adequately represented as the di-σ-bonded olefin. Hence, it was proposed that the (111) faces would be inactive for acetylene adsorption due to geometrical requirements in that adsorption mode. However, LEED[35] experiments performed on platinum single crystals showed that ethyne readily adsorbs on the (111) planes. Following work published by Rooney *et al*[36,37,38], it has generally been assumed that the active adsorbed form of ethyne in hydrogenation reactions is the π-adsorbed complex, formed between the π-bond and two metal atoms.

1.6 Hydrogenation of Acetylenic Hydrocarbons

The hydrogenation of acetylenes is a critical reaction in the petrochemical industry[39]. Some basic chemical processes require large quantities of olefins of reagent grade purity with a very low concentration of acetylene impurity. This aim is normally met by the application of supported metal catalysts, typically low loaded Pd/Al_2O_3 which selectively reduce the acetylene impurity to the desired olefin. However, even with the best catalysts[40,41], the hydrogenation of acetylenes rarely reaches the low levels required without the accompanied formation of the alkane. Therefore, an acetylene will generally hydrogenate to yield both the olefin and alkane, and the system may show a preference for either product depending on the catalyst and operating conditions employed. This situation is made somewhat more

complicated when the acetylene contains four or more carbon atoms. In these circumstances, partial hydrogenation of the acetylene can yield a number of isomeric olefins as well as the alkane. The extent to which the acetylene hydrogenates to the olefin as opposed to the alkane is termed the selectivity, and is determined in part by the adsorption characteristics of both the olefin and acetylene.

1.6.1 Catalyst Selectivity

Two different types of selectivity in catalytic reactions are known. Consider the hydrogenation of the acetylene, C_nH_{2n-2}, shown in Figure 1.1.8.

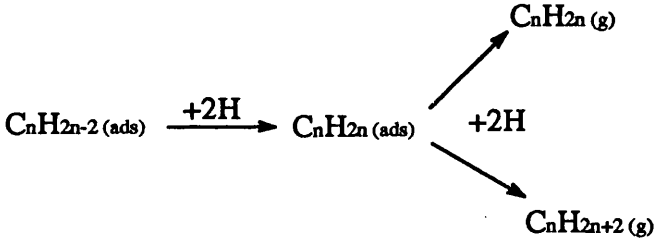

Figure 1.1.8 : *Acetylene Hydrogenation Scheme*

In the first type of selectivity, the reaction can be given as in Figure 1.1.9.

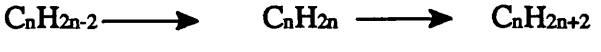

Figure 1.1.9 : *Consecutive Reaction Route*

The extent to which the olefin is formed is related to how much more strongly the acetylene is chemisorbed at the surface than the olefin. Therefore, if the difference between the free energies of adsorption of these two species is considerable, such that the olefin is effectively excluded from

the surface, then the formation of the alkane from the olefin will not occur. This phenomenon is called the *thermodynamic factor.*

The second type of selectivity related to such systems is termed the *mechanistic factor.* In this case, the hydrogenation of the acetylene may proceed to yield both the olefin and alkane simultaneously. This is shown in Figure 1.2.0.

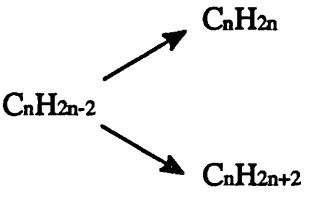

Figure 1.2.0 : *Parallel Reaction Routes*

The initial adsorption of the acetylene may proceed to an adsorbed olefin, which on desorption gives a high selectivity value. However, the adsorption of the acetylene may proceed at the surface to produce the alkane through one surface visit, as the step involving readsorption of the olefin in the presence of adsorbed acetylene is unlikely.

In the hydrogenation of acetylenes both types of selectivity occur, and therefore, the full reaction scheme can be given as shown in Figure 1.2.1.

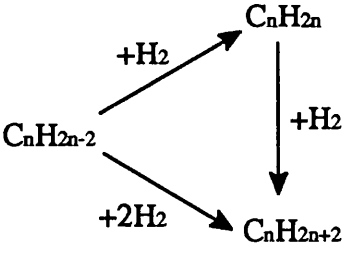

Figure 1.2.1 : *Competitive Routes*

1.6.2 Hydrogenation Mechanisms

^{14}C-tracer studies performed by Webb and Al-Ammar[42] on the hydrogenation of ethyne over silica-supported palladium, platinum and iridium in the presence of ^{14}C-ethene, showed that with each catalyst, the amount of alkane formed directly from ethene was small. They discovered that the major route to ethane formation was from ethyne hydrogenation, and that ethene did not adsorb on the ethyne hydrogenation sites. This mechanistic study suggested that the hydrogenation of ethyne and ethene occurred on different types of surface site.

Ethyne hydrogenation has been well documented[43,44,45,46,47,48] over the years, with less work on the hydrogenation of substituted acetylenes being reported. For the purposes of this section of the introduction the hydrogenation of acetylenes containing three or more carbon atoms will be considered.

The study of propyne hydrogenation reactions over metal catalysts has been little discussed, with the majority of the work published in this area relating to static reaction experiments[49]. Mann and Khulbe[50] studied the hydrogenation of propyne over both pumice-supported and unsupported platinum and iridium catalysts. Over a range of reactant ratios and temperatures the order of reaction with respect to hydrogen and propyne was determined. Over unsupported iridium these workers found that the order of reaction in propyne was zero or slightly negative and dependent on temperature. For hydrogen the reaction order was found to be positive. This suggests that propyne is more strongly chemisorbed at the surface than hydrogen. Therefore, the surface coverage for propyne would be very high, while that of hydrogen would be low in comparison. Similar results were obtained by Bond and Wells[51] using Pd/Al_2O_3 in the hydrogenation of ethyne.

More recent work on propyne hydrogenation has been published by Jackson and Kelly[52]. Using a Pt/SiO_2 catalyst, the reactions were performed in a pulse-flow system using various reactant ratios and temperatures. The order of reaction with respect to propyne was found to change with reaction temperature and, similar to the results of Bond and Sheridan[49], they concluded that the propyne is indeed strongly adsorbed at the surface. The effect of reactant ratio was also determined in this study. At high temperatures an increase in the hydrogen concentration was found to favour the formation of propane over propene suggesting that the activation energy for propane formation was higher than that of propene.

Jackson and Casey[53] reported the results of propyne hydrogenation reactions performed in both a static and pulse-flow system, and full characterisation of the intermediates was achieved by *in-situ* infra-red spectroscopy. The pulse-flow reactions displayed significant quantities of carbon being deposited over the catalyst surface resulting in the attainment of a steady-state regime. This behaviour undoubtedly relates to the build up of hydrocarbonaceous overlayers on the surface[54]. On all supported palladium catalysts examined by this group, the selectivity toward propene formation was found to be 100%. Clearly the reaction which predominates is the conversion of propyne to propene. Characterisation of the reaction intermediates was performed by *in-situ* IR spectroscopy. Similar to work published earlier by Jackson *et al*[27] on highly dispersed Pd/ZrO_2, this technique allowed the elucidation of all adsorbed surface intermediates involved in the reaction. The spectra obtained were found to contain bands similar to those observed by Shahid and Sheppard[25] for propene chemisorption. Bands attributed to a di-σ-bonded propene species (I) and the propylidyne molecule (II) were obtained, as was a σ-bonded propyne species (III), as shown in Figure 1.2.2.

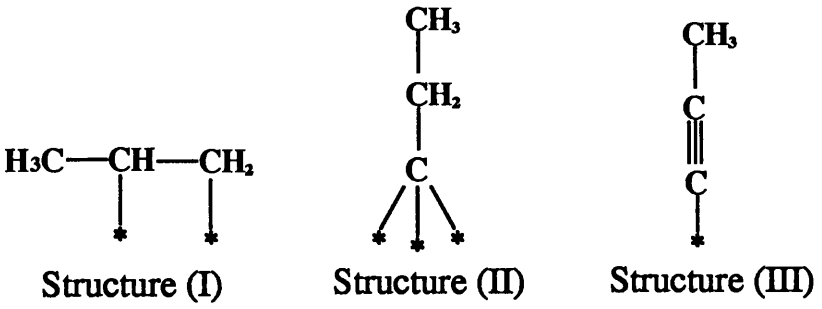

Figure 1.2.2 : *Adsorbed States of Propyne*

These results were consistent with work published by Koestner[55] for propyne and propene adsorption on a Pt (111) single crystal. A general mechanism for propyne hydrogenation over group 8-10 metals was therefore postulated in view of this work and radiotracer work by Webb *et al*[56] on ethyne hydrogenation.

Similar studies have been carried out using 1-butyne and 2-butyne, both of which give rise to stereospecific reactions. Maetz *et al*[57] studied the hydrogenation of 1-butyne over alumina- and silica-supported platinum catalysts with differing dispersions. They found that those catalysts with high metal dispersions and hence, smaller particles were less active than all others. Similar to propyne hydrogenation work by Jackson *et al*[27], the build up of hydrocarbonaceous deposits at the surface led to a change in catalyst behaviour for subsequent reactions, with the selectivity toward 1-butene formation enhanced. This was believed to be the result of the metal sites becoming poisoned by a π-adsorbed 1-butyne molecule which converts to a vinylic adsorbed species. Carbonaceous overlayers block the active metal sites thereby inhibiting further evolution of the adsorbed species to further hydrogenated molecules, thus making butane formation impossible. The formation of butane was believed to occur on non-selective edge and corner sites of the metal crystallites. The effect of metal particle size in the

hydrogenation of 1-butyne over platinum and rhodium catalysts has also been discussed by Boitiaux *et al*[58].

In the hydrogenation reactions of disubstituted acetylenes, the formation of the *cis* isomer of the olefin is favoured using supported palladium and copper catalysts. Burwell and Hamilton[59] examined the hydrogenation of 2-butyne in a flow system using a low loaded Pd/Al_2O_3 catalyst. In the presence of the acetylene, only trace amounts of butane and *trans*-2-butene were observed with the major product being *cis*-2-butene. Similar to propyne and ethyne hydrogenation, on the removal of the acetylene from the system, the *cis*-olefin underwent both isomerisation to *trans*-2-butene and hydrogenation to butane. The stereoselective nature of these reactions was best shown in the work of Meyer and Burwell[60] employing deuterium as a tracer. Approximately 99% of the product was found to be *cis*-2-butene-2,3,-d_2, provided unconverted 2-butyne was present. NMR spectroscopy showed that two deuterium atoms were present on the second and third carbon atoms only. 2-butyne itself did not undergo exchange, but did reduce the rate of hydrogen exchange by a factor of forty.

Using alumina-supported osmium and ruthenium catalysts, Webb and Wells[61] reported the formation of all three butenes in the hydrogenation of 2-butyne using a static reaction system. This work showed that although the activity of osmium and ruthenium for 2-butyne hydrogenation was similar to that of the face centred cubic metals, the stereoselective behaviour of palladium, platinum and nickel could not be mimicked. It has been shown that the highest selectivity of all transition metals is to be found in the first row metals with lower selectivities obtained on descending the groups.

1.7 Carbonaceous Overlayers

It is generally accepted that the hydrogenation of unsaturated hydrocarbons at catalytic surfaces is accompanied by the deposition of surface carbonaceous overlayers[62]. The discovery of this phenomenon is not a new one, with Beeck *et al*[63] reporting the formation of surface carbonaceous residues in a study into the interaction of ethene with evaporated metal films. Similar conclusions were reported by Dus[64] from ethene hydrogenation experiments performed over evaporated palladium films. He claimed that two adsorbed ethene layers where present at the surface; the first layer produced by dissociative adsorption of ethene and the second by associative adsorption of the olefin. It was on this second carbonaceous overlayer that the hydrogenation step occurred. Using supported metal catalysts, Al-Ammar and Webb[65,66,67] provided ^{14}C-radiotracer evidence for the existence of such overlayers in ethene and ethyne adsorption studies. At ambient temperature, the adsorption of ^{14}C-ethene and ^{14}C-ethyne was found to occur in two distinct stages. In the first stage, the species were dissociatively adsorbed at the surface, and self-hydrogenation occured to produce ethane. At higher pressures, a secondary adsorption region was evident, and those species which undergo hydrogenation do so on this surface overlayer. Similar conclusions were presented by Kesmodel *et al*[36] for the hydrogenation of ethyne on a platinum (111) surface, where the hydrogenation step was found to proceed on a secondary adsorbed carbonaceous layer.

1.7.1 Effects of Carbonaceous Overlayers on Catalyst Behaviour

Sheppard *et al*[20,21,68] reported the ability of carbonaceous overlayers to reversibly store hydrogen, using infra-red spectroscopy. This group found that when a hydrocarbon precovered surface was exposed to hydrogen, the band

intensities in the (C-H) region increased, whilst subsequent evacuation of the surface resulted in a loss in band intensity in this region. The hydrogen storage capacity of carbonaceous overlayers was also reported by Somorjai and Zaera[69] using platinum single crystals. This work showed that the presence of active carbonaceous residues containing CH or CH_2 fragments were capable of storing approximately ten times as much hydrogen as a clean metal surface.

Jackson and Kelly[52] noted the selectivity enhancing properties of such deposits in the hydrogenation of propyne over Pt/SiO_2. Using reactant ratios of differing hydrogen concentration, it was discovered that the selectivity of the catalyst toward propene formation was enhanced when the carbonaceous residues were found in a hydrogenated form. When dehydrogenated, these residues no longer acted as hydrogen transfer species.

On the basis of radiochemical studies, Thomson and Webb[62] proposed a general mechanism for the metal catalysed hydrogenation of unsaturated hydrocarbons. It was proposed that the reactions occurred through hydrogen transfer between an adsorbed hydrocarbon, $M\text{-}C_xH_y$, and the adsorbed olefin, rather than by direct hydrogen addition to the adsorbed olefin. This is shown in Figure 1.2.3.

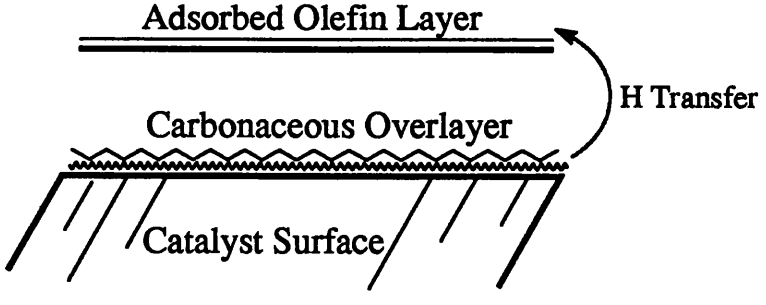

Figure 1.2.3 : *Hydrogen Transfer from Carbonaceous Residues*

A second detrimental feature of carbonaceous overlayer formation is catalyst deactivation[43,44]. Salmeron and Somorjai[70] found that extensive carbon deposition was predominantly found on flat surfaces that are well populated; a phenomenon also observed with larger particles. Therefore, reactions that occur preferentially at these surfaces are then suppressed by the deposition of carbon which diminishes the number of exposed atom clusters. This has the effect of lowering the activity of the catalyst for further reaction, since the number of active sites have been reduced.

Generally, catalyst regeneration can be achieved by treating the catalyst with oxygen at high temperatures, effectively burning off the carbon as the oxygenated product. However, the removal of carbon is irreversible when the carbonaceous overlayers become graphitic[71].

Chapter Two

OBJECTIVES OF STUDY

The principle aim of this project was to examine the hydrogenation reactions of a number of mono- and di-substituted acetylenic hydrocarbons over supported palladium and platinum catalysts. For the purposes of this study, three acetylenes have been examined; propyne, 2-butyne and phenylacetylene. Four supported metal catalysts (Pd/SiO_2, $Pd/\gamma\text{-}Al_2O_3$, Pt/SiO_2, $Pt/\gamma\text{-}Al_2O_3$) have been tested for activity and selectivity in these hydrogenation reactions.

The hydrogenation reactions of propyne have been performed in the gas phase at ambient temperature. The effect of hydrogen concentration was examined by using two different acetylene to hydrogen ratios; an equimolar ratio ($1 : 1 :: C_3H_4 : H_2$), and a three fold excess of hydrogen ($1 : 3 :: C_3H_4 : H_2$).

Hydrogenation of the di-substituted acetylene 2-butyne, was performed over a range of temperatures using gas mixtures of the same ratio as in the propyne hydrogenation reactions.

Phenylacetylene hydrogenation was initially performed as a liquid phase study, with reactions carried out in a stirred autoclave. Similar reactions were also performed for styrene and a co-hydrogenation mixture of styrene and phenylacetylene. These reactions were also examined in a gas phase continuous flow system.

It was hoped that the above reactions would yield valuable information into such surface processes, with a view to :

(a) determining the effects of the adsorbed acetylene structure on

(i) the selectivity and hence, the mechanism of the reaction, with particular reference to the nature and involvement of the adsorbed acetylenic species.

(ii) the ease of formation and nature of permanently retained hydrocarbonaceous surface residues, and the influence of such species on catalyst selectivity and activity.

(b) determining possible correlations between the various effects noted in (a) and the structure of the supported metal catalyst.

Chapter Three

EXPERIMENTAL

Experimental

3.1 Introduction

Three of the four catalysts used in this study were prepared at Glasgow using a wet impregnation method of preparation. The Pt/silica catalyst, also prepared by wet impregnation, was supplied by ICI Katalco.

Catalyst characterisation performed on all four samples included chemisorption measurements, temperature programmed reduction (TPR), thermal gravimetric analysis (TGA), transmission electron microscopy (TEM), atomic absorption spectroscopy (AAS), surface area determination (BET) and UV/Visible diffuse reflectance spectroscopy (UVDRS). The results of these characterisation procedures are given in the results chapter (Section 4.1).

3.2 CATALYST PREPARATION

3.2.1 Metal Precursors and Supports

Supported catalysts were prepared from hexachloroplatinic acid, H_2PtCl_6 (Johnson Matthey Chemicals Ltd, minimum Pt assay 40%) and anhydrous palladium (II) chloride (Fluka Chemicals Ltd, minimum Pd assay 60%). The supports used were silica (M5 Cab-O-Sil) and γ-alumina (Degussa Aluminium Oxid C).

3.2.2 Preparation

The platinum catalysts were prepared by dissolving hexachloroplatinic acid in 725ml of deionised water in a round bottomed flask. The required support material was then added and the solution stirred for approximately two hours forming a gel-like suspension. A further 375mls of water was added to

complete dissolution of the salt. This procedure was continued until all the support material had been introduced, with the total volume of water required being 2.0l. The flask was then attached to a Buchi rotary evaporator and the water slowly removed by maintaining the flasks contents at 80°C under a nitrogen atmosphere. This was continued until all the water had evaporated off producing a free-flowing powder.

In the case of the palladium catalysts a similar procedure was adopted. However, since $PdCl_2$ has limited solubility in water, concentrated HCl was added dropwise to the flasks containing the aqueous salt solutions until dissolution had occurred. At this stage, catalyst preparation followed the route given above. All catalysts were then dried for 12 hours at 100°C.

3.3 CATALYST CHARACTERISATION

3.3.1. Temperature Programmed Reduction (TPR)

Reduction is a necessary step in the preparation of a metallic catalyst. If this is not done correctly the catalyst may sinter or may not reach its optimum state of reduction. The reduction of the metal precursor, MCl_2 by hydrogen is described by the equation

$$MCl_2 + nH_2 \Rightarrow M + 2nHCl \qquad \textbf{Equation 2}$$

Therefore, when the temperature of a catalyst precursor is increased linearly in a stream of reducing gas, typically H_2/N_2, hydrogen will be consumed as a function of the temperature/reactivity relationship of the precursor species. This technique is termed temperature programmed reduction (TPR). TPR is a highly useful technique, providing quick

characterisation, and most important, critical information on the temperature needed for the complete reduction of the catalyst.

The experiments were performed in the system given in Figure 3.3.1. The temperature of the catalyst sample was increased linearly using an electric furnace attached to a Eurotherm temperature programmer. The reduction procedure initially involved placing 0.20g of catalyst into the reactor and purging the system with helium, until the chart recorder displayed a steady baseline.

The reducing gas mixture used was 6% H_2/N_2, which was passed through an oxygen trap, 5% Pd/WO_3, and dried by passing through a Linde 5Å molecular sieve trap. The extent of metal precursor reduction was monitored using a thermal conductivity detector (TCD), which operates by detecting changes in the composition of the effluent gas, as hydrogen is consumed. The removal of reduction products was achieved by incorporating a cold trap, consisting of acetone and dry ice, to protect the TCD filaments from possible corrosion.

The flow of reducing gas was set at 45ml min^{-1} and the sample temperature raised by $5^{o}\,min^{-1}$. The consumption of hydrogen was monitored by the TCD and the reduction of distinct surface species producing a peak on the chart recorder at a specific temperature. This procedure was adopted for all four catalysts, providing information on the number of species present and, more importantly, the minimum temperature at which complete reduction occurs for each catalyst before use in the hydrogenation reactions.

3.3.2 Chemisorption

To achieve a greater understanding of any supported metal catalyst it is important to have a knowledge of the catalyst surface. For the purpose of

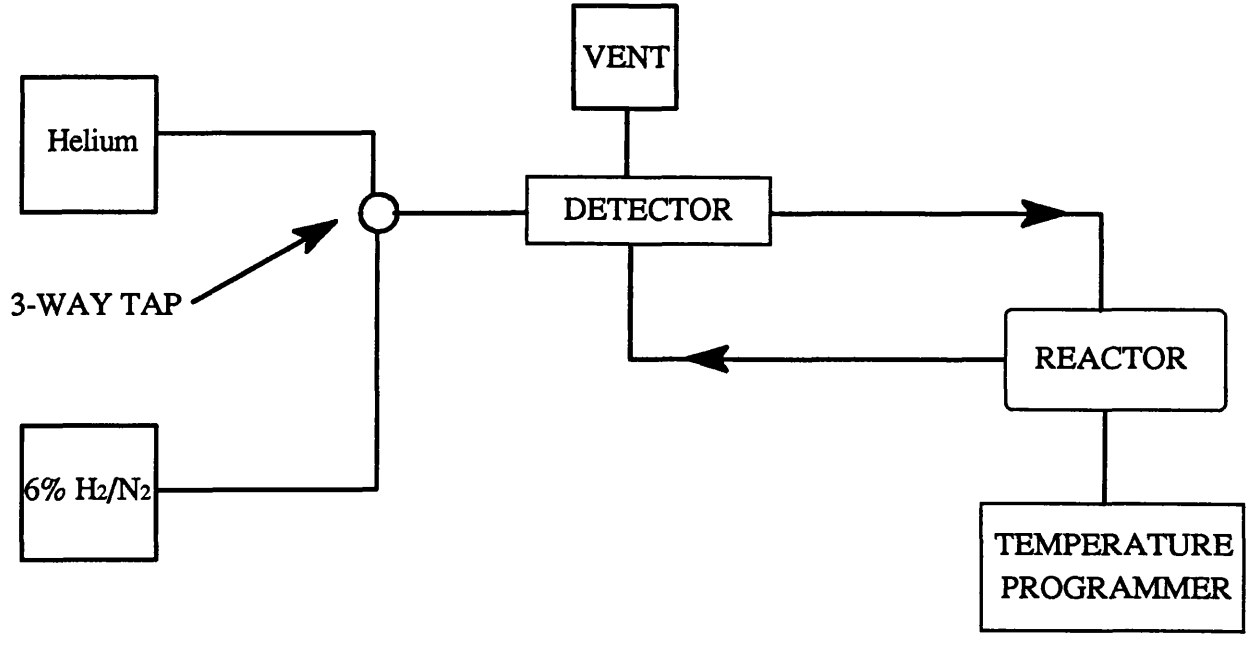

FIGURE 3.3.1 : BLOCK DIAGRAM OF TPR APPARATUS

further reaction chemistry it was deemed necessary to determine the fraction of the total number of metal atoms which were exposed at the surface. This was achieved by the adsorption of carbon monoxide and oxygen in separate experiments. Since the modes of adsorption of both of these gases is simple over palladium and platinum, the number of surface metal atoms could readily be obtained. This allows the determination of the catalyst dispersion, where

$$\% \text{ Dispersion} = \frac{\text{No. Surface Metal Atoms}}{\text{Total No. Metal Atoms Per Sample}} \qquad \textbf{Equation 3}$$

When a known volume of an adsorbate gas is pulsed over a freshly reduced catalyst, a quantity of that gas will be chemisorbed at the surface, forming a fraction of a monolayer. Continued pulsing will result in more gas being adsorbed until a monolayer has been achieved, at which time no more gas will react at the surface, with flow chemisorption only determining the amount of material permanently retained at the adsorption temperature. This model suggests that there is little or no contribution from the support to the observed chemisorption process, hence, a direct stoichiometry between the number of exposed metal atoms and adsorbed gas molecules can be applied.

Carbon monoxide and oxygen adsorption experiments were performed on all catalysts as a means of determining the degree of metal atom dispersion over the support materials, and also to determine the average metal crystallite sizes.

The experiments were performed on the pulse-flow gas chemisorption apparatus shown in Figure 3.3.2. The rig consisted of a vacuum section, a flow line and a known volume sample loop. The vacuum of 10^{-4} Torr or better was achieved by combining both a rotary oil pump and a mercury diffusion pump. This was measured directly using a Pirani Gauge. Cold traps

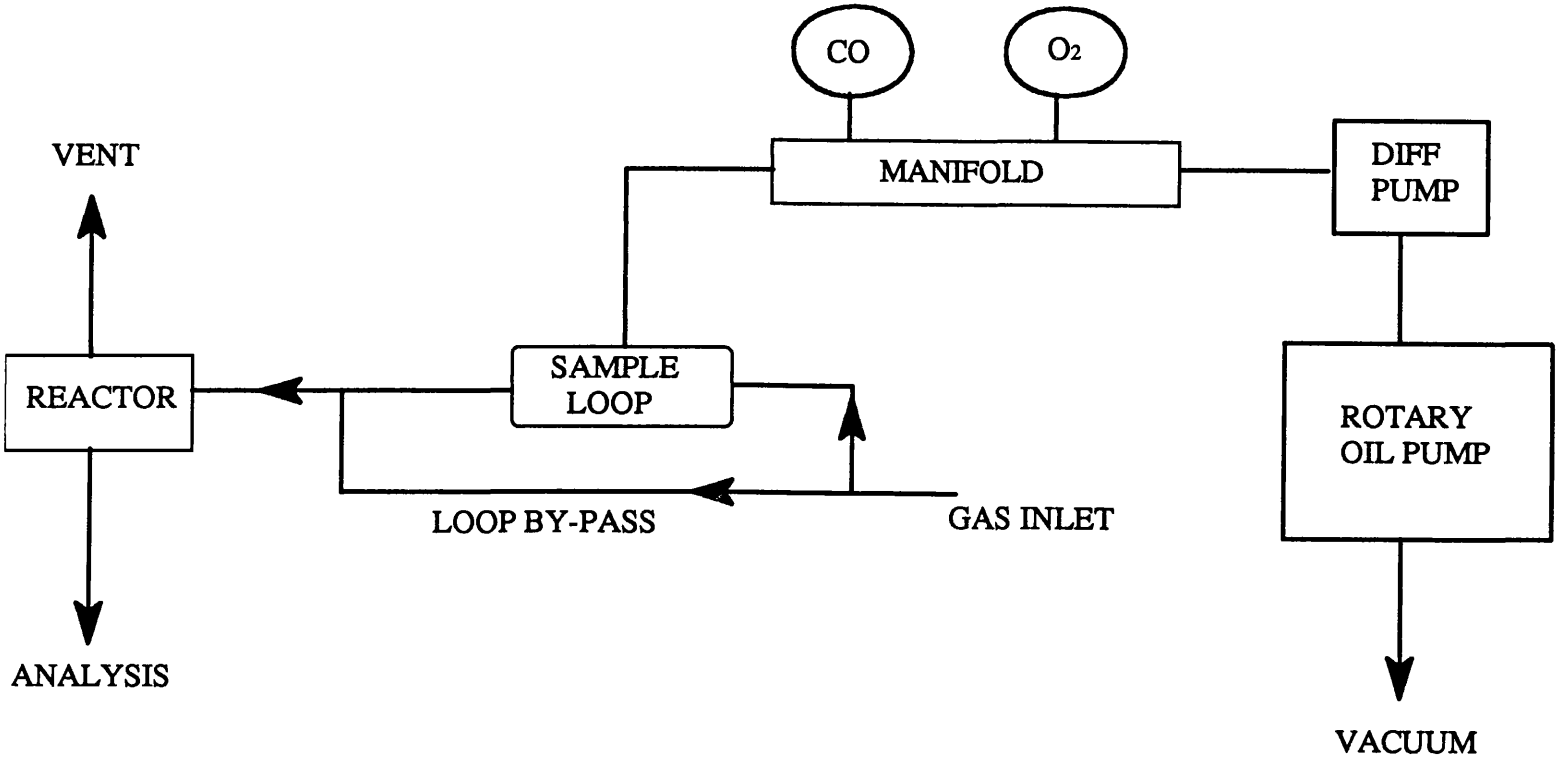

FIGURE 3.3.2 : GAS ADSORPTION APPARATUS

containing liquid nitrogen were used to remove the possibility of mercury vapour poisoning the catalysts, and to protect the oil pump from condensable gases.

The adsorbate gases were stored in bulbs attached to the line via a manifold. By isolating the manifold from the vacuum section, the adsorbate gas could be admitted into the known volume loop and the pressure measured by a mercury manometer. This known amount of gas ($4.70cm^3$, 10mmHg) was then injected into a helium carrier gas flow and over the reduced catalyst. A TCD placed in the gas flow allowed direct monitoring of any changes in the gas composition.

For the purposes of these chemisorption experiments approximately 0.10g of catalyst was reduced *in situ* in a flow of 6% H_2/N_2 at the required elevated temperature. When catalyst activation was complete, the reducing gas mixture was changed to helium and the sample allowed to cool to ambient temperature. Both gas flows were purified before reaching the catalyst, by passage over a deoxygenating catalyst, 5% Pd/WO_3, and subsequently dried by passing through a molecular sieve trap.

Before adsorption experiments could be performed, it was necessary to calibrate the system. This was achieved by pulsing standard pulses of the adsorbate into the helium flow and hence, through the output from which was fed a TCD a Hewlett Packard 3395 Integrator. These pulses by-passed the catalyst reactor and produced distinct peaks on the integrator. Once three identical pulses had been obtained on by-pass, pulses of known size were directed over the catalyst, and the uptake of gas measured as the difference in the eluted peaks and the calibration peaks. This procedure was continued until three peaks of equal area were obtained, indicating the formation of a monolayer. A typical chemisorption trace is given in Figure 3.3.3.

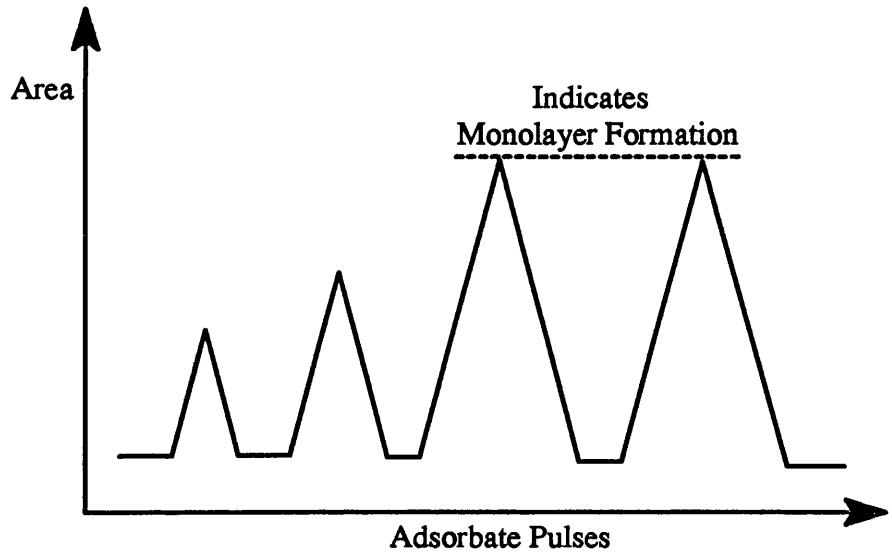

Figure 3.3.3 : *Typical Chemisorption Trace*

3.3.3 UV/Visible Diffuse Reflectance Spectroscopy (UVDRS)

The electronic ground state of the catalyst precursors was investigated by UVDRS. This method of characterisation determines the diffuse reflectance of UV-visible radiation (5000 - 50 cm^{-1}) by finely divided solids.

For powdered solids which are insoluble, or for which solution will perturb the absorbing species, the solid state UV absorption spectra can be obtained by measuring the reflectance of UV light from the absorbing solid. This technique allows the assignation of electronic transitions between metals in different oxidation states, (d-d) transitions within a given metal atom, or transitions from metal to ligand or *vice versa.*

UV-visible diffuse reflectance spectroscopy was performed on all solid catalyst samples, using $BaSO_4$ as a standard, over the range 190 - 900nm using a Philips 8800 UV-vis spectrometer with a diffuse reflectance attachment to determine the electronic spectra. Samples for examination were ground to a fine powder and mounted into a $1cm^3$ cell.

3.3.4 Transmission Electron Microscopy (TEM)

For studying supported catalysts, TEM is a commonly applied form of electron microscopy. Generally, the detection of the supported metal particles is possible provided that there is sufficient contrast between metal and support material. However, this may impede the application of TEM on highly dispersed supported oxide catalysts.

This technique was applied to correlate particle size measurements with those determined from the chemisorption experiments.

Samples were prepared by grinding approximately 0.10g of catalyst into a fine powder, which was then suspended in distilled water and ultrasonically dispersed for 15 minutes. A drop of the fine suspension was then placed on a 300 square mesh Cu carbon coated grid. This was then put in an oven overnight to dry at 40°C. The impregnated grid was placed in the microscope and measurements made using a Philips 1200 electron microscope.

3.3.5 Thermogravimetric Analysis (TGA)

This technique was applied to all catalyst samples using a Du Pont 951 Thermogravimetric analyser. This procedure involves monitoring the mass of the sample against temperature, whilst the temperature is ramped in a reducing gas atmosphere.

The TGA curve obtained expresses the dependence of the weight change on temperature, thus yielding information on the sample composition, thermal stability and the products formed during heating.

Samples of approximately 5mg were placed inside a furnace and subjected to a flow of 6% H_2/N_2 at 60ml min^{-1}, whilst the temperature was raised by 5^{o} min^{-1}. The subsequent loss of sample weight was recorded by a thermobalance and plotted as a function of temperature.

3.3.6 Atomic Absorption Spectroscopy (AAS)

AAS is an analytical method for the determination of elements in small quantities and is based on the absorption of radiation by free atoms.

An absorption spectrum is obtained when the atoms are irradiated with radiation of the appropriate wavelength. Quantitative results can only be obtained by comparison of the catalyst solutions with reference solutions. The calibration graph is established by plotting the absorbance readings for a series of standards against the concentration.

The calibration method used is an interpolation method, which means that all catalyst solutions must lie between the lowest and highest readings of all the standard solutions.

Actual metal loadings in each of the catalysts were obtained using a Perkin Elmer M1100 spectrometer, with both palladium and platinum samples being irradiated with the appropriate radiation wavelength : Pd (247.6nm), Pt (265.9nm).

In order to obtain a calibration curve, 10 to 60ppm platinum standard solutions and 1 to 10 ppm palladium standard solutions, all in 5% HNO_3, were prepared and their absorbances determined. These absorbances were plotted against concentration, and the actual metal loadings for each of the four catalysts calculated.

3.3.7 Surface Area Measurements (BET)

The volume of gas adsorbed per unit mass of solid depends on the equilibrium pressure P, the absolute temperature T, and the nature of the gas and solid. The pressure is usually expressed in terms of P/P_s, the relative pressure, where P_s is the saturation vapour pressure of the adsorbing gas. At a constant adsorption temperature, a series of measurements plotted as

Volume of gas adsorbed / unit mass solid versus P / P_s

yields a graph called an *adsorption isotherm.*

Surface area determination involves admitting an adsorbing gas to a sample of known weight, which has been previously dried, weighed and removed of any adsorbed gases and atmospheric vapours by subjecting it to elevated temperature and evacuation procedures. The adsorbate, which for the purposes of BET measurements is nitrogen, is admitted to the sample in incremental amounts. Some of the gas will be physisorbed by the sample at low temperatures, usually that of liquid nitrogen. The adsorption temperature of this process is critical, and is typically near the boiling point of the adsorbing gas. This procedure is repeated until no more adsorbate gas is taken up by the catalyst sample.

BET surface areas (N_2, 77K) were performed by Coulter Scientific Instruments using a Coulter SA 3100 surface area instrument.

3.4 CATALYST ACTIVATION

Catalyst activation was achieved by loading the catalyst sample into the U-tube flow reactor, which contained a silica sinter to support the sample against the downward flow of gas. The reducing gas mixture, 6% H_2/N_2, was set at 30ml min^{-1}, and the temperature of the catalyst bed increased by 5^{o} min^{-1} using a Eurotherm temperature programmer. The samples were heated to a predetermined temperature which would ensure complete reduction of the precursors to the active metal; palladium samples (200°C, 2hrs) and platinum samples (300°C, 2hrs). After this step was complete, the samples were flushed with pure hydrogen gas for approximately 0.50hrs, after which time they were flushed with helium at the reduction temperature for 0.50hrs, before being set to the reaction temperature.

3.5 Pulse-Flow Microcatalytic Reactor System

A conventional high vacuum system, shown in Figure 3.3.4, was used for hydrogenation reactions in the gas phase. This system incorporated both a high vacuum section and a pulse flow section. Both sections were joined through a sample loop of known volume, ($V = 5.83 cm^3$) through which gas mixtures could be isolated and hence, injected into a helium carrier stream, and over the catalyst.

Similar to the chemisorption apparatus, the vacuum within the system was achieved by combining both a rotary oil pump and a mercury diffusion pump, allowing the system to be evacuated to pressures of 10^{-4} Torr or better.

The vacuum line incorporated four glass bulbs for the storage of hydrogen and reactant hydrocarbons. Reaction mixtures of the required compositions were pre-mixed and stored before use.

The pressure of gas within the line could be monitored at all times using a pressure transducer (Edwards Medium Vacuum control unit 251).

3.5.1 Sample Loop

For the hydrogenation reactions of propyne, the sample loop used consisted of three spring loaded glass taps, all of which could be lubricated using Apiezon N tap grease. However, for the purposes of further hydrogenation experiments on 2-butyne, this grease was found to be unsuitable, in that the gas readily dissolved in the vacuum grease. To avoid this problem, it was deemed necessary to adapt the loop to incorporate only Youngs vacuum taps.

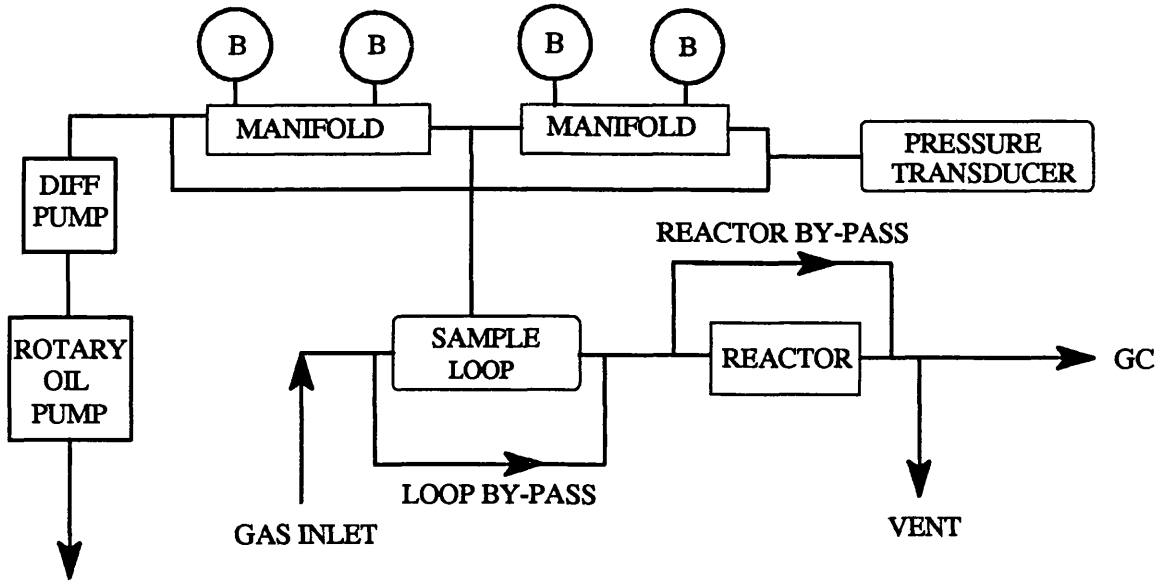

B : GLASS STORAGE BULB

FIGURE 3.3.4: SCHEMATIC DIAGRAM OF PULSE-FLOW MICROCATALYTIC REACTOR

3.5.2 Sample Loop Volume Determination

This was achieved by the use of several known volume bulbs. A standard volume flask was attached to the line, and filled with helium of a known pressure. The line was then evacuated, and the contents of the bulb allowed to expand within the system. The pressure obtained was measured using a pressure transducer. This procedure was carried out several times with both the loop open and closed. The difference between both sets of values allows V_{loop} to be determined. This procedure was repeated with several bulbs until three reproducible V_{loop} values were obtained.

3.5.3 Gas Supply

The gas supply for the vacuum flow system consisted of helium, hydrogen and 6% H_2/N_2. All were supplied by B.O.C (99% purity), and were purified using the deoxygenating and drying traps described in section 3.3.1.

3.5.4 Materials

Propyne

Cylinder propyne (BDH Chemicals Ltd, minimum purity 96%) was purified through two bulb to bulb distillations before use.

2-Butyne

Cylinder 2-butyne (CK Gas Products, minimum assay 96%) was purified as described for propyne, above.

Propane and Propene

Both, supplied by BOC (minimum assay 99%), were found to contain no impurities detectable by gas chromatography, and were merely degassed before use.

Butane and 2-Butene Isomers

Butane (BOC Ltd, minimum assay 99%) was found to contain no impurities detectable by gas chromatography, and similar to the above, was degassed before use. The 2-butene isomers were degassed before use.

Phenylacetylene

Supplied by Aldrich Ltd (minimum purity 98%), this was frozen, pumped and thawed several times before use in the gas phase, to remove dissolved gases. Degassing was completed by bubbling hydrogen through the liquid (25ml min^{-1}) for one hour before use.

Styrene

Supplied by Aldrich Ltd (minimum purity 99%), this was frozen at liquid nitrogen temperatures, pumped and thawed before use in the gas phase. Similar to phenylacetylene, hydrogen was also bubbled through the hydrocarbon before use.

Ethylbenzene

Supplied by Hopkins and Williams Ltd (minimum purity 98%), this was purified using a similar method to that used for styrene and phenylacetylene.

3.6 PULSE-FLOW EXPERIMENTAL PROCEDURE

3.6.1 Hydrogenation Reactions

A mixture of hydrocarbon and hydrogen was prepared by admitting a known pressure of hydrocarbon into a mixing bulb and condensing it in a cold finger. Hydrogen gas was then admitted to the bulb until the desired ratio of hydrocarbon to hydrogen was obtained. The mixture was then allowed to warm to ambient temperature over several hours before use.

Hydrogenation reactions were performed by admitting a known pressure of the reaction mixture into the sample loop. Once isolated, this mixture could be injected into the helium carrier gas flow and hence, over the catalyst bed. Product analysis was achieved by gas chromatography.

3.6.2 Gas Phase Analysis System

Analysis of reaction products was performed by gas chromatography, using a Shimadzu GC-14A chromatograph fitted with a TCD. An on-line computer terminal (Labnet) and Chromjet integrator allowed direct analysis of the chromatographic data.

Analysis of the propyne hydrogenation products was achieved using a stainless steel column (2.2m x 0.125inch, packed with Poropak QS 50-80 mesh).

2-Butyne hydrogenation products were also seperated using a stainless steel column (12ft x 0.125 inch, Carbowax 1500 on Carbopack C 80-100 mesh).

A stainless steel column was also employed for the separation of phenylacetylene hydrogenation products; (12ft x 0.125 inch; Carbowax 20M on Chromosorb W-NAW 60-80 mesh).

3.7 Liquid Phase Hydrogenation Apparatus

For the purposes of this section of the work, a 1.0l, stirred, autoclave was employed. This apparatus as shown in Figure 3.3.5, incorporated a hydrogen-on-demand system, which bubbled under the surface of the solvent. The temperature of the reactor could be altered by the use of a circulating water bath, which kept the system isothermal throughout the course of the reaction. The pressure of gas within the reactor could be measured directly from a gauge, and the incorporation of a bursting disc ensured the reactor pressure did not exceed 4 Bar. The reactor had a built-in sample point through which the hydrogen to the reactor could be by-passed and samples removed during the course of the reaction.

3.7.1 Palladium Catalysed Reactions

The procedure for these reactions involved purging the closed reactor with nitrogen for a period of between 0.5hrs and 1.0hr. At this stage 340ml of ethanol (HPLC Grade >99%) was added. A sample of catalyst, typically 25mg, was added to the reactor as a slurry in ethanol. The reactor was then heated to 50°C and the system purged with hydrogen (BOC >99%), and the stirrer set at 750rpm. Over a period of 2.0hrs the system was put through a series of pressure/depressure cycles by increasing the hydrogen pressure to 2Bar, then reducing to 1Bar, hence allowing diffusion of the gas through the solvent and substrate. At the end of this procedure the reactor was cooled to 30°C and the reactant(s) added in a volume of ethanol. For phenylacetylene and styrene hydrogenation reactions, approximately 1ml of reactant was employed. For the purposes of co-hydrogenation experiments, 1ml of both reactants was used. The final volume of solvent used was 400ml. The hydrogen pressure was set at 2Bar, and this was maintained throughout the

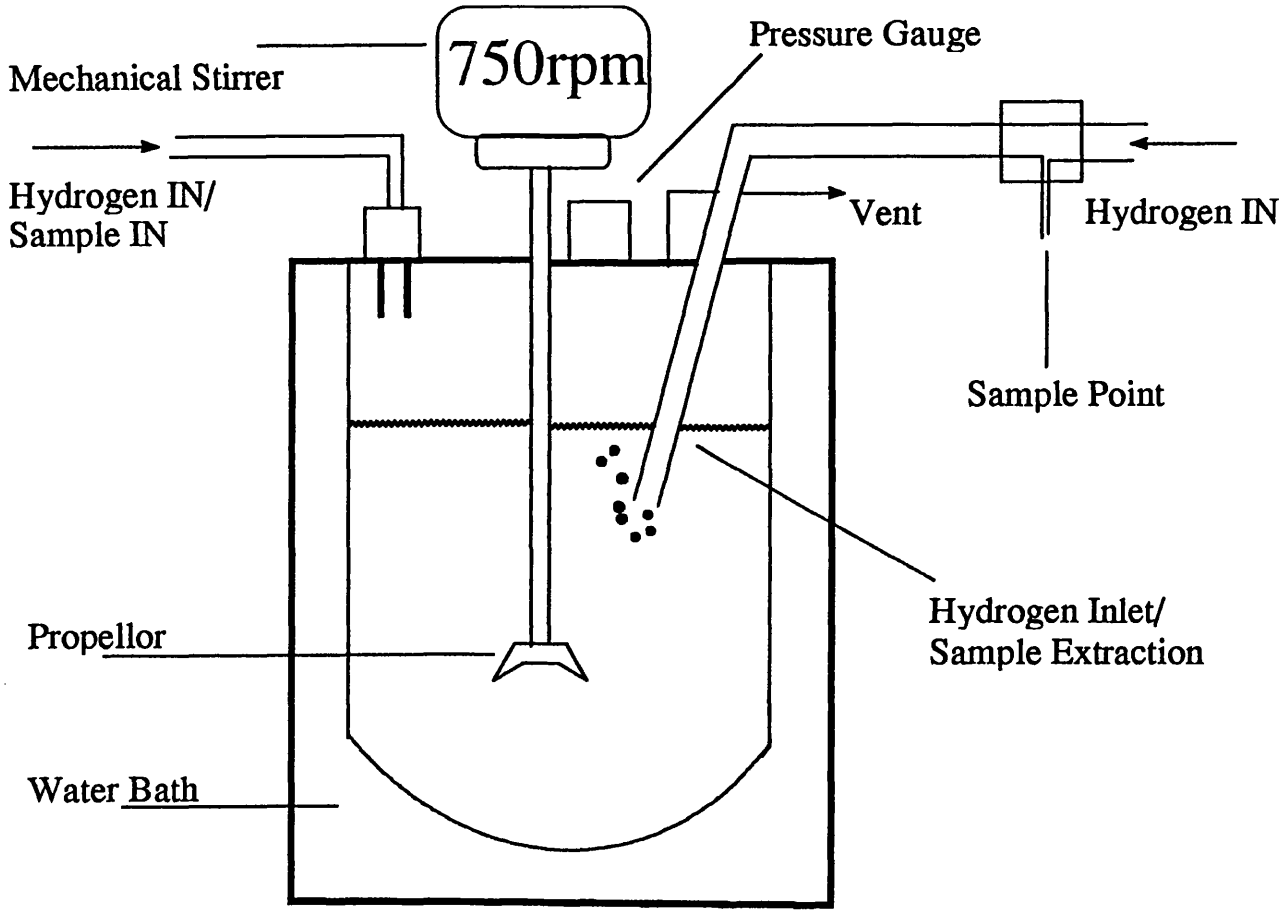

Figure 3.3.5: High Pressure Liquid Phase Hydrogenation System

course of the experiment. Samples for GC analysis were removed every 5mins for the first 45mins, and finally after one hour of reaction.

3.7.2 Platinum Catalysed Reactions

Due to the higher temperatures required for activation of the above catalysts, the reductions were performed under flowing conditions, as in pulse-flow reactions. The catalysts were then transferred into the reactor in a small volume of degassed solvent. At this stage, the experimental procedure was as in the palladium cases, above.

3.7.3 Liquid Phase Analysis System

Analysis of the liquid phase hydrogenation products was achieved using a Chrompack 9001 GC fitted with a flame ionisation detector (FID). Separation was achieved using a Carbowax 20M column as detailed in section 3.6.2.

3.8 Infra-Red Spectroscopy

This section details the procedure used for the characterisation of surface structures present in the hydrogenation of 2-butyne over silica-supported palladium, using an equimolar ratio of 2-butyne and hydrogen.

3.8.1 Diffuse Reflectance Infra Red Spectroscopy (DRIFTS)

DRIFTS spectra were obtained at $4cm^{-1}$ resolution using a Nicolet Magna 550 FTIR spectrometer. The DRIFTS environmental cell was installed onto an optical bench and a sample of catalyst loaded into an elevated holder.

The cell was connected to a low pressure (10^{-4} - 10^{-5} Torr) vacuum line, and was water cooled, to reduce the effects of heat transfer when operating the cell at elevated temperatures. The spectrometer was equipped with a purging facility, which allowed the optical bench to be operated under flowing nitrogen, to reduce the concentration of atmospheric moisture in the spectra taken.

The reducing gas mixture, 6% H_2/N_2, was then passed over the catalyst via the vacuum line. Standard activation procedures were followed (Section 3.4) before cooling the sample to ambient temperature in flowing helium.

The reactant gas mixture (1:1 :: C_4H_6 : H_2) was introduced to the catalyst via a known volume sample loop, with the pressure of gas (80 Torr) recorded by a Baratron capacitance manometer.

A background spectrum was acquired after the activation procedure. Spectra were then obtained immediately after adsorbate pulsing, and are presented as background subtracted spectra, referenced to the clean catalyst.

3.8.2 Transmission Infra Red Spectroscopy

The above experiments were performed using the same instrument as detailed in Section 3.8.1 above. The *in situ* infra red cell used in these experiments contained a catalyst wafer holder. Two KBr windows, sealed in stainless steel rings, were connected to both ends of the cell, with a heating element connected to an external thermocouple, allowing the catalyst to be activated *in situ*. This cell was connected to a low pressure vacuum line which allowed the system to be pumped or subjected to injected gases. Samples for examination (typically, 50mg catalyst; 150mg KBr) were pressed into wafer thin discs and mounted on the sample holder.

Activation of the catalyst samples was achieved by heating the cell to 200°C and charging the cell with a pressure of hydrogen (200 Torr). This was

pumped away after one hour and then repeated. The remaining hydrogen was again pumped away, and the temperature of the substrate increased to 220°C to remove any retained surface hydrogen. On completion of this stage, the catalyst temperature was reduced to 100°C.

At this stage, individual pulses of the reaction mixture (20, 70 and 100 Torr) were passed over the catalyst and left for approximately five minutes to equilibrate.

Spectra were recorded after each pulse and on pumping all the gases from the cell.

3.9 Continuous Flow Hydrogenations

The hydrogenation reactions of phenylacetylene and styrene were also performed in a gas phase study. Due to the relatively low vapour pressures of both hydrocarbons, it was necessary to carry out the reactions in a continuous flow mode.

The experimental set up for these reactions is shown in Figure 3.3.6. The hydrocarbon was contained in a Dreschel type vessel, through which hydrogen gas was bubbled (25ml min^{-1}), which transported the hydrocarbon vapour over the catalyst bed. For the purposes of controlling the reaction chemistry, it was necessary to lower the vapour pressure still further. This was achieved by surrounding the Dreschel bottle in ice.

The reaction lifetimes were found to be critically dependant on the concentration of catalyst used. For this reason, catalyst weights of approximately 5-10mg were used in this study. As both phenylacetylene and styrene have relatively high melting points, all reactions were performed at 425K to prevent condensation of the hydrocarbon onto the catalyst.

The products formed were analysed via a gas sampling valve which was connected to a gas chromatograph.

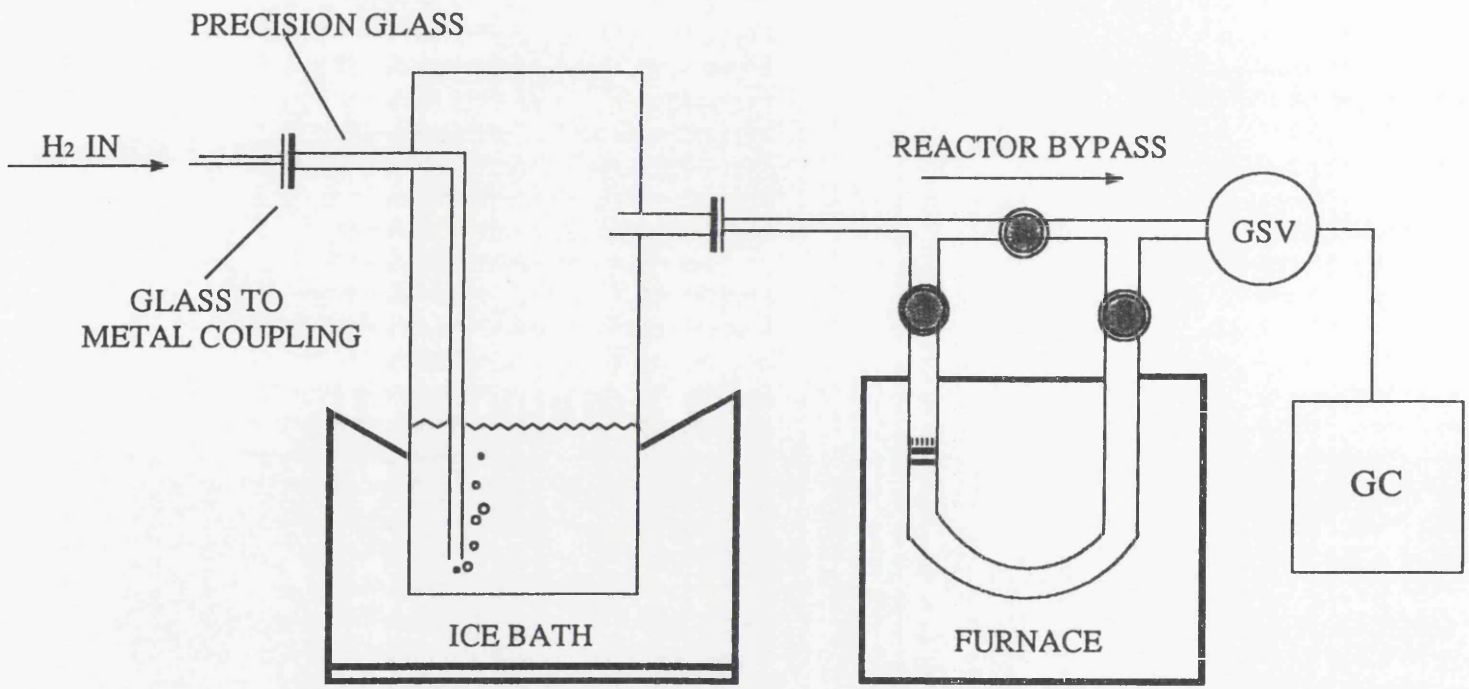

FIGURE 3.3.6 : CONTINUOUS FLOW HYDROGENATION APPARATUS

Chapter Four

RESULTS

Section One

Catalyst Characterisation

4.1.1 Temperature Programmed Reduction (TPR)

Only the TPR profiles of the supported-platinum catalysts were obtained as the chemisorption of hydrogen on the palladium samples was observed to occur at ambient temperature. For both Pt/silica and Pt/alumina, where reduction occurred at elevated temperatures, Table 4.1.1 shows the temperature at which hydrogen chemisorption initially occurred (T_{min}), and the optimum temperature determined for the complete conversion of the metal precursor to the active metallic state; T_{max}.

Table 4.11: *TPR Results for Platinum Catalysts*

Catalyst	T_{min} (°C)	Optimum Reduction Temp. : T_{max} (°C)
Pt/silica	195	245
Pt/alumina	188	231

Both catalysts exhibited one near symmetrical peak which could be assigned to the reduction of Pt^{4+} to metallic Pt^0.

4.1.2 CO/O_2 Chemisorption

To quantify the results of CO and O_2 adsorption experiments, the mode and hence, stoichiometry of such adsorption reactions was required. It is well documented[72] that the chemisorption of CO on platinum occurs by an associative mechanism, with both a linear and bridging model possible. In practice however, the linear model is known to predominate. This result has

best been quantified by the application of infra-red spectroscopy as a means of measuring the metallic area of supported metal catalysts. Over various platinum catalysts Gruber[73] has established that the existence of the bridging mode is highly dependent on metal dispersion.

Similarly, for supported palladium catalysts, the adsorption of CO is known to occur both linearly and as a bridged species. For dispersion calculations a ratio of 2Pd : 1CO was applied.

Both metals dissociatively adsorb O_2 such that two metal atoms are required for the surface chemisorption of one oxygen atom. Therefore, a ratio of 2Pt : 1O was taken for the purposes of dispersion calculations. Table 4.1.2 shows the calculated fraction of exposed metal atoms for each of the catalysts.

4.1.3 UV-Visible Diffuse Reflectance Spectroscopy (UVDRS)

4.1.3(a) Platinum Catalysts

The absorption maxima and band assignments for both Pt/silica and Pt/alumina are shown in Table 4.1.3(a).

Table 4.1.3(a) : *UV Band Assignments for Platinum Catalysts*

Catalyst	Transitions (nm)		LMCT (nm)
	$^1A_{1g} \rightarrow {}^3T_{2g}$	$^1A_{1g} \rightarrow {}^1T_{1g}$	
Pt/silica	456	375	260, 205
Pt/alumina	450	350	220

Table 4.1.2 : *CO/O_2 Chemisorption Results*

Catalyst	Total (CO) Adsorbed at Sat^n x10^{18}	Total (O_2) Adsorbed at Sat^n x10^{18}	No. Surface Metal Atoms (CO) x10^{18}	No. Surface Metal Atoms (O_2) x10^{18}	Total Metal Atoms Present x10^{19}	Dispersion (CO) [%]	Dispersion (O_2) [%]
Pd/silica	0.292	0.369	5.58	7.04	5.66	9.86	12.44
Pd/alumina	0.564	0.677	10.64	12.78	5.66	18.80	22.60
Pt/silica	0.195	1.099	16.29	20.59	3.08	52.77	66.80
Pt/alumina	0.175	0.221	3.22	4.08	3.08	10.43	13.22

The UV data obtained for both catalysts compares well with the literature presently available regarding Pt^{4+} species in an octahedral environment. The spectrum of the Pt/silica precursor state is very similar to that of aqueous hexachloroplatinic acid. In the case of the alumina-supported catalyst, the deviation of the ligand to metal charge transfer (LMCT) band to 220nm is in direct correlation with the UV spectrum of PtO_2/alumina, in which an absorption band at 209nm was assigned to an oxygen to platinum charge transfer process. The band at 220nm has been assigned by Jackson *et al*[74] to the formation of an oxychloro species, $[PtCl_5OH]^{2-}$ from the exchange between $[PtCl_6]^{2-}$ and water in aqueous solution.

4.1.3(b) Palladium Catalysts

The UV results for both palladium catalysts are given in Table 4.1.3(b). In the preparation of the supported-palladium catalysts, the dissolution of the precursor salt, $PdCl_2$, was aided by the addition of concentrated HCl. This results in the formation of the tetrachloropalladate anion, $[PdCl_4]^{2-}$ as H_2PdCl_4. This molecule is unlike H_2PtCl_6 in that it adopts a square planar geometry in solution, with the central Pd^{2+} ion coordinated to four Cl^- ions.

Table 4.1.3(b) : *UV Band Assigments for Palladium Catalysts*

Catalyst	Transition (nm)		LMCT (nm)
	$^1A_{1g} \rightarrow {}^1A_{2g}$	$^1A_{1g} \rightarrow {}^1B_{1g}$	
Pd/silica	490	360	278
Pd/alumina	500	346	283, 233

The UV band assignments for the supported palladium catalysts were therefore achieved by comparison with the absorption spectrum of the dipotassium salt of $[PdCl_4]^{2-}$, K_2PdCl_4[75].

4.1.4 Transmission Electron Microscopy (TEM)

The TEM results are detailed in Table 4.1.4 below, which shows the average particle sizes determined for each of the catalysts. These values were obtained by scanning over several different areas of the catalyst and examining a large number of particles. However, in the case of the highly dispersed Pt/silica catalyst, poor resolution coupled with sample decomposition due to prolonged time in the microscope resulted in beam damage, thus preventing determination of the metal crystallite sizes.

In the case of the Pd/silica catalyst, the surface appeared to contain several areas where metallic palladium was encapsulated by the support material. This may well be a consequence of the preparation procedure, and would explain the relatively low metal dispersion calculated from CO and O_2 chemisorption experiments.

Table 4.1.4 : *TEM Results and Dispersion Calculation Particle Sizes*

Catalyst	TEM Values (nm)	Chemisorption Values (nm)
Pd/silica	9.04	8.68
Pd/alumina	4.29	4.83
Pt/alumina	4.66	7.88

4.1.5 Thermogravimetric Analysis (TGA)

The main feature of the TGA data obtained for all catalysts was a period of gradual weight loss which was most probably the result of water loss in the gas flow. However, in the Pd/alumina catalyst, a series of weight fluctuations were observed. A weight loss of w/w 1.50% which corresponded to the total chlorine content in the precursor state was observed in the temperature region, 25-50°C. This is in good agreement with the TPR data obtained which showed hydrogen chemisorption occuring at ambient temperature, suggesting the removal of chlorine as HCl. Further regions of weight variation in the TGA plot were assigned to the absorption of hydrogen into the sample bulk.

4.1.6 Atomic Absorption Spectroscopy (AAS)

Table 4.1.6 below details the actual metal loadings obtained for all four catalysts.

Table 4.1.6 : *Actual Metal Loadings from AAS*

Catalyst	Actual Metal Content (%)
Pd/silica	0.97
Pd/alumina	1.00
Pt/silica	1.14
Pt/alumina	1.30

The metal loadings of both platinum catalysts could be the result of support loss in the evaporation stage of catalyst preparation, thus explaining the higher than expected metal content.

4.1.7 Surface Area Measurements (BET)

All catalysts exhibited similar adsorption isotherm curves in the surface area determination experiments. The isotherm plot is shown in Figure 4.7.

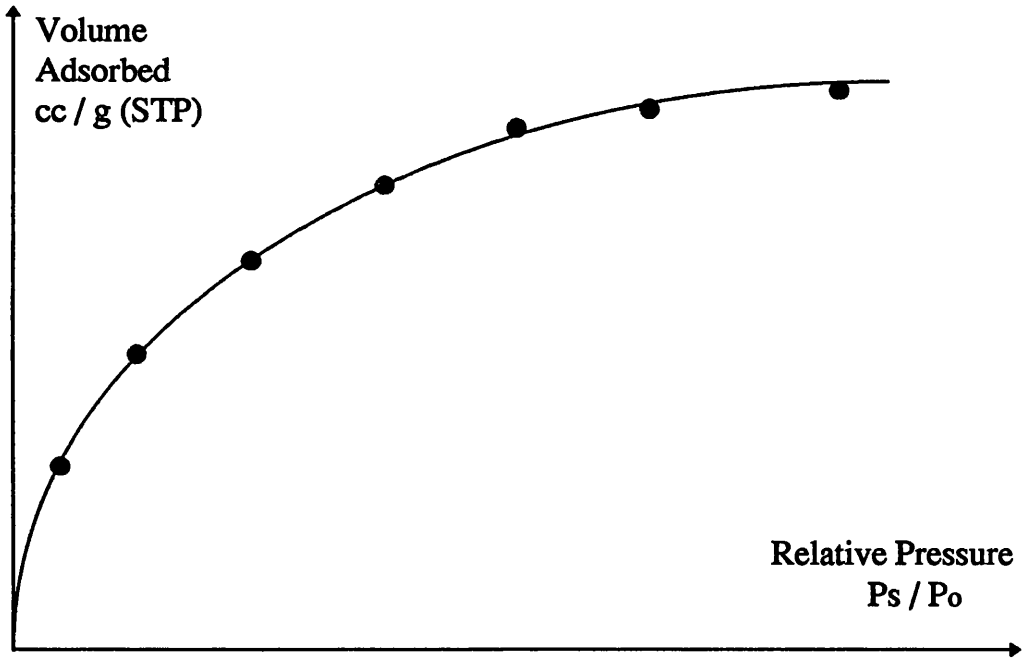

Figure 4.7 : *Adsorption Isotherm for Nitrogen Physisorption on Catalysts*

Table 4.1.7 overleaf shows the results obtained from the BET measurements.

Table 4.1.7 : *Total Surface Area Data*

Catalyst	BET Surface Area (m^2/g)
Pd/silica	213
Pd/alumina	107
Pt/silica	187
Pt/alumina	95

4.1.8 Sample Loop Volume Results

Table 4.1.8 shows the results obtained for the sample loop volume used in the 2-butyne hydrogenation reactions.

Table 4.1.8 : *Sample Loop Volume Results*

Bulb Volume (cm^3)	Sample Loop Volume (cm^3)
Bulb A (170.22)	6.99
Bulb B (195.93)	6.91
Bulb C (123.43)	7.15

Therefore, for calculation purposes, the sample volume was taken as the average of the above values; $V = 7.00cm^3$.

4.2 Hydrogenation Results

This section details the results obtained in the hydrogenation reactions of propyne and 2-butyne using the pulse-flow microcatalytic reactor system. The determination of product distributions, reaction selectivities and conversions were obtained from quantitative GC calibration for the products observed. Calibration for the reactants and products was achieved by passing known pressures of gas over the GC. This procedure allowed a relationship to be drawn between the number of molecules of gas and the area response of the chromatograph detector. Carbon balance data was achieved by relating the amount of carbon injected over the catalyst in each pulse, with the amount of eluted products and reactant. The difference between these two values (Δcarbon), yielded information as to whether carbon was retained by the catalyst (Δcarbon value positive) or carbon was removed from the catalyst (Δcarbon value negative).

Standard procedure for the hydrogenation reactions involved passing a mixture of hydrogen and the acetylene over a freshly reduced catalyst sample, typically of weight, 0.20g. For the purposes of these reactions, the concentration of hydrogen in the reaction mixtures was varied. Reactions were performed using either a three fold excess of hydrogen, or an equimolar acetylene/hydrogen mixture.

The following section details the hydrogenation reactions of propyne performed at ambient temperature. The equation applied for the determination of catalyst selectivity toward olefin formation is shown in Equation 4. Conversion calculations were determined as the difference in the amount of acetylene, before and after pulsing. This is shown in Equation 5.

$$\text{Selectivity} = \frac{\text{Olefin}}{\text{Olefin + Alkane}} \times 100\% \qquad \textbf{Equation 4}$$

The conversion values were given by :

$$\text{Conversion} = \frac{[\text{Acetylene In - Acetylene Out}]}{\text{Acetylene In}} \times 100\% \qquad \textbf{Equation 5}$$

4.3 Carbon Mass Balance

The amount of carbon passing over the catalyst during each individual pulse could be determined from the pressure of gas in the sample loop. From this the number of moles of acetylene could be calculated. Multiplying this value by Avogadrós number (N_a = 6.022 x 10^{23}) yielded the number of reactant molecules in each pulse. With the number of carbon atoms given as :

[No. molecules of acetylene x No. carbon atoms].

Propyne, containing three carbon atoms produced

[3 x no. molecules of propyne] atoms per pulse

2-butyne, containing four carbon atoms produced

[4 x no. molecules of 2-butyne] atoms per pulse

From the above calculations, the number of carbon atoms lost or retained by the catalyst could be measured.

Section Two

PROPYNE HYDROGENATION

4.4.1 The Hydrogenation of Propyne over Silica-Supported Palladium

The hydrogenation of propyne over silica-supported palladium using an equimolar reactant mixture exhibited complete selectivity toward propene production, as shown in Table 5.1.1. The amount of propene produced over a series of ten pulses was constant, with the corresponding yield of propyne found to increase with increasing number of pulses, until a steady state was reached. The amount of carbon retained by the catalyst was observed to decrease with increasing number of pulses.

Changing the composition of hydrogen in the reaction mixture (1:3 :: C_3H_4 : H_2), produced both propane and propene. However, it was not until the second pulse that the olefin was produced (Table 5.1.3). The yield of propene was found to increase to a seemingly steady-state (quasi-steady state), before increasing still further until a limiting value was reached. Similar to the equimolar reaction, the conversion of propyne, although initially high, decreased with increasing number of pulses. In these reactions the activity of the catalyst decreased at a much slower rate, with the final conversion of propyne greater than that observed in the equimolar reactions. The deposition of carbon was found to decrease with increasing number of pulses, until the twentieth pulse, from which point, carbon was removed from the surface (Figure 5.1.5).

Table 5.1.1 : Hydrogenation of Propyne (Equimolar Ratio) over Pd/silica at 293K.

Pulse Number	Sample Pressure (mB)	Moles of Alkyne In / 10^5	Moles of Alkene Out / 10^5	Moles of Alkane Out / 10^5	Moles of Alkyne Out / 10^5	Selectivity (%)	Conversion (%)
1	100	11.95	1.94	0.00	3.64	100.0	34.77
2	100	11.95	1.98	0.00	3.87	100.0	33.81
3	100	11.95	1.84	0.00	5.22	100.0	28.15
4	100	11.95	1.78	0.00	6.45	100.0	23.03
5	100	11.95	1.92	0.00	7.10	100.0	20.29
6	100	11.95	1.98	0.00	8.06	100.0	16.27
7	100	11.95	1.95	0.00	8.11	100.0	16.07
8	100	11.95	1.95	0.00	8.38	100.0	14.85
9	100	11.95	1.96	0.00	7.77	100.0	17.49
10	100	11.95	1.98	0.00	7.49	100.0	18.66

Figure 5.1.1 : Variation of Product Distribution with Pulse Number for the Hydrogenation of Propyne (Equimolar Ratio) over Pd/silica at 293K

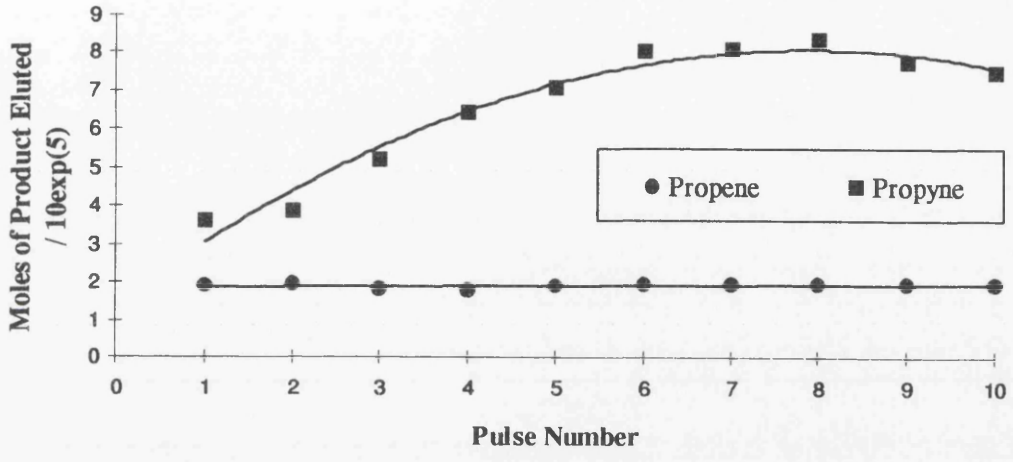

Figure 5.1.2 : Carbon Mass Balance for the Hydrogenation of Propyne (Equimolar Ratio) over Pd/silica at 293K

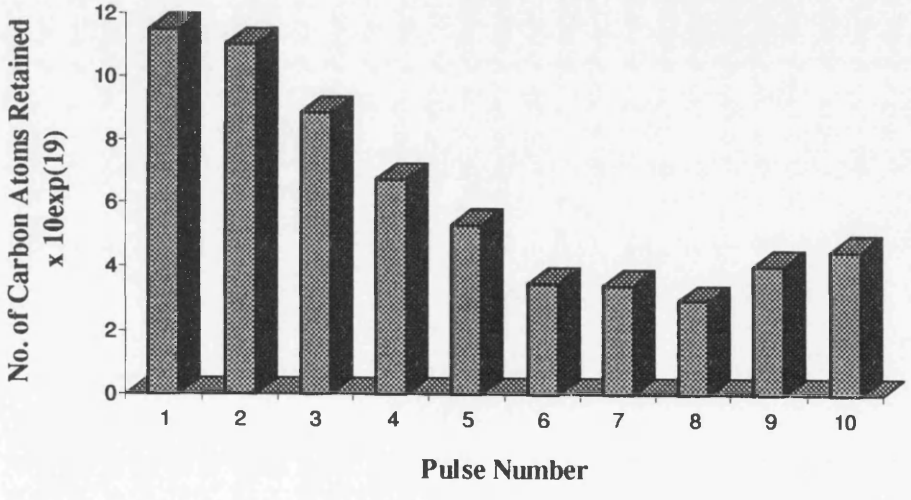

Table 5.1.2 : Carbon Deposition Data for the Hydrogenation of Propyne (Equimolar Ratio) over Pd/silica at 293K

Pulse Number	No. of Carbon Atoms Deposited (x 10^{19})	
	Per Pulse	Cumulative
1	11.50	11.50
2	11.00	22.50
3	8.83	31.33
4	6.72	38.05
5	5.29	43.34
6	3.45	46.79
7	3.41	50.20
8	2.93	53.13
9	4.01	57.14
10	4.48	61.62

Table 5.1.3 : Hydrogenation of Propyne (Excess Hydrogen) over Pd/silica at 293K

Pulse Number	Sample Pressure (mB)	Moles of Alkyne In / 10^5	Moles of Alkene Out / 10^5	Moles of Alkane Out / 10^5	Moles of Alkyne Out / 10^5	Selectivity (%)	Conversion (%)
1	120	7.17	0.00	1.87	0.80	0.00	88.84
2	120	7.17	1.43	1.60	0.93	47.10	87.00
3	120	7.17	1.50	1.66	1.00	47.40	86.05
4	120	7.17	1.62	1.87	1.04	48.10	85.49
5	120	7.17	1.69	1.79	1.08	48.60	84.94
6	120	7.17	1.75	1.83	1.12	48.80	84.38
7	120	7.17	1.81	2.00	1.15	47.45	83.96
8	120	7.17	1.87	2.05	1.22	47.70	82.98
9	120	7.17	1.90	2.17	1.26	47.05	82.43
10	120	7.17	1.93	2.40	1.29	44.50	82.00
11	120	7.17	1.88	1.69	1.31	52.60	81.73
12	120	7.17	1.91	1.73	1.34	52.45	81.31
13	120	7.17	1.94	1.73	1.39	52.90	80.61
14	120	7.17	1.97	1.76	1.41	52.77	80.33
15	120	7.17	2.01	1.81	1.46	52.47	79.64
16	120	7.17	2.13	2.27	1.54	52.33	78.52
17	120	7.17	2.33	2.07	1.55	52.91	78.38
18	120	7.17	2.53	2.23	1.63	53.17	77.27
19	120	7.17	2.81	2.52	1.77	52.66	75.31
20	120	7.17	3.20	2.74	1.85	53.85	74.19
21	120	7.17	3.08	2.61	1.87	54.10	73.92
22	120	7.17	3.10	2.60	1.90	54.35	73.50
23	120	7.17	3.12	2.66	2.00	53.88	72.10
24	120	7.17	3.05	2.61	2.10	53.85	70.71
25	120	7.17	3.06	2.76	2.22	54.90	69.04
26	120	7.17	3.01	2.51	2.22	54.50	69.04
27	120	7.17	3.03	2.46	2.23	55.10	68.89
28	120	7.17	3.05	2.42	2.24	55.77	68.75
29	120	7.17	3.06	2.45	2.31	55.49	67.78
30	120	7.17	3.07	2.39	2.40	56.20	66.53

Figure 5.1.3 : Variation of Product Distribution with Pulse Number for the Hydrogenation of Propyne (Excess Hydrogen) over Pd/silica at 293K

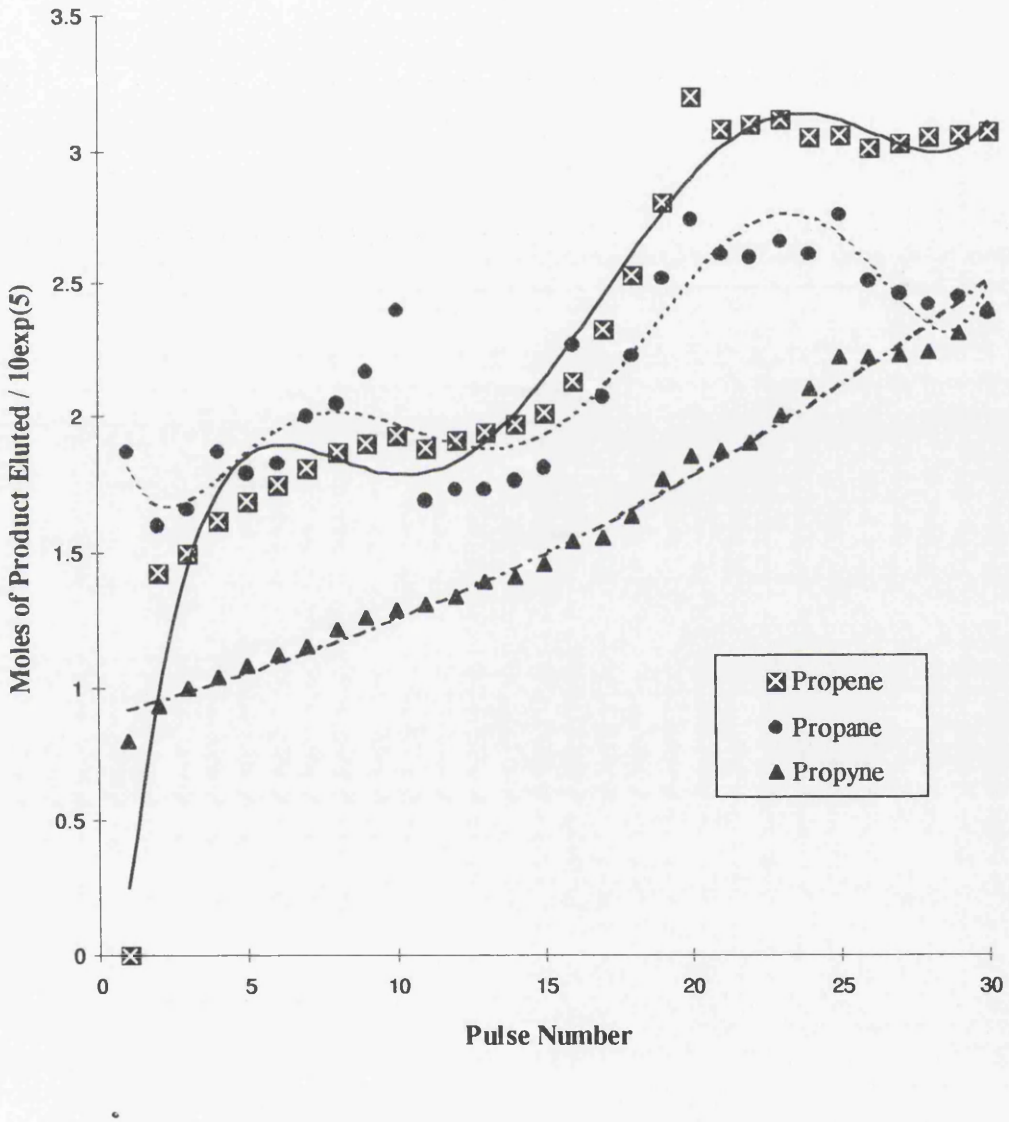

Figure 5.1.4 : Variation of Conversion with Pulse Number for the Hydrogenation of Propyne (Excess Hydrogen) over Pd/silica at 293K

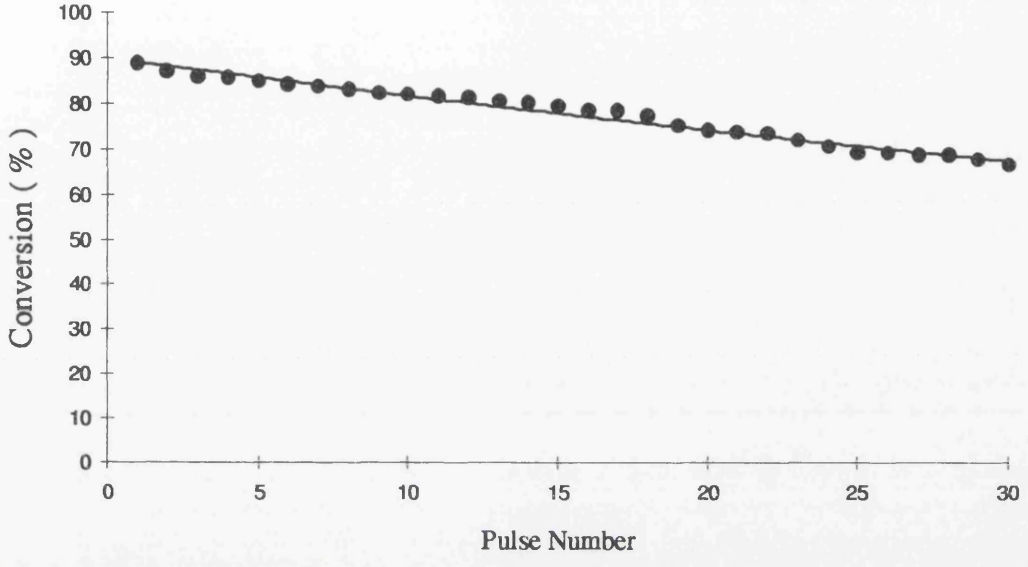

Figure 5.1.5 : Carbon Mass Balance for the Hydrogenation of Propyne (Excess Hydrogen) over Pd/silica at 293K

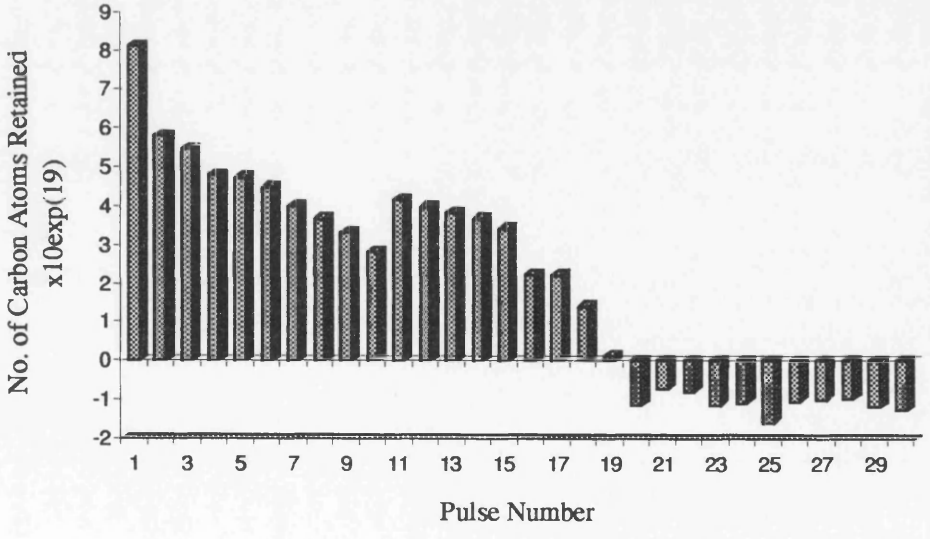

Table 5.1.4 : Carbon Deposition Data for the Hydrogenation of Propyne (Excess Hydrogen) over Pd/silica at 293K

Pulse Number	No. of Carbon Atoms Deposited (x 10^{19})	
	Per Pulse	Cumulative
1	8.13	8.13
2	5.79	13.92
3	5.44	19.36
4	4.77	24.13
5	4.72	28.85
6	4.46	33.31
7	3.99	37.30
8	3.67	40.97
9	3.32	44.29
10	2.80	47.09
11	4.14	51.05
12	3.96	55.01
13	3.82	58.83
14	3.67	62.50
15	3.41	65.91
16	2.22	68.13
17	2.20	70.33
18	1.41	71.74
19	0.13	71.87
20	-1.12	70.75
21	-0.71	70.04
22	-0.77	69.27
23	-1.10	68.17
24	-1.06	67.11
25	-1.57	65.54
26	-1.03	64.51
27	-0.99	63.52
28	-0.97	62.55
29	-1.17	61.38
30	-1.25	60.13

4.4.2 The Hydrogenation of Propyne over Alumina-Supported Palladium

Over alumina-supported palladium, the hydrogenation of propyne displayed lower selectivity toward the olefin than Pd/silica, when an equimolar ratio was employed (Table 5.1.5). The selectivity in this case was found to remain at approximately 48% over ten pulses, with the yield of both propene and propane constant throughout. Similar to the Pd/silica catalyst, the initially low catalyst activity for propyne hydrogenation was found to decrease with increased number of pulses. The amount of carbon retained by the catalyst decreased over ten pulses, until practically no more carbon was deposited at the surface (Figure 5.1.7).

Increasing the concentration of hydrogen increased the catalyst's activity for hydrogenation. Over the first fifteen pulses, propyne was completely converted, with both propane and propene produced. However, the formation of the olefin was not observed until the fifth pulse (Figure 5.1.8), with propane produced from the onset. The yield of propene remained constant from pulse five on, with the amount of propane formed found to decrease to a limiting value. The product distribution curves for both propene and propane in these reactions appear to be mirror images of each other, with the yield of propane decreasing at the expense of an increase in the amount of propene produced.

From pulse one to fifteen, carbon from the injected pulses was retained by the catalyst. On the production of propene, the amount of carbon lost from the catalyst was observed to increase.

Table 5.1.5 : Hydrogenation of Propyne (Equimolar Ratio) over Pd/alumina at 293K.

Pulse Number	Sample Pressure (mB)	Moles of Alkyne In / 10^5	Moles of Alkene Out / 10^5	Moles of Alkane Out / 10^5	Moles of Alkyne Out / 10^5	Selectivity (%)	Conversion (%)
1	100	11.95	1.74	1.79	5.20	48.30	28.25
2	100	11.95	1.72	1.80	5.61	48.90	26.55
3	100	11.95	1.73	1.86	5.70	48.15	26.15
4	100	11.95	1.71	1.87	5.75	47.10	25.95
5	100	11.95	1.69	1.83	5.94	48.03	25.14
6	100	11.95	1.67	1.84	6.21	47.74	24.20
7	100	11.95	1.69	1.86	6.83	47.56	21.42
8	100	11.95	1.66	1.83	7.59	47.65	18.22
9	100	11.95	1.65	1.79	8.05	47.91	16.31
10	100	11.95	1.63	1.80	8.39	47.49	14.89

Figure 5.1.6 : Variation of Product Distribution with Pulse Number for the Hydrogenation of Propyne (Equimolar Ratio) over Pd/alumina at 293K

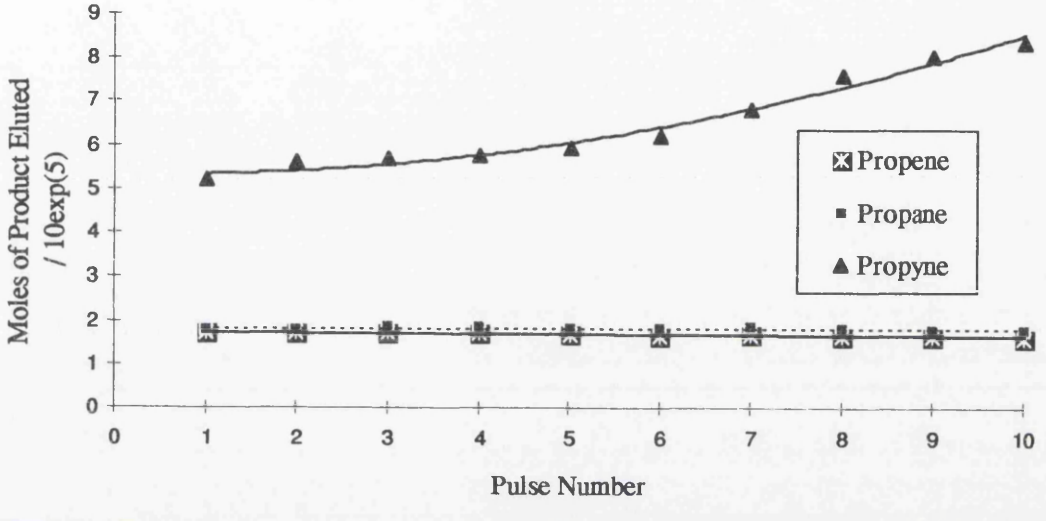

Figure 5.1.7 : Carbon Mass Balance for the Hydrogenation of Propyne (Equimolar Ratio) over Pd/alumina at 293K

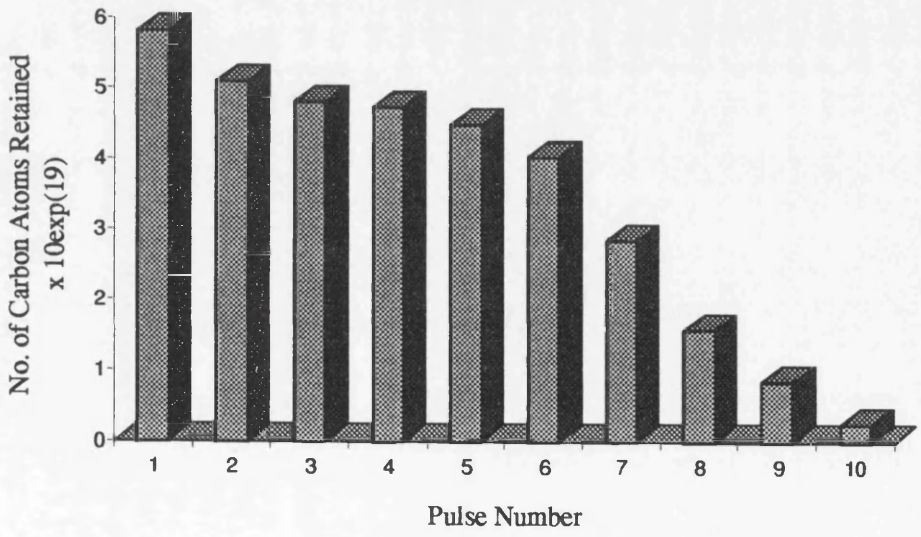

Table 5.1.6 : Carbon Deposition Data for the Hydrogenation of Propyne (Equimolar Ratio) over Pd/alumina at 293K

Pulse Number	No. of Carbon Atoms Deposited (x 10^{19})	
	Per Pulse	Cumulative
1	5.81	5.81
2	5.09	10.90
3	4.80	15.70
4	4.73	20.43
5	4.49	24.92
6	4.03	28.95
7	2.83	31.78
8	1.57	33.35
9	0.83	34.18
10	0.24	34.42

Table 5.1.7 : Hydrogenation of Propyne (Excess Hydrogen) over Pd/alumina at 293K

Pulse Number	Sample Pressure (mB)	Moles of Alkyne In / 10^5	Moles of Alkene Out / 10^5	Moles of Alkane Out / 10^5	Moles of Alkyne Out / 10^5	Selectivity (%)	Conversion (%)
1	100	5.98	0.00	3.62	0.00	0.00	100.0
2	100	5.98	0.00	3.58	0.00	0.00	100.0
3	100	5.98	0.00	3.66	0.00	0.00	100.0
4	100	5.98	0.00	3.50	0.00	0.00	100.0
5	100	5.98	1.43	3.60	0.00	28.27	100.0
6	100	5.98	1.49	3.12	0.00	32.33	100.0
7	100	5.98	1.48	2.27	0.00	39.41	100.0
8	100	5.98	1.54	1.82	0.00	45.72	100.0
9	100	5.98	1.49	1.76	0.00	45.82	100.0
10	100	5.98	1.46	1.78	0.00	46.10	100.0
11	100	5.98	1.47	1.66	0.00	46.91	100.0
12	100	5.98	1.43	1.59	0.00	47.20	100.0
13	100	5.98	1.50	1.73	0.00	46.39	100.0
14	100	5.98	1.51	1.77	0.00	46.09	100.0
15	100	5.98	1.57	1.78	0.00	46.72	100.0
16	100	5.98	1.59	1.86	3.25	45.99	45.60
17	100	5.98	1.54	1.75	3.32	46.71	44.48
18	100	5.98	1.58	1.79	3.51	46.90	41.30
19	100	5.98	1.60	1.84	3.65	46.53	38.96
20	100	5.98	1.57	1.82	3.68	46.20	38.44
21	100	5.98	1.57	1.82	3.73	46.30	37.60
22	100	5.98	1.57	1.80	3.82	46.55	36.10
23	100	5.98	1.58	1.84	3.85	46.22	35.59
24	100	5.98	1.58	1.79	3.99	46.77	33.20
25	100	5.98	1.58	1.83	4.21	46.42	29.57
26	100	5.98	1.59	1.80	4.16	46.90	30.43
27	100	5.98	1.58	1.79	4.13	46.87	30.87
28	100	5.98	1.57	1.80	4.23	46.53	29.31
29	100	5.98	1.57	1.79	4.19	46.59	29.96
30	100	5.98	1.58	1.79	3.61	47.00	39.48

Figure 5.1.8 : Variation of Product Distribution with Pulse Number for the Hydrogenation of Propyne (Excess Hydrogen) over Pd/alumina at 293K

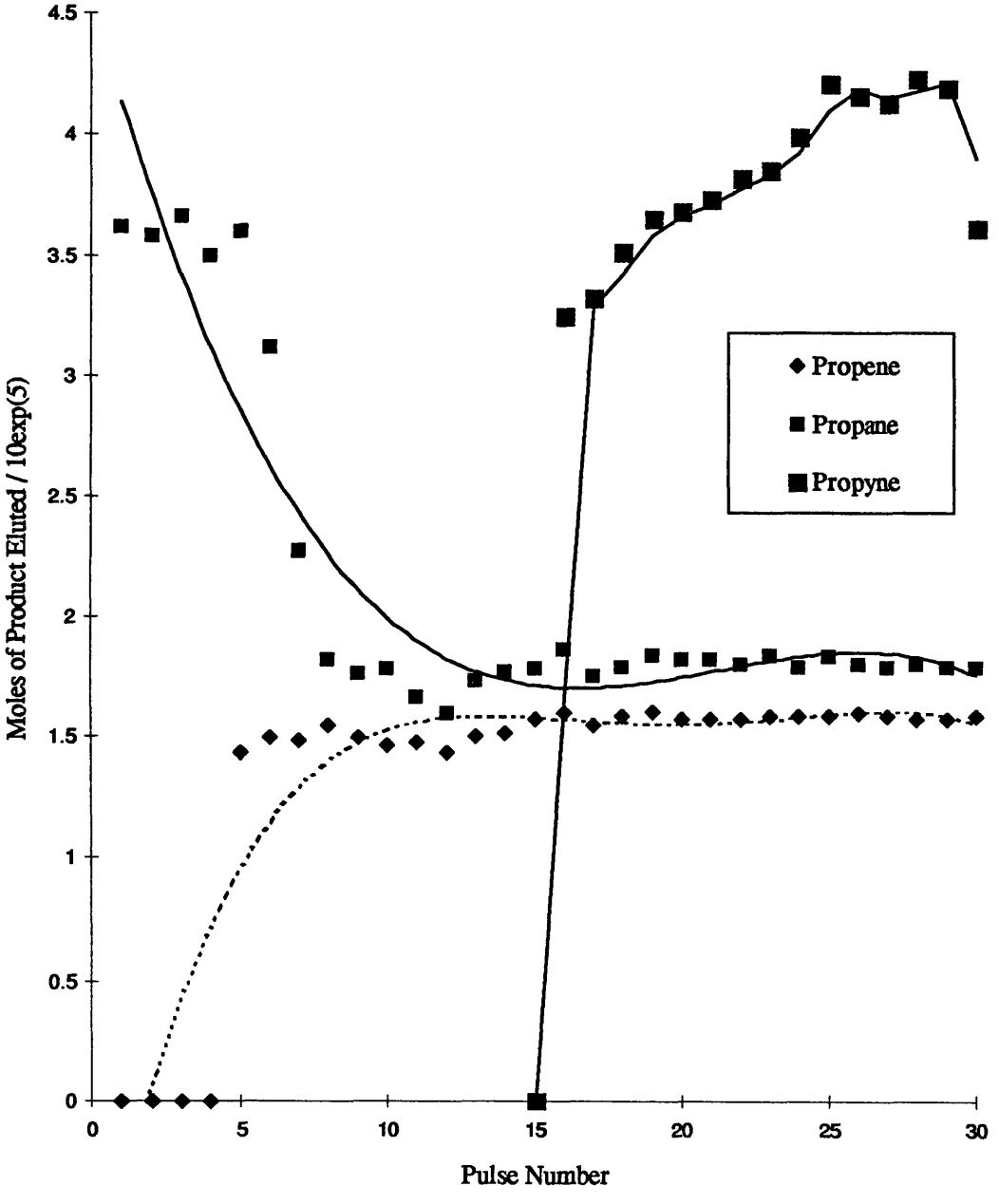

Figure 5.1.9 : Variation of Conversion with Pulse Number for the Hydrogenation of Propyne (Excess Hydrogen) over Pd/alumina at 293K

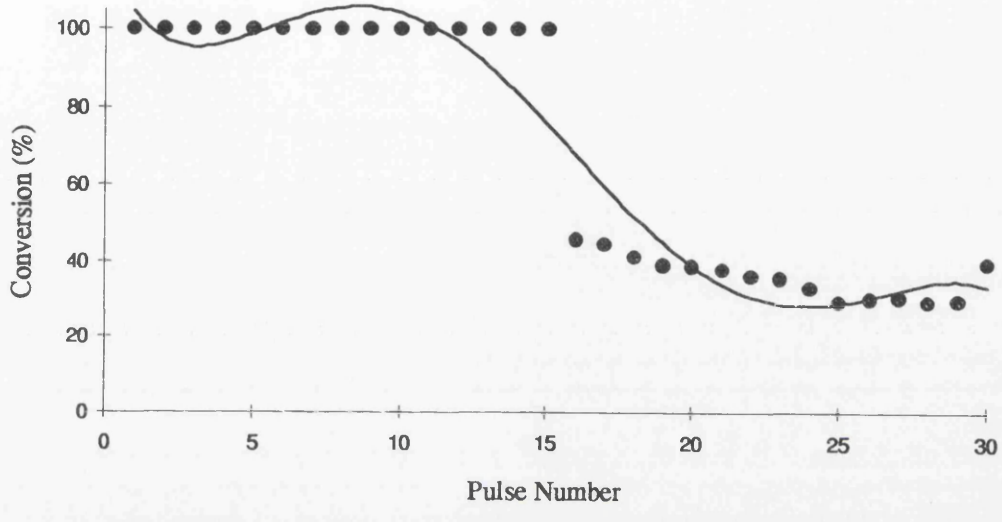

Figure 5.2.0 : Carbon Mass Balance for the Hydrogenation of Propyne (Excess Hydrogen) over Pd/alumina at 293K

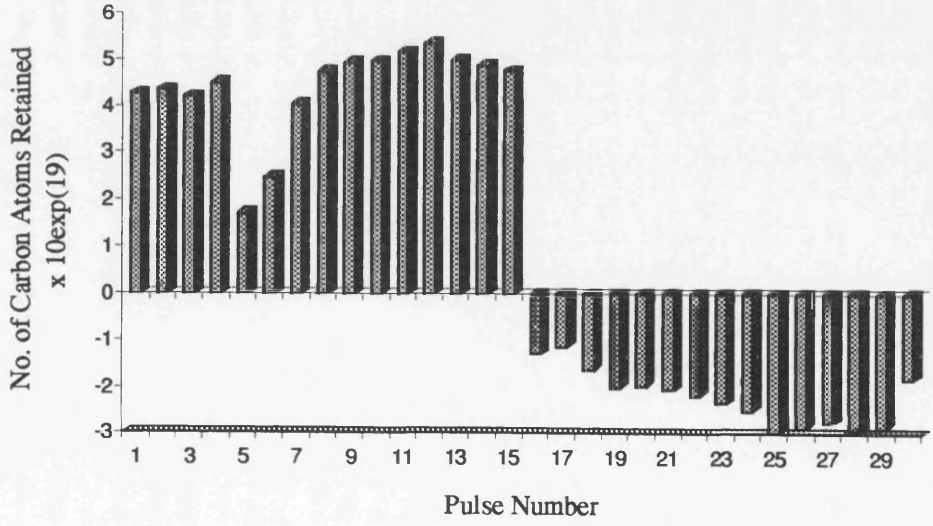

Table 5.1.8 : Carbon Deposition Data for the Hydrogenation of Propyne (Excess Hydrogen) over Pd/alumina at 293K

Pulse Number	No. of Carbon Atoms Deposited (x 10^{19})	
	Per Pulse	Cumulative
1	4.26	4.26
2	4.33	8.59
3	4.19	12.78
4	4.48	17.26
5	1.71	18.97
6	2.47	21.44
7	4.03	25.47
8	4.73	30.20
9	4.93	35.13
10	4.95	40.08
11	5.15	45.23
12	5.35	50.19
13	4.96	55.15
14	4.87	60.02
15	4.75	64.77
16	-1.30	63.47
17	-1.14	61.85
18	-1.62	60.23
19	-2.00	58.23
20	-1.97	56.26
21	-2.06	54.20
22	-2.18	52.02
23	-2.33	49.69
24	-2.49	47.20
25	-2.96	44.24
26	-2.83	41.41
27	-2.75	38.66
28	-2.93	35.73
29	-2.84	32.89
30	-1.81	31.08

4.4.3 The Hydrogenation of Propyne over Silica-Supported Platinum

The hydrogenation of propyne (1:1 :: C_3H_4:H_2) over silica-supported platinum, produced both propane and propene with very low conversions of propyne. In the first pulse (Table 5.1.9), the only hydrogenation product was propane, with approximately 75% of the initial propyne content of the pulse unreacted. From pulse two onward, the yield of propane decreased, with the amount of propene formed remaining constant over ten pulses. The activity of the catalyst dropped sharply from pulse one to pulse two (25% to 6%), and continued to decrease until there was effectiviely no hydrogenation occurring at the surface.

The amount of carbon retained by the catalyst was large in the first pulse. The retention of carbon at the surface was observed to decrease sharply in pulse two, and decreased further over the remaining eight pulses (Figure 5.2.2).

The hydrogenation of propyne (1:3 :: C_3H_4:H_2) over Pt/silica displayed relatively high conversions of propyne which decreased with an increase in the number of pulses, until a steady state was achieved (Table 5.2.1). However, the marked difference in this system compared to the others, was in the product distributions observed in the reaction. Over the first sixteen pulses the only observed products were unreacted propyne and propane. From pulse seventeen to thirty, propene was also produced (Figure 5.2.3). This propene production was accompanied by a decrease in the yield of propane, with the amount of propyne eluted increasing to a limiting value. The initially high amounts of retained carbon decreased in pulse seventeen onward, with effectively no carbon being retained at the catalyst surface.

Table 5.1.9 : Hydrogenation of Propyne (Equimolar Ratio) over Pt/silica at 293K.

Pulse Number	Sample Pressure (mB)	Moles of Alkyne In / 10^5	Moles of Alkene Out / 10^5	Moles of Alkane Out / 10^5	Moles of Alkyne Out / 10^5	Selectivity (%)	Conversion (%)
1	100	11.95	0.00	0.49	9.08	0.00	24.00
2	100	11.95	0.22	0.32	11.23	44.60	5.95
3	100	11.95	0.23	0.28	11.30	44.60	5.43
4	100	11.95	0.22	0.26	11.38	46.90	4.69
5	100	11.95	0.20	0.26	11.45	44.30	4.20
6	100	11.95	0.19	0.22	11.54	47.20	3.40
7	100	11.95	0.20	0.22	11.56	48.58	3.21
8	100	11.95	0.20	0.23	11.67	47.50	2.34
9	100	11.95	0.20	0.23	11.67	47.30	2.27
10	100	11.95	0.20	0.22	11.68	47.99	2.20

Figure 5.2.1 : Variation of Product Distribution with Pulse Number for the Hydrogenation of Propyne (Equimolar Ratio) over Pt/silica at 293K

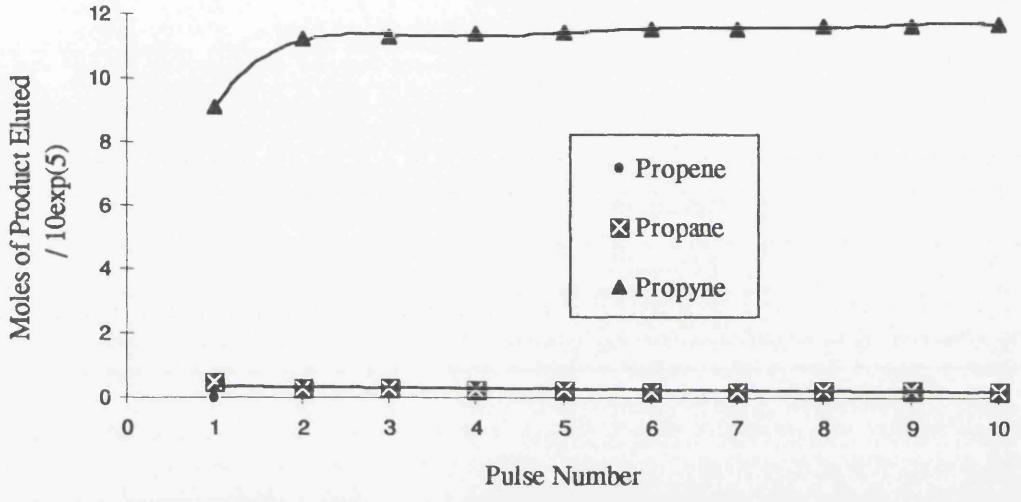

Figure 5.2.2 : Carbon Mass Balance for the Hydrogenation of Propyne (Equimolar Ratio) over Pt/silica at 293K

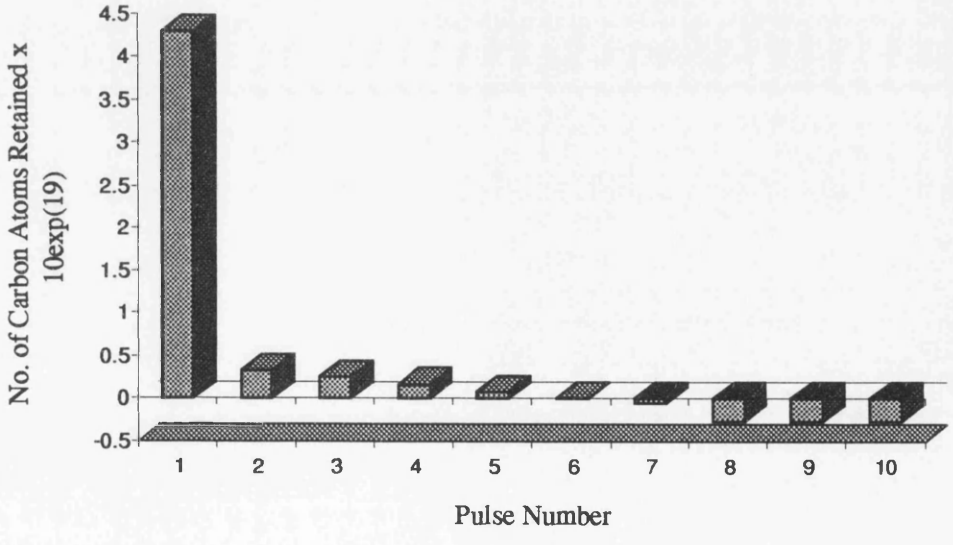

Table 5.2.0 : Carbon Deposition Data for the Hydrogenation of Propyne (Equimolar Ratio) over Pt/silica at 293K

Pulse Number	No. of Carbon Atoms Deposited (x 10^{19})	
	Per Pulse	Cumulative
1	4.29	4.29
2	0.32	4.61
3	0.25	4.86
4	0.16	5.02
5	0.07	5.09
6	0.00	5.09
7	-0.05	5.04
8	-0.27	4.77
9	-0.27	4.50
10	-0.27	4.23

Table 5.2.1 : Hydrogenation of Propyne (Excess Hydrogen) over Pt/silica at 293K

Pulse Number	Sample Pressure (mB)	Moles of Alkyne In / 10^5	Moles of Alkene Out / 10^5	Moles of Alkane Out / 10^5	Moles of Alkyne Out / 10^5	Selectivity (%)	Conversion (%)
1	100	5.98	0.00	2.36	1.48	0.00	75.19
2	100	5.98	0.00	2.42	1.52	0.00	74.62
3	100	5.98	0.00	1.84	1.52	0.00	74.55
4	100	5.98	0.00	2.01	1.59	0.00	73.45
5	100	5.98	0.00	2.04	1.67	0.00	71.94
6	100	5.98	0.00	2.02	1.70	0.00	71.55
7	100	5.98	0.00	1.97	1.49	0.00	74.96
8	100	5.98	0.00	2.43	2.16	0.00	63.95
9	100	5.98	0.00	2.03	2.56	0.00	57.13
10	100	5.98	0.00	1.53	2.76	0.00	53.90
11	100	5.98	0.00	1.53	2.81	0.00	52.98
12	100	5.98	0.00	1.55	2.87	0.00	52.00
13	100	5.98	0.00	1.60	2.81	0.00	52.95
14	100	5.98	0.00	1.56	2.56	0.00	57.26
15	100	5.98	0.00	1.54	2.85	0.00	52.30
16	100	5.98	0.00	1.54	2.20	0.00	63.21
17	100	5.98	1.78	1.52	2.72	54.03	54.50
18	100	5.98	1.80	1.51	2.75	54.45	53.94
19	100	5.98	1.71	1.55	2.56	52.49	57.18
20	100	5.98	1.70	1.53	2.63	52.53	56.03
21	100	5.98	1.70	1.53	2.61	52.69	56.31
22	100	5.98	1.71	1.55	2.59	52.40	56.67
23	100	5.98	1.70	1.53	2.34	52.75	60.83
24	100	5.98	1.69	1.56	2.86	52.04	52.05
25	100	5.98	1.67	1.55	2.67	51.90	55.25
26	100	5.98	1.67	1.54	2.74	51.99	54.11
27	100	5.98	1.71	1.49	2.75	53.41	54.02
28	100	5.98	1.69	1.49	2.81	53.18	52.90
29	100	5.98	1.68	1.50	2.87	52.83	52.09
30	100	5.98	1.69	1.52	2.81	52.73	53.01

Figure 5.2.3 : Variation of Product Distribution with Pulse Number for the Hydrogenation of Propyne (Excess Hydrogen) over Pt/silica at 293K

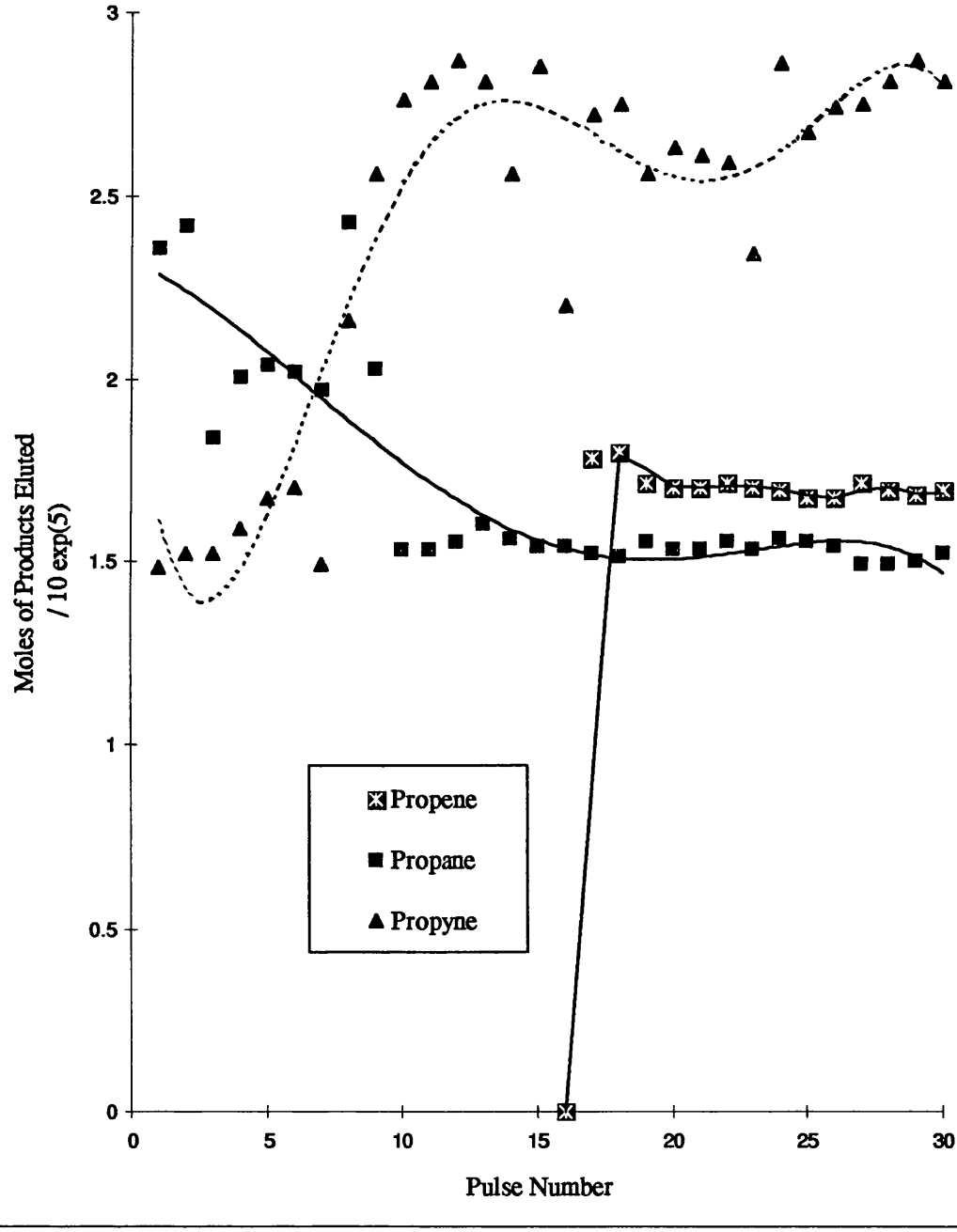

Figure 5.2.4 : Variation of Conversion with Pulse Number for the Hydrogenation of Propyne (Excess Hydrogen) over Pt/silica at 293K

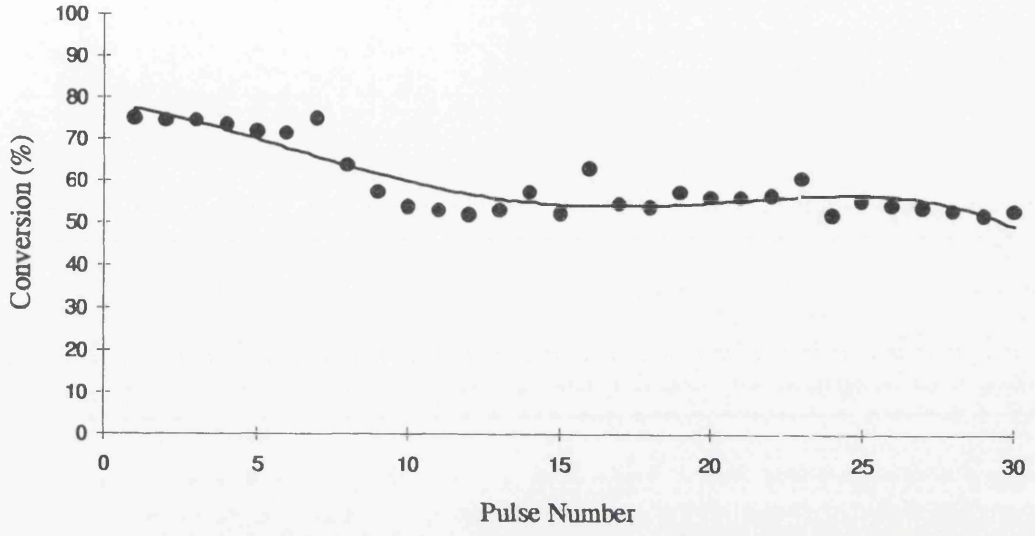

Figure 5.2.5 : Carbon Mass Balance for the Hydrogenation of Propyne (Excess Hydrogen) over Pt/silica at 293K

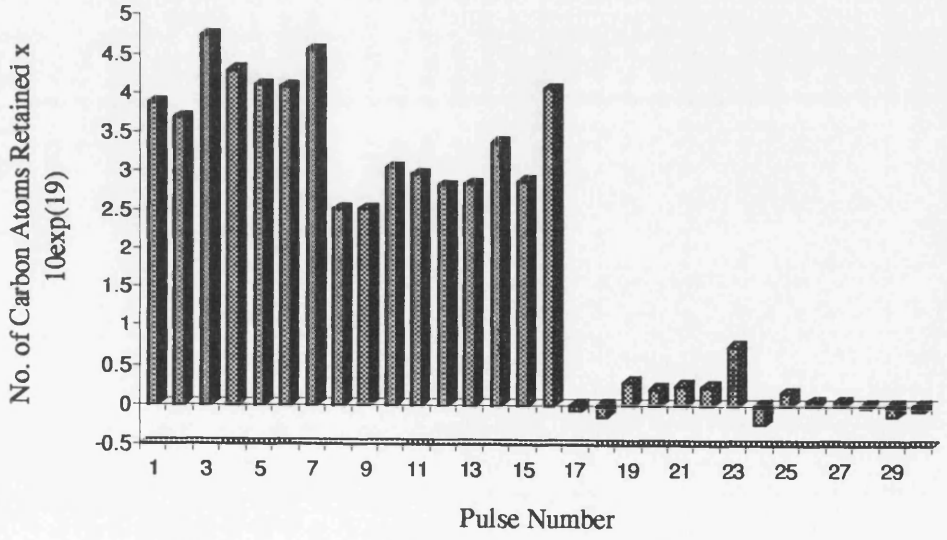

Table 5.2.2 : Carbon Deposition Data for the Hydrogenation of Propyne (Excess Hydrogen) over Pt/silica at 293K

Pulse Number	No. of Carbon Atoms Deposited (x 10^{19})	
	Per Pulse	Cumulative
1	3.87	3.87
2	3.68	7.55
3	4.73	12.28
4	4.29	16.57
5	4.10	20.67
6	4.08	24.75
7	4.55	29.30
8	2.51	31.81
9	2.51	34.32
10	3.05	37.37
11	2.96	40.33
12	2.82	43.15
13	2.84	45.99
14	3.36	49.35
15	2.87	52.22
16	4.05	56.27
17	-0.07	56.20
18	-0.14	56.06
19	0.29	56.35
20	0.21	56.56
21	0.25	56.81
22	0.23	57.04
23	0.74	57.78
24	-0.24	57.54
25	0.16	57.80
26	0.05	57.85
27	0.05	57.90
28	-0.02	57.88
29	-0.13	57.75
30	-0.07	57.68

4.4.4 The Hydrogenation of Propyne over Alumina-Supported Platinum

Similar to silica-supported palladium, the hydrogenation of propyne using an equimolar reactant ratio produced propene, over Pt/alumina. However, the activity of this catalyst for hydrogenation was low, even in the first pulse, and was observed to decrease still further with an increased number of pulses. In pulse one, approximately 66% of the reactant propyne remained unreacted, compared to pulse ten in which over 80% of the freshly injected propyne was unconverted. The yield of propene was unaltered over ten pulses with the corresponding retention of carbon at the surface found to drop significantly over the first eight pulses. From pulse nine and ten, in Figure 5.2.7, it can be seen that the catalyst loses carbon to the system.

Increasing the concentration of hydrogen in the reaction mixture, produced both propene and propane over Pt/alumina. As with all other catalyst, there was an induction period before propene was produced, as can be seen in Figure 5.2.8. Over this catalyst, the hydrogenation of propyne produced only propane over the first five pulses (Table 5.2.5). An increase in the number of pulses resulted in propene formation. The yield of propane was found to oscillate over the course of the experiments, while that of propene increased to an apparently steady value. The retention of carbon on the catalyst was found to decrease with an increasing number of pulses.

Table 5.2.3 : Hydrogenation of Propyne (Equimolar Ratio) over Pt/alumina at 293K

Pulse Number	Sample Pressure (mB)	Moles of Alkyne In / 10^5	Moles of Alkene Out / 10^5	Moles of Alkane Out / 10^5	Moles of Alkyne Out / 10^5	Selectivity (%)	Conversion (%)
1	100	11.95	1.82	0.00	8.42	100.0	14.78
2	100	11.95	1.77	0.00	8.73	100.0	13.25
3	100	11.95	1.71	0.00	8.93	100.0	12.64
4	100	11.95	1.59	0.00	9.06	100.0	12.09
5	100	11.95	1.61	0.00	9.11	100.0	11.88
6	100	11.95	1.57	0.00	9.17	100.0	11.69
7	100	11.95	1.65	0.00	9.32	100.0	11.00
8	100	11.95	2.03	0.00	9.65	100.0	9.60
9	100	11.95	1.88	0.00	10.10	100.0	7.74
10	100	11.95	1.63	0.00	10.35	100.0	6.69

Figure 5.2.6 : Variation of Product Distribution with Pulse Number for the Hydrogenation of Propyne (Equimolar Ratio) over Pt/alumina at 293K

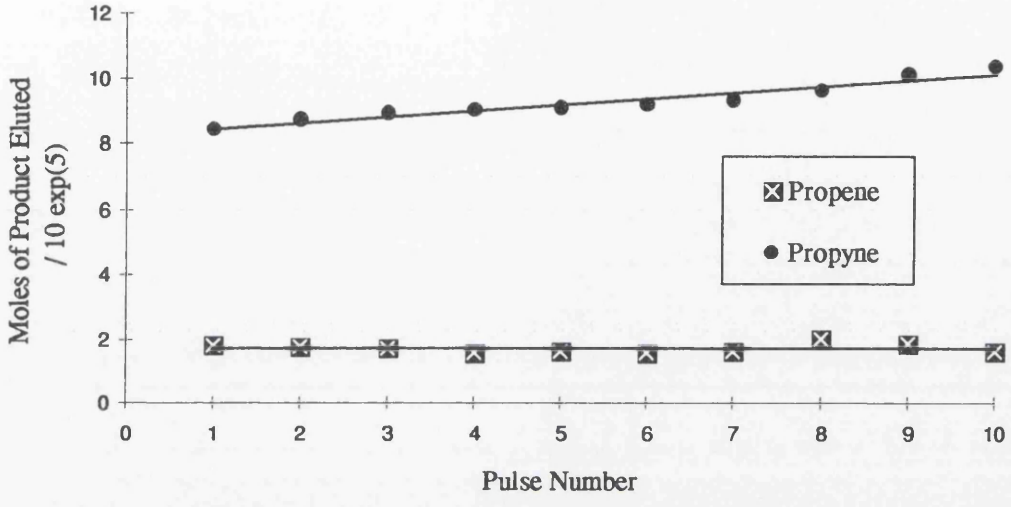

Figure 5.2.7 : Carbon Mass Balance for the Hydrogenation of Propyne (Equimolar Ratio) over Pt/alumina at 293K

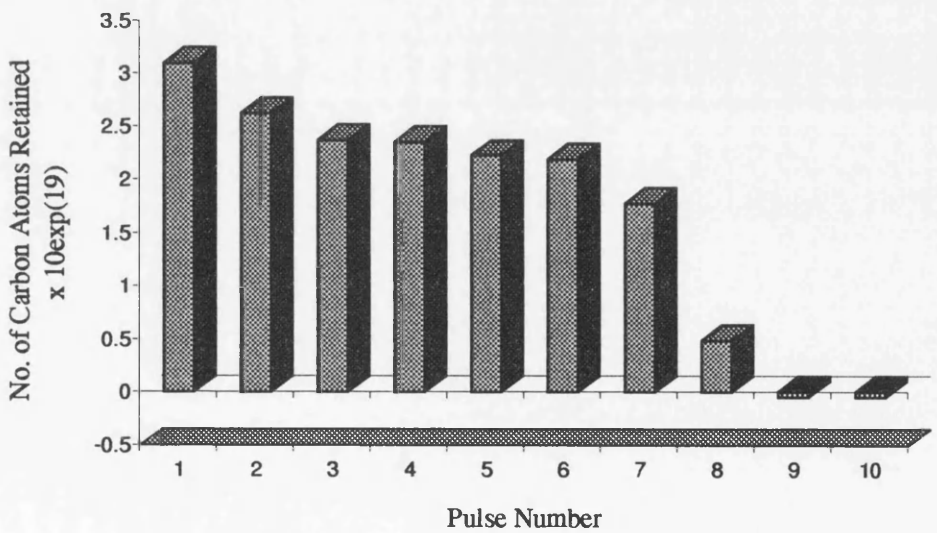

Table 5.2.4 : Carbon Deposition Data for the Hydrogenation of Propyne (Equimolar Ratio) over Pt/alumina at 293K

Pulse Number	No. of Carbon Atoms Deposited (x 10^{19})	
	Per Pulse	Cumulative
1	3.09	3.09
2	2.62	5.71
3	2.36	8.07
4	2.35	10.42
5	2.22	12.64
6	2.18	14.82
7	1.77	16.59
8	0.48	17.07
9	-0.05	17.02
10	-0.05	16.93

Table 5.2.5 : Hydrogenation of Propyne (Equimolar Ratio) over Pt/alumina at 293K

Pulse Number	Sample Pressure (mB)	Moles of Alkyne In / 10^5	Moles of Alkene Out / 10^5	Moles of Alkane Out / 10^5	Moles of Alkyne Out / 10^5	Selectivity (%)	Conversion (%)
1	100	5.98	0.00	1.61	0.88	0.00	85.28
2	100	5.98	0.00	1.58	0.86	0.00	85.62
3	100	5.98	0.00	1.63	0.90	0.00	84.90
4	100	5.98	0.00	1.59	0.90	0.00	84.90
5	100	5.98	0.00	1.56	0.92	0.00	84.60
6	100	5.98	1.62	1.77	0.92	47.70	84.60
7	100	5.98	1.54	1.58	0.94	49.30	84.20
8	100	5.98	1.59	1.50	0.935	51.44	84.36
9	100	5.98	1.60	1.55	0.96	50.78	83.94
10	100	5.98	1.57	1.51	0.98	51.07	83.55
11	100	5.98	1.51	1.46	1.05	50.90	82.44
12	100	5.98	1.57	1.50	1.14	51.11	80.93
13	100	5.98	1.62	1.61	1.19	50.05	80.10
14	100	5.98	1.50	1.43	1.29	51.19	78.42
15	100	5.98	1.56	1.59	1.45	49.50	75.65
16	100	5.98	1.63	1.59	1.51	50.62	74.75
17	100	5.98	1.50	1.44	1.44	50.96	75.91
18	100	5.98	1.49	1.46	1.42	50.54	76.20
19	100	5.98	1.53	1.41	1.43	51.99	76.00
20	100	5.98	1.60	1.46	1.39	51.93	76.44
21	100	5.98	1.58	1.48	1.60	51.66	73.22
22	100	5.98	1.57	1.51	1.70	50.98	71.49
23	100	5.98	1.58	1.55	1.99	50.42	66.72
24	100	5.98	1.59	1.57	2.30	50.30	61.39
25	100	5.98	1.59	1.65	2.63	48.90	56.00
26	100	5.98	1.61	1.66	2.64	49.24	55.82
27	100	5.98	1.62	1.66	2.68	49.44	55.09
28	100	5.98	1.61	1.57	2.73	50.54	54.32
29	100	5.98	1.62	1.57	2.75	50.75	53.92
30	100	5.98	1.65	1.53	2.78	51.70	53.43

Figure 5.2.8 : Variation of Product Distribution with Pulse Number for the Hydrogenation of Propyne (Excess Hydrogen) over Pt/alumina at 293K

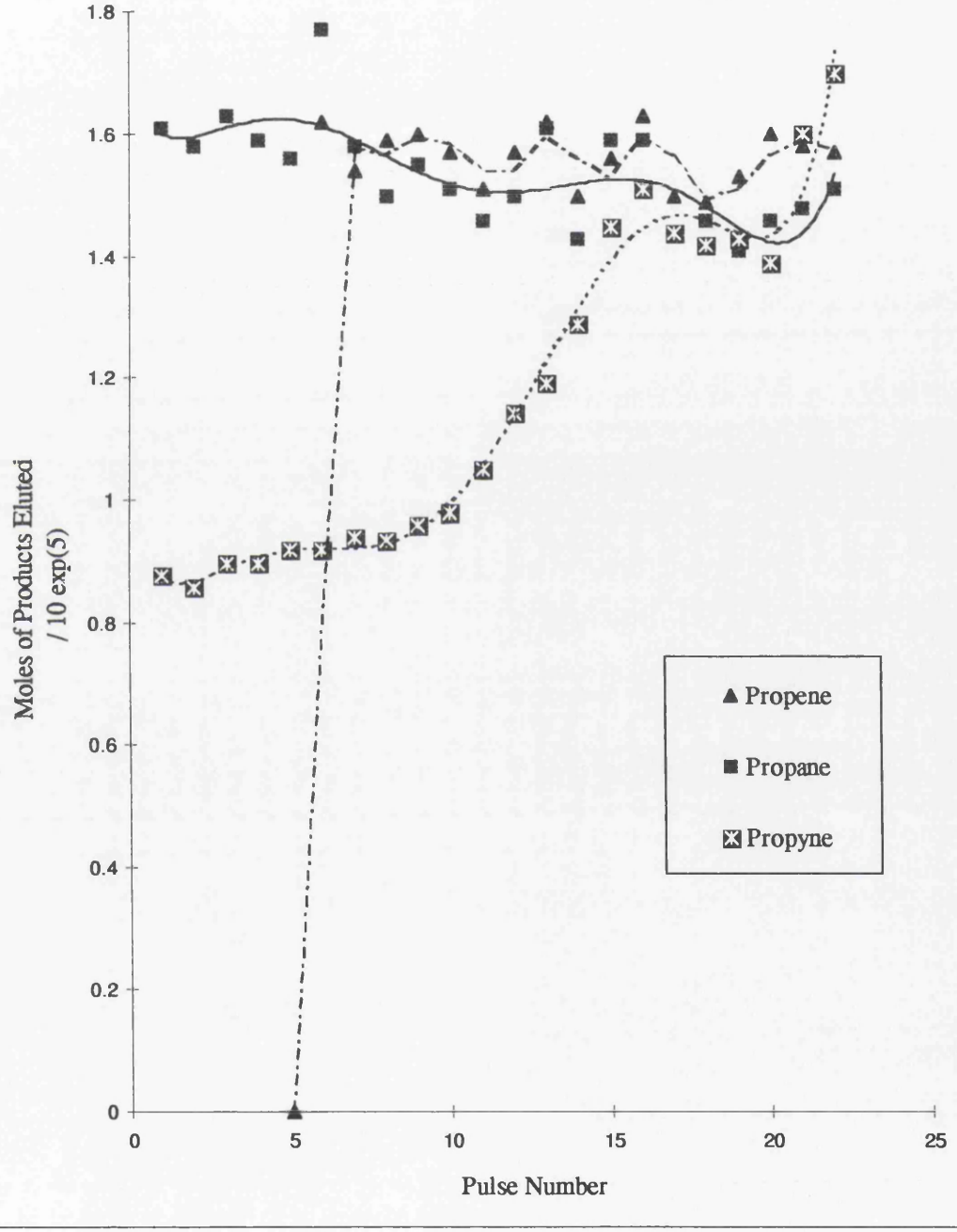

Figure 5.2.9 : Variation of Conversion with Pulse Number for the Hydrogenation of Propyne (Excess Hydrogen) over Pt/alumina at 293K

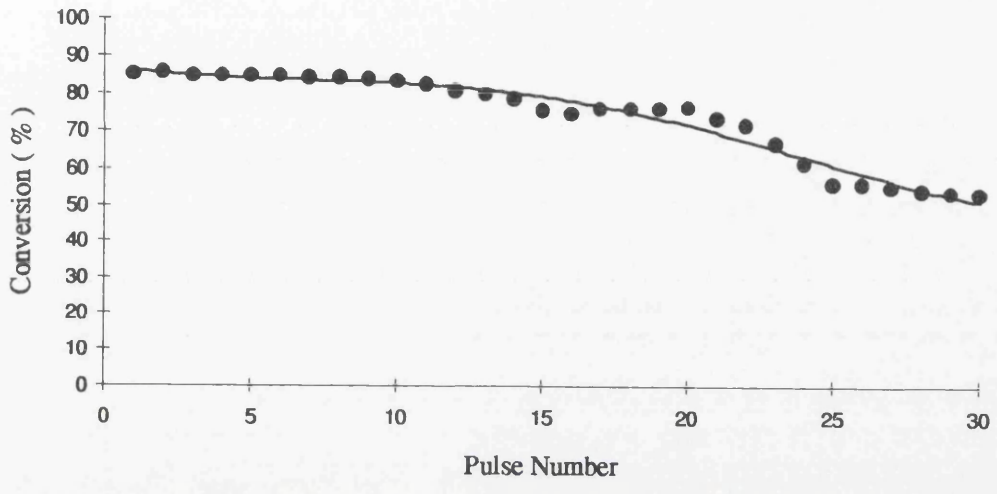

Figure 5.3.0 : Carbon Mass Balance for the Hydrogenation of Propyne (Excess Hydrogen) over Pt/alumina at 293K

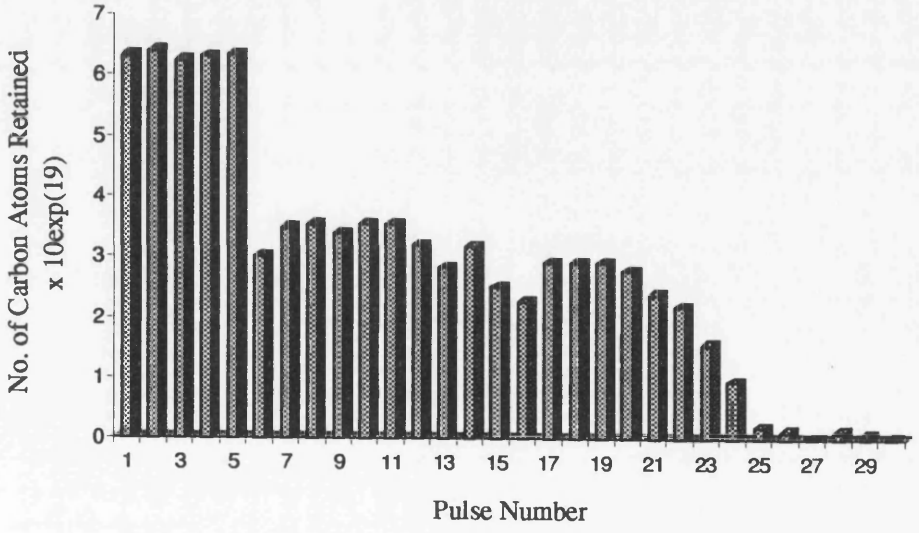

Table 5.2.6 : Carbon Deposition Data for the Hydrogenation of Propyne (Excess Hydrogen) over Pt/alumina at 293K

Pulse Number	No. of Carbon Atoms Deposited (x 10^{19})	
	Per Pulse	Cumulative
1	6.31	6.31
2	6.39	12.70
3	6.23	18.93
4	6.30	25.23
5	6.32	31.55
6	3.01	34.56
7	3.47	38.03
8	3.53	41.56
9	3.38	44.94
10	3.54	48.48
11	3.54	52.02
12	3.19	55.21
13	2.82	58.03
14	3.17	61.20
15	2.49	63.69
16	2.26	65.95
17	2.89	68.84
18	2.90	71.74
19	2.90	74.64
20	2.76	77.40
21	2.38	79.78
22	2.17	81.95
23	1.55	83.50
24	0.94	84.44
25	0.19	84.63
26	0.13	84.76
27	0.04	84.80
28	0.13	84.93
29	0.07	85.00
30	0.04	85.04

Section Three

2-BUTYNE HYDROGENATION

4.4.5 The Hydrogenation of 2-Butyne over Silica-Supported Palladium

The hydrogenation of 2-butyne over silica-supported palladium has been investigated using two different reactant ratios, and various reaction temperatures.

Using an equimolar reactant ratio, the hydrogenation of 2-butyne over Pd/silica at 465K produced both the *cis* and *trans*-olefin isomers. The yield of *cis* isomer was far greater than the *trans* isomer, but was observed to decrease with increasing number of pulses, before increasing again to its initial value. The *trans* isomer in this reaction was produced in trace amounts, and was relatively constant over a series of ten pulses (Table 5.2.7). The activity of the catalyst for 2-butyne hydrogenation was initially complete (100%), but decreased before increasing again. The amount of carbon retained in each pulse decreased (negative in pulse 3), and fluctuated from pulse four to ten (Figure 5.3.2).

The hydrogenation of 2-butyne with excess hydrogen (1:3 :: C_4H_6:H_2) over Pd/silica, at the same reaction temperature, gave complete removal of the acetylene over thirty pulses. This high acetylene conversion was accompanied by continual carbon deposition, which did not dimininsh the catalysts efficiency for 2-butyne hydrogenation. The only observed hydrogenation products were *n*-butane and methane, the latter product formed by hydrogenolysis of the adsorbed acetylene. The yield of methane was relatively constant throughout a series of thirty pulses (Figure 5.3.4), with the yield of *n*-butane found to increase with an increase in the number of pulses.

2-Butyne hydrogenation over the above catalyst at 373K (equimolar reactant ratio) produced *cis*-2-butene as the sole hydrogenation product. The conversion of 2-butyne was constant at 100% over the first two pulses. This activity decreased with increasing number of pulses, but as with the reaction performed at 465K, the conversion of acetylene increased in the later pulses. The

yield of *cis*-2-butene was relatively constant over the ten pulses (Figure 5.3.6). Carbon mass balance data shows that the amount of carbon retained by the catalyst in each pulse decreases before increasing again. The yield of 2-butyne and the amount of carbon retained at the surface seem to be mirror images of each other, such that as one increased the other decreased.

Increasing the hydrogen concentration, produced only *n*-butane over Pd/silica at 373K. Similar to the reactions performed at 465K, the conversion of the acetylene was complete over a series of thirty pulses and was accompanied by a fluctuating yield of the alkane. The carbon mass balance data shows that the amount of carbon held at the surface fluctuated from pulse to pulse (Figure 5.4.0).

When an equimolar ratio of 2-butyne and hydrogen was injected over silica-supported palladium at 330K, there was no hydrogenation observed. Indeed, the only reaction was the partial loss of acetylene to the catalyst surface, which can be attributed to a poisoning process. There seems to be no relation between the amount of acetylene pulsed over the catalyst and the amount of carbon retained (Table 5.3.1).

At room temperature, the hydrogenation of 2-butyne, using an equimolar reactant ratio over the above catalyst produced *cis*-2-butene, with complete conversion of the acetylene over the first nine pulses. In pulse ten, the activity of the catalyst decreased such that approximately 33% of the injected 2-butyne remained unreacted. The yield of the olefin was found to decrease with increased number of pulses, with the amount of carbon held at the catalyst surface increasing from pulse one to nine (Figure 5.4.1), before decreasing in pulse ten.

Table 5.2.7 : Hydrogenation of 2-Butyne (Equimolar Ratio) over Pd/silica at 465K

Pulse Number	Sample Pressure (mB)	Moles of Alkyne In / 10^5	Moles of **c-2-B** Out / 10^5	Moles of **t-2-B** Out / 10^5	Moles of Alkyne Out / 10^5	Conversion (%)	No. of Carbon Atoms In $x10^{19}$	No. of Carbon Atoms Out $x10^{19}$	ΔCarbon Atoms $x10^{19}$
1	40	5.65	3.19	0.08	0.00	100.0	13.60	7.87	5.73
2	40	5.65	2.62	0.00	1.42	74.87	13.60	9.73	3.87
3	40	5.65	2.33	0.28	3.41	39.65	13.60	14.50	-0.90
4	40	5.65	2.05	0.28	3.18	43.76	13.60	13.27	0.33
5	40	5.65	1.97	0.27	2.86	49.30	13.60	12.28	1.32
6	40	5.65	1.88	0.28	3.02	46.50	13.60	12.48	1.12
7	40	5.65	2.36	0.31	2.52	55.30	13.60	12.50	1.10
8	40	5.65	2.42	0.25	2.19	61.20	13.60	11.70	1.90
9	40	5.65	3.14	0.22	2.27	59.85	13.60	13.56	0.04
10	40	5.65	3.26	0.23	1.88	66.75	13.60	12.93	0.67

Figure 5.3.1 : Variation of Product Distribution with Pulse Number for the Hydrogenation of 2-Butyne (Equimolar Ratio) over Pd/silica at 465K

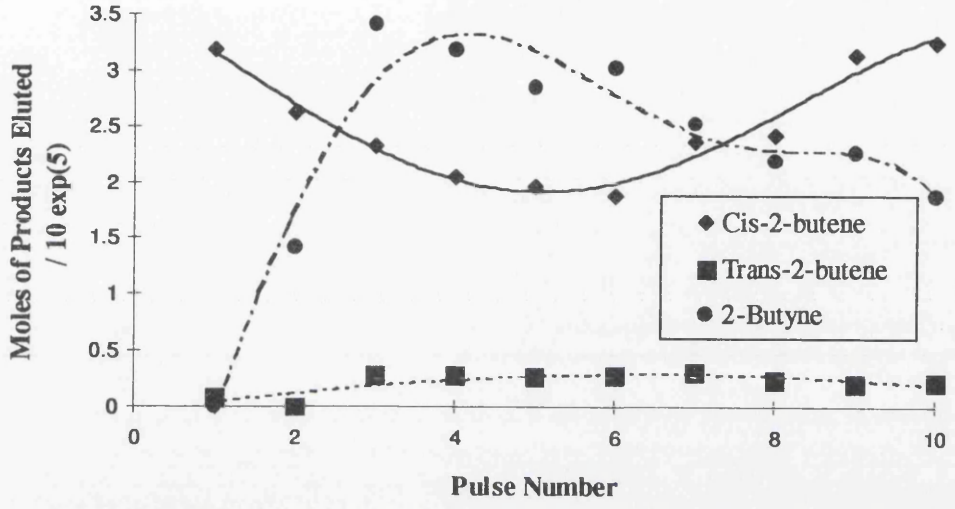

Figure 5.3.2 : Carbon Mass Balance for the Hydrogenation of 2-Butyne (Equimolar Ratio) over Pd/silica at 465K

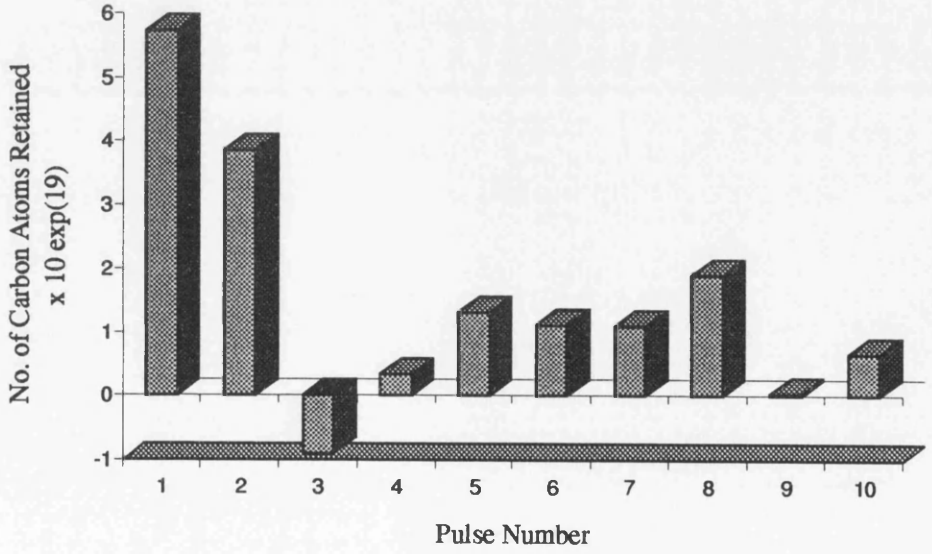

Figure 5.3.3 : Variation of Conversion with Pulse Number for the Hydrogenation of 2-Butyne (Equimolar Ratio) over Pd/silica at 465K

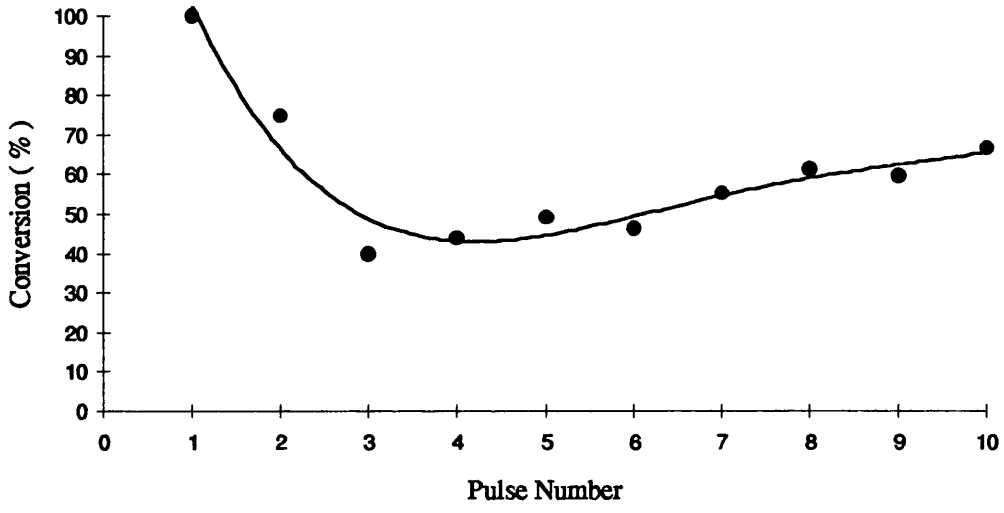

Table 5.2.8 : Hydrogenation of 2-Butyne (Excess Hydrogen) over Pd/silica at 465K

Pulse Number	Sample Pressure (mB)	Moles of Alkyne In / 10^5	Moles of n-B Out / 10^5	Moles of CH_4 Out / 10^5	No. of Carbon Atoms In $x10^{19}$	No. of Carbon Atoms Out $x10^{19}$	ΔCarbon atoms $x10^{19}$
1	30	2.12	0.77	1.06	5.10	2.50	2.60
2	30	2.12	0.83	0.81	5.10	2.49	2.61
3	30	2.12	0.95	0.85	5.10	2.79	2.31
4	30	2.12	1.04	0.72	5.10	2.94	2.16
5	30	2.12	0.98	0.86	5.10	2.87	2.23
6	30	2.12	1.16	0.76	5.10	3.25	1.85
7	30	2.12	1.28	0.73	5.10	3.52	1.58
8	30	2.12	0.87	0.65	5.10	2.48	2.62
9	30	2.12	1.20	0.73	5.10	3.33	1.77
10	30	2.12	1.18	0.80	5.10	3.32	1.78
11	30	2.12	1.42	0.82	5.10	3.91	1.19
12	30	2.12	1.12	1.33	5.10	3.49	1.61
13	30	2.12	1.00	0.97	5.10	2.99	2.11
14	30	2.12	1.02	0.97	5.10	3.04	2.06
15	30	2.12	1.23	0.82	5.10	3.45	1.65
16	30	2.12	1.18	0.79	5.10	3.31	1.79
17	30	2.12	1.24	0.76	5.10	3.44	1.66
18	30	2.12	1.41	0.77	5.10	3.85	1.25
19	30	2.12	1.35	0.80	5.10	3.73	1.37
20	30	2.12	1.09	0.77	5.10	3.09	2.01
21	30	2.12	1.29	0.70	5.10	3.52	1.58
22	30	2.12	1.36	0.66	5.10	3.66	1.44
23	30	2.12	1.13	0.80	5.10	3.20	1.90
24	30	2.12	1.44	0.76	5.10	3.92	1.18
25	30	2.12	1.54	0.78	5.10	4.17	0.93
26	30	2.12	1.39	0.80	5.10	3.83	1.27
27	30	2.12	1.33	0.91	5.10	3.75	1.35
28	30	2.12	1.29	0.78	5.10	3.56	1.54
29	30	2.12	1.30	0.94	5.10	3.69	1.41
30	30	2.12	1.22	0.98	5.10	3.53	1.57

Figure 5.3.4 : Variation of Product Distribution with Pulse Number for the Hydrogenation of 2-Butyne (Excess Hydrogen) over Pd/silica at 465K

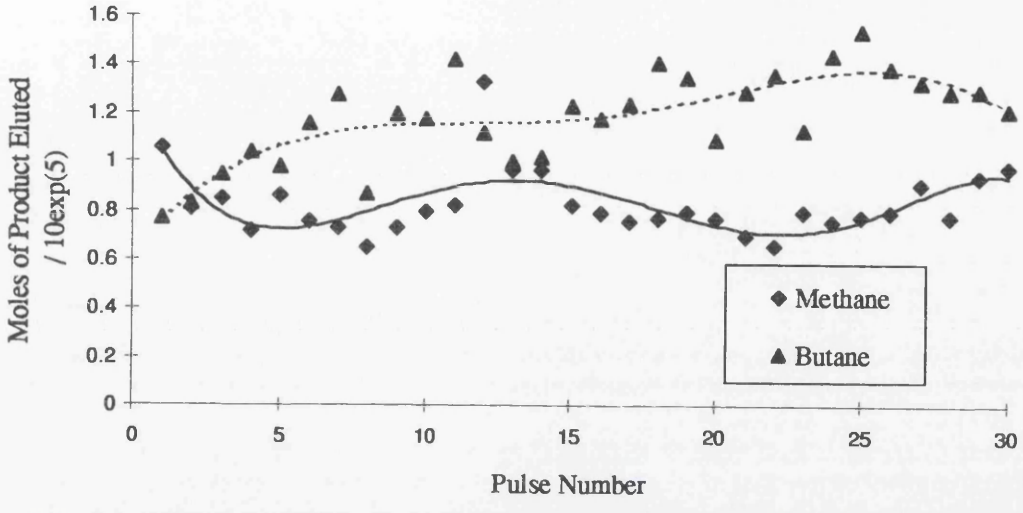

Figure 5.3.5 : Carbon Mass Balance for the Hydrogenation of 2-Butyne (Excess Hydrogen) over Pd/silica at 465K

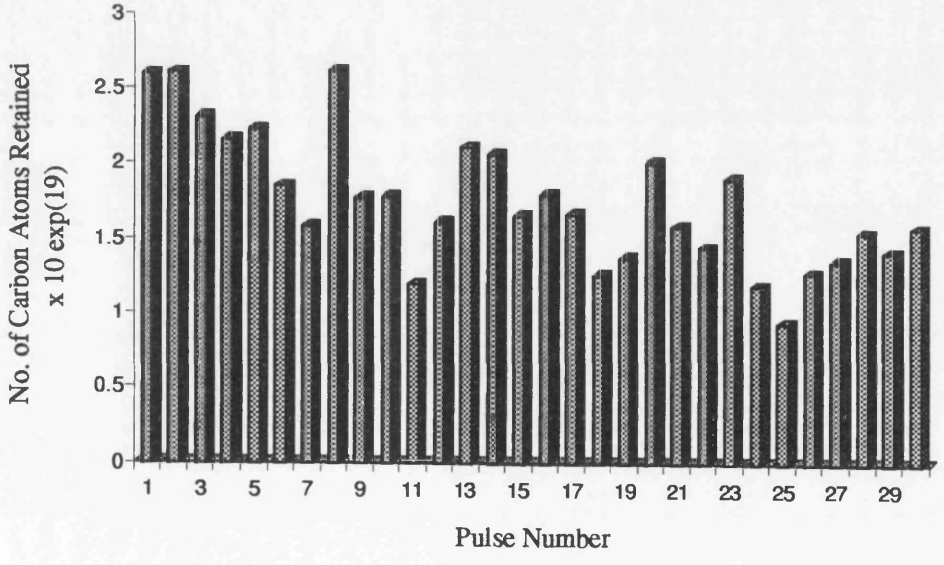

Table 5.2.9 : Hydrogenation of 2-Butyne (Equimolar Ratio) over Pd/silica at 373K

Pulse Number	Sample Pressure (mB)	Moles of Alkyne In / 10^5	Moles of c-2-B Out / 10^5	Moles of Alkyne Out / 10^5	Conversion (%)	No. of Carbon Atoms In $x10^{19}$	No. of Carbon Atoms Out $x10^{19}$	ΔCarbon Atoms $x10^{19}$
1	30	4.24	2.64	0.00	100.0	10.20	6.36	3.84
2	30	4.24	2.30	0.98	76.88	10.20	7.90	2.30
3	30	4.24	2.87	0.72	83.02	10.20	8.65	1.55
4	30	4.24	2.32	1.09	74.29	10.20	8.21	1.99
5	30	4.24	2.40	1.09	74.29	10.20	8.40	1.80
6	30	4.24	2.36	0.94	77.83	10.20	7.95	2.25
7	30	4.24	2.34	0.90	78.77	10.20	7.80	2.4
8	30	4.24	2.15	1.01	76.18	10.20	7.61	2.59
9	30	4.24	2.26	0.00	100.0	10.20	5.44	4.76
10	30	4.24	2.31	0.00	100.0	10.20	5.56	4.64

Figure 5.3.6 : Variation of Product Distribution with Pulse Number for the Hydrogenation of 2-Butyne (Equimolar Ratio) over Pd/silica at 373K

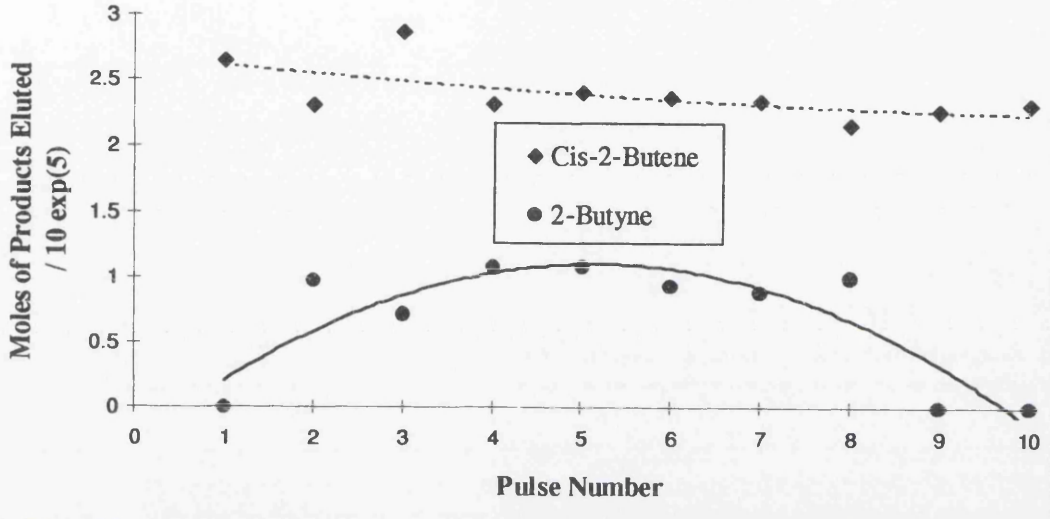

Figure 5.3.7 : Carbon Mass Balance for the Hydrogenation of 2-Butyne (Equimolar Ratio) over Pd/silica at 373K

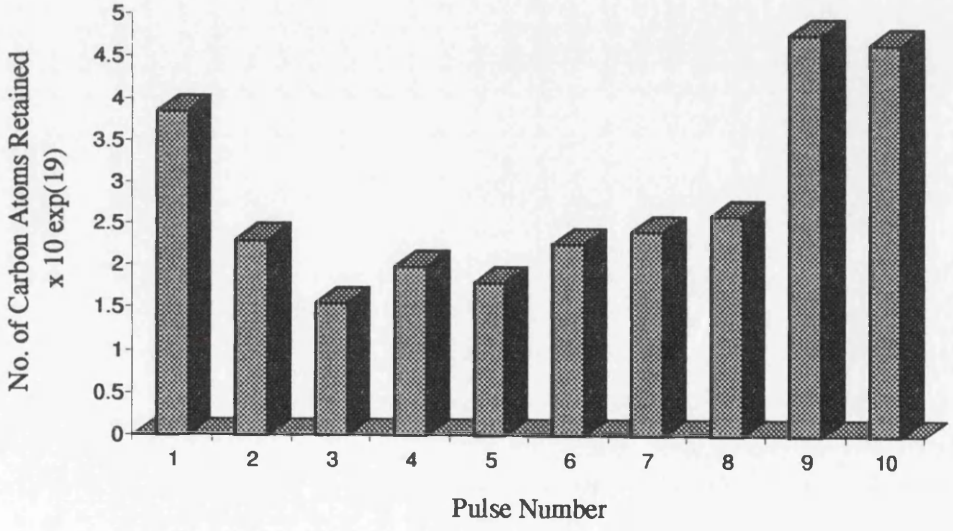

Figure 5.3.8 : Variation of Conversion with Pulse Number for the Hydrogenation of 2-Butyne (Equimolar Ratio) over Pd/silica at 373K

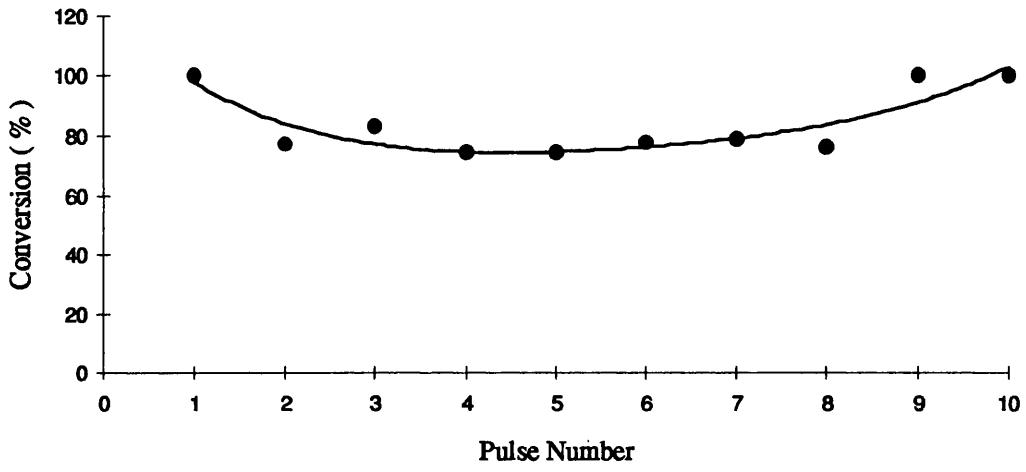

Table 5.3.0 : Hydrogenation of 2-Butyne (Excess Hydrogen) over Pd/silica at 373K

Pulse Number	Sample Pressure	Moles of Alkyne In / 10^5	Moles of n-B Out / 10^5	No. of Carbon Atoms In $x10^{19}$	No. of Carbon Atoms Out $x10^{19}$	ΔCarbon Atoms $x10^{19}$
1	40	2.82	2.17	6.79	5.23	1.56
2	40	2.82	2.48	6.79	5.98	0.81
3	40	2.82	2.39	6.79	5.76	1.03
4	40	2.82	2.86	6.79	6.89	-0.10
5	40	2.82	2.44	6.79	5.88	0.91
6	40	2.82	2.92	6.79	7.04	-0.25
7	40	2.82	3.13	6.79	7.54	-0.75
8	40	2.82	2.62	6.79	6.30	0.49
9	40	2.82	2.49	6.79	5.99	0.80
10	40	2.82	2.62	6.79	6.30	0.49
11	40	2.82	2.91	6.79	7.01	-0.22
12	40	2.82	2.87	6.79	6.92	-0.13
13	40	2.82	2.86	6.79	6.89	-0.10
14	40	2.82	2.61	6.79	6.29	0.50
15	40	2.82	2.87	6.79	6.92	-0.13
16	40	2.82	3.01	6.79	7.25	-0.46
17	40	2.82	3.07	6.79	7.40	-0.61
18	40	2.82	2.74	6.79	6.59	0.20
19	40	2.82	3.23	6.79	7.78	-0.99
20	40	2.82	3.22	6.79	7.76	-0.97
21	40	2.82	3.34	6.79	8.06	-0.13
22	40	2.82	3.14	6.79	7.56	-0.77
23	40	2.82	2.60	6.79	6.26	0.53
24	40	2.82	2.48	6.79	5.97	0.82
25	40	2.82	2.77	6.79	6.67	0.12
26	40	2.82	2.66	6.79	6.42	0.37
27	40	2.82	2.46	6.79	5.93	0.86
28	40	2.82	2.57	6.79	6.18	0.61
29	40	2.82	2.66	6.79	6.42	0.37
30	40	2.82	2.74	6.79	6.60	0.19

Figure 5.3.9 : Variation of Butane Formation with Pulse Number for the Hydrogenation of 2-Butyne (Excess Hydrogen) over Pd/silica at 373K

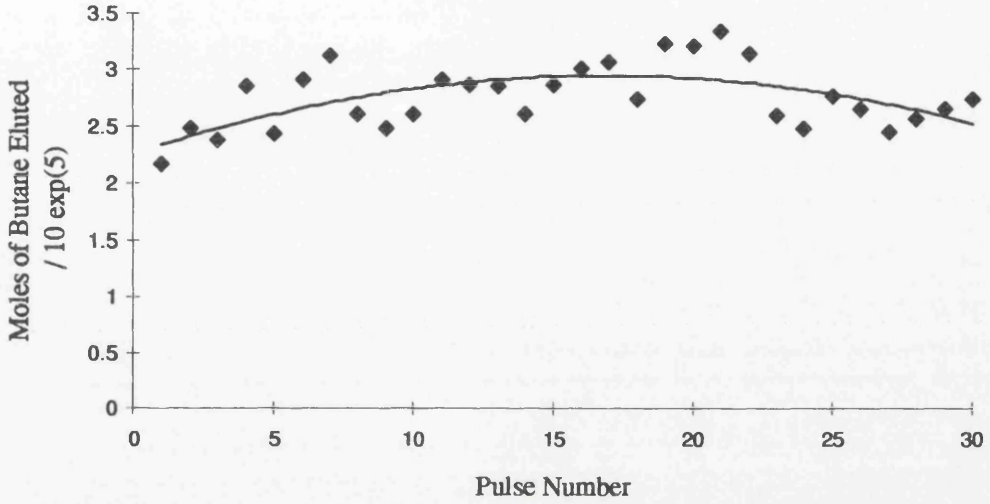

Figure 5.4.0 : Carbon Mass Balance for the Hydrogenation of 2-Butyne (Excess Hydrogen) over Pd/silica at 373K

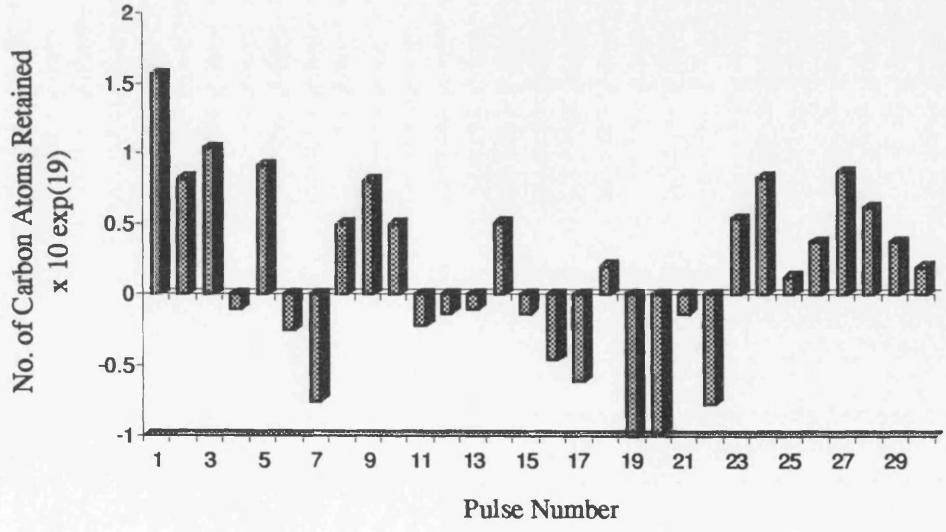

Table 5.3.1 : Hydrogenation of 2-Butyne (Equimolar Ratio) over Pd/silica at 330K

Pulse Number	Sample Pressure (mB)	Moles of Alkyne In / 10^5	Moles of Alkyne Out / 10^5	Conversion (%)	No. of Carbon Atoms In x10^{19}	No. of Carbon Atoms Out x10^{19}	ΔCarbon Atoms x10^{19}
1	48	6.78	6.33	6.64	16.33	15.24	1.09
2	48	6.78	5.26	22.41	16.33	12.67	3.66
3	48	6.78	6.91	-1.92	16.33	16.64	-0.31
4	48	6.78	5.55	18.14	16.33	13.37	2.96
5	48	6.78	6.33	6.64	16.33	15.25	1.08
6	48	6.78	6.05	10.77	16.33	14.57	1.76
7	48	6.78	4.96	26.84	16.33	11.95	4.38
8	48	6.78	6.25	7.82	16.33	15.06	1.27
9	48	6.78	6.65	1.92	16.33	16.02	0.31
10	48	6.78	5.76	15.04	16.33	13.87	2.46

Table 5.3.2 : Hydrogenation of 2-Butyne (Equimolar Ratio) over Pd/silica at 298K

Pulse Number	Sample Pressure (mB)	Moles of Alkyne In / 10^5	Moles of **c-2-B** Out / 10^5	Moles of Alkyne Out / 10^5	Conversion (%)	No. of Carbon Atoms In $x10^{19}$	No. of Carbon Atoms Out $x10^{19}$	ΔCarbon Atoms $x10^{19}$
1	30	4.24	2.82	0.00	100.0	10.20	6.79	3.41
2	30	4.24	2.87	0.00	100.0	10.20	6.91	3.29
3	30	4.24	2.69	0.00	100.0	10.20	6.48	3.72
4	30	4.24	2.70	0.00	100.0	10.20	6.50	3.70
5	30	4.24	2.82	0.00	100.0	10.20	6.79	3.41
6	30	4.24	2.77	0.00	100.0	10.20	6.67	3.53
7	30	4.24	2.27	0.00	100.0	10.20	5.46	4.74
8	30	4.24	2.40	0.00	100.0	10.20	5.78	4.42
9	30	4.24	1.90	0.00	100.0	10.20	4.57	5.63
10	30	4.24	1.95	1.55	63.44	10.20	8.43	1.77

Figure 5.4.1 : Variation of Product Distribution with Pulse Number for the Hydrogenation of 2-Butyne (Equimolar Ratio) over Pd/silica at 298K

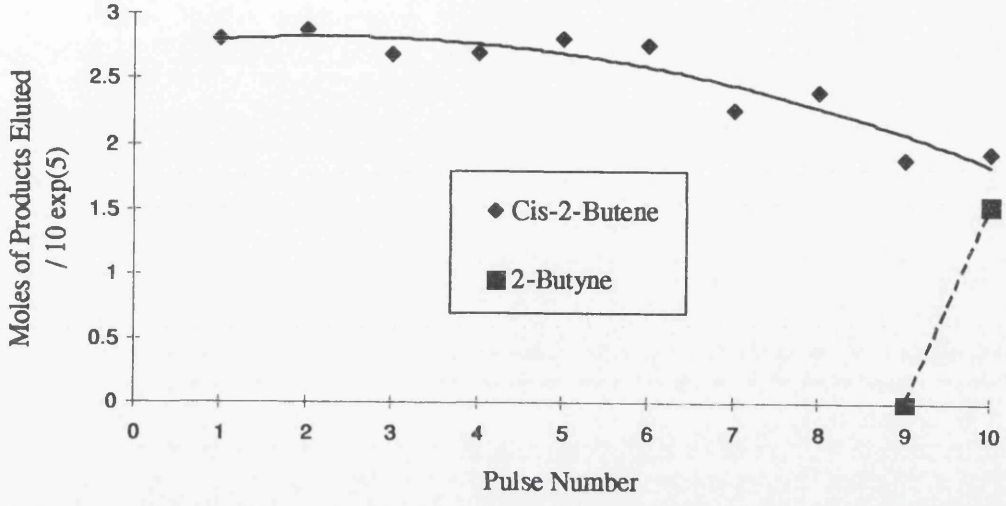

Figure 5.4.2 : Carbon Mass Balance for the Hydrogenation of 2-Butyne (Equimolar Ratio) over Pd/silica at 298K

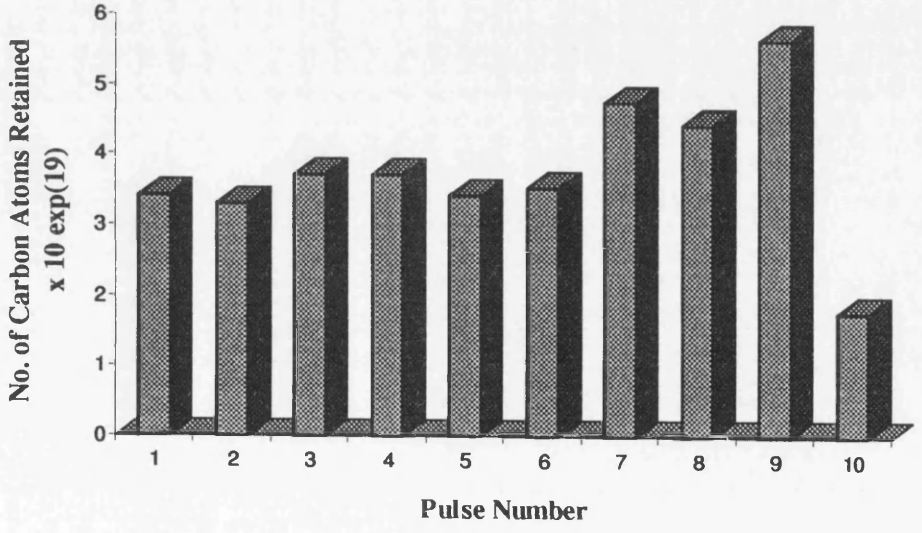

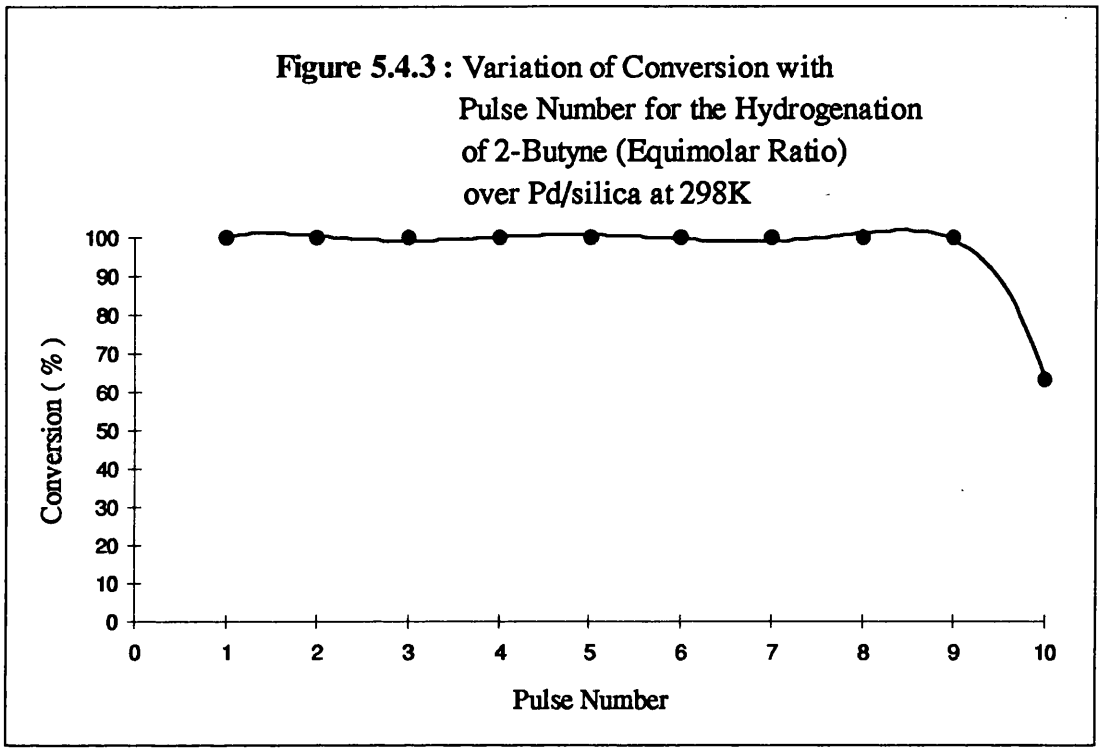

Figure 5.4.3 : Variation of Conversion with Pulse Number for the Hydrogenation of 2-Butyne (Equimolar Ratio) over Pd/silica at 298K

4.4.6 The Hydrogenation of 2-Butyne over Alumina-Supported Palladium

The hydrogenation of 2-butyne over alumina-supported palladium at 373K yielded *cis*-2-butene as the sole reduction product when an equimolar reactant ratio was employed. The activity of the catalyst was far superior to that observed under the same conditions for Pd/silica. Complete removal of 2-butyne was maintained over a series of ten pulses. The yield of the olefin was observed to decrease slightly, but was essentially stable throughout. The catalyst was prone to carbon laydown, and the quantity of carbon deposited at the surface tended to increase over the first five pulses (Figure 5.4.5), before decreasing. On reaching the final pulse, the propensity of this catalyst to produce surface carbon was again enhanced, with the amount of carbon deposited observed to increase.

Using a three-fold excess of hydrogen, the hydrogenation of 2-butyne over Pd/alumina produced only *n*-butane. The complete conversion of 2-butyne was maintained over a thirty pulse period. The amount of butane eluted was relatively constant throughout these pulses, with the corresponding deposition of carbon tending to fluctuate (Figure 5.4.7).

At 298K, the hydrogenation of 2-butyne over Pd/alumina (equimolar ratio), again produced only the *cis*-olefin isomer. The conversion of 2-butyne at this temperature was lower than that seen at 373K. The conversion of 2-butyne was found to oscillate over ten pulses, with the yield *cis*-2-butene observed to decrease (Table 5.3.5). The deposition of carbon at the catalyst surface was initially low, but increased with increased pulsing (Figure 5.4.9).

Using an excess of hydrogen resulted in the formation of both *n*-butane and methane over Pd/alumina at 298K. Similar to all other excess hydrogen reactions, the conversion of the acetylene was unaltered over thirty pulses. The amounts of methane and *n*-butane formed were constant over the course of the

experiments, with butane constituting approximately 80% of the eluted gas mixture. This catalyst showed no indication of losing surface carbon, with carbon being retained in each individual pulse.

Table 5.3.3 : Hydrogenation of 2-Butyne (Equimolar Ratio) over Pd/alumina at 373K.

Pulse Number	Sample Pressure (mB)	Moles of Alkyne In / 10^5	Moles of c-2-B Out / 10^5	Moles of Alkyne Out / 10^5	Conversion (%)	No. of Carbon Atoms In $x10^{19}$	No. of Carbon Atoms Out $x10^{19}$	ΔCarbon Atoms $x10^{19}$
1	30	4.24	3.85	0.00	100.0	10.20	9.27	0.93
2	30	4.24	3.12	0.00	100.0	10.20	7.52	2.68
3	30	4.24	3.12	0.00	100.0	10.20	7.52	2.68
4	30	4.24	3.58	0.00	100.0	10.20	8.62	1.58
5	30	4.24	2.44	0.00	100.0	10.20	5.87	4.33
6	30	4.24	2.82	0.00	100.0	10.20	6.78	3.42
7	30	4.24	2.77	0.00	100.0	10.20	6.68	3.52
8	30	4.24	3.03	0.00	100.0	10.20	7.29	2.91
9	30	4.24	3.60	0.00	100.0	10.20	8.67	1.53
10	30	4.24	2.64	0.00	100.0	10.20	6.36	3.84

Figure 5.4.4 : Variation of Cis-2-Butene Formation with Pulse Number for the Hydrogenation of 2-Butyne (Equimolar Ratio) over Pd/alumina at 373K

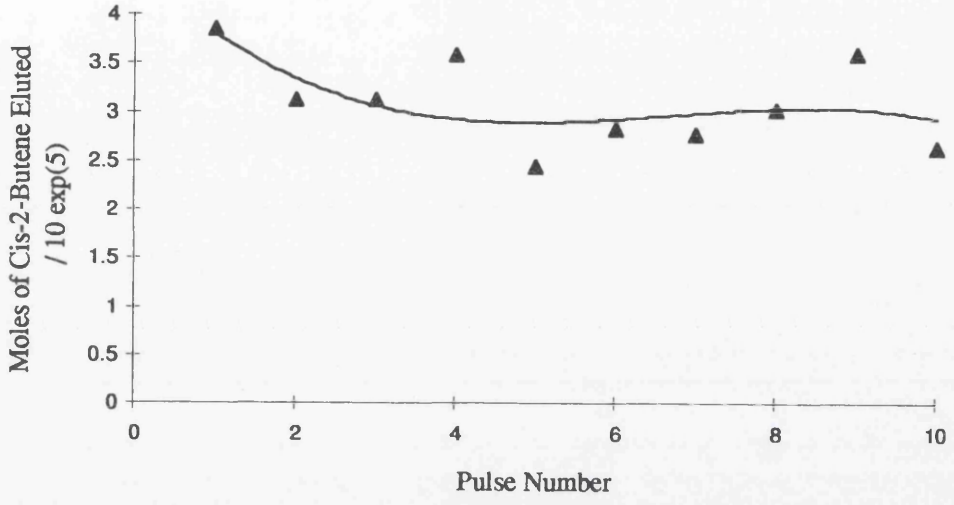

Figure 5.4.5 : Carbon Mass Balance for the Hydrogenation of 2-Butyne (Equimolar Ratio) over Pd/alumina at 373K

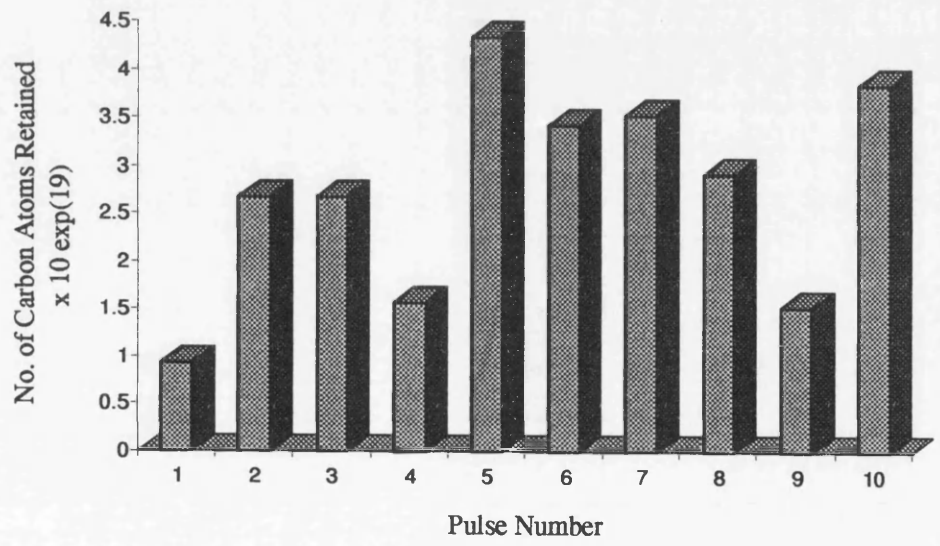

Table 5.3.4 : Hydrogenation of 2-Butyne (Excess Hydrogen) over Pd/alumina at 373K

Pulse Number	Sample Pressure (mB)	Moles of Alkyne In / 10^5	Moles of n-B Out / 10^5	No. of Carbon Atoms In x10^{19}	No. of Carbon Atoms Out x10^{19}	ΔCarbon Atoms x10^{19}
1	40	2.82	2.82	6.79	6.78	0.01
2	40	2.82	2.71	6.79	6.53	0.26
3	40	2.82	2.54	6.79	6.13	0.66
4	40	2.82	2.68	6.79	6.45	0.34
5	40	2.82	2.86	6.79	6.89	-0.10
6	40	2.82	2.90	6.79	6.99	-0.20
7	40	2.82	2.51	6.79	6.05	0.74
8	40	2.82	2.64	6.79	6.37	0.42
9	40	2.82	3.00	6.79	7.22	-0.43
10	40	2.82	2.47	6.79	5.94	0.85
11	40	2.82	3.05	6.79	7.36	-0.57
12	40	2.82	2.91	6.79	7.01	-0.22
13	40	2.82	2.77	6.79	6.68	0.11
14	40	2.82	3.08	6.79	7.41	-0.62
15	40	2.82	2.95	6.79	7.11	-0.32
16	40	2.82	2.42	6.79	5.82	0.97
17	40	2.82	2.52	6.79	6.08	0.71
18	40	2.82	2.35	6.79	5.66	1.13
19	40	2.82	2.46	6.79	5.92	0.87
20	40	2.82	3.05	6.79	7.34	-0.55
21	40	2.82	2.39	6.79	5.77	1.02
22	40	2.82	2.40	6.79	5.79	1.00
23	40	2.82	2.50	6.79	6.03	0.76
24	40	2.82	2.41	6.79	5.79	1.00
25	40	2.82	2.63	6.79	6.32	0.47
26	40	2.82	2.61	6.79	6.28	0.51
27	40	2.82	2.53	6.79	6.09	0.70
28	40	2.82	2.54	6.79	6.12	0.65
29	40	2.82	2.66	6.79	6.42	0.37
30	40	2.82	2.66	6.79	6.41	0.38

Figure 5.4.6 : Variation of Butane Formation with Pulse Number for the Hydrogenation of 2-Butyne (Excess Hydrogen) over Pd/alumina at 373K

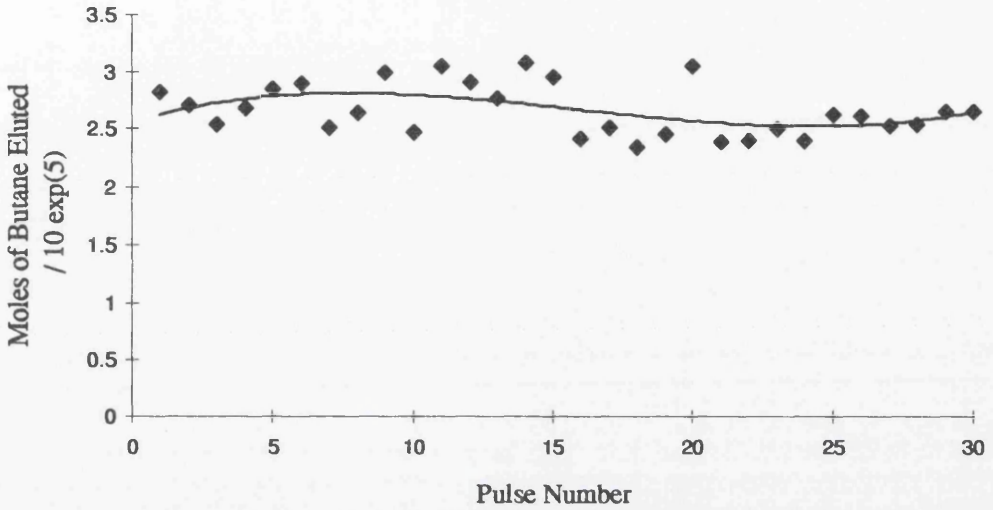

Figure 5.4.7 : Carbon Mass Balance for the Hydrogenation of 2-Butyne (Excess Hydrogen) over Pd/alumina at 373K

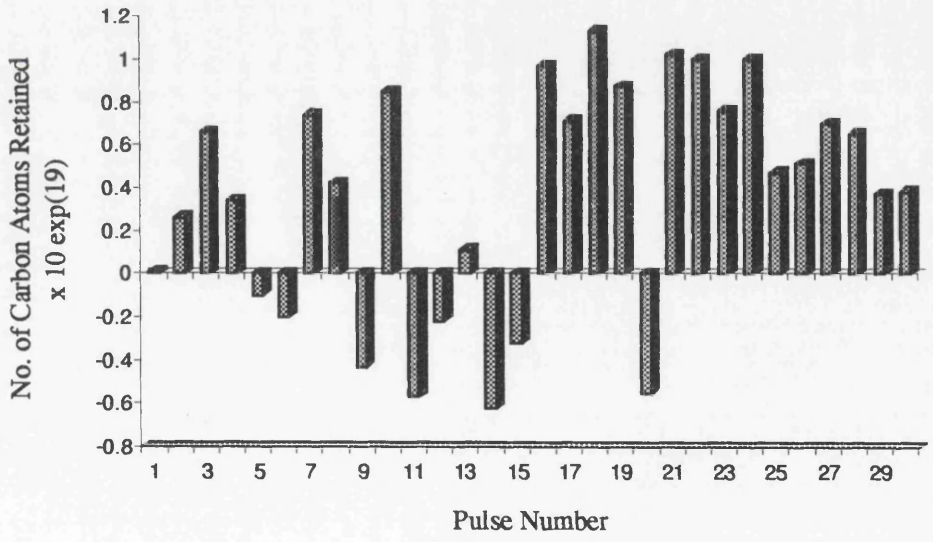

Table 5.3.5 : Hydrogenation of 2-Butyne (Equimolar Ratio) over Pd/alumina at 298K.

Pulse Number	Sample Pressure (mB)	Moles of Alkyne In / 10^5	Moles of **c-2-B** Out / 10^5	Moles of **t-2-B** Out / 10^5	Moles of Alkyne Out / 10^5	Conversion (%)	No. of Carbon Atoms In $x10^{19}$	No. of Carbon Atoms Out $x10^{19}$	ΔCarbon Atoms $x10^{19}$
1	30	4.24	2.02	0.00	2.05	51.50	10.20	9.80	0.40
2	30	4.24	2.02	0.00	2.36	44.30	10.20	10.55	-0.35
3	30	4.24	1.88	0.00	1.82	57.21	10.20	8.91	1.29
4	30	4.24	1.75	0.00	1.55	63.50	10.20	7.94	2.26
5	30	4.24	1.74	0.00	1.52	64.20	10.20	7.85	2.35
6	30	4.24	1.77	0.00	1.75	58.70	10.20	8.48	1.72
7	30	4.24	1.71	0.00	1.48	65.00	10.20	7.68	2.52
8	30	4.24	1.85	0.00	1.79	57.80	10.20	8.76	1.44
9	30	4.24	1.92	0.00	1.73	59.12	10.20	8.79	1.41
10	30	4.24	1.85	0.00	1.74	58.90	10.20	8.64	1.56

Figure 5.4.8 : Variation of Product Distribution with Pulse Number for the Hydrogenation of 2-Butyne (Equimolar Ratio) over Pd/alumina at 298K

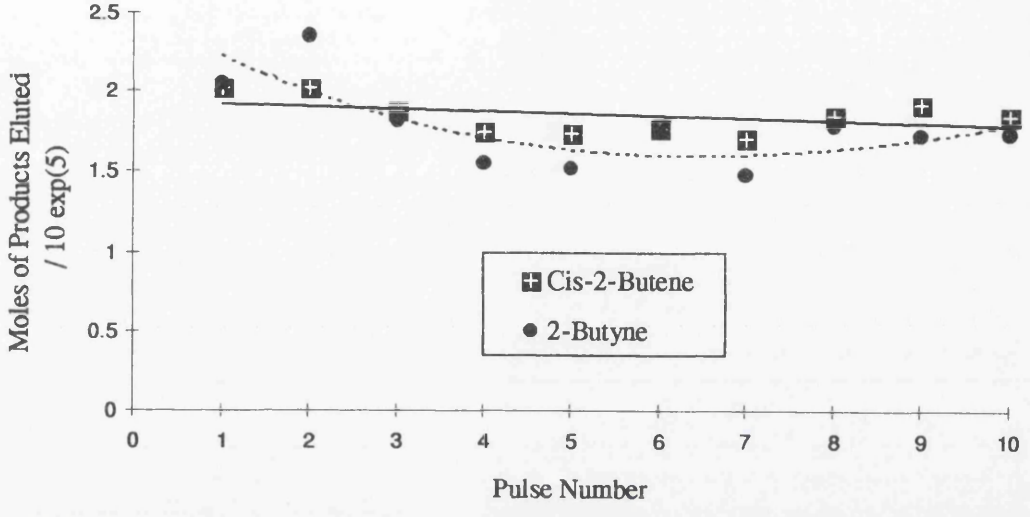

Figure 5.4.9 : Carbon Mass Balance for the Hydrogenation of 2-Butyne (Equimolar Ratio) over Pd/alumina at 298K

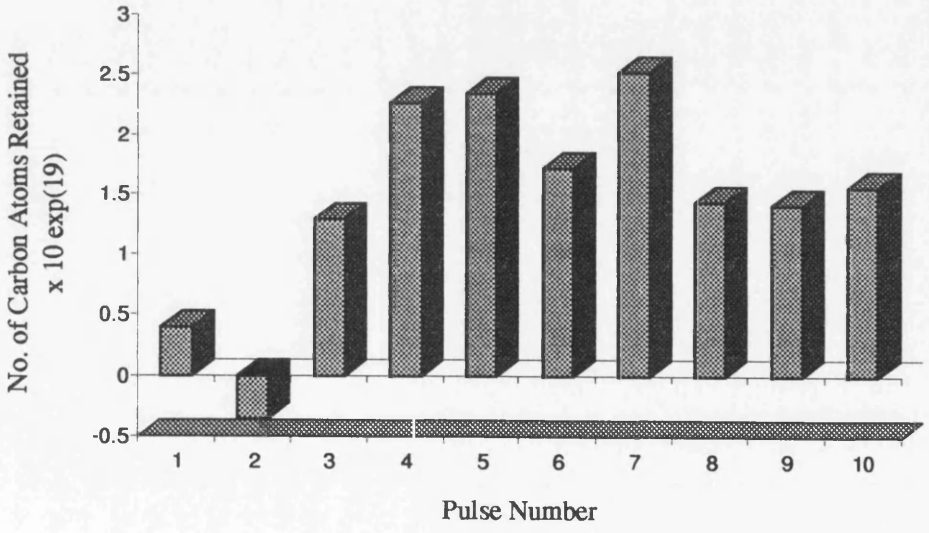

Figure 5.5.0 : Variation of Conversion with Pulse Number for the Hydrogenation of 2-Butyne (Equimolar Ratio) over Pd/alumina at 298K

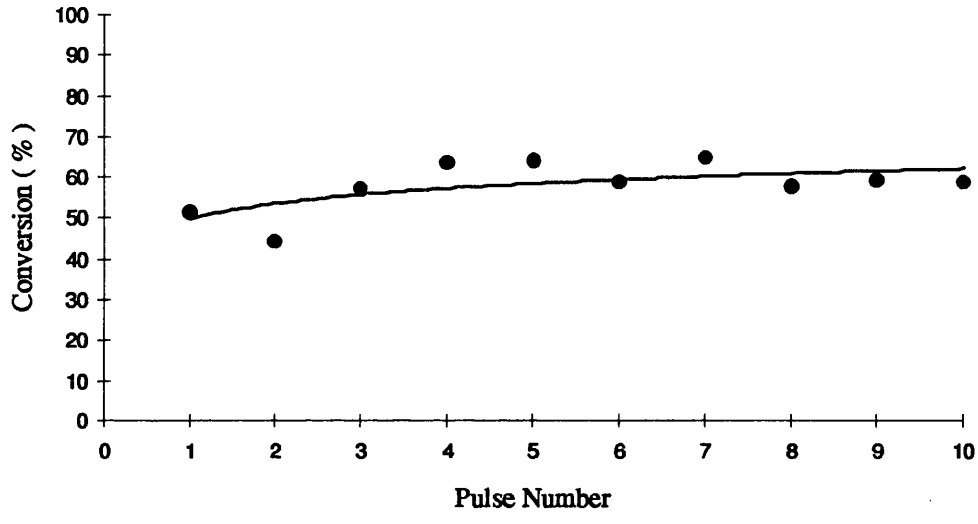

Table 5.3.6 : Hydrogenation of 2-Butyne (Excess Hydrogen) over Pd/alumina at 298K

Pulse Number	Sample Pressure (mB)	Moles of Alkyne In / 10^5	Moles of n-B Out / 10^5	Moles of CH_4 Out / 10^5	No. of Carbon Atoms In $x10^{19}$	No. of Carbon Atoms Out $x10^{19}$	ΔCarbon Atoms $x10^{19}$
1	30	2.12	1.68	0.24	5.10	4.18	0.92
2	30	2.12	1.73	0.20	5.10	4.28	0.82
3	30	2.12	1.77	0.28	5.10	4.43	0.67
4	30	2.12	1.81	0.20	5.10	4.48	0.62
5	30	2.12	1.86	0.22	5.10	4.61	0.49
6	30	2.12	1.78	0.28	5.10	4.45	0.65
7	30	2.12	1.69	0.21	5.10	4.19	0.92
8	30	2.12	1.74	0.23	5.10	4.33	0.77
9	30	2.12	1.96	0.19	5.10	4.83	0.27
10	30	2.12	1.86	0.21	5.10	4.60	0.50
11	30	2.12	1.61	0.21	5.10	4.00	1.10
12	30	2.12	1.68	0.28	5.10	4.22	0.88
13	30	2.12	1.73	0.34	5.10	4.37	0.73
14	30	2.12	1.62	0.39	5.10	4.13	0.97
15	30	2.12	1.72	0.27	5.10	4.30	0.80
16	30	2.12	1.65	0.29	5.10	4.14	0.96
17	30	2.12	1.82	0.26	5.10	4.54	0.56
18	30	2.12	1.74	0.32	5.10	4.38	0.72
19	30	2.12	1.69	0.30	5.10	4.25	0.75
20	30	2.12	1.72	0.41	5.10	4.39	0.71
21	30	2.12	1.77	0.48	5.10	4.55	0.55
22	30	2.12	1.85	0.42	5.10	4.70	0.40
23	30	2.12	1.81	0.40	5.10	4.60	0.50
24	30	2.12	1.80	0.40	5.10	4.57	0.53
25	30	2.12	1.74	0.44	5.10	4.45	0.65
26	30	2.12	1.68	0.38	5.10	4.28	0.82
27	30	2.12	1.72	0.49	5.10	4.43	0.67
28	30	2.12	1.89	0.34	5.10	4.76	0.34
29	30	2.12	1.83	0.40	5.10	4.65	0.45
30	30	2.12	1.85	0.29	5.10	4.62	0.48

Figure 5.5.1 : Variation of Product Distribution with Pulse Number for the Hydrogenation of 2-Butyne (Excess Hydrogen) over Pd/alumina at 298K

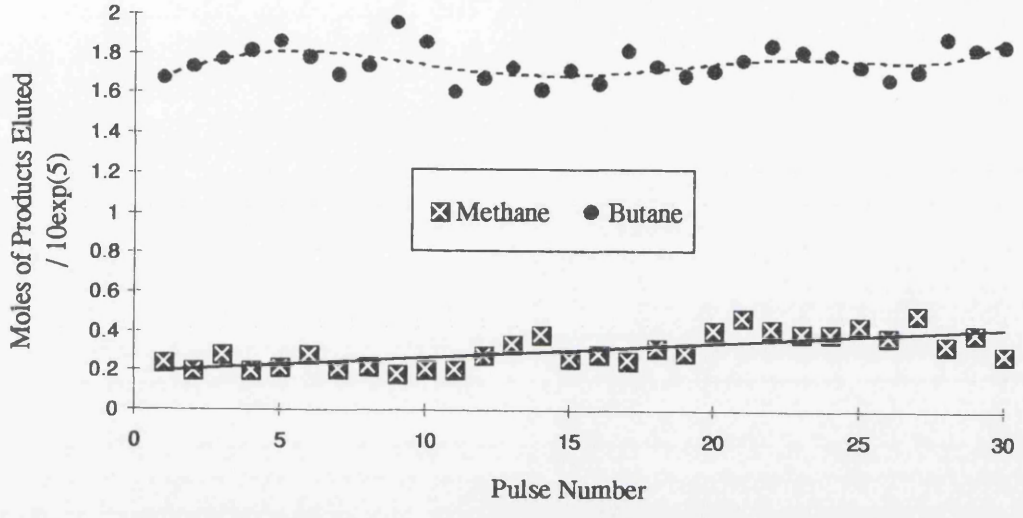

Figure 5.5.2 : Carbon Mass Balance for the Hydrogenation of 2-Butyne (Excess Hydrogen) over Pd/alumina at 298K

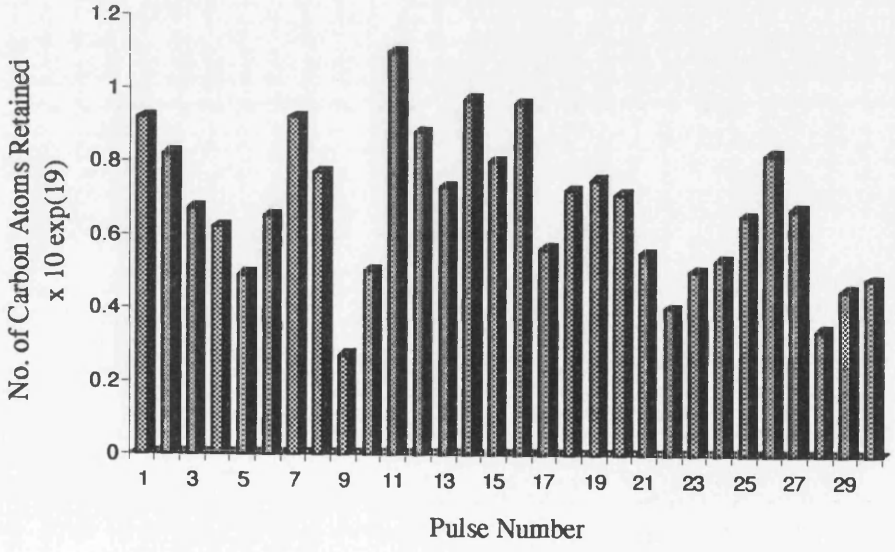

4.4.7 The Hydrogenation of 2-Butyne over Silica-Supported Platinum

Over highly dispersed silica-supported platinum, the hydrogenation of 2-butyne (1:1 :: C_4H_6:H_2) at 465K, produced both olefin isomers. The amount of *trans*-2-butene detected was small, with the yield of *cis*-2-butene observed to decrease with increasing number of pulses, until a limiting value was reached (Figure 5.5.3). The conversion of 2-butyne was maintained at 100% over the first three pulses before decreasing to approximately 60%. The amount of carbon lost to the surface increased and then decreased, until carbon was being removed from the surface (C_{total} positive).

Using excess hydrogen, the hydrogenation of 2-butyne over Pt/silica at 465K, produced *cis*-2-butene as the major product, with 100% conversion of the acetylene maintained over thirty pulses. Over the first two pulses the *trans* isomer was also detected, but only in trace amounts (Table 5.3.8). The yield of *cis*-2-butene was observed to increase (unsteadily) to a limiting value, with the catalyst observed to retain and lose carbon (C_{total} positive).

At 373K, the reaction between 2-butyne and hydrogen (equimolar ratio) over Pt/silica produced *cis*-2-butene. The conversion of 2-butyne was found to decrease sharply after six pulses, from 100% to approximately 27% (Table 5.3.6). The amount of olefin produced decreased with increased number of pulses, with the laydown of surface carbon decreasing from pulse five onward, until negative (C_{total} positive).

Using excess hydrogen, the reaction produced only *cis*-2-butene. The yield of the olefin was observed to fluctuate from pulse to pulse, with the resulting product curve showing behaviour indicative of an oscillating system. This oscillatory behaviour was also seen in the carbon mass balance data (Figure 5.6.3).

Table 5.3.7 : Hydrogenation of 2-Butyne (Equimolar Ratio) over Pt/silica at 465K

Pulse Number	Sample Pressure (mB)	Moles of Alkyne In / 10^5	Moles of **c-2-B** Out / 10^5	Moles of **t-2-B** Out / 10^5	Moles of Alkyne Out / 10^5	Conversion (%)	No. of Carbon Atoms In $x10^{19}$	No. of Carbon Atoms Out $x10^{19}$	ΔCarbon Atoms $x10^{19}$
1	30	4.24	3.89	0.00	0.00	100.0	10.20	9.37	0.83
2	30	4.24	3.67	0.00	0.00	100.0	10.20	8.84	1.36
3	30	4.24	3.11	0.00	0.00	100.0	10.20	7.49	2.71
4	30	4.24	3.32	0.00	0.79	81.33	10.20	9.90	0.30
5	30	4.24	3.25	0.00	1.12	73.46	10.20	10.52	-0.32
6	30	4.24	3.08	0.03	1.37	67.53	10.20	10.79	-0.59
7	30	4.24	2.89	0.04	1.51	64.33	10.20	10.69	-0.49
8	30	4.24	2.85	0.07	1.65	61.00	10.20	11.00	-0.80
9	30	4.24	2.83	0.09	1.67	60.46	10.20	11.06	-0.86
10	30	4.24	2.82	0.10	1.69	60.13	10.20	11.10	-0.90

Figure 5.5.3 : Variation of Product Distribution with Pulse Number for the Hydrogenation of 2-Butyne (Equimolar Ratio) over Pt/silica at 465K

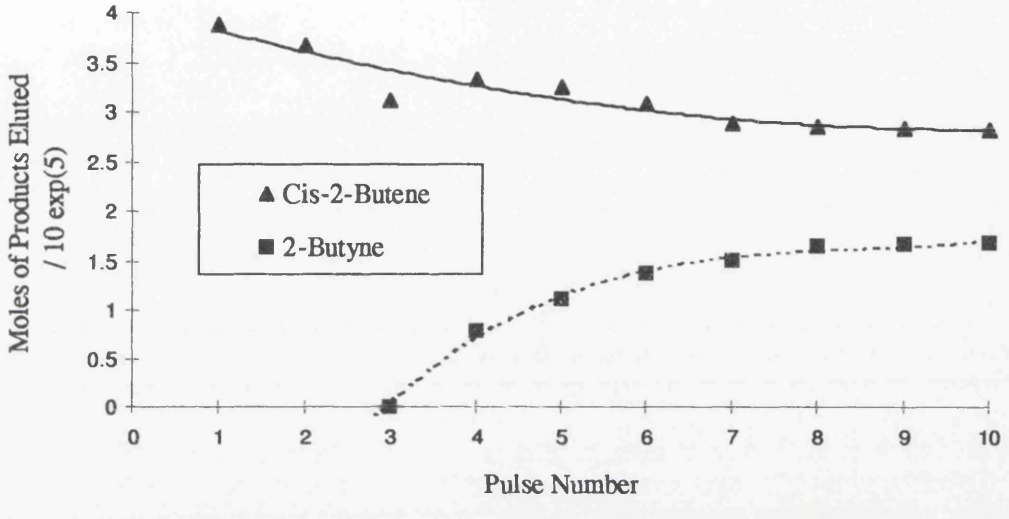

Figure 5.5.4 : Carbon Mass Balance for the Hydrogenation of 2-Butyne (Equimolar Ratio) over Pt/silica at 465K

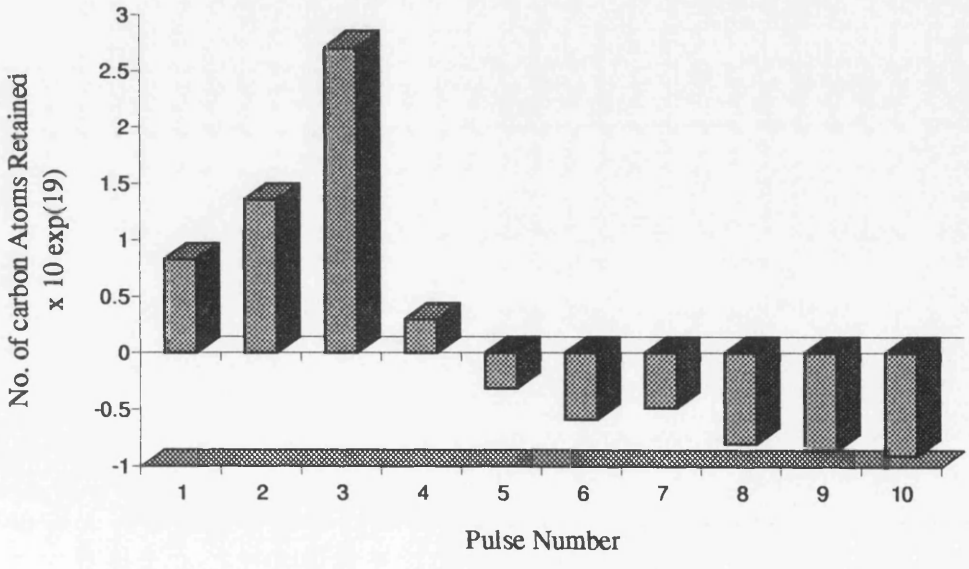

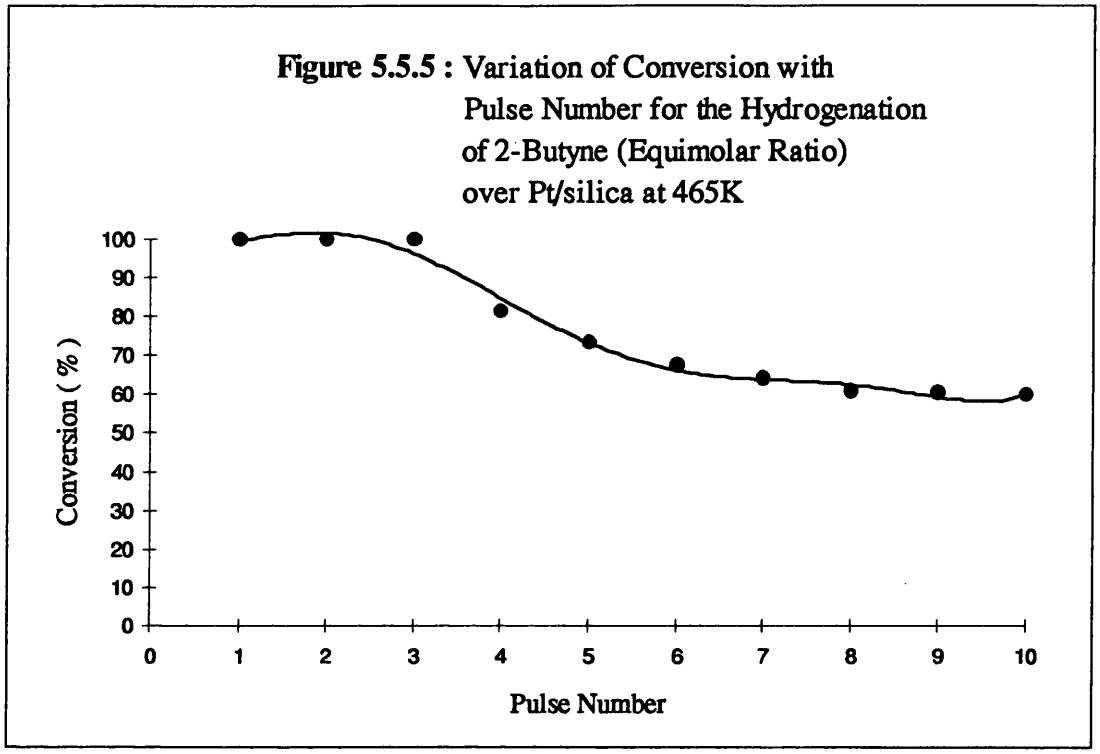

Figure 5.5.5 : Variation of Conversion with Pulse Number for the Hydrogenation of 2-Butyne (Equimolar Ratio) over Pt/silica at 465K

Table 5.3.8 : Hydrogenation of 2-Butyne (Excess Hydrogen) over Pt/silica at 465K

Pulse Number	Sample Pressure (mB)	Moles of Alkyne In / 10^5	Moles of c-2-B Out / 10^5	Moles of t-2-B Out / 10^5	No. of Carbon Atoms In $x10^{19}$	No. of Carbon Atoms Out $x10^{19}$	ΔCarbon Atoms $x10^{19}$
1	30	2.12	0.82	0.55	5.10	3.30	1.80
2	30	2.12	0.94	0.24	5.10	2.84	2.26
3	30	2.12	1.48	0.00	5.10	3.56	1.54
4	30	2.12	1.80	0.00	5.10	4.34	0.76
5	30	2.12	1.64	0.00	5.10	3.95	1.15
6	30	2.12	2.01	0.00	5.10	4.84	0.26
7	30	2.12	1.89	0.00	5.10	4.55	0.55
8	30	2.12	0.88	0.00	5.10	2.12	2.98
9	30	2.12	1.50	0.00	5.10	3.60	1.50
10	30	2.12	1.71	0.00	5.10	4.12	0.98
11	30	2.12	1.82	0.00	5.10	4.38	0.72
12	30	2.12	2.12	0.00	5.10	5.10	0.00
13	30	2.12	1.91	0.00	5.10	4.60	0.50
14	30	2.12	2.00	0.00	5.10	4.81	0.29
15	30	2.12	2.02	0.00	5.10	4.86	0.24
16	30	2.12	2.25	0.00	5.10	5.41	-0.31
17	30	2.12	2.36	0.00	5.10	5.68	-0.58
18	30	2.12	2.33	0.00	5.10	5.61	-0.51
19	30	2.12	2.22	0.00	5.10	5.34	-0.24
20	30	2.12	2.10	0.00	5.10	5.06	0.04
21	30	2.12	2.17	0.00	5.10	5.22	-0.12
22	30	2.12	2.20	0.00	5.10	5.29	-0.19
23	30	2.12	2.27	0.00	5.10	5.47	-0.37
24	30	2.12	2.24	0.00	5.10	5.39	-0.29
25	30	2.12	1.92	0.00	5.10	4.62	0.48
26	30	2.12	2.21	0.00	5.10	5.32	-0.22
27	30	2.12	2.21	0.00	5.10	5.32	-0.22
28	30	2.12	1.98	0.00	5.10	4.77	0.33
29	30	2.12	1.89	0.00	5.10	4.55	0.55
30	30	2.12	2.09	0.00	5.10	5.03	0.07

Figure 5.5.6 : Variation of Product Distribution with Pulse Number for the Hydrogenation of 2-Butyne (Excess Hydrogen) over Pt/silica at 465K

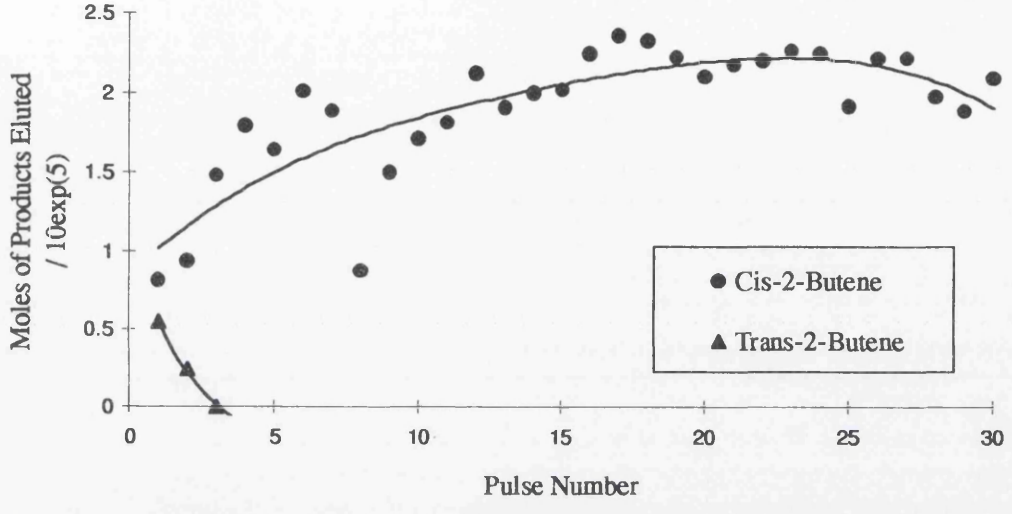

Figure 5.5.7 : Carbon Mass Balance for the Hydrogenation of 2-Butyne (Excess Hydrogen) over Pt/silica at 465K

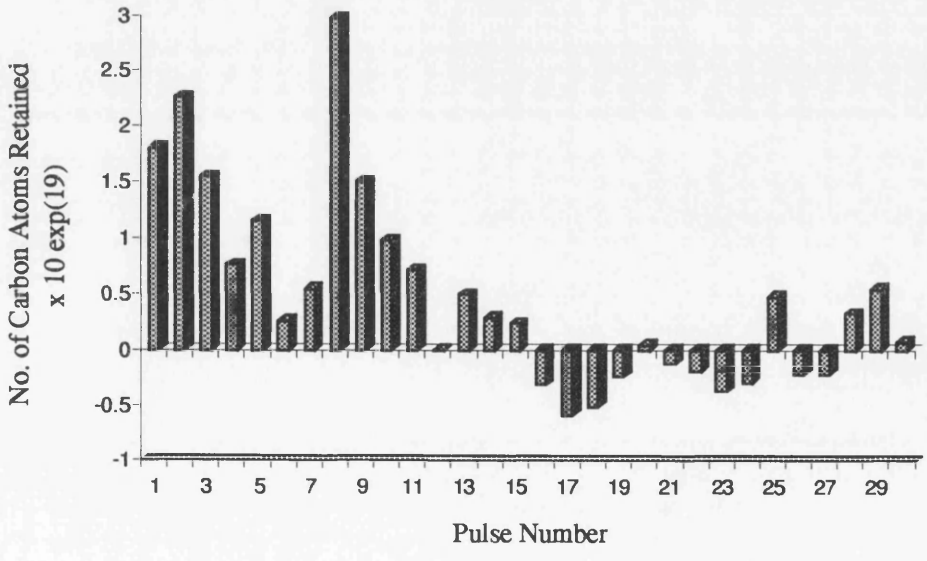

Table 5.3.9 : Hydrogenation of 2-Butyne (Equimolar Ratio) over Pt/silica at 373K

Pulse Number	Sample Pressure (mB)	Moles of Alkyne In / 10^5	Moles of **c-2-B** Out / 10^5	Moles of Alkyne Out / 10^5	Conversion (%)	No. of Carbon Atoms In $x10^{19}$	No. of Carbon Atoms Out $x10^{19}$	ΔCarbon Atoms $x10^{19}$
1	30	4.24	3.02	0.00	100.0	10.20	7.27	2.93
2	30	4.24	2.73	0.00	100.0	10.20	6.57	3.63
3	30	4.24	2.89	0.00	100.0	10.20	6.96	3.24
4	30	4.24	2.37	0.00	100.0	10.20	5.70	4.50
5	30	4.24	2.50	0.00	100.0	10.20	6.02	4.18
6	30	4.24	1.73	3.10	26.89	10.20	11.63	-1.43
7	30	4.24	1.86	2.90	31.60	10.20	11.46	-1.26
8	30	4.24	1.44	2.57	39.38	10.20	9.66	0.54
9	30	4.24	2.79	2.13	49.64	10.20	11.85	-1.65
10	30	4.24	2.60	2.60	38.68	10.20	12.53	-2.33

Figure 5.5.8 : Variation of Product Distribution with Pulse Number for the Hydrogenation of 2-Butyne (Equimolar Ratio) over Pt/silica at 373K

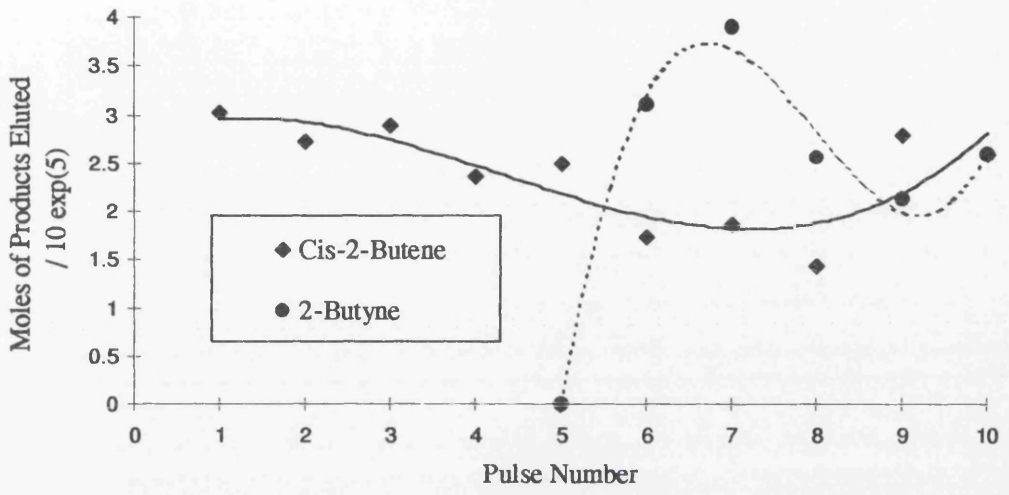

Figure 5.5.9 : Carbon Mass Balance for the Hydrogenation of 2-Butyne (Equimolar Ratio) over Pt/silica at 373K

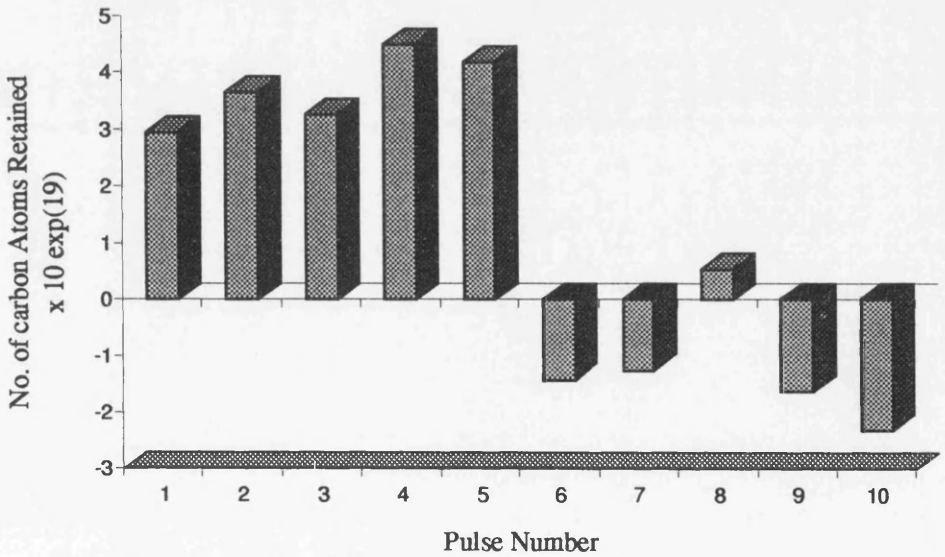

Figure 5.6.0 : Variation of Conversion with Pulse Number for the Hydrogenation of 2-Butyne (Equimolar Ratio) over Pt/silica at 373K

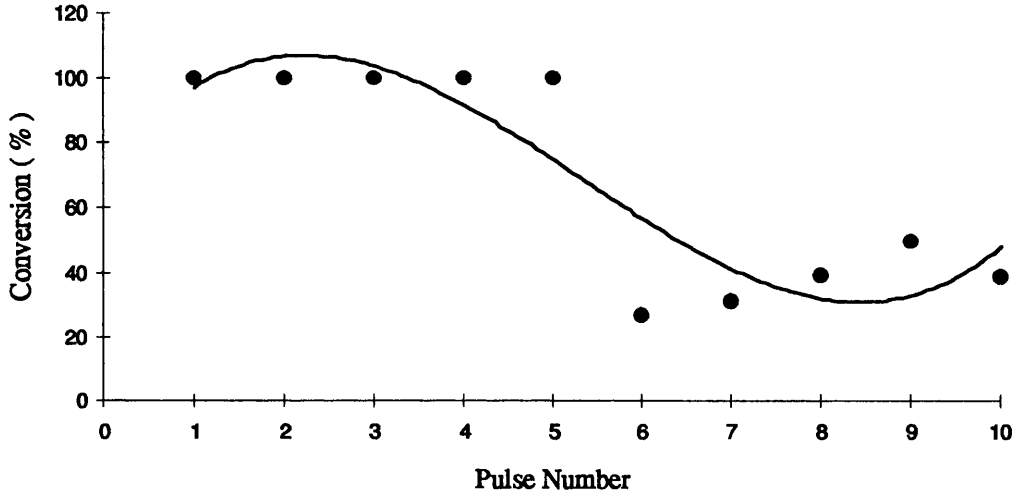

Table 5.4.0 : Hydrogenation of 2-Butyne (Excess Hydrogen) over Pt/silica at 373K

Pulse Number	Sample Pressure (mB)	Moles of Alkyne In / 10^5	Moles of c-2-B Out / 10^5	No. of Carbon Atoms In $x10^{19}$	No. of Carbon Atoms Out $x10^{19}$	ΔCarbon Atoms $x10^{19}$
1	40	2.82	1.36	6.80	3.28	3.52
2	40	2.82	2.97	6.80	7.15	-0.35
3	40	2.82	2.73	6.80	6.59	0.21
4	40	2.82	2.82	6.80	6.80	0.00
5	40	2.82	3.15	6.80	7.58	-0.78
6	40	2.82	2.50	6.80	6.02	0.78
7	40	2.82	2.61	6.80	6.29	0.51
8	40	2.82	2.95	6.80	7.10	-0.30
9	40	2.82	2.51	6.80	6.06	0.74
10	40	2.82	3.04	6.80	7.32	-0.52
11	40	2.82	2.47	6.80	5.95	0.85
12	40	2.82	2.52	6.80	6.07	0.73
13	40	2.82	3.00	6.80	7.22	-0.42
14	40	2.82	2.82	6.80	6.80	0.00
15	40	2.82	2.96	6.80	7.14	-0.34
16	40	2.82	2.44	6.80	5.87	0.93
17	40	2.82	3.04	6.80	7.33	-0.53
18	40	2.82	2.80	6.80	6.74	0.06
19	40	2.82	2.93	6.80	7.05	-0.25
20	40	2.82	1.78	6.80	4.28	2.52
21	40	2.82	2.99	6.80	7.20	-0.40
22	40	2.82	2.12	6.80	5.12	1.68
23	40	2.82	2.24	6.80	5.40	1.40
24	40	2.82	2.49	6.80	5.99	0.81
25	40	2.82	2.15	6.80	5.17	1.63
26	40	2.82	2.25	6.80	5.42	1.38
27	40	2.82	2.36	6.80	5.69	1.11
28	40	2.82	2.56	6.80	6.17	0.63
29	40	2.82	2.36	6.80	5.70	1.10
30	40	2.82	2.67	6.80	6.44	0.36

Figure 5.6.1 : Variation of Cis-2-Butene Formation with Pulse Number for the Hydrogenation of 2-Butyne (Excess Hydrogen) over Pt/silica at 373K

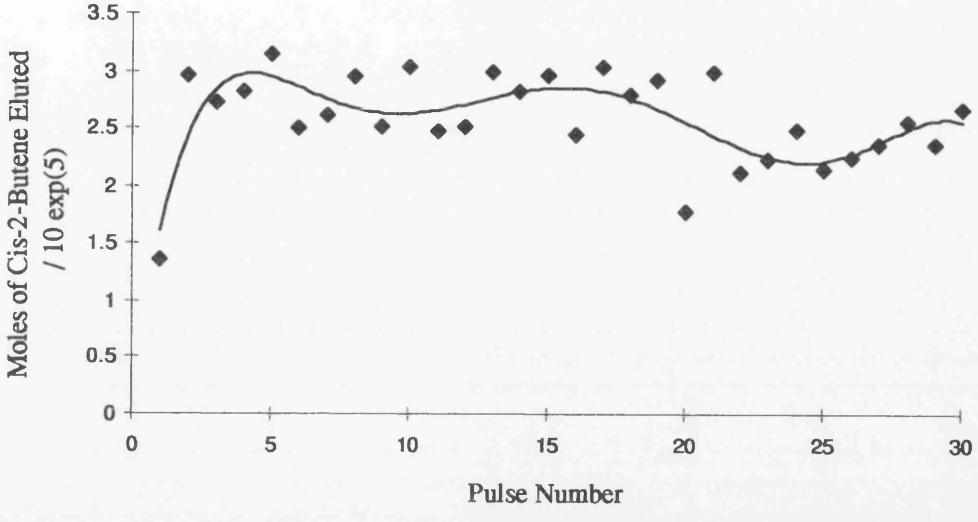

Figure 5.6.2 : Carbon Mass Balance for the Hydrogenation of 2-Butyne (Excess Hydrogen) over Pt/silica at 373K

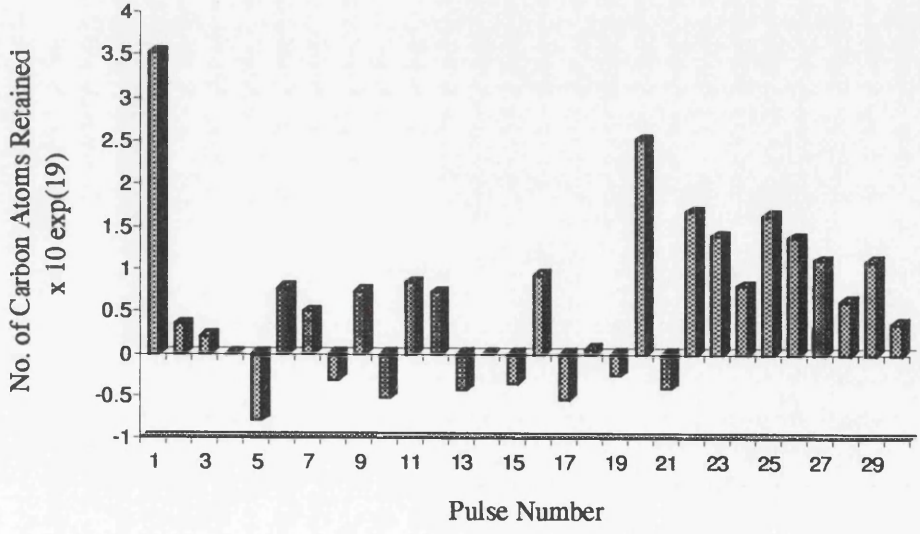

4.4.8 The Hydrogenation of 2-Butyne over Alumina-Supported Platinum

For Pt/alumina, the reaction between 2-butyne and hydrogen (equimolar ratio) at 465K produced both olefin isomers, with the conversion of 2-butyne observed to be low. However, although the initial conversion values for this reaction were less than that seen on the other catalysts, the activity of this substrate was essentially constant over ten pulses. The yield of both *cis* and *trans*-2-butene were near constant, although the latter increased initially before achieving steady state. The deposition of carbon in these reactions was found to decrease (pulse 4 negative), before increasing again (Figure 5.6.4).

Using an excess of hydrogen produced both *n*-butane and methane at 465K. The complete removal of 2-butyne was again observed over thirty pulses, with the amount of butane formed increasing to a limiting value (Figure 5.6.6). Methane production decreased with increased number of pulses, and was non-existent by pulse eleven. The catalyst took up most carbon in pulses six and seven, and over the course of the pulses, no carbon was lost from the surface.

Cis-2-butene was the sole hydrogenation product of 2-butyne over Pt/alumina at 373K, when an equimolar reactant ratio was employed. The conversion of the acetylene decreased with increased number of pulses, as seen in Table 5.4.3, with the yield of the olefin oscillating slightly throughout. The trend of carbon laydown, as shown in Figure 5.6.9, displayed increasing deposition as the yield of olefin decreased, and *vice versa.*

With excess hydrogen, *n*-butane was produced, and 2-butyne was totally converted over thirty pulses (Table 5.4.4). The yield of alkane fluctuated over thirty pulses, with similar behaviour observed in the carbon deposition data.

Table 5.4.1 : Hydrogenation of 2-Butyne (Equimolar Ratio) over Pt/alumina at 465K

Pulse Number	Sample Pressure (mB)	Moles of Alkyne In / 10^5	Moles of **c-2-B** Out / 10^5	Moles of **t-2-B** Out / 10^5	Moles of Alkyne Out / 10^5	Conversion (%)	No. of Carbon Atoms In $x10^{19}$	No. of Carbon Atoms Out $x10^{19}$	ΔCarbon Atoms $x10^{19}$
1	30	4.24	1.25	0.12	1.72	59.40	10.20	7.44	2.76
2	30	4.24	0.87	0.33	2.57	39.30	10.20	9.08	1.12
3	30	4.24	0.84	0.39	2.14	49.60	10.20	8.11	2.09
4	30	4.24	1.62	0.64	2.28	46.20	10.20	10.93	-0.73
5	30	4.24	1.44	0.59	2.15	49.30	10.20	10.07	0.13
6	30	4.24	1.23	0.53	2.08	51.00	10.20	9.25	0.95
7	30	4.24	1.10	0.49	1.73	59.00	10.20	7.99	2.21
8	30	4.24	1.33	0.53	1.84	56.50	10.20	8.91	1.29
9	30	4.24	1.25	0.51	1.88	55.60	10.20	8.76	1.44
10	30	4.24	1.19	0.50	1.81	57.30	10.20	8.43	1.77

Figure 5.6.3 : Variation of Product Distribution with Pulse Number for the Hydrogenation of 2-Butyne (Equimolar Ratio) over Pt/alumina at 465K

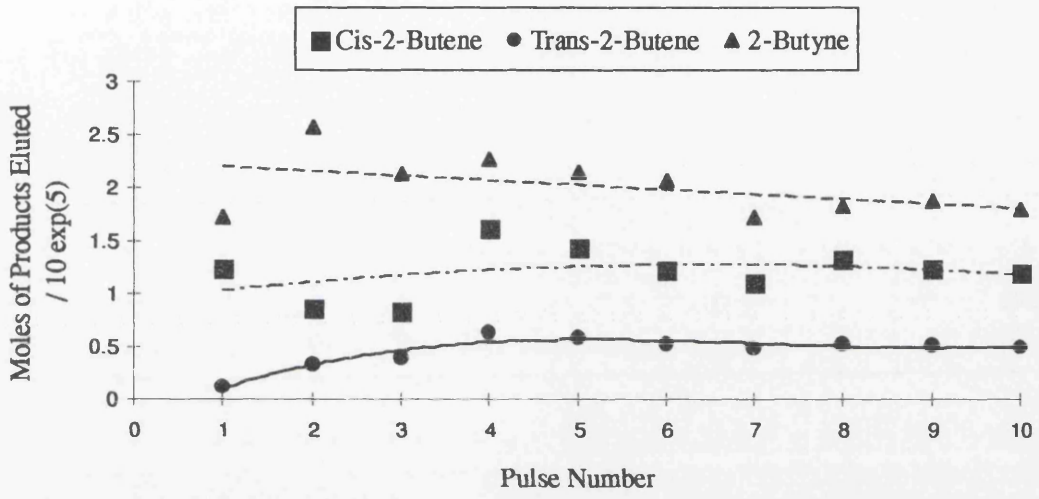

Figure 5.6.4 : Carbon Mass Balance for the Hydrogenation of 2-Butyne (Equimolar Ratio) over Pt/alumina at 465K

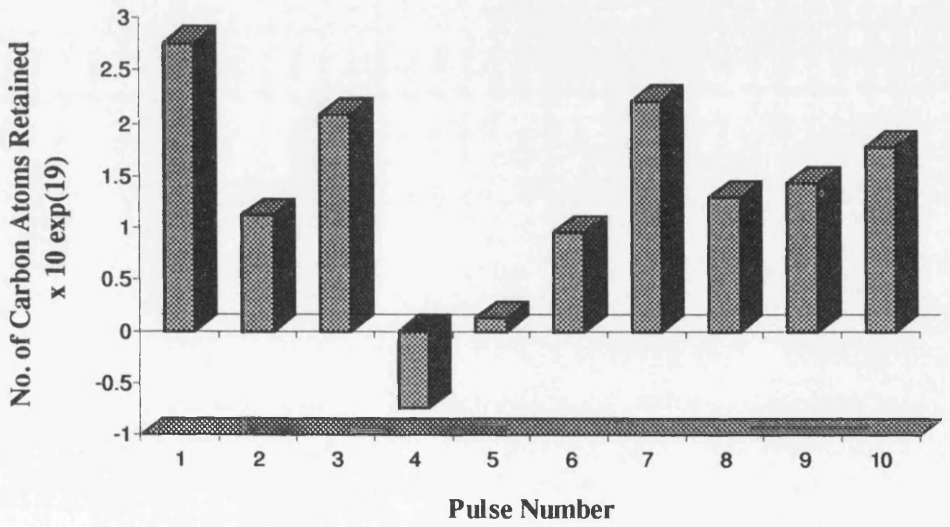

Figure 5.6.5 : Variation of Conversion with Pulse Number for the Hydrogenation of 2-Butyne (Equimolar Ratio) over Pt/alumina at 465K

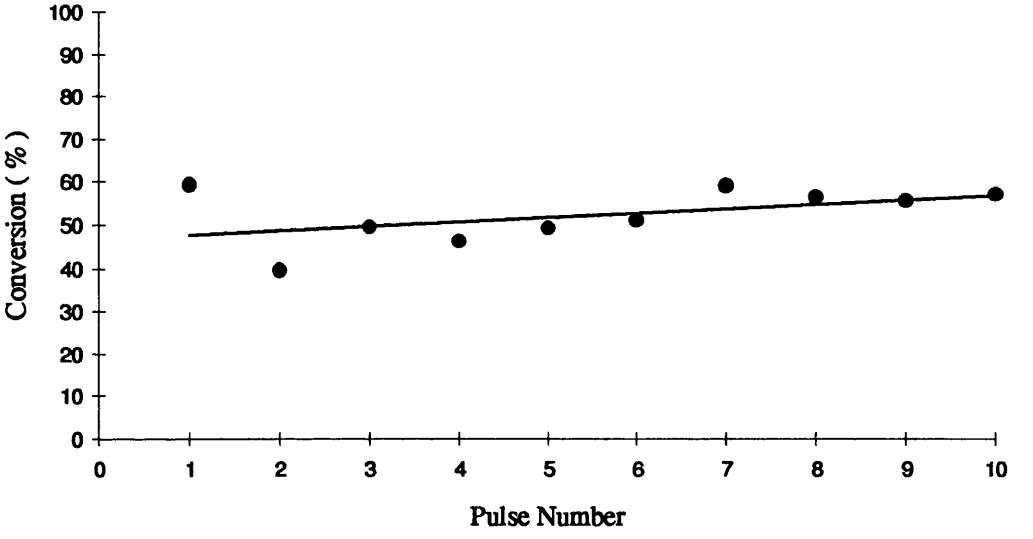

Table 5.4.2 : Hydrogenation of 2-Butyne (Excess Hydrogen) over Pt/alumina at 465K

Pulse Number	Sample Pressure (mB)	Moles of Alkyne In / 10^5	Moles of n-B Out / 10^5	Moles of CH_4 Out / 10^5	No. of Carbon Atoms In $x10^{19}$	No. of Carbon Atoms Out $x10^{19}$	ΔCarbon atoms $x10^{19}$
1	30	2.12	1.09	0.72	5.10	3.05	2.05
2	30	2.12	1.44	0.59	5.10	3.81	1.29
3	30	2.12	1.92	0.27	5.10	4.79	0.31
4	30	2.12	1.94	0.28	5.10	4.84	0.26
5	30	2.12	1.84	0.23	5.10	4.57	0.53
6	30	2.12	0.73	0.62	5.10	2.12	2.98
7	30	2.12	0.52	0.61	5.10	1.62	3.48
8	30	2.12	1.54	0.85	5.10	4.21	0.89
9	30	2.12	1.78	0.49	5.10	4.57	0.53
10	30	2.12	1.90	0.53	5.10	4.89	0.21
11	30	2.12	1.91	0.00	5.10	4.60	0.50
12	30	2.12	1.94	0.00	5.10	4.67	0.43
13	30	2.12	1.70	0.00	5.10	4.09	1.01
14	30	2.12	1.88	0.00	5.10	4.53	0.57
15	30	2.12	1.77	0.00	5.10	4.26	0.84
16	30	2.12	1.95	0.00	5.10	4.69	0.41
17	30	2.12	1.90	0.00	5.10	4.58	0.52
18	30	2.12	1.83	0.00	5.10	4.41	0.69
19	30	2.12	1.91	0.00	5.10	4.60	0.50
20	30	2.12	1.92	0.00	5.10	4.62	0.48
21	30	2.12	1.99	0.00	5.10	4.79	0.31
22	30	2.12	2.02	0.00	5.10	4.86	0.24
23	30	2.12	1.96	0.00	5.10	4.72	0.38
24	30	2.12	1.97	0.00	5.10	4.75	0.35
25	30	2.12	2.10	0.00	5.10	5.06	0.04
26	30	2.12	2.07	0.00	5.10	4.98	0.12
27	30	2.12	2.11	0.00	5.10	5.08	0.02
28	30	2.12	2.03	0.00	5.10	4.89	0.21
29	30	2.12	1.96	0.00	5.10	4.72	0.38
30	30	2.12	2.01	0.00	5.10	4.84	0.26

Figure 5.6.6 : Variation of Product Distribution with Pulse Number for the Hydrogenation of 2-Butyne (Excess Hydrogen) over Pt/alumina at 465K

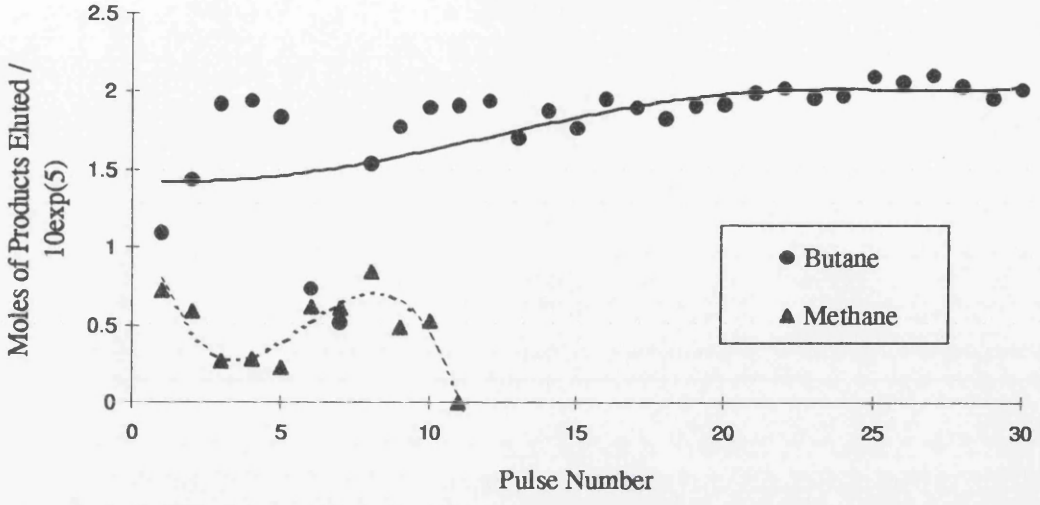

Figure 5.6.7 : Carbon Mass Balance for the Hydrogenation of 2-Butyne (Excess Hydrogen) over Pt/alumina at 465K

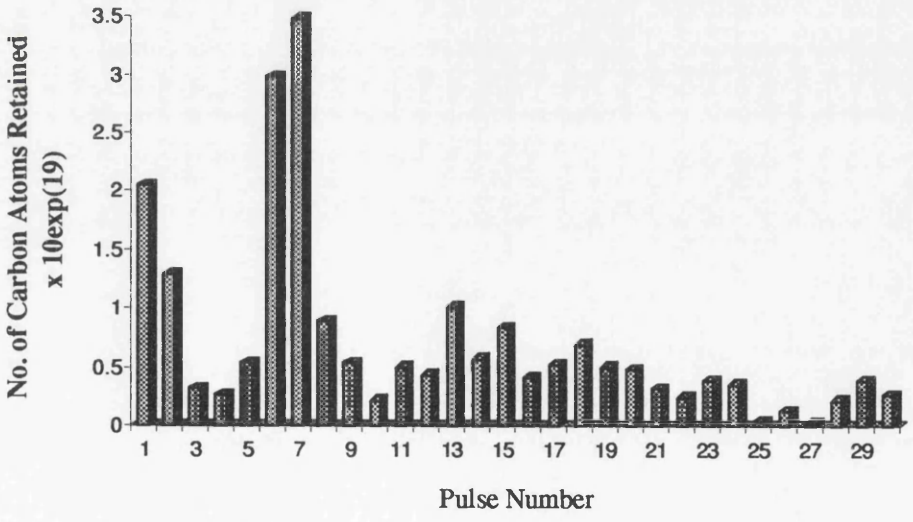

Table 5.4.3 : Hydrogenation of 2-Butyne (Equimolar Ratio) over Pt/alumina at 373K

Pulse Number	Sample Pressure (mB)	Moles of Alkyne In / 10^5	Moles of **c-2-B** Out / 10^5	Moles of Alkyne Out / 10^5	Conversion (%)	No. of Carbon Atoms In $x10^{19}$	No. of Carbon Atoms Out $x10^{19}$	ΔCarbon Atoms $x10^{19}$
1	30	4.24	4.12	0.00	100.0	10.20	9.92	0.28
2	30	4.24	3.91	0.00	100.0	10.20	9.42	0.78
3	30	4.24	3.99	0.00	100.0	10.20	9.61	0.59
4	30	4.24	3.22	0.56	86.79	10.20	9.10	1.10
5	30	4.24	2.75	0.63	85.14	10.20	8.14	2.06
6	30	4.24	2.91	0.65	84.67	10.20	8.65	1.55
7	30	4.24	3.01	0.70	83.37	10.20	8.93	1.27
8	30	4.24	3.12	0.69	83.77	10.20	9.17	1.03
9	30	4.24	3.23	0.70	83.46	10.20	9.47	0.73
10	30	4.24	3.19	0.71	83.13	10.20	9.39	0.81

Figure 5.6.8 : Variation of Product Distribution with Pulse Number for the Hydrogenation of 2-Butyne (Equimolar Ratio) over Pt/alumina at 373K

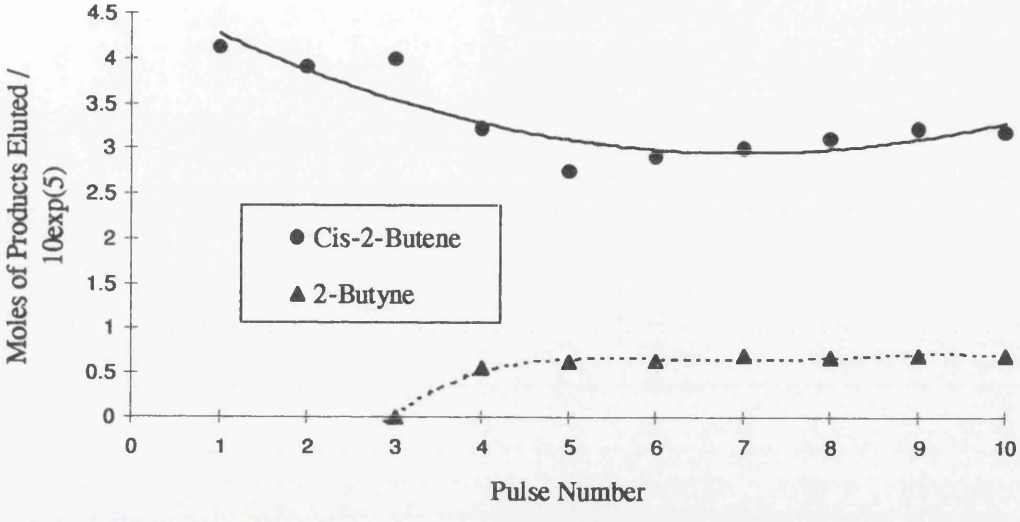

Figure 5.6.9 : Carbon Mass Balance for the Hydrogenation of 2-Butyne (Equimolar Ratio) over Pt/alumina at 373K

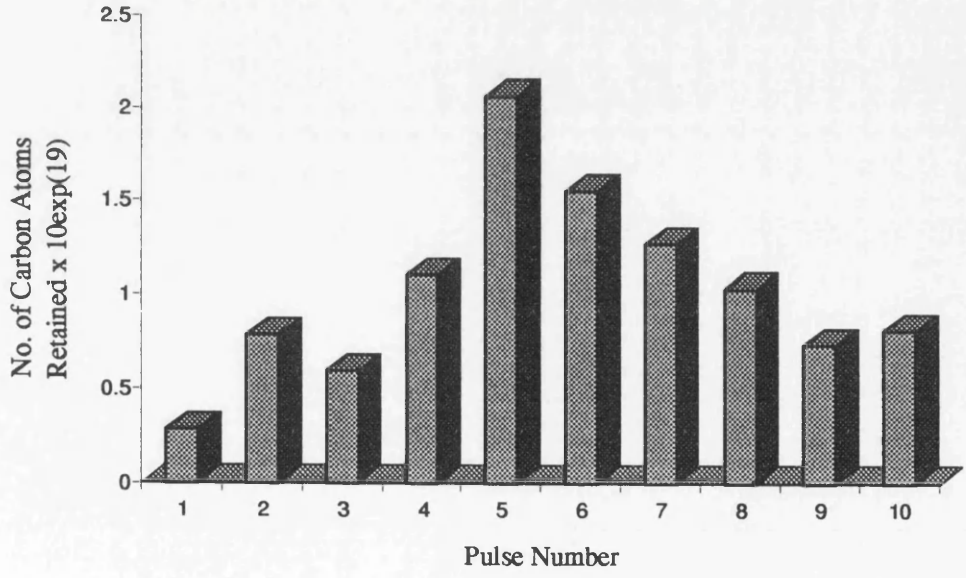

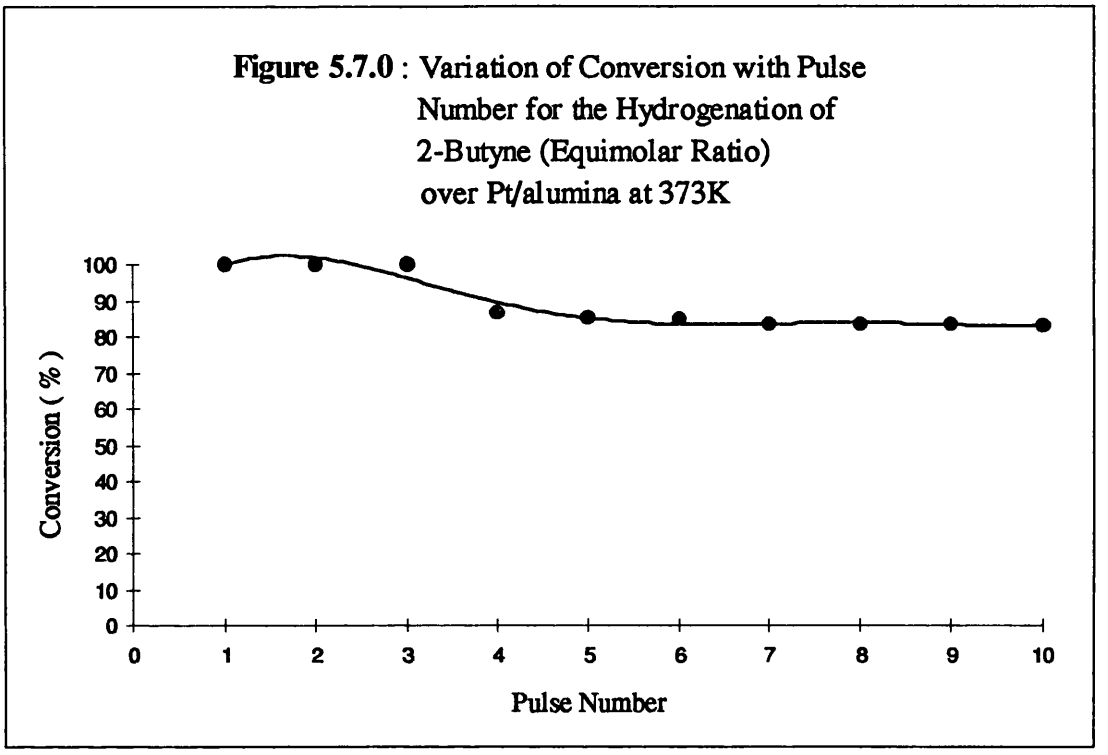

Figure 5.7.0 : Variation of Conversion with Pulse Number for the Hydrogenation of 2-Butyne (Equimolar Ratio) over Pt/alumina at 373K

Table 5.4.4 : Hydrogenation of 2-Butyne (Excess Hydrogen) over Pt/alumina at 373K

Pulse Number	Sample Pressure (mB)	Moles of Alkyne In / 10^5	Moles of n-B Out / 10^5	No. of Carbon Atoms In x10^{19}	No. of Carbon Atoms Out x10^{19}	ΔCarbon Atoms x10^{19}
1	40	2.82	2.20	6.80	5.29	1.51
2	40	2.82	2.76	6.80	6.64	0.16
3	40	2.82	3.11	6.80	7.50	-0.70
4	40	2.82	2.80	6.80	6.74	0.06
5	40	2.82	2.51	6.80	6.03	0.77
6	40	2.82	2.63	6.80	6.33	0.47
7	40	2.82	2.76	6.80	6.64	0.16
8	40	2.82	2.57	6.80	6.18	0.62
9	40	2.82	3.22	6.80	7.76	-0.96
10	40	2.82	2.56	6.80	6.16	0.64
11	40	2.82	3.27	6.80	7.88	-1.08
12	40	2.82	3.32	6.80	8.00	-1.20
13	40	2.82	2.63	6.80	6.34	0.46
14	40	2.82	2.69	6.80	6.49	0.31
15	40	2.82	2.61	6.80	6.28	0.52
16	40	2.82	3.19	6.80	7.68	-0.88
17	40	2.82	2.62	6.80	6.32	0.48
18	40	2.82	2.92	6.80	7.03	-0.23
19	40	2.82	2.67	6.80	6.44	0.36
20	40	2.82	2.60	6.80	6.25	0.55
21	40	2.82	2.50	6.80	6.03	0.77
22	40	2.82	2.45	6.80	5.90	0.90
23	40	2.82	2.34	6.80	5.64	1.16
24	40	2.82	2.50	6.80	6.03	0.73
25	40	2.82	2.73	6.80	6.59	0.21
26	40	2.82	2.53	6.80	6.09	0.71
27	40	2.82	2.63	6.80	6.33	0.47
28	40	2.82	2.50	6.80	6.01	0.79
29	40	2.82	2.50	6.80	6.02	0.78
30	40	2.82	2.57	6.80	6.18	0.62

Figure 5.7.1 : Variation of Butane Formation with Pulse Number for the Hydrogenation of 2-Butyne (Excess Hydrogen) over Pt/alumina at 373K

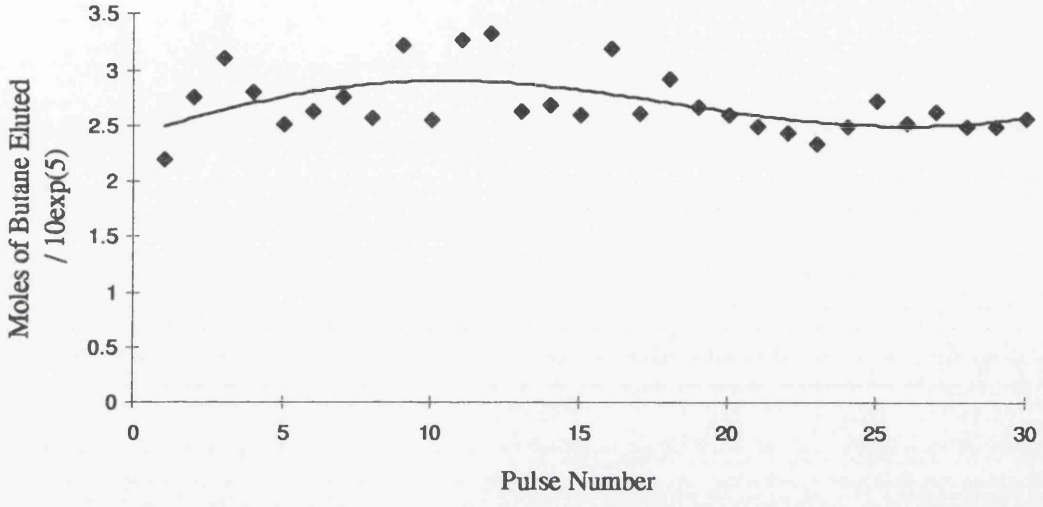

Figure 5.7.2 : Carbon Mass Balance for the Hydrogenation of 2-Butyne (Excess Hydrogen) over Pt/alumina at 373K

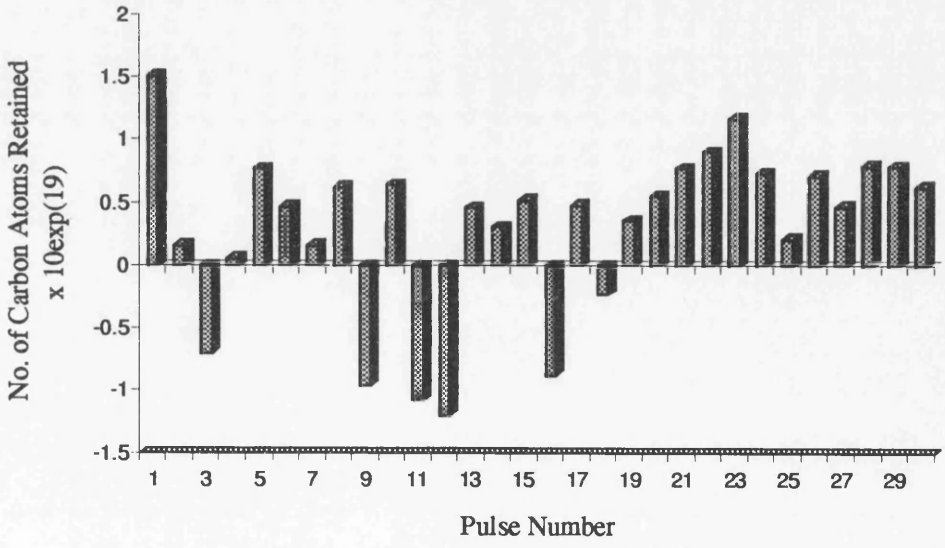

Section Four

INFRA-RED SPECTROSCOPY RESULTS

4.4.9 Infra-Red Spectroscopy Results for 2-Butyne/Hydrogen Chemisorption on Silica-Supported Palladium

This section details the results obtained from the diffuse reflectance and transmission infra-red studies performed *in situ* on the adsorption of a 2-butyne/hydrogen mixture over silica-supported palladium. The results of reaction chemistry show that the hydrogenation of 2-butyne over Pd/silica using an equimolar reactant ratio, yields *cis*-2-butene as the sole product at ambient temperature.

It was the aim of this section of work to apply infra-red spectroscopy to ascertain the nature of the acetylene adsorption, and hence, identify the correct reaction mechanism.

Figure 5.7.3 shows the spectra obtained from sequential pulsing of the hydrogenation mixture over the activated catalyst, with the number of pulses increasing as the y-axis is scaled (For transmission, pulses increase as y-axis is descended). Table 5.4.5 compares the bands obtained for the adsorption experiments and those observed for gas phase 2-butyne (Figure 5.7.4).

Table 5.4.5 : *Assigment of IR Bands for 2-Butyne(g) and Adsorbed 2-Butyne*

2-Butyne (g)	2-Butyne on Pd/silica	Assignments
		Vibration
$2927_{(s)}$	$2933_{(s)}$	$\upsilon CH_{3(asym)}$
$2868_{(s)}$	$2870_{(s)}$	$\upsilon CH_{3(sym)}$
$2742_{(w)}$	$2757_{(w)}$	$2\delta CH_{3(sym)}$
$1387_{(w)}$	$1375_{(w)}$	$\delta CH_{3(sym)}$
$1452_{(s)}$	----	$\delta CH_{3(asym)}$

Figure 5.7.3 : DRIFTS Spectra of Pd/silica Reaction
with (1 : 1 :: 2-Butyne : Hydrogen)

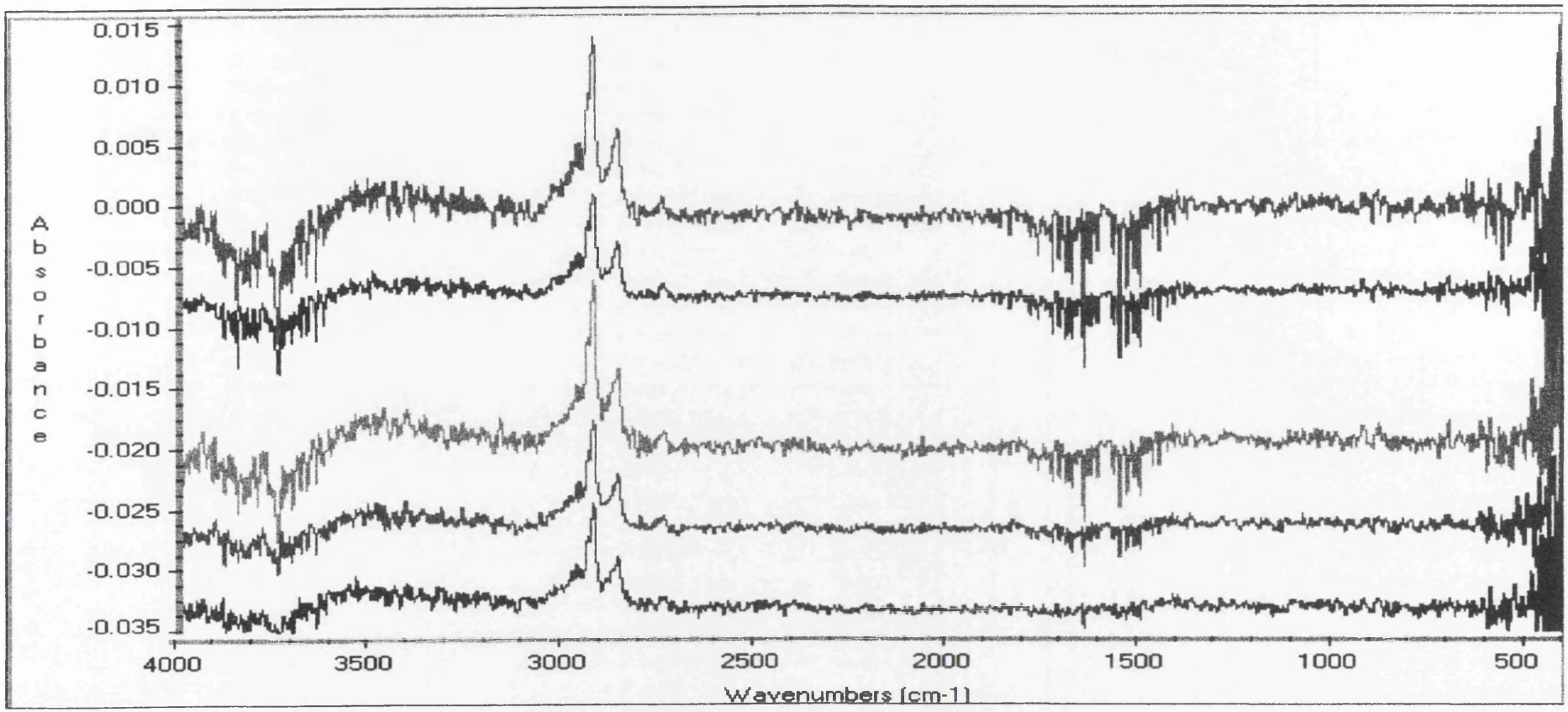

Figure 5.7.4 : Gas Phase 2-Butyne Spectrum

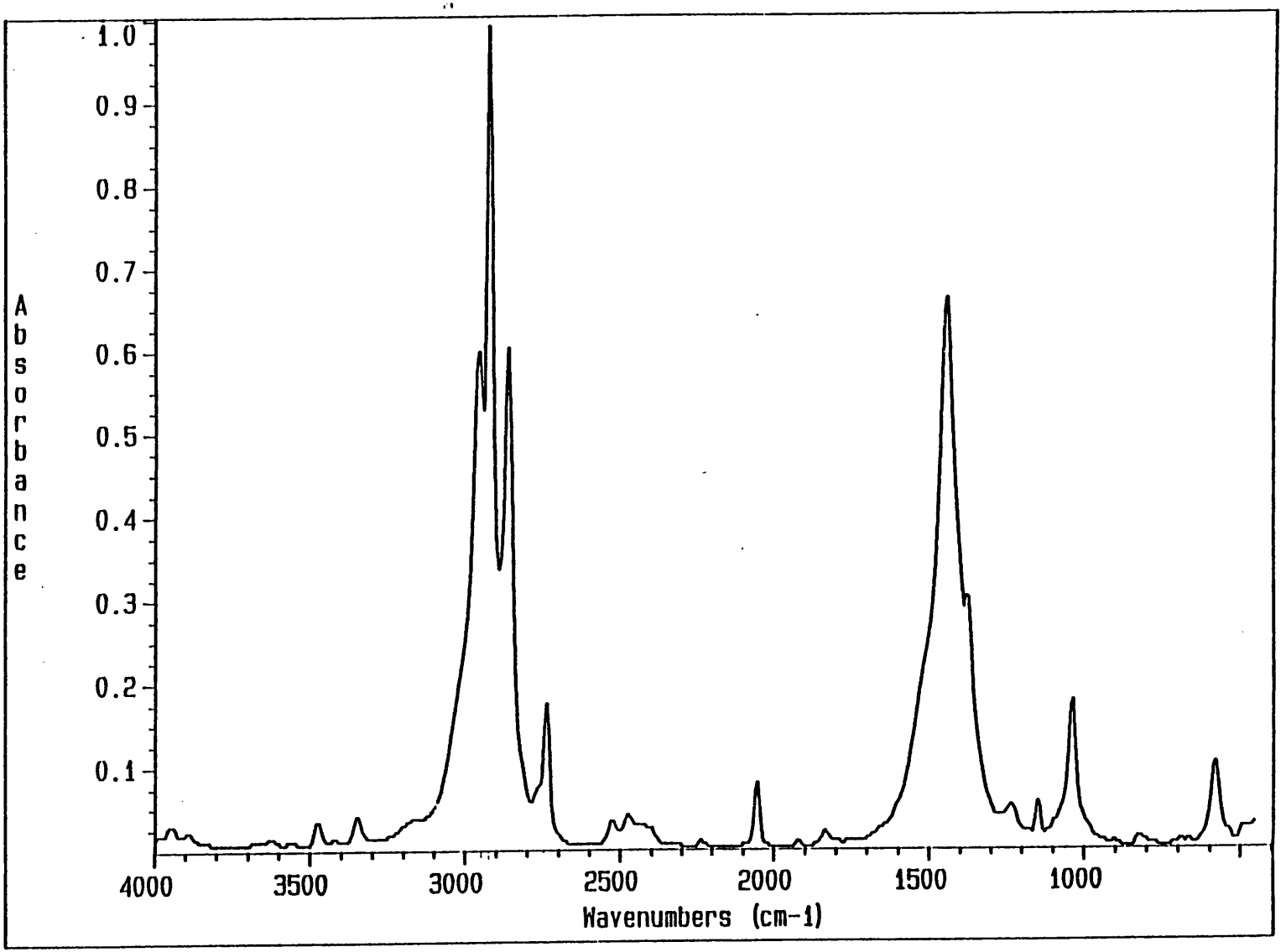

Figure 5.7.5 : Transmission Infra-Red Spectra of Pd/silica Reaction with Equimolar 2-Butyne/Hydrogen Mixture

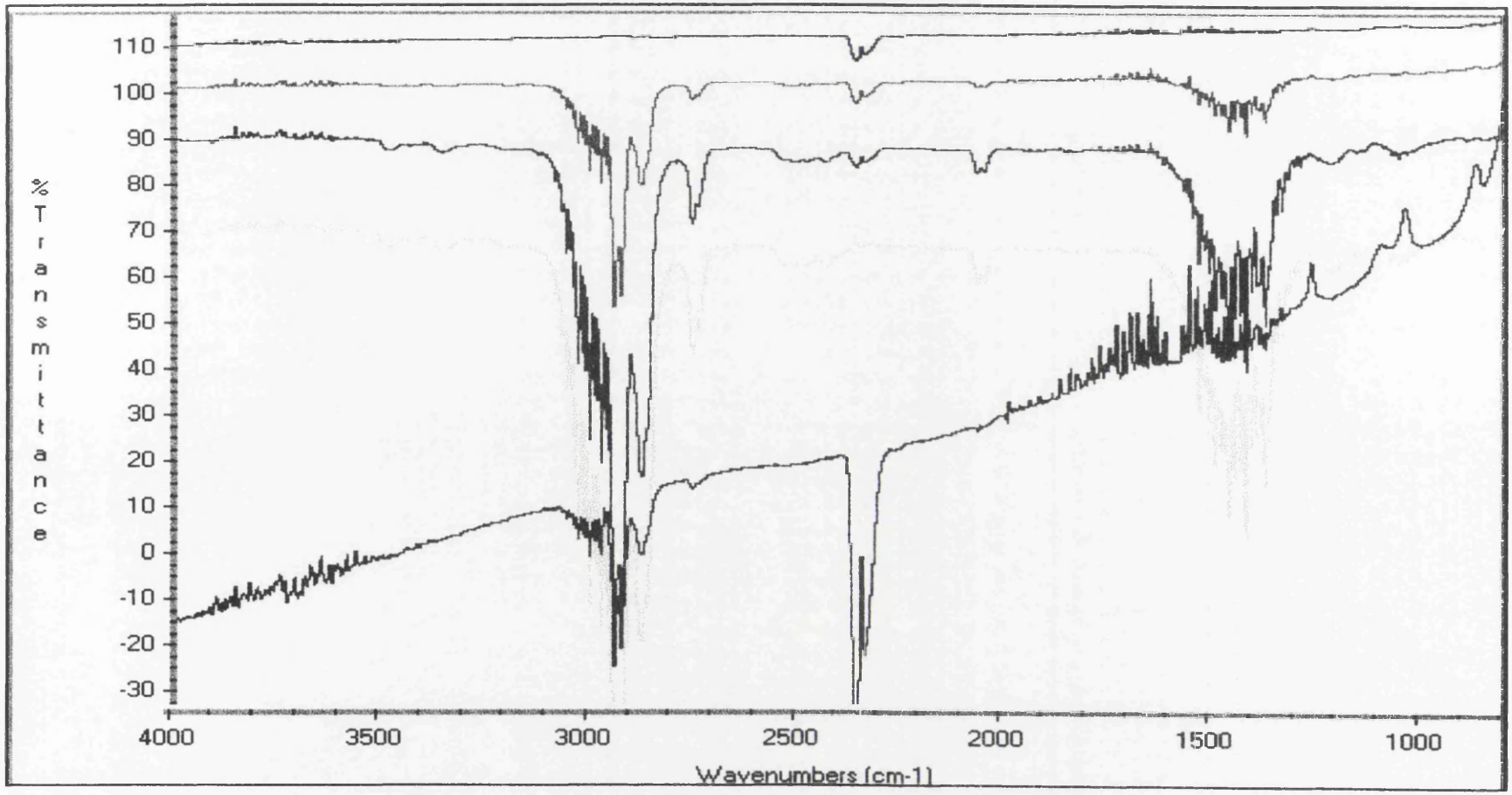

On subjecting the catalyst to a series of five pulses, the symmetric CH_3 bands were observed to decrease in intensity when left in flowing helium for 0.20hrs. Attempts to adsorbed CO onto the used catalyst produced a spectrum which was consistent with the presence of gas phase CO.

The results of the transmission infra-red experiments are shown in Figure 5.7.5. These bands are similar to those found in the DRIFTS study, in that they are indicative of molecularly adsorbed species. Similar to the DRIFTS experiments, it was found that the intensity of these bands decreased when the catalyst' chamber was evacuated over a period of 0.20hrs.

Section Five

LIQUID PHASE HYDROGENATION

4.5.1 The Hydrogenation of Phenylacetylene and Styrene over Palladium/silica

The liquid phase hydrogenation of phenylacetylene over Pd/silica produced both styrene and ethylbenzene, with the removal of the acetylene from the system complete after approximately twenty-five minutes of reaction. At this stage the yield of styrene decreased, suggesting that the hydrogenation of styrene to ethylbenzene predominated. As can be seen in Figure 5.7.6, the rate of styrene formation in the early stages of reaction is approximately double that of ethylbenzene.

The hydrogenation of styrene over Pd/silica yielded ethylbenzene. However, unlike the phenylacetylene reaction, the complete removal of the reactant was not observed, as displayed in Figure 5.8.4. The kinetics of this reaction obeyed a simple first order mechanism, with the rate of reaction determined.

When a co-hydrogenation reaction between phenylacetylene and styrene was performed, complete consumption of the acetylene occurred inside twenty minutes of reaction. In the presence of the acetylene, both styrene and ethylbenzene were produced, as shown in Figure 5.9.2. Similar to the hydrogenation of phenylacetylene, the adsorption and hydrogenation of styrene only predominated on removal of phenylacetylene from the system.

4.5.2 The Hydrogenation of Phenylacetylene and Styrene over Palladium/alumina

Phenylacetylene hydrogenation over alumina-supported palladium yielded both ethylbenzene and styrene. However, the rate of phenylacetylene consumption was less than that observed over Pd/silica. On removal of the acetylene, the hydrogenation of the olefin proceeded to produce ethylbenzene, which explains the decrease in styrene yield after forty-five minutes of reaction (Figure 5.7.8).

Styrene hydrogenation over the above catalyst again yielded ethylbenzene. Over Pd/alumina, the complete removal of the olefin was observed after approximately forty-five minutes of reaction (Figure 5.8.6). Therefore, comparing both Pd/silica and Pd/alumina, indicates that the latter is slightly more active for styrene hydrogenation. Similar to Pd/silica, the hydrogenation of styrene followed first order kinetics, with the corresponding rate coefficient determined.

The hydrogenation of an equimolar mixture of phenylacetylene and styrene proceeded with the initial formation of both ethylbenzene and styrene (Figure 5.9.3). Removal of the acetylene resulted in the hydrogenation of styrene to ethylbenzene predominating.

4.5.3 The Hydrogenation of Phenylacetylene and Styrene over Platinum/silica

Over Pt/silica, the rate of phenylacetylene hydrogenation was very slow. Even after one hour of reaction, the reaction liquor consisted of approximately 30% phenylacetylene. Both the olefin and alkane were produced from the onset,

with the rate of olefin production far greater than that of the alkane (Figure 5.8.0).

Styrene hydrogenation catalysed by Pt/silica, exhibited very low conversion to the alkane. After one hour of reaction, the reaction mixture consisted of approximately 90% styrene and 10% ethylbenzene. As with the supported-palladium catalysed reactions of styrene, the first order rate coefficient was determined (Table 5.4.7).

Co-hydrogenation of phenylacetylene/styrene over Pt/silica again displayed very low catalyst activity for phenylacetylene hydrogenation. Over the course of the analysis, the composition of phenylacetylene and styrene were observed to slightly decrease and increase, respectively (Figure 5.9.4).

4.5.4 The Hydrogenation of Phenylacetylene and Styrene over Platinum/alumina

As shown in Figure 5.8.2, phenylacetylene hydrogenation over Pt/alumina exhibited low conversion of the acetylene with increasing reaction time. On reaching one hour of reaction, the amount of reactant in the final reaction liquor was approximately 50%. Similar to Pt/silica, the rate of olefin production was far greater than that of the alkane.

Styrene hydrogenation over Pt/alumina was almost identical to that observed using Pt/silica, with very low conversion of olefin to alkane over a one hour period, as shown in Figure 5.9.0.

Using a co-hydrogenation mixture, there was a slight increase in the amount of styrene and ethylbenzene in the system. The accompanying loss of phenylacetylene was very small over a one hour period.

Figure 5.7.6 : Variation of Product Distribution with Time for the Hydrogenation of Phenylacetylene over Pd/silica at 303K

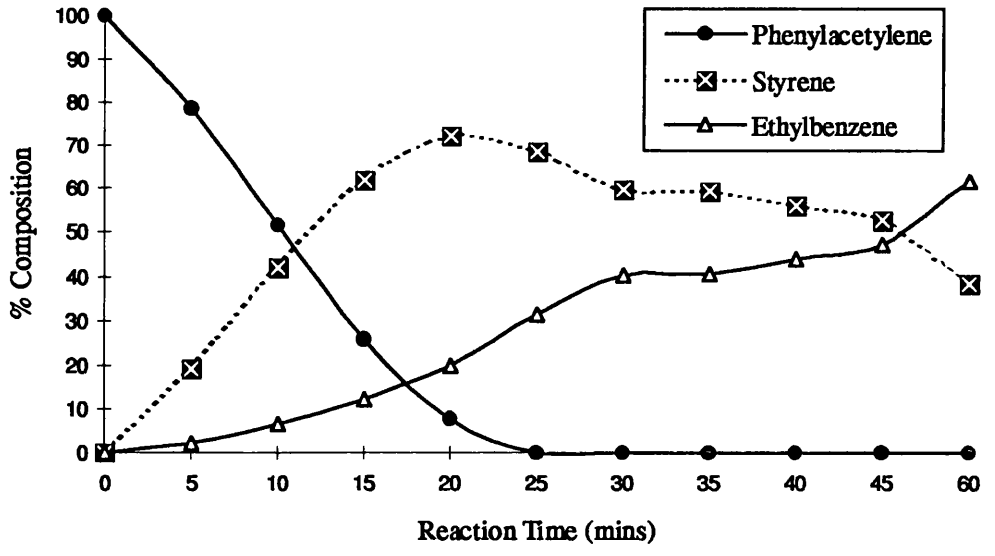

Figure 5.7.7 :Variation of Catalyst Selectivity with Conversion for the Hydrogenation of Phenylacetylene over Pd/silica at 303K

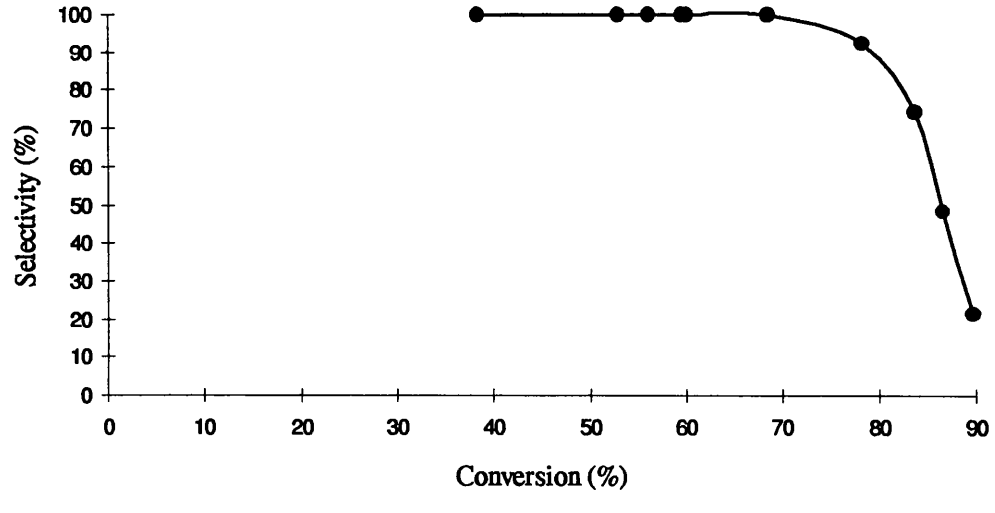

Figure 5.7.8 : Variation of Product Distribution with Time for the Hydrogenation of Phenylacetylene over Pd/alumina at 303K

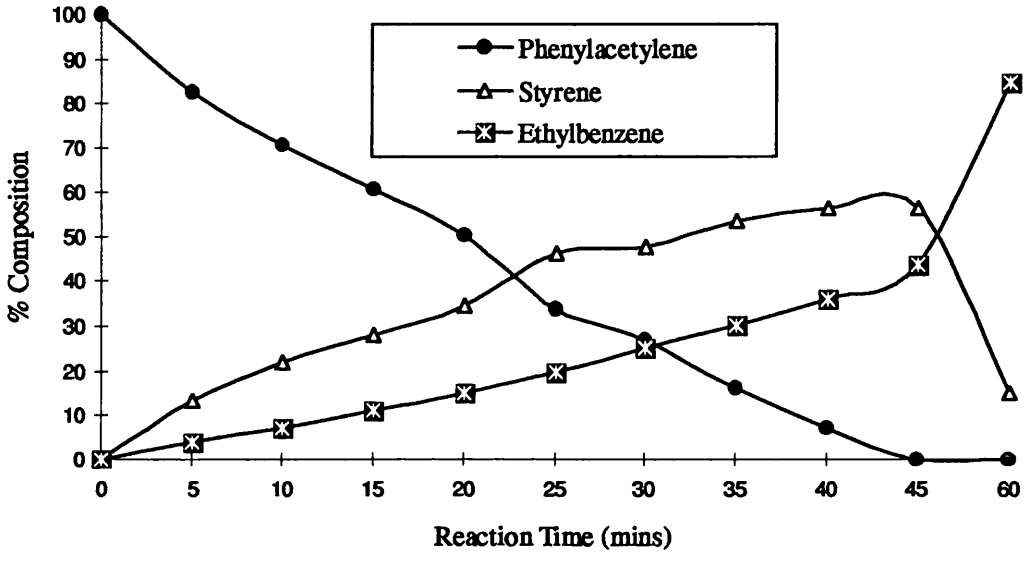

Figure 5.7.9 : Variation of Catalyst Selectivity with Conversion for the Hydrogenation of Phenylacetylene over Pd/alumina at 303K

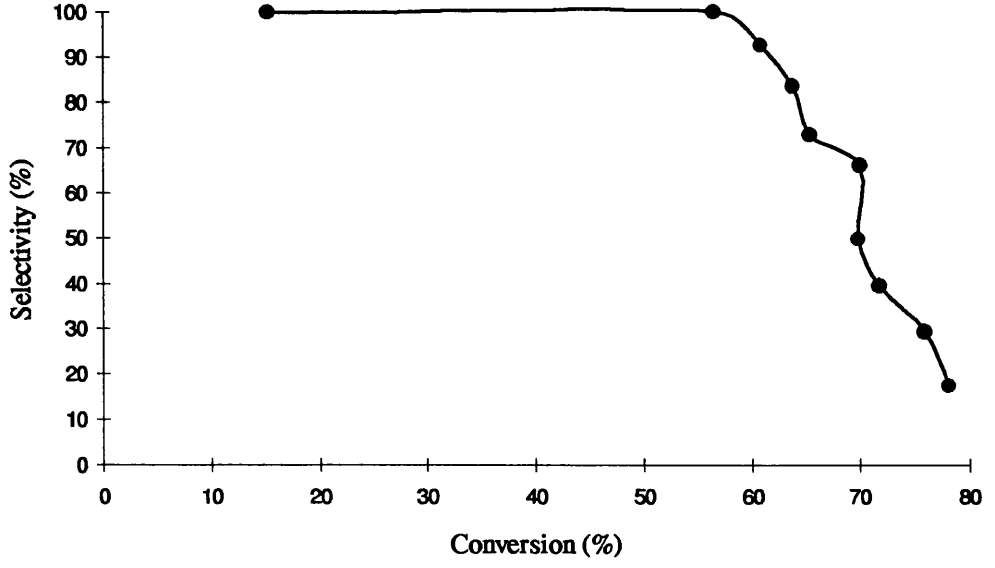

Figure 5.8.0 : Variation of Product Distribution with Time for the Hydrogenation of Phenylacetylene over Pt/silica at 333K

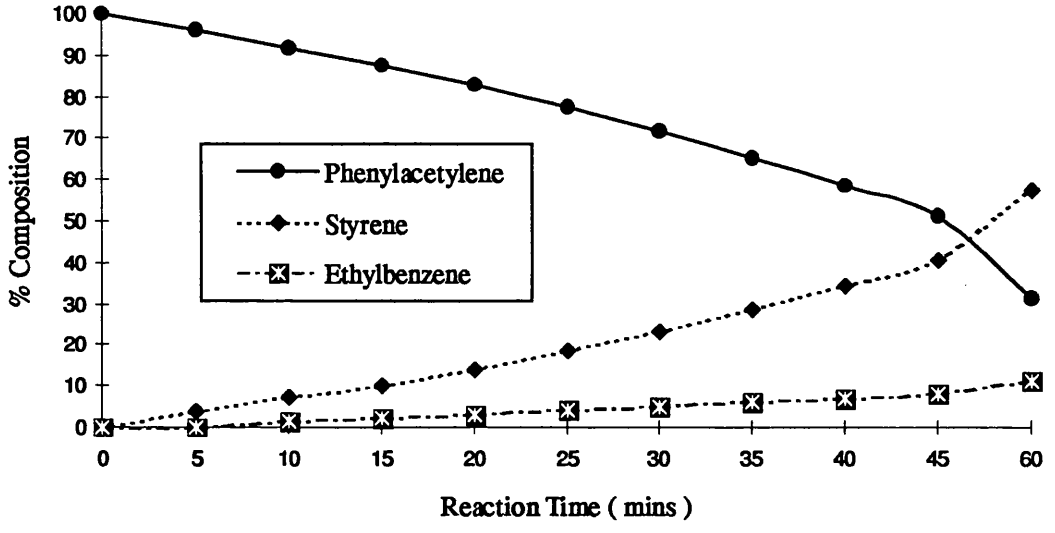

Figure 5.8.1 : Variation of Conversion with Selectivity for the Hydrogenation of Phenylacetylene over Pt/silica at 333K

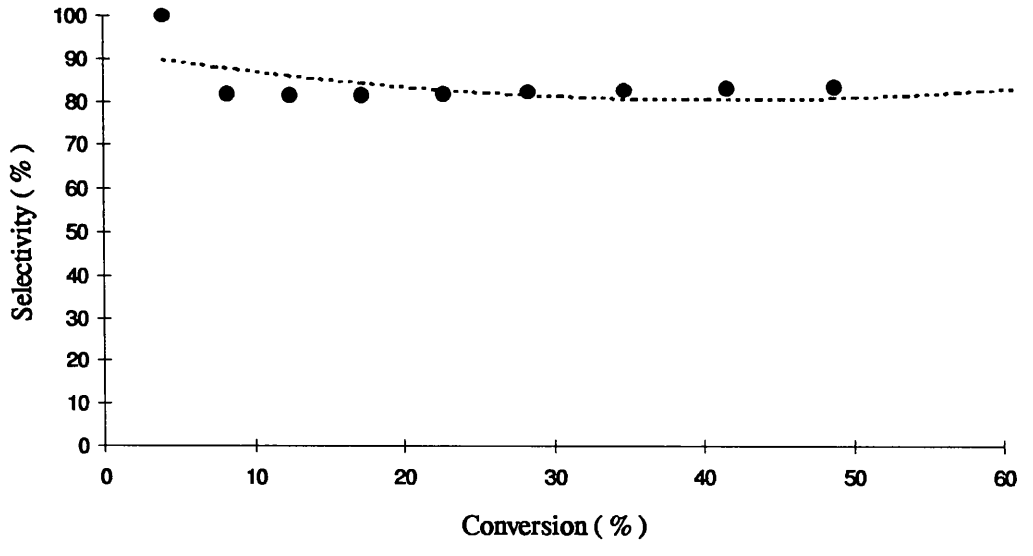

Figure 5.8.2 : Variation of Product Distribution with Time for the Hydrogenation of Phenylacetylene over Pt/alumina at 333K

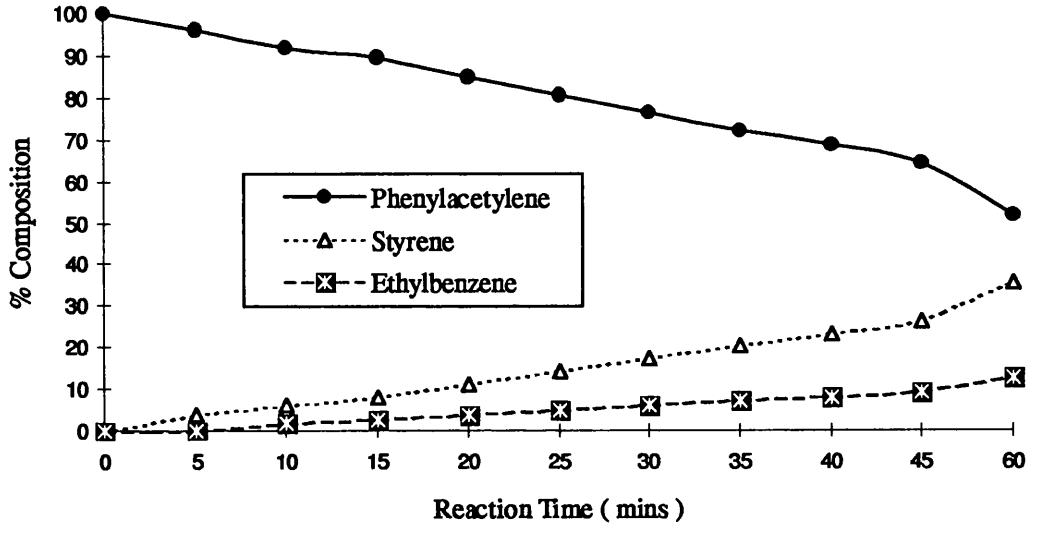

Figure 5.8.3 : Variation of Conversion with Selectivity for the Hydrogenation of Phenylacetylene over Pt/alumina at 333K

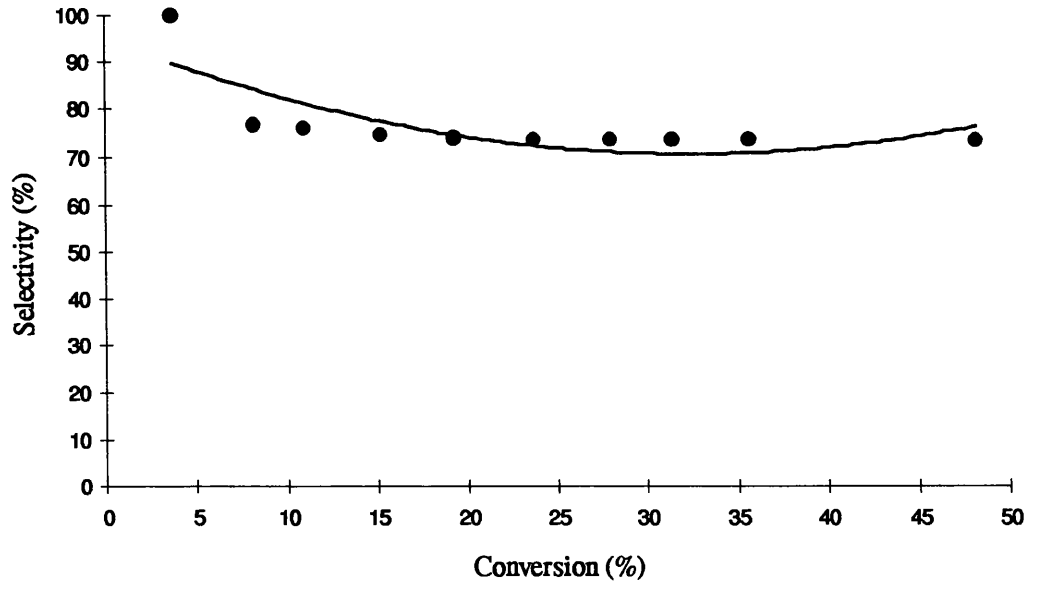

Figure 5.8.4 : Variation of Product Distribution with Time for the Hydrogenation of Styrene over Pd/silica at 303K.

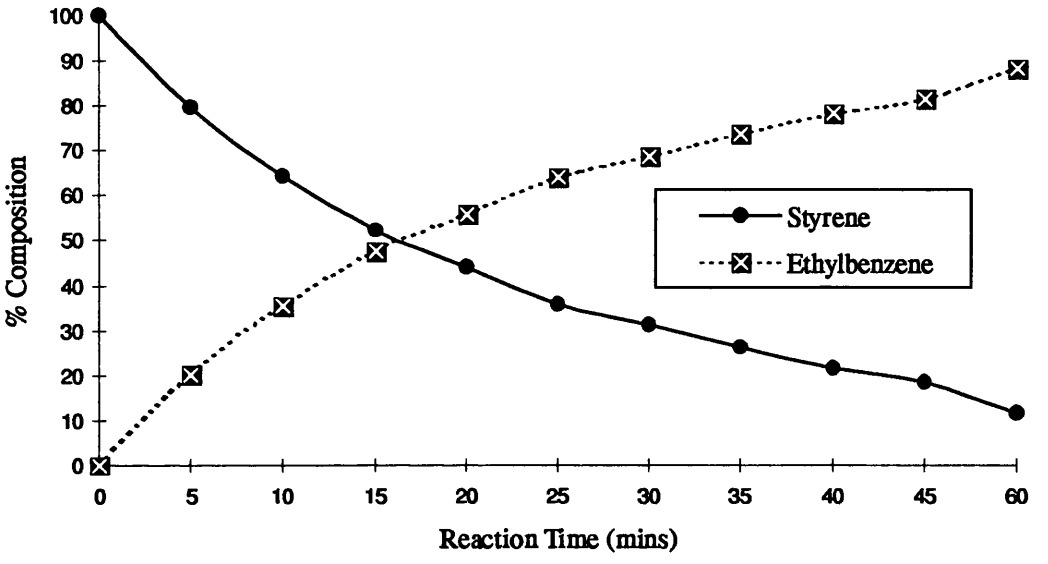

Figure 5.8.5 : Rate Coefficient Determination Graph for the Hydrogenation of Styrene over Pd/silica at 303K.

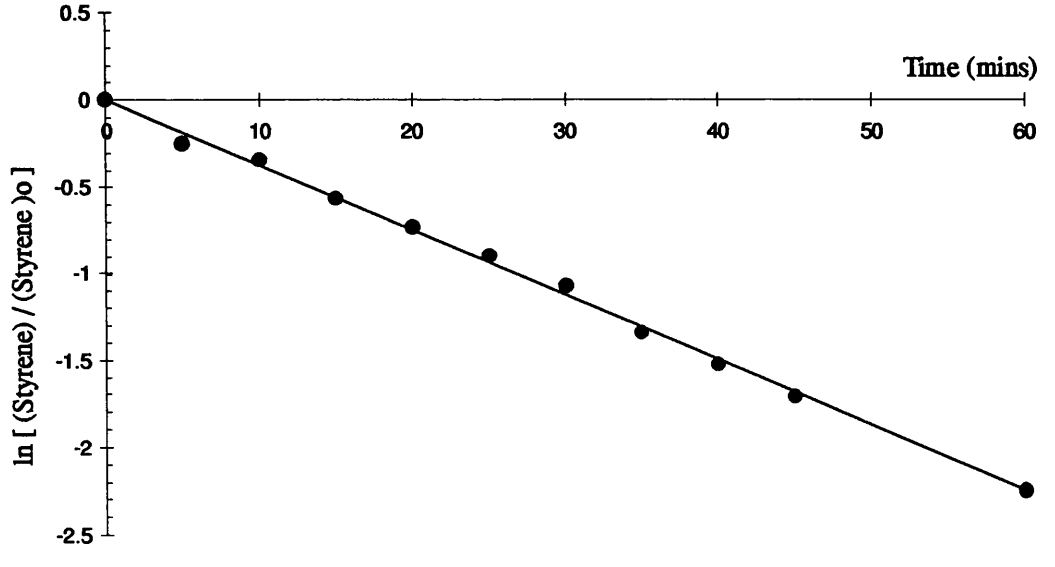

Figure 5.8.6 : Variation of Product Distribution with Time for the Hydrogenation of Styrene over Pd/alumina at 303K

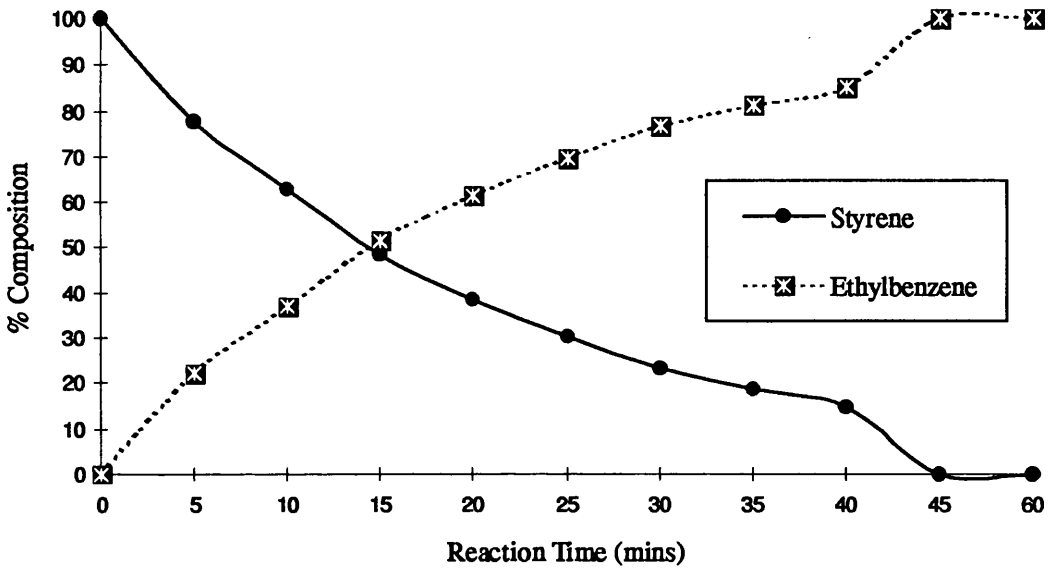

Figure 5.8.7 : Rate Coefficient Determination Graph for the Hydrogenation of Styrene over Pd/alumina at 303K

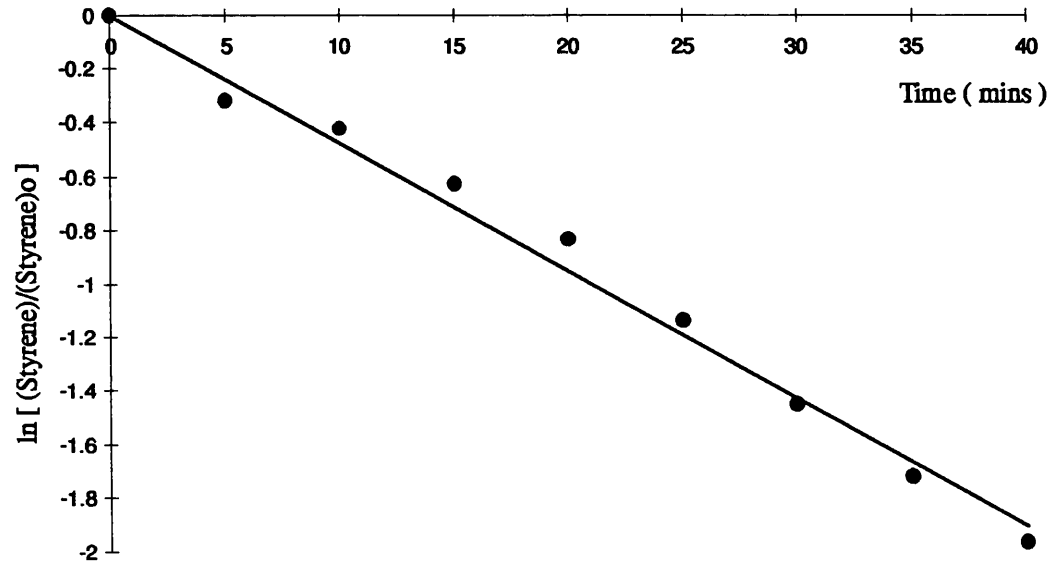

The rate coefficients for styrene hydrogenation over both supported-palladium catalysts, are shown in Table 5.4.6. The kinetics of the reactions were found to fit a first order mechanism, with the rate of styrene removal given as :

$$-d\,[\text{styrene}]/dt = k\,[\text{styrene}]$$

Integration of this equation, given that at $t = 0$, $[\text{styrene}] = [\text{styrene}]_o$, yields

$$[\text{styrene}] = [\text{styrene}]_o e^{-kt}$$

Table 5.4.6 : *Rate Coefficients for Styrene Hydrogenation*

Catalyst	Rate Coefficient (min^{-1})
Pd/silica	3.74×10^{-2}
Pd/alumina	4.70×10^{-2}

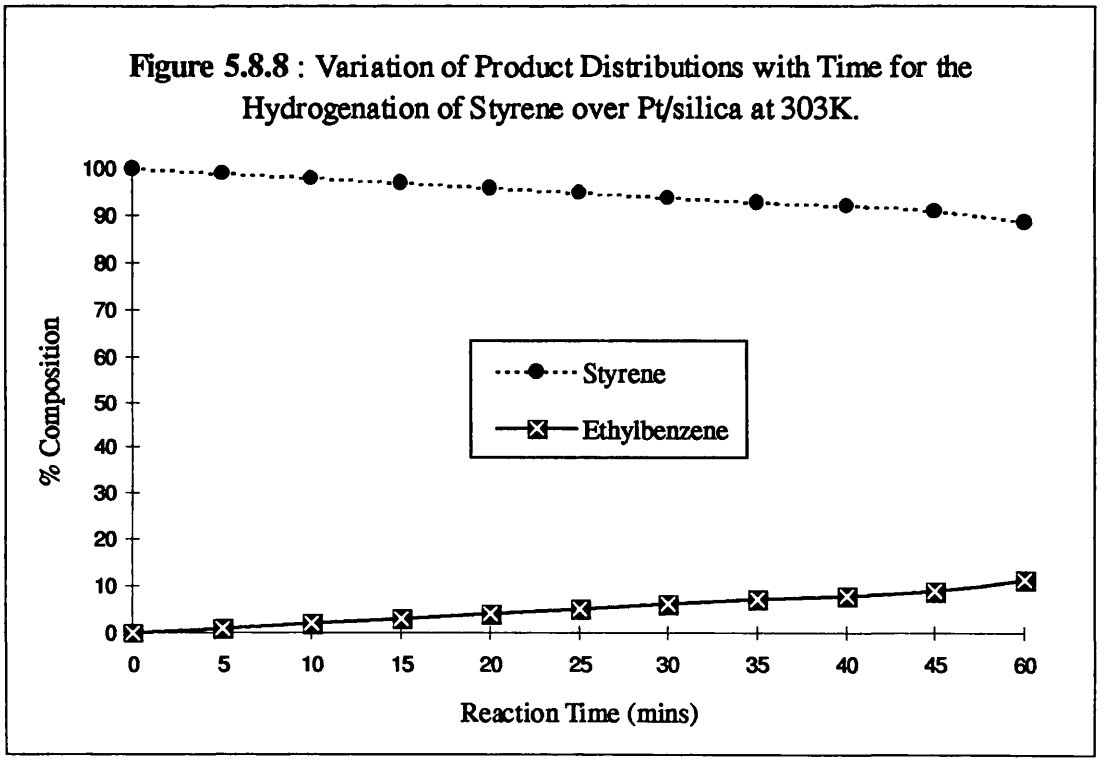

Figure 5.8.9 : Rate Coefficient Determination Graph for the Hydrogenation of Styrene over Pt/silica at 303K.

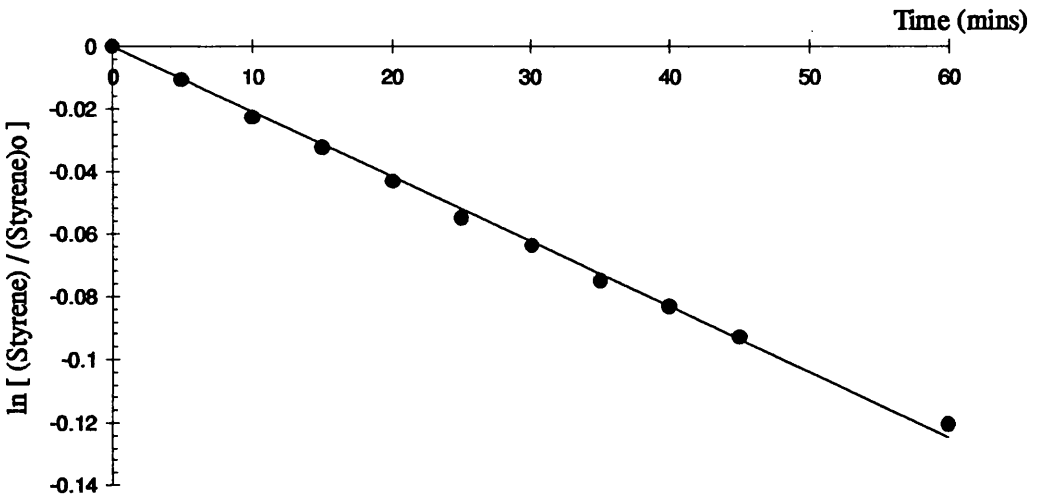

Figure 5.9.0 : Variation of Product Distributions with Time for the Hydrogenation of Styrene over Pt/alumina at 303K.

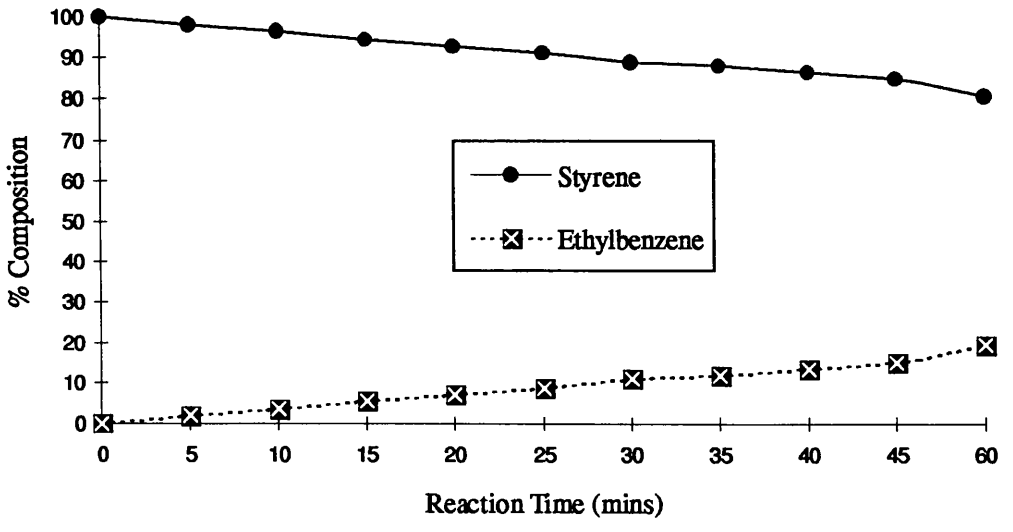

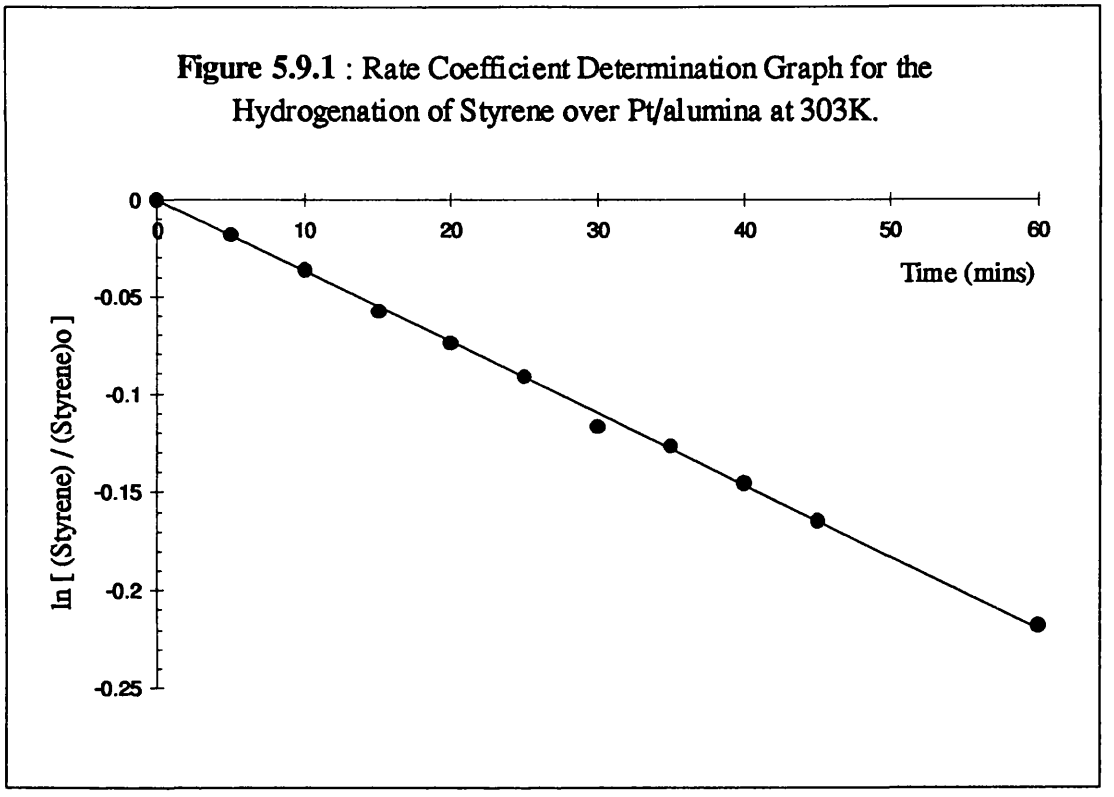

Figure 5.9.1 : Rate Coefficient Determination Graph for the Hydrogenation of Styrene over Pt/alumina at 303K.

Similar to the hydrogenation reactions of styrene over supported palladium, both platinum catalysts obeyed first order kinetics, although the rate of styrene removal was found to be an order of magnitude less than the corresponding palladium reactions. Table 5.4.7 shows the rate coefficient values obtained.

Table 5.4.7 : *Rate Coefficients for Platinum Catalysed Hydrogenation of Styrene*

Catalyst	Rate Coefficients (min^{-1})
Pt/silica	2.10×10^{-3}
Pt/alumina	3.70×10^{-3}

Figure 5.9.2 : Variation of Product Distributions with Time for the Co-Hydrogenation of (Phenylacetylene and Styrene) over Pd/silica at 303K

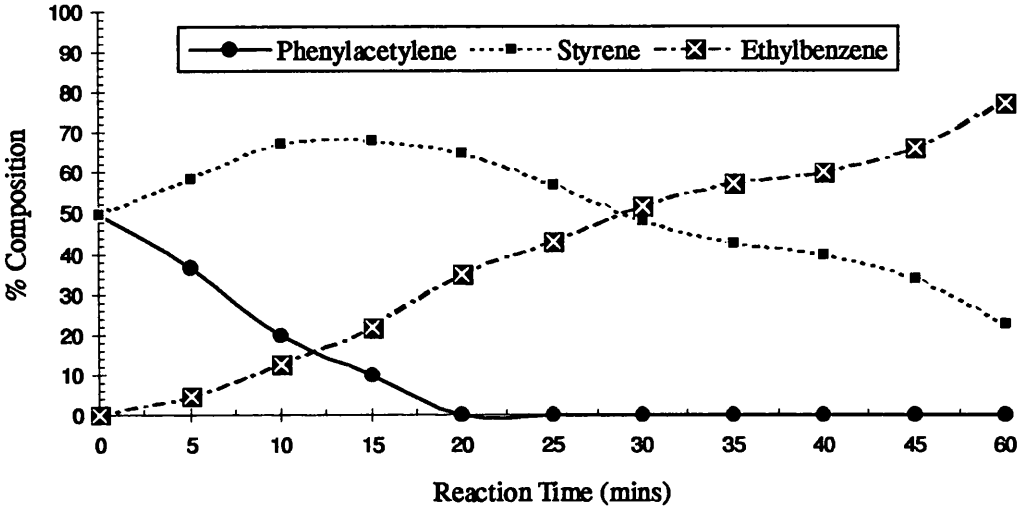

Figure 5.9.3 : Variation of Product Distributions with Time for the Co-Hydrogenation of (Phenylacetylene and Styrene) over Pd/alumina at 303K.

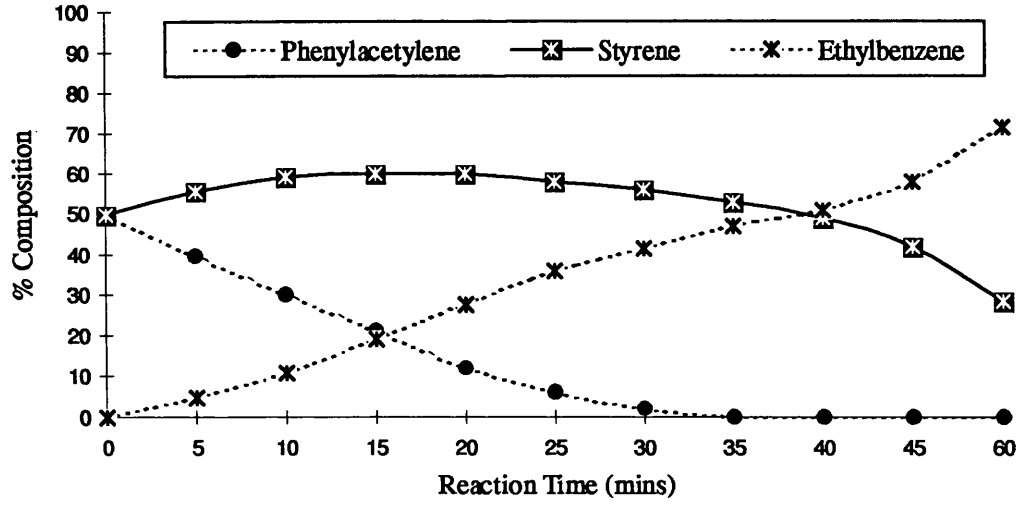

Figure 5.9.4 : Variation of Product Distributions with Time for the Co-Hydrogenation of (Phenylacetylene and Styrene) over Pt/silica at 303K.

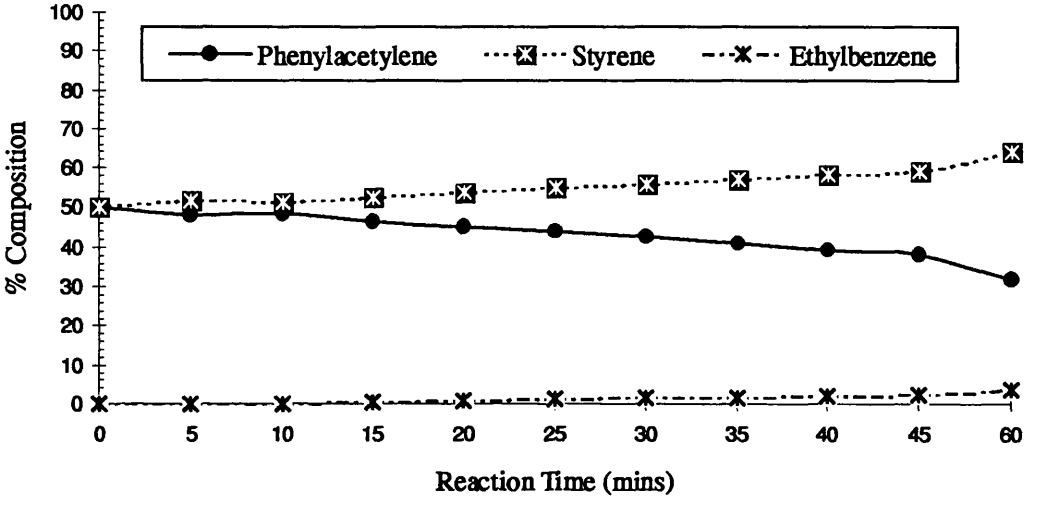

Figure 5.9.5 : Variation of Product Distributions with Time for the Co-Hydrogenation of (Phenylacetylene and Styrene) over Pt/alumina at 303K.

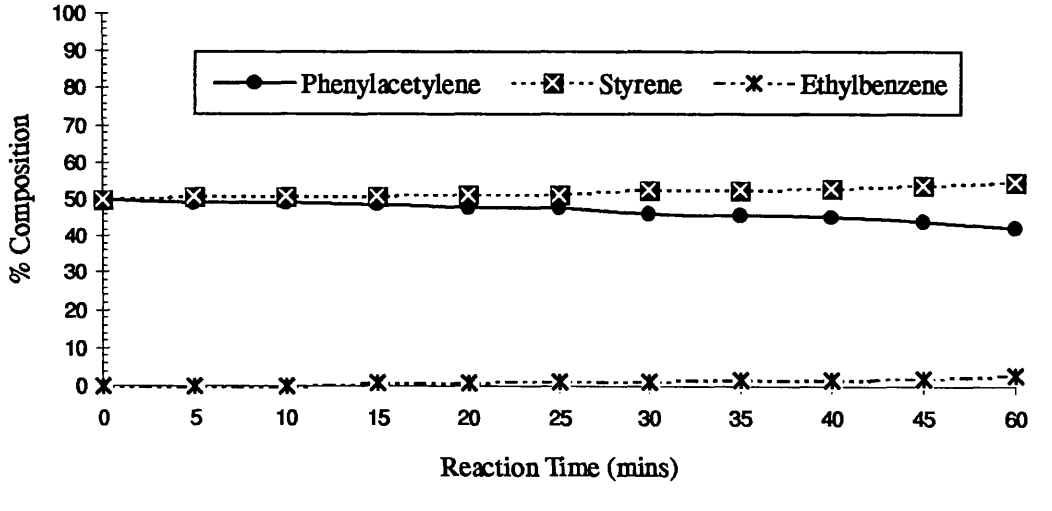

Section Six

CONTINUOUS FLOW HYDROGENATION

4.6 Continuous Flow Hydrogenation Reactions

The hydrogenation of phenylacetylene in the continuous flow mode produced only ethylbenzene. Over silica-supported palladium, the conversion of the acetylene was found to increase with increasing time on-line. Increasing the weight of catalyst resulted in the attainment of a steady state (with respect to catalyst activity and product(s) yield) from the onset of the reaction.

Alumina-supported palladium produced constant amounts of ethylbenzene and unreacted phenylacetylene over the course of the reaction. On increasing the weight of catalyst, ethylbenzene formation could be followed as a function of time. This continued until a constant yield of the alkane was achieved.

Both platinum catalysts displayed near constant product distributions in the hydrogenation of phenylacetylene. However, when alumina-supported platinum was used, the conversion of phenylacetylene was observed to decrease with increasing reaction.

Styrene hydrogenation produced ethylbenzene over both supported-palladium and platinum. However, the hydrogenation activity of palladium was found to be low, with low concentrations of ethylbenzene produced. In contrast, the hydrogenation of styrene over supported-platinum resulted in the rapid formation of ethylbenzene, with complete conversion of the olefin over a one hour period.

i) Hydrogenation of Phenylacetylene over 5mg Pd/silica at 425K

Figure 5.9.6 : Variation of Product Distribution with Time On-Line for the Hydrogenation of Phenylacetylene over 5mg Pd/silica at 425K

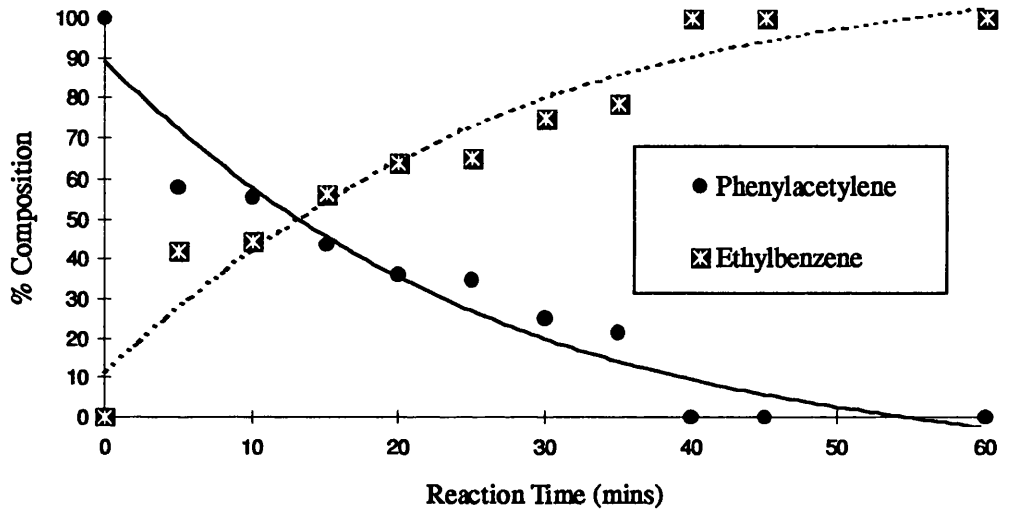

Figure 5.9.7 : Variation of Conversion with Time On-Line for the Gas Phase Hydrogenation of Phenylacetylene over 5mg Pd/silica at 425K

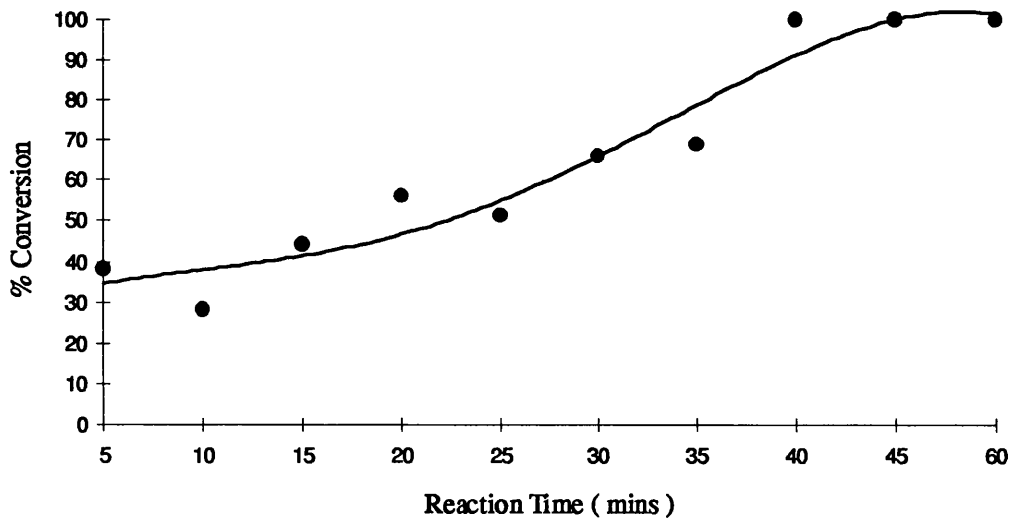

ii) Hydrogenation of Phenylacetylene over 50mg Pd/silica at 425K

This reaction was analysed over a one hour period, over which time only ethylbenzene was produced. The activity of the catalyst for phenylacetylene hydrogenation remained at 100% over the analysis time, indicating that the catalyst was operating in a steady state regime with respect to alkane production.

iii) Hydrogenation of Phenylacetylene over 5mg Pd/alumina at 425K

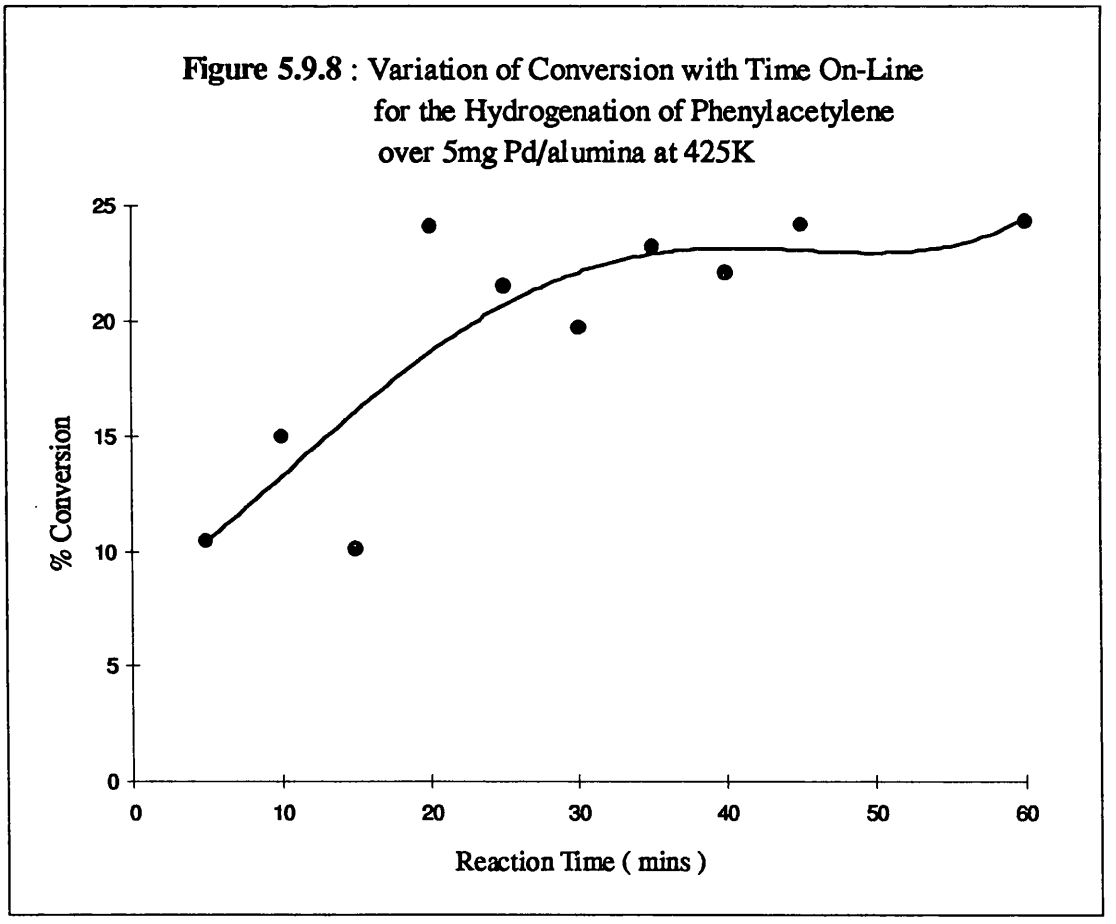

Figure 5.9.8 : Variation of Conversion with Time On-Line for the Hydrogenation of Phenylacetylene over 5mg Pd/alumina at 425K

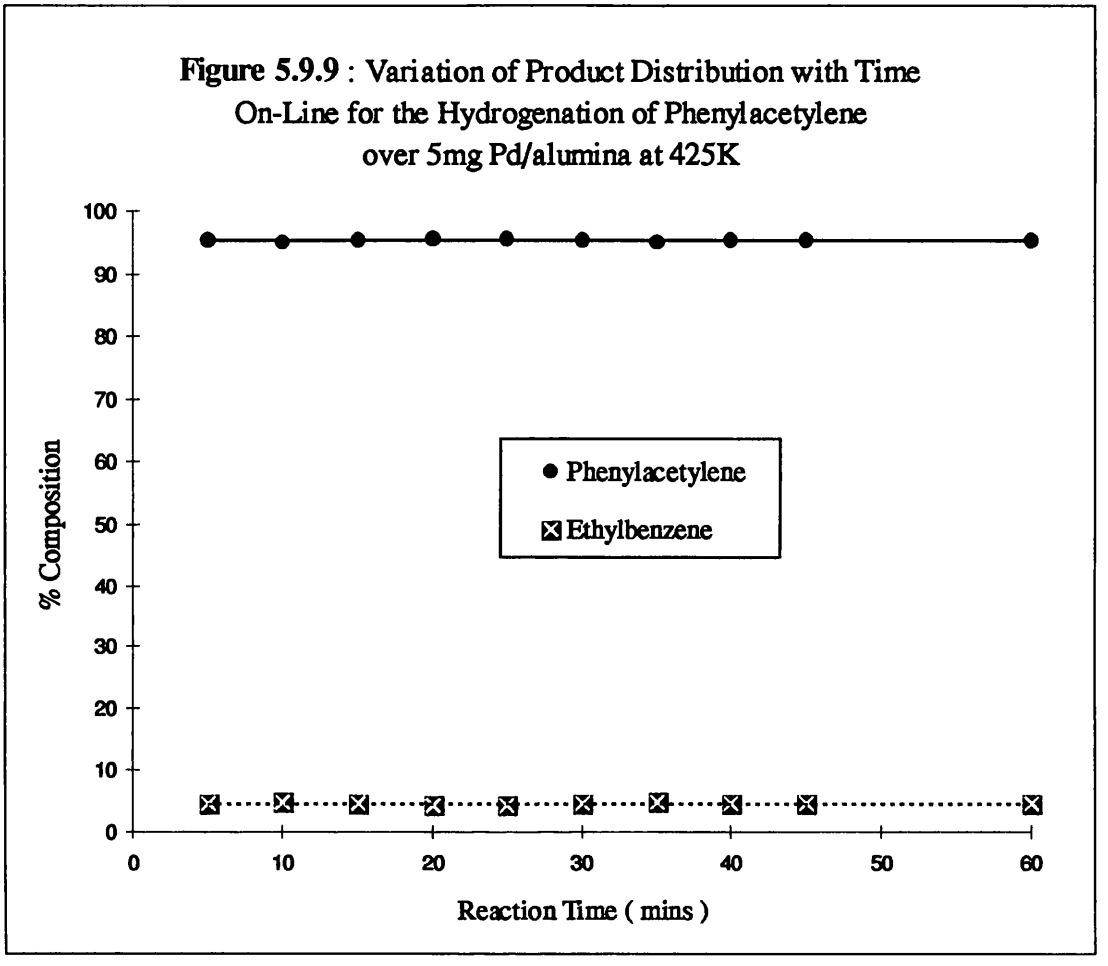

iv) Reaction of Phenylacetylene over 10mg Pd/alumina at 425K

Complete removal of the acetylene was observed after five minutes of reaction, with the yield of ethylbenzene found to increase to a limiting value after twenty-five minutes of reaction. The rate of ethylbenzene formation as a function of time is shown in Figure 6.0.0 overleaf.

Figure 6.0.0 : Rate of Ethylbenzene Formation in the Hydrogenation of Phenylacetylene over 10mg Pd/alumina at 425K

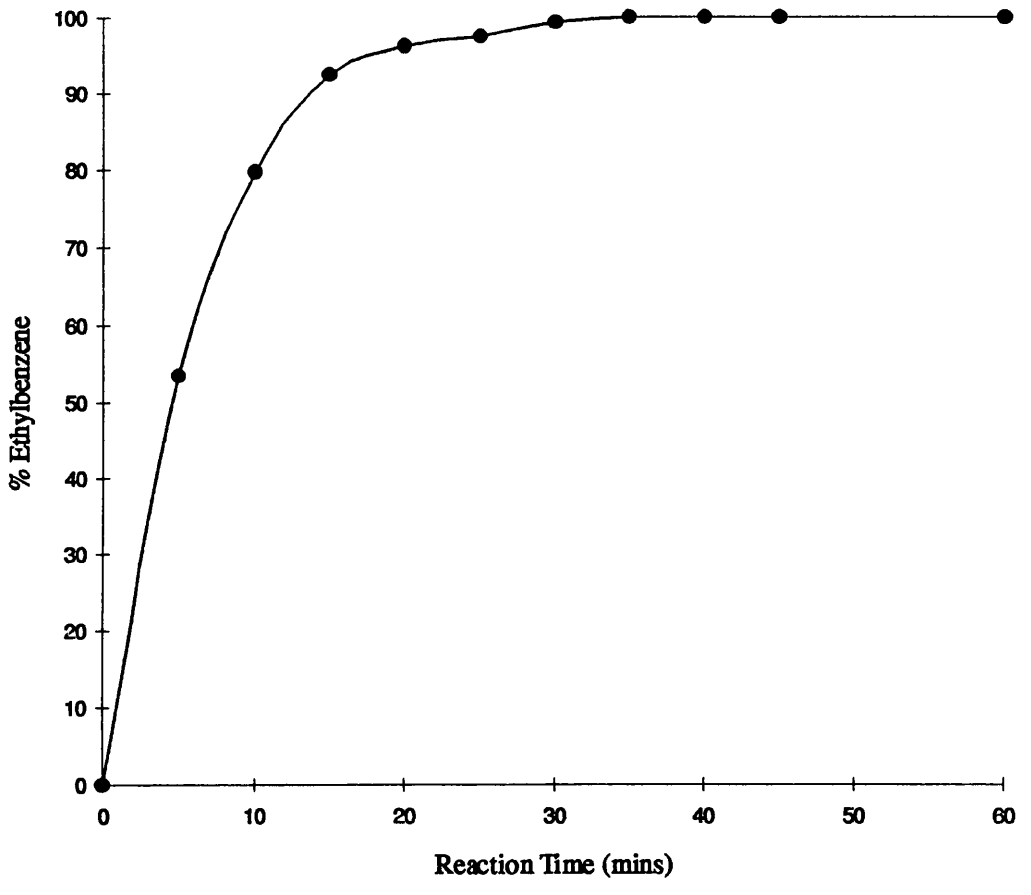

v) Hydrogenation of Phenylacetylene over 7mg Pt/silica at 425K

Similar to the supported-palladium catalysed reactions, the above reaction afforded no selectivity to styrene, with ethylbenzene produced from the onset. The yield of both ethylbenzene and unconverted phenylacetylene was constant over a period of two hours.

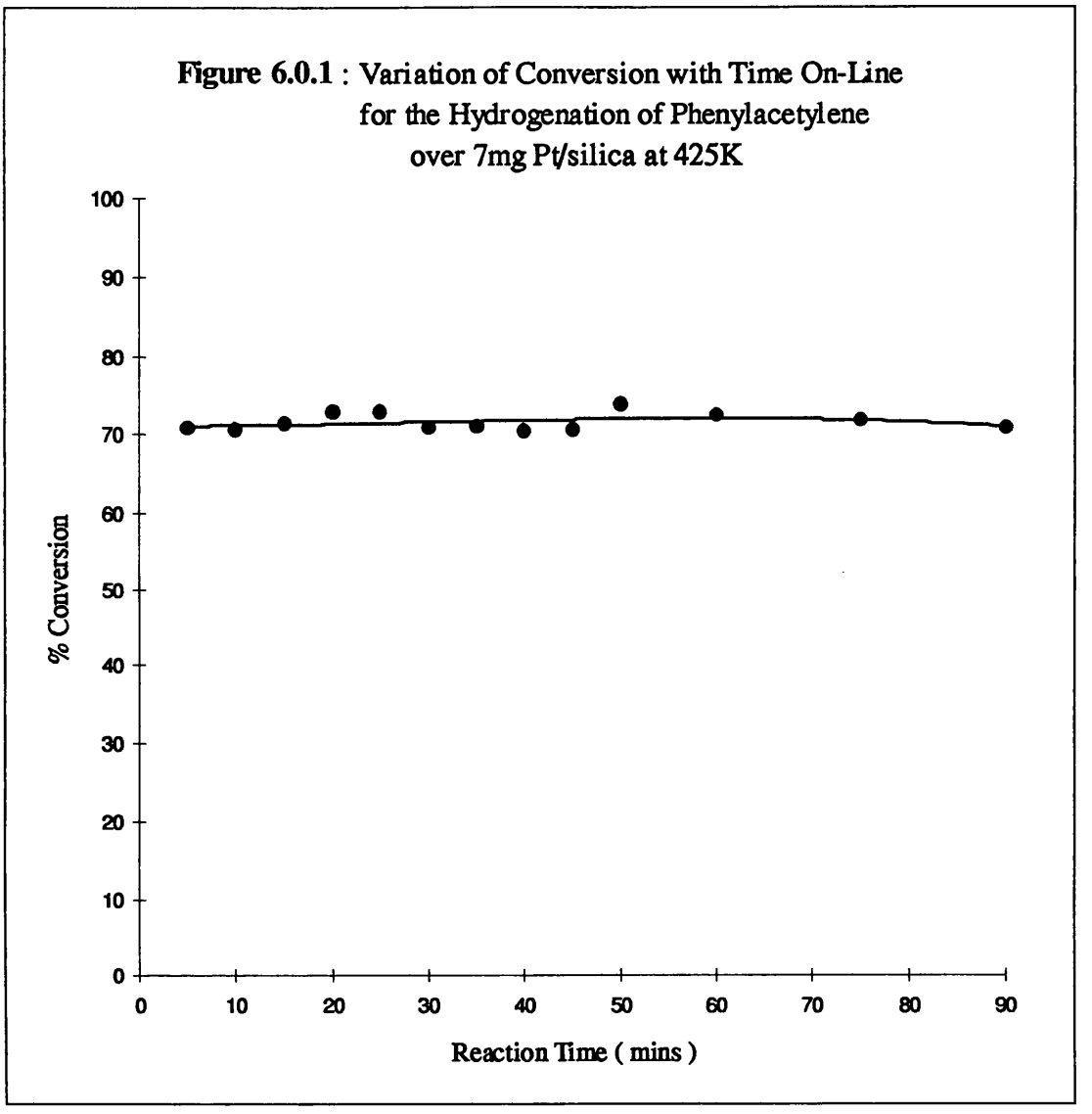

vi) Hydrogenation of Phenylacetylene over 7mg Pt/alumina at 425K

The above catalyst produced both ethylbenzene and unreacted phenylacetylene as the sole reaction products. The yield of the former was found to increase with increasing time on-line, until a steady state was achieved. The variation of both acetylene conversion and product distributions are shown in Figures 6.0.2 and 6.0.3 respectively.

Figure 6.0.2 : Variation in Conversion with Time On-Line for the Hydrogenation of Phenylacetylene over 7mg Pt/alumina at 425K

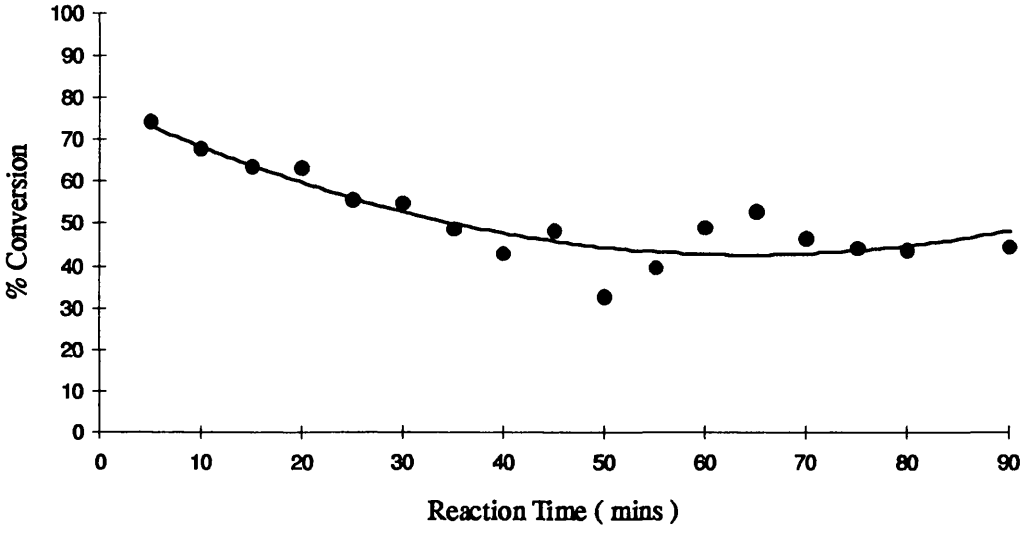

Figure 6.0.3 : Variation of Product Distribution with Time On-Line for the Hydrogenation of Phenylacetylene over 7mg Pt/alumina at 425K

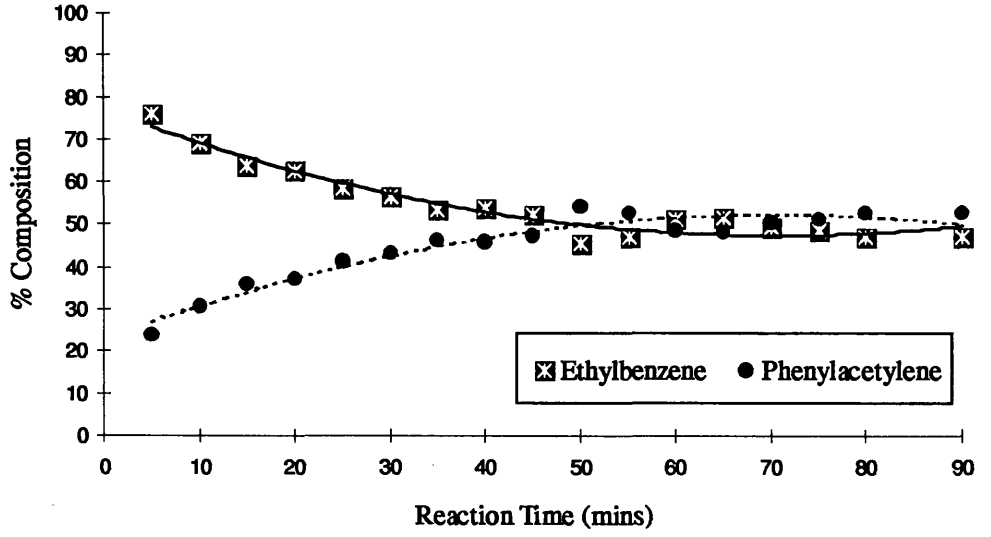

vii) Hydrogenation of Styrene over 6mg Pd/silica at 425K

Figure 6.0.4 : Variation in Conversion with Time On-Line for the Hydrogenation of Styrene Over 6mg Pd/silica at 425K

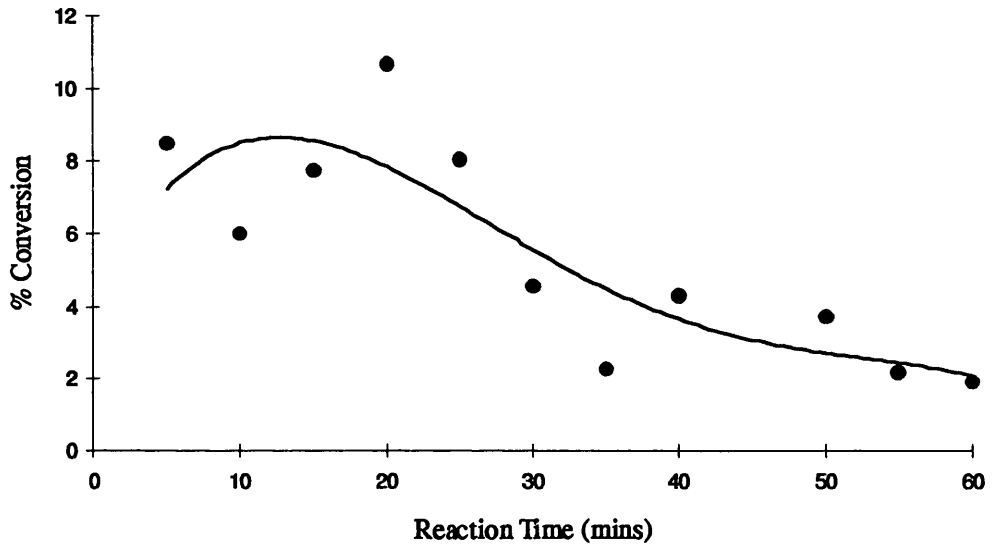

Figure 6.0.5 : Variation of Product Distribution with Time On-Line for the Hydrogenation of Styrene over 6mg Pd/silica at 425K

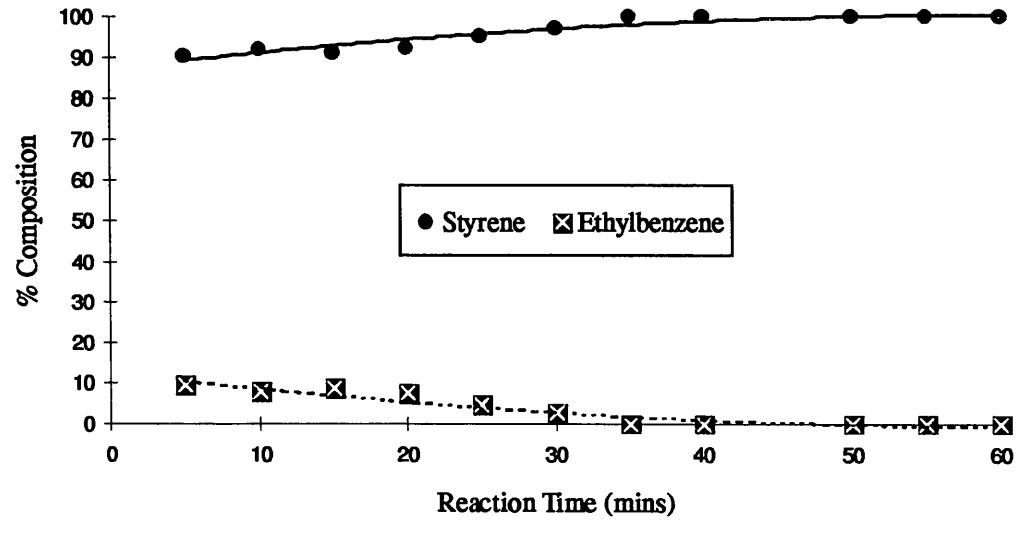

viii) Hydrogenation of Styrene over 6mg Pd/alumina at 425K

Figure 6.0.6 : Variation of Conversion with Time On-Line for Hydrogenation of Styrene over 6mg Pd/alumina at 425K

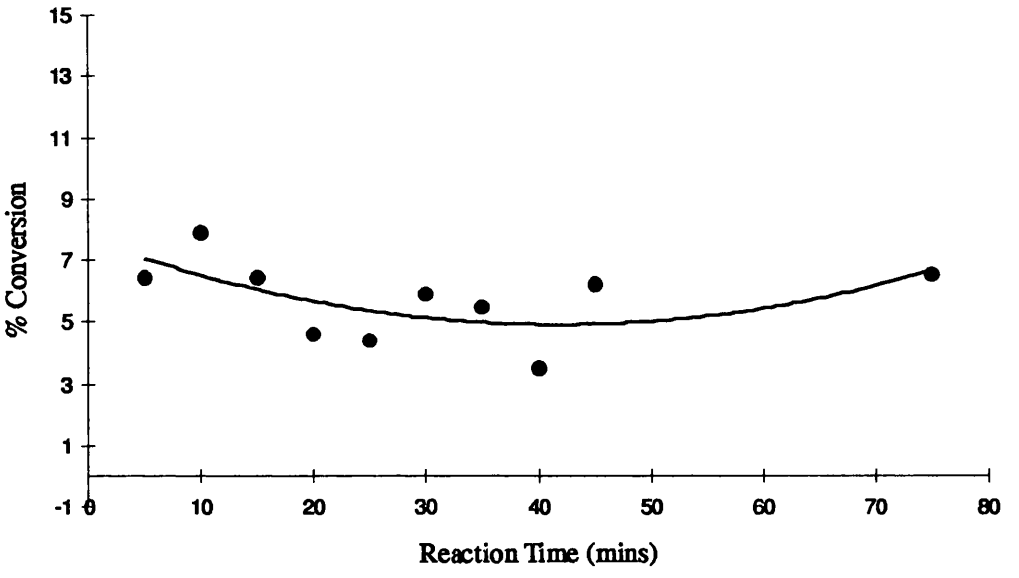

Figure 6.0.7 : Variation in Product Distribution with Time On-Line for the Hydrogenation of Styrene over 6mg Pd/alumina at 425K

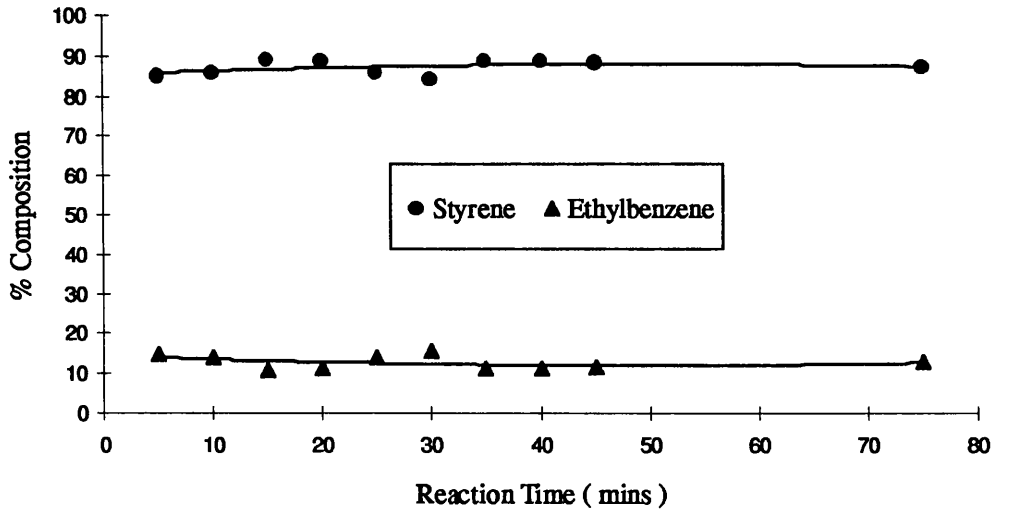

ix) Hydrogenation of Styrene over 7mg Pt/silica at 425K

The reaction between hydrogen and styrene over the above substrate produced ethylbenzene from five minutes onward. Similar to the hydrogenation of phenylacetylene, the yield of the alkane remained unaltered over a period of one hour, and was accompanied by complete conversion of the olefin.

x) Hydrogenation of Styrene over 7mg Pt/alumina at 425K

Styrene hydrogenation produced a constant yield of the alkane with complete removal of the olefin maintained throughout the analysis time.

Chapter Five

DISCUSSION

Discussion

5.1 Introduction

The previous section detailed the results of the various hydrogenation reactions which were performed using propyne, 2-butyne and phenylacetylene as reactants. This final chapter will discuss the observed product distributions, catalyst behaviour and the effect of surface retained carbon species on the reaction chemistry.

It is the aim of this section to present possible explanations for the observed reactions; in particular, the nature and involvement of the adsorbed acetylenic species, the effect of catalyst structure on reaction chemistry and the role of any surface carbonaceous residues. By understanding these effects, it is hoped that a more detailed understanding of the mechanism of these hydrogenation reactions, and their pathways can be elucidated.

5.1.1 Preface

For the purposes of this discussion, the definition of conversion and catalyst selectivity will be, as shown below:

$$\text{Conversion (\%)} = \frac{\text{Acetylene In - Acetylene Out}}{\text{Acetylene In}} \text{x100\%}$$

$$\text{Selectivity (\%)} = \frac{\text{Olefin}}{\text{Olefin + Alkane}} \text{x100\%}$$

The reaction routes shown in Figure 6.0.8 will also be used as a general scheme detailing the possible reaction products, and will be referred to in the discussion which follows.

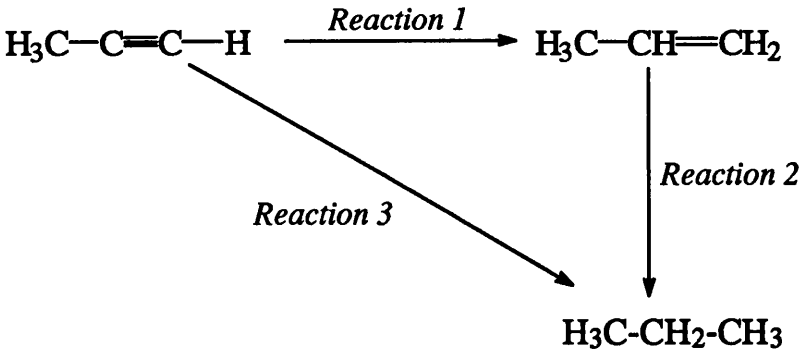

Figure 6.0.8 : *General Hydrogenation Scheme for Propyne*

5.1.2 The Interaction of Propyne with Metal Surfaces

Before the reactions of propyne and hydrogen over supported palladium and platinum are discussed, the mode of interaction of the acetylene at the surface must first be considered. Conclusions by Webb and Al-Ammar[65,66,67] relating to the hydrogenation of ethyne include the involvement of both associatively and dissociatively adsorbed ethyne derivatives in the hydrogenation process, with a σ/π-adsorbed olefinic species postulated as a possible precursor to ethane formation. It is therefore reasonable to assume that an analogous species could be active for propane formation via a dissociatively adsorbed propyne derivative. More recently, Jackson and Casey[53] have provided evidence for the existence of a σ-bonded acetylenic species (I), which behaves as a precursor for the formation

of the corresponding alkylidyne, propylidyne[27] (II), which may be coordinated through three distinct metal atoms, as shown in Figure 6.0.9.

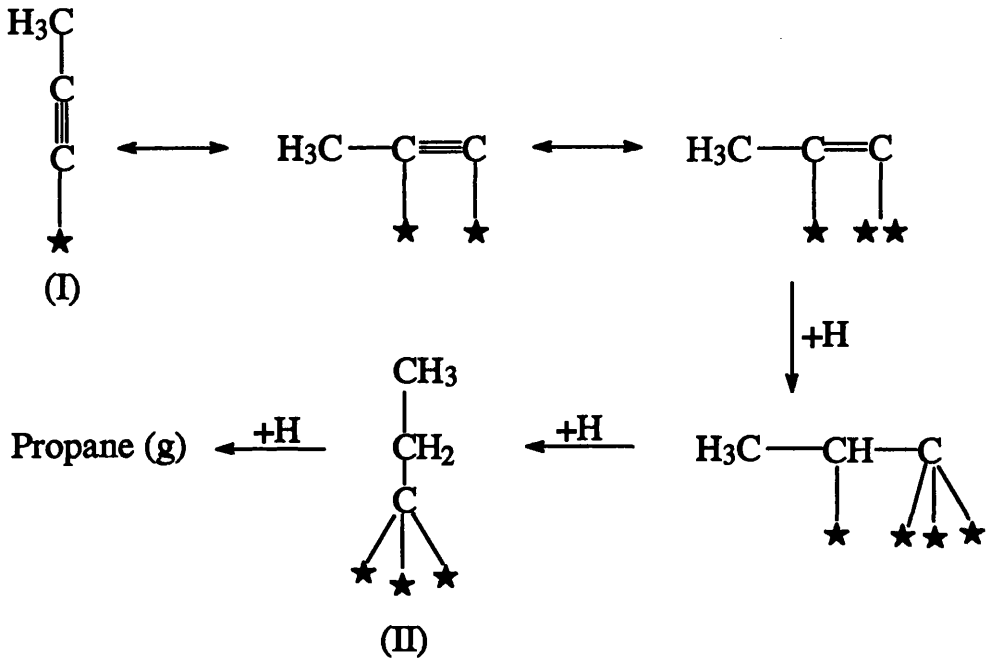

Figure 6.0.9 : *A Possible Route to the Formation of Propane via Dissociative Adsorption of Propyne*

The propylidyne species may also be an important precursor to further surface hydrocarbonaceous overlayers, which could be produced from (i) dehydrogenation of this alkylidyne or (ii) cleavage of one or more of the (C-C) bonds. Therefore, in view of this it is reasonable to assume that both the alkane precursor and the hydrocarbonaceous residues will co-exist at the surface. Therefore we can propose that the formation of either the alkane or surface hydrocarbonaceous overlayers will be dependent on the rate of hydrogen supply to the alkane or overlayer precursor sites. Those reactions where the alkane

predominates can be considered to reflect a greater rate of hydrogen supply to the alkane formation sites and *vice versa.*

The involvement of an associatively adsorbed propyne species can be proposed as the precursor to formation of the olefin, propene. The adsorption of acetylenes at metal surfaces is well documented (Section 1.5), thus olefin formation can be envisaged as progressing from a di-π-adsorbed propyne entity. The mechanism for the hydrogenation of this species is explained in detail in Section 5.1.5.

Therefore, the overall scheme for the adsorption and hydrogenation of propyne can be envisaged as occurring as shown in Figure 6.1.0, a scheme which incorporates the catalysts ability to form the olefin, alkane and surface hydrocarbonaceous overlayers.

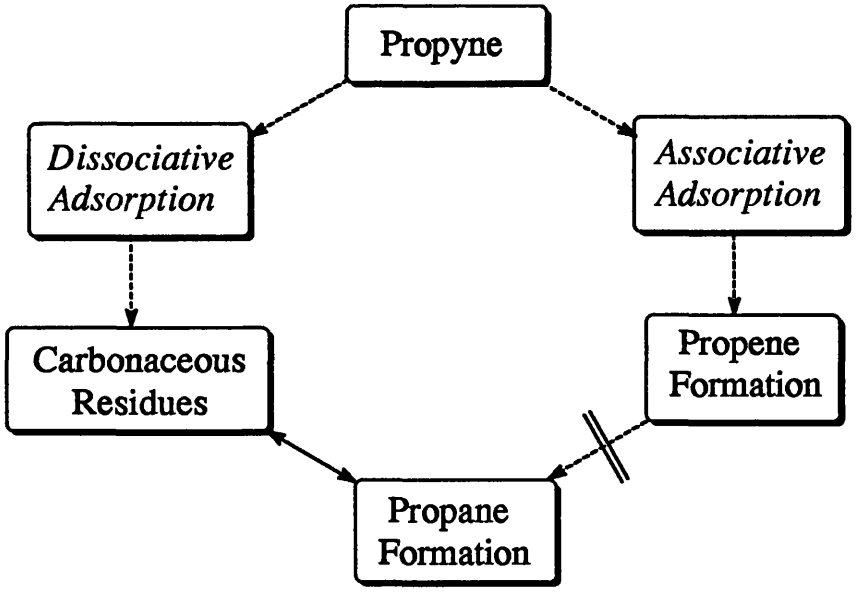

Figure 6.1.0 : *Overall Scheme for Propyne Adsorption and Hydrogenation*

5.1.3 The Reaction of Propyne with Hydrogen over Supported Palladium

When propyne was hydrogenated using an equimolar reactant mixture, the silica-supported palladium catalyst displayed complete selectivity toward the formation of propene (Table 5.1.1). However, over a series of ten pulses, the turnover of propyne to propene was found to decrease with increasing number of pulses (Figure 5.1.1). This decrease in catalyst activity is termed deactivation, and was accompanied by a decrease in the amount of carbon retained by the catalyst (11.5 $x10^{19}$ atoms [pulse 1] $\rightarrow$ 4.48 $x10^{19}$ atoms [pulse 10]: C_{total} = 11.5 $x10^{19}$ atoms [pulse 1], 61.62 $x10^{19}$ atoms [pulse 10]). The loss of activity is attributed to the ability of surface carbonaceous residues to diminish the number of active metal clusters, thus inhibiting the initial adsorption of the propyne molecule. The initially low conversion values for this reaction tends to suggest that either the surface contains relatively few sites for propyne adsorption, or the availability of surface hydrogen is limited (θ_H low). This latter conclusion would result in the desorption of propyne before hydrogenation had occurred. Comparing the high selectivity and low conversion values suggests that either (i) only sites for the hydrogenation of propyne to propene are available, and the existence of surface sites for propane formation, if any, are blocked by the retained carbon, or (ii) that the surface hydrogen coverage is too low to meet the demands of propane formation. Since the amount of propene produced was relatively constant throughout the ten pulses, the decreasing conversion and carbon retention suggests that the surface carbon residues, which give rise to catalyst deactivation, originate from propyne.

When the pressure of hydrogen in the reactant mixture was increased (3-fold excess), the conversion of propyne was initially much greater than in the equimolar experiments (Table 5.1.3). However, similar to the equimolar

reactions, this conversion was observed to decrease over a series of thirty pulses. The hydrogenation of propyne under these conditions gave rise to both propene and propane. The amount of propane detected over the course of the thirty pulses was found to oscillate (Figure 5.1.3), while propene was only observed from pulse two onward. Similar to the result of Jackson and Kelly[52], it is believed that the formation of the olefin is a consequence of hydrocarbonaceous overlayers acting as hydrogen transfer species[62], and furnishing the propyne molecule with activated hydrogen atoms. The deposition of carbon, determined quantitatively, was observed to decrease (8.13×10^{19} atoms [pulse 1]), until a point at which carbon was being removed from the surface (-1.25×10^{19} atoms [pulse 30]). The yield of propene was observed to pass through two cycles before reaching an apparent steady state value. This can be related to the rate of hydrogen supply to the sites of associatively adsorbed propyne, such that when the yield of propene was low the rate of hydrogen supply could be considered to be low also. When the amount of propene increased with pulsing, the availabilty of hydrogen was greater at the surface.

The oscillations in the propane composition from pulse to pulse are indicative of the concentration of hydrogen in the hydrocarbonaceous residues varying. The existence of an equilibrium between the precursor states for propane and hydrocarbonaceous residue formation, would result in the amount of product formed varying with pulsing, with the rate of hydrogen supply to the relevant sites dictating the predominant reaction.

Using alumina-supported palladium, the reaction of propyne and hydrogen (1:1 ratio) afforded both propene and propane (Table 5.1.5). This relatively low selectivity for a palladium catalyst was accompanied by low conversions of propyne ($\leq$ 28%). Similiar to the silica-supported palladium catalyst, this

reaction also gave rise to significant amounts of retained carbon which was deemed responsible for the drop in catalyst activity for hydrogenation.

The low turnover of propyne, even in pulse one, is in contrast with the expected chemisorption strength of an acetylene at a metal surface. Generally, the heats of adsorption for such processes are high, but the deposition of carbon in the first reaction pulse may be responsible for perturbing the electronic nature of the 'modified' metal surface. It is the existence of this carbon containing surface which gives rise to the desorption of unreacted propyne. Clearly, the production of both propane and propene indicates that sites for the formation of both hydrocarbons are available at the surface. Coupling this with the relatively low conversions of propyne, leads to the conclusion that since both products are only formed in small amounts, the formation of propane can be considered to occur by hydrogenation of surface hydrocarbonaceous overlayers. Under these circumstances we can state that the consecutive reaction pathway, where propane is produced via one surface visit from dissociatively adsorbed propyne is likely. The selective hydrogenation of propyne to propene will occur from the adsorption of an associatively adsorbed propyne species on the hydrogen covered overlayers.

Using an excess of hydrogen in the reactant mixture resulted in complete removal of propyne from the gas eluent stream over a period of sixteen pulses (Table 5.1.7). This high turnover was found to decrease by approximately 55% in pulse seventeen. As with all the previous reactions, this loss of catalyst activity is a function of the poisoning abilities of surface carbonaceous residues. Unlike the silica-supported palladium catalyst, the formation of propene was not evident until after the fifth pulse. This catalyst selectivity increased from zero to approximately 46%, and remained constant at this value over the remaining pulses.

With the amount of propene formed remaining relatively constant, the reaction pathway for propene formation from propyne hydrogenation can be considered to be unaffected by the deposition of carbon at the surface. However, the composition of propane produced was found to vary with pulsing, and the overall trend seems to be one of poisoning of the propane formation sites (decreases by 1.83 $x10^{-5}$ moles over 30 pulses). From Figure 6.0.8, we can state that:

(i) propene production will be the result of the hydrogenation of an associatively adsorbed acetylenic species (*Reaction 1*)

(ii) formation of propane (from hydrogenation of dissociatively adsorbed propyne) will be susceptible to poisoning through carbon deposition (*Reaction 3*)

With the yield of propene effectively unaltered throughout, propane production must occur from direct hydrogenation of the acetylene, with the yield of the alkane therefore decreasing at lower propyne conversions.

5.1.4 The Reaction of Propyne with Hydrogen over Supported Platinum

The hydrogenation of propyne over highly dispersed silica-supported platinum, using an equimolar reactant mixture, produced both propene and propane (Table 5.1.9). The conversion of propyne, although initially low, was found to decrease further over ten pulses. The yield of the olefin and alkane was also small, with the amount of alkane produced decreasing to a limiting value (0.49 $x10^{-5}$ moles $\rightarrow$ 0.22 $x10^{-5}$ moles over 10 pulses). In the case of the olefin,

the amount detected increased from zero in pulse one to a constant amount (0.20 $x10^{-5}$ moles [pulse 6]), suggesting the attainment of a steady state regime.

The conversion of propyne over this catalyst decreased to near zero after ten pulses. Under these circumstances, where all the propyne passed over the catalyst is unreacted, it seems reasonable to propose that both propene and propane detected at this stage of the reaction must be the product of carbonaceous residue hydrogenation. This is in good agreement with the carbon mass balance data which shows that carbon was removed from the surface in the later pulses.

The initially low conversion of propyne could be the result of one or both of two factors. First, the accompanying carbon laydown may act as a poison for subsequent reactions. Second, the catalyst surface, which contains a large fraction of exposed metal atoms, may have insufficient adsorption sites of the required geometric and/or electronic arrangement for propyne chemisorption. The metal particles which have an average diameter of 1-2nm will behave more electrophilically, such that the electron rich acetylenic bond will be chemisorbed more strongly at the surface, thus contributing to the laydown of surface carbon. This would effectively poison the active sites for further propyne adsorption. Coupled with the low concentration of hydrogen atoms at these sites, the carbonaceous residues would become carbidic and deactivate the catalyst.

The selectivity of this reaction shows that the hydrogenation of propyne to yield both propene and propane is still feasible. Since only propane is detected in pulse one, the direct hydrogenation of propyne to produce propane is important. This is most probably a reflection of a primary adsorption period where only dissociative adsorption of propyne occurs directly on the metal to yield the alkane. The production of propene from pulse two onwards suggests that the enhancement of the catalyst selectivity is again a consequence of the hydrocarbonaceous residues acting as hydrogen suppliers for the hydrogenation

of associatively adsorbed propyne species. Since the amount of propene produced is relatively small (and constant) throughout, we can assume that the concentration of propene sites is unaltered by carbon deposition.

In the case of the alkane, an increase in the number of pulses is accompanied by a decreasing propane yield, indicating that the opposite is true for these sites, and that propane formation sites on this surface are susceptible to poisoning; at least until a steady concentration of sites has been attained. Therefore, in relation to the general reaction route described in Figure 6.0.8, we can state that the initial stages of the reaction are (i) the dissociative adsorption of propyne to form surface hydrocarbonaceous residues and (ii) the hydrogenation of adsorbed propyne to produce propane. When the number of pulses increased, the amount of propane eluted decreased, indicating the propensity of these sites to undergo poisoning through carbon build-up. An induction period precedes the formation of propene, the production of which will be the result of hydrogen supply to a di-π-propyne entity from the carbonaceous overlayers.

Increasing the hydrogen content of the reactant mixture (3-fold excess) has a marked effect on both catalyst activity and selectivity. The conversion of propyne under these conditions was initially greater than in the equimolar reactions (Table 5.2.1), which clearly shows that the adsorbed propyne in the former reactions was starved of hydrogen. In the early stages of these reactions the formation of propane occurred exclusively. This reaction predominated until the seventeenth pulse, at which point propene was simultaneously formed. Therefore, it is clear that in order for the hydrogenation of propyne and desorption of adsorbed propene to commence, the accumulation of surface hydrocarbonaceous residues must have progressed in parallel with propane formation.

The amount of propane eluted throughout these reactions was observed to decrease, while the yield of propene increased from zero to a steady value (Figure 5.2.3). Therefore, with regard to the available reaction pathways we can state that those sites which govern propane formation by direct hydrogenation of a dissociatively adsorbed propyne species predominated during the initial sixteen pulses. However, since the amount of propane formed decreased with increasing number of pulses, we can state that these sites are susceptible to deactivation. The large induction period before the detection of propene may be the result of the reluctance of smaller metal particles to form carbonaceous residues[76], which act as hydrogenation species when hydrogen rich[52].

From the carbon mass balance data, it is evident that the amount of carbon retained by the catalyst is increasing as a function of decreasing propyne hydrogenation. Therefore, it is reasonable to assume that both the retained associatively and dissociatively adsorbed surface species must originate from the olefin and alkane precursors.

Propyne hydrogenation over alumina-supported platinum employing a 1:1 mixture displayed complete selectivity toward the production of propene, with low conversion of propyne (Table 5.2.3). As with all other reactions, the turnover of propyne decreased with increasing number of pulses, and was accompanied by significant carbon deposition. The high catalyst selectivity points to (i) the effective exclusion of the olefin from the surface, such that no competition for sites occurs or (ii) the low surface hydrogen coverage favouring olefin formation. The hydrogenation of propyne to yield propene will proceed on a carbon covered surface, and the lack of propane suggests that any sites for dissociative adsorption and hydrogenation of propyne are inactive due to the low concentration of hydrogen at the surface.

The low conversion of propyne indicates that chemisorption on this carbon covered surface is unfavourable. Those molecules which do adsorb either undergo partial hydrogenation to produce propene, or give rise to further carbonaceous residues.

The selectivity of this catalyst is diminished on increasing the amount of hydrogen in each pulse (Table 5.2.5). Essentially, this mixture contains sufficient hydrogen to hydrogenate propyne to propene or propane. The fact that only propane is produced in the early stages of these reactions indicates a route to propane by direct hydrogenation of propyne from one surface visit. The subsequent build up of surface carbon as well as the excess supply of hydrogen from the gas phase inevitably results in the formation of hydrogenated residues, which enable associative adsorption of propyne to produce propene. Since the yield of olefin was relatively unaltered over the course of the pulses, these new surface sites can be deemed resistant to poisoning.

The alkane yield changes slightly from pulse to pulse (Figure 5.2.8), but is constant within experimental error in most cases. Those pulses in which the yield of propane changes dramatically i.e. pulses five, six and seven, are indicative of the varying availability of hydrogen at the propane formation sites.

The actual amount of carbon retained by the catalyst drops to a point at which there is no carbon being retained or removed (0.04×10^{19} atoms [pulse 30]). Under these conditions, all adsorbed propyne is either hydrogenated to propene or propane. Therefore, with the yield of both hydrogenation products remaining constant either (i) the concentration of sites for propene/propane formation or (ii) the rate of propyne hydrogenation is constant.

The decrease in propyne turnover coupled with the decrease in the amount of carbon deposited at the surface suggests that the hydrocarbonaceous overlayers which are produced are acetylenic in origin. Therefore, with the yields of both

propane and propene relatively constant, we can propose that the formation of the alkane will occur from hydrogenation of propyne and surface hydrocarbonaceous residues.

5.1.5 Mechanism for Propyne Hydrogenation to Propene

In order to postulate a mechanism for the reactions described earlier, it is necessary to define the nature of the adsorbed propyne species involved in propene formation, since it is this species which will inevitably give rise to the semi-hydrogenation product.

From the work of Mann and Khulbe[50], the reaction of propyne with hydrogen under dynamic conditions was found to obey Langmuir-Hinshelwood kinetics, with the heat of adsorption of propyne being higher than that of hydrogen. However, this relatively weak adsorption of hydrogen is a crucial step in the hydrogenation process. The mechanism shown in Figure 6.1.1 shows a possible route to propene from an associatively adsorbed propyne species.

The chemisorption of propyne is a two site process, producing an adsorbed di-π-propyne species. The addition of one hydrogen atom to this entity yields the σ/π-propenyl molecule. Subsequent hydrogenation yields the π-adsorbed olefin, which will undergo desorption in favour of the more strongly adsorbed di-π-propyne species. The route to propane formation from an initially adsorbed propyne dissociation product has been discussed earlier (Section 5.1.3).

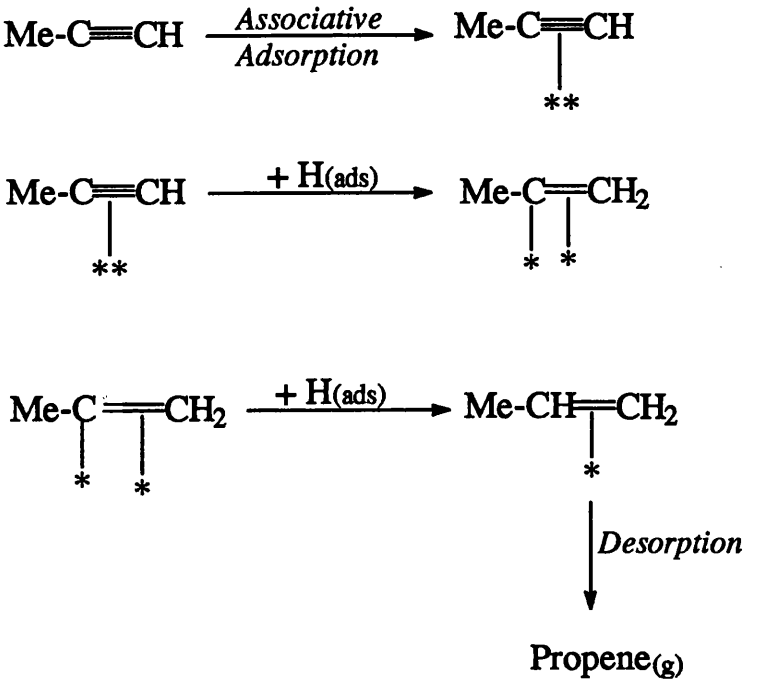

Figure 6.1.1 : *Possible Propyne Hydrogenation Mechanism*

The role of carbonaceous deposits is clearly important in all the reactions described. One major disadvantage, from an industrial viewpoint, is the ease of deactivation of such substrates through coking. Carbonaceous residues which have little or no hydrogen will give rise to carbidic species which reduce the activity of the catalyst for further reaction. The formation of carbonaceous residues in propyne hydrogenation was first identified by Bond and Sheridan[49]. These workers reported the ability of surface adsorbed radical species to undergo a hydropolymerisation reaction to produce surface polymers. This is shown in Figure 6.1.2. The presence of methyl groups on the adsorbed propyne molecules are believed to prevent any extensive polymerisation in the chemisorbed layer due to steric constraints which interfere with (C-C) bond formation.

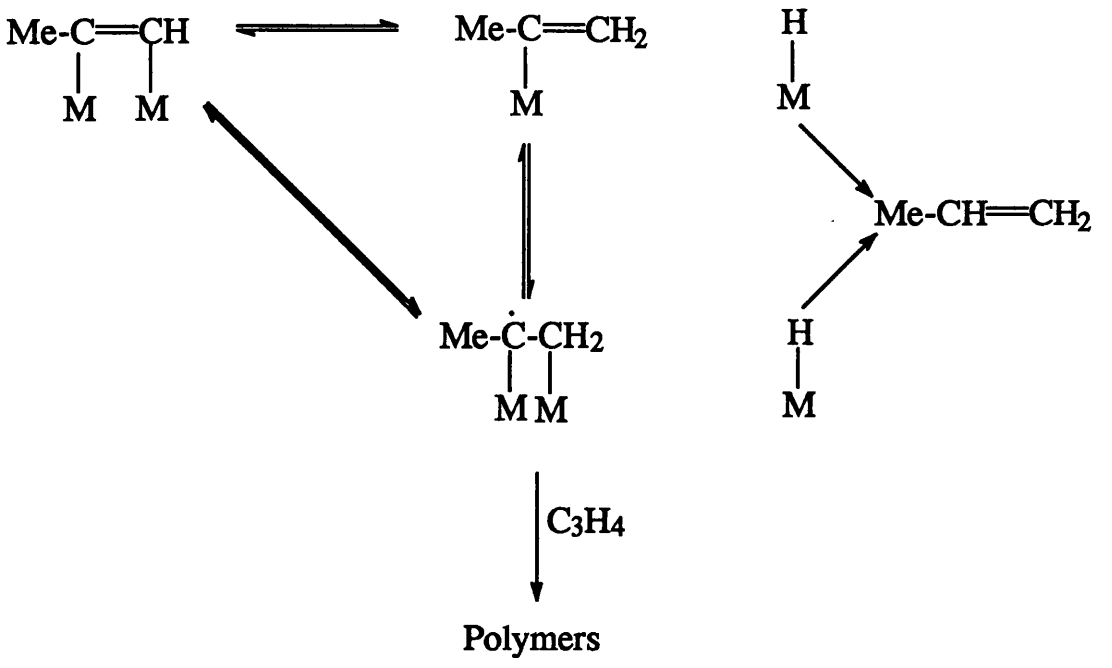

Figure 6.1.2 : *Polymerisation of Propyne Radicals on Metal Surfaces*

5.1.6 Propyne Hydrogenation - Conclusions

5.1.6.1 Equimolar Ratio of Propyne and Hydrogen

The hydrogenation of propyne over silica-supported palladium and alumina-supported platinum is completely selective for the formation of propene. In the case of the palladium catalyst, this may be the result of the metals ability to absorb hydrogen and hence, its high selectivity will be a result of a lower concentration of surface hydrogen. In this case, the hydrogenation will occur as hydrogen diffuses through the metal bulk to attack the chemisorbed propyne.

Bond[77] suggests that this dissolved hydrogen has the ability to alter the electronic nature of the metal and its propensity to attract the π-electrons of the olefin.
For alumina-supported platinum, the above argument cannot be applied so readily. In this case it seems that the formation of propene is either (i) a consequence of propyne excluding propene from the surface [$\Delta H_a(C_3H_4) >> \Delta H_a(C_3H_6)$] or that (ii) the rate of hydrogen supply to dissociatively adsorbed propyne sites is limited.

Both alumina-supported palladium and silica-supported platinum exhibit low selectivities for propene formation. The existence of both propene and propane suggests that both catalysts contain similar concentrations of sites for associative and dissociative propyne adsorption. For highly dispersed platinum, the electrophilicity of the metal particles may be enhanced toward the acetylenic bonds. Therefore, the residence time of the acetylene will be increased, allowing propane production to occur.

Over alumina-supported palladium, the formation of both propene and propane indicates that this surface also has sites for propyne hydrogenation to propene and/or propane. The metal also has the ability to occlude large quantities of hydrogen, which may play an active role in furnishing the adsorbed propyne molecules with hydrogen atoms. The formation of both propene and propane will occur on carbon covered surfaces which does not alter the yield of either product.

5.1.6.2 Excess Hydrogen Reactions

All catalysts were prone to deactivation through carbon deposition. The promoting ability of hydrocarbonaceous residues was more pronounced in these

reactions, most notably in the case of silica-supported platinum. The large induction period before the detection of propene using this substrate may well be the result of the smaller metal particles being more reluctant to form surface carbonaceous residues, which act to supply hydrogen to associatively adsorbed di-π-propyne species. Salmeron and Somorjai[71] reported the preferential deposition of carbon on flat catalytic planes that are well populated with large particles. Therefore, small metal particles, which contain fewer flat faces will be less sensitive to self poisoning through carbon deposition. The low selectivities in these reactions is a product of the greater availability of hydrogen at the surface, a condition which will favour propane production.

5.1.6.3 Physical Nature of Catalysts - Effect on Product Selectivities

In order to fully characterise the hydrogenation reactions of propyne over supported palladium and platinum catalysts, it is necessary to consider the nature of the catalytic surface. The first factor which may be taken into account is the role of the support material in the observed reactions. Clearly the support has an influential role in the reaction chemistry, with both Pd/silica and Pt/alumina exhibiting complete selectivity toward the olefin. However, since these differing supports have identical products, we can assume that the hydrogen atoms associated with each support are not important in relation to the hydrogenation reactions. However, where the support may be important is in the catalyst preparation stages. Both Pd/silica and Pt/alumina have comparable particle sizes (~10 nm from TEM/chemisorption), while Pt/silica and Pd/alumina have smaller particle diameters; 1-2 nm and 5nm respectively. Therefore, the hydrogenation of

propyne over supported palladium and platinum may be governed by the relative metal particle sizes.

This may be summarised in terms of the electrophilicity of smaller metal particles toward electron rich bonds. With both Pd/alumina and Pt/silica exhibiting low selectivities to the olefin, we can propose that this is merely a result of the metal particles ability to retain the acetylene at the surface, with the increase in retention time favouring saturation of the acetylene, to yield the alkane. Those catalysts which are completely selective toward propene (and have larger metal particles) will be less electrophilic, and hence, more likely to allow desorption of the olefin before saturation occurs.

5.2.1 The Interaction of 2-Butyne with Metal Surfaces

The results of the 2-butyne hydrogenation reactions, detailed in the previous chapter, show that with low concentrations of surface hydrogen, 2-butyne hydrogenation favoured production of the *cis*-olefin isomer. At high reaction temperatures, the formation of trace amounts of *trans*-2-butene was also evident.

At high coverages of hydrogen, the major reaction over almost all catalysts was the hydrogenation of 2-butyne to *n*-butane. Unlike the C-3 hydrogenation reactions, the conversion of the acetylene (detailed in Section 5.1.2) was complete, such that all 2-butyne passed over the catalyst was either converted to the alkane or was retained in the form of surface hydrocarbonaceous residues.

The existence of methane in several of the "excess hydrogen" reactions suggests that the dissociative adsorption of 2-butyne on bare metal sites is feasible, as shown in Figure 6.1.3. Therefore, we can conclude that similar to

propyne hydrogenation, the reaction of hydrogen and 2-butyne over supported palladium and platinum will proceed by both dissociative and associative adsorption of the acetylene.

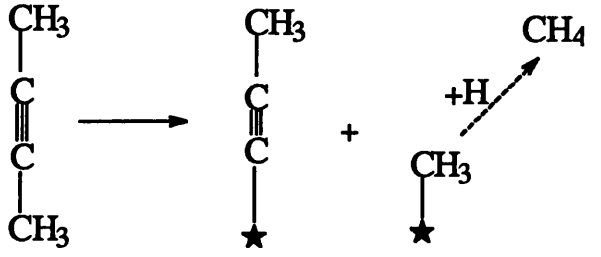

Figure 6.1.3 : *Dissociative Adsorption of 2-Butyne to Yield Methane*

(I) The dissociative process will give rise to surface hydrocarbonaceous residues and/or hydrogenolysis products

(ii) The associative process will proceed via a di-π-adsorbed butyne species that undergoes sequential hydrogen addition to yield the corresponding alkane or olefin.

5.2.2 The Reaction of 2-Butyne with Hydrogen over Supported Palladium

Using an equimolar ratio of H_2/C_4H_6, silica-supported palladium produced *cis*-2-butene as the major hydrogenation product over a range of reaction temperatures. The initial adsorbed state of the acetylene can therefore be envisaged as occurring as a di-π-adsorbed species. Similar to the conclusions of Webb *et al*[78], this chemisorption will be accompanied by a deviation from linearity of the 2-butyne molecule. Due to steric interference experienced by

each of the substituent methyl groups, both from each other and from the surface metal atoms, the angle between the surface plane and these substituent groups will be increased, such that they are directed away from the surface, hence, adopting a *syn* conformation. Therefore, under hydrogenation conditions, the approach of dissociated hydrogen atoms will yield the *cis*-olefin isomer.

At 465K, silica-supported palladium also produced trace amounts of the *trans*-olefin isomer. The argument invoked above will invariably present unfavourable conditions for the formation of this isomer, since addition of the two hydrogen atoms occurs on the same side of the acetylenic bond. For this reason, and also the fact that this isomer was only produced at high temperatures, the formation of the *trans* isomer can be considered to occur by either (i) isomerisation of the *cis*-olefin isomer at the surface or (ii) the adsorption of the acetylene on a low co-ordination site of high energy, such as a step or edge site.

The possibility of *trans* isomer formation by isomerisation will proceed by hydrogen addition to a free radical form of the half-hydrogenated state, which will exist in equilibrium with the normal form. This intermediatory species is shown in Figure 6.1.4.

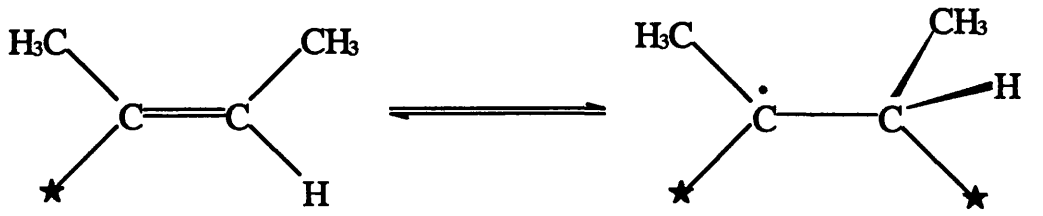

Figure 6.1.4 : *Formation of Trans-2-Butene from Cis Isomer Isomerisation*

Alternatively, hydrogen addition may occur at either side of the acetylenic bond, as shown in Figure 6.1.5. This pathway will undoubtedly yield only a small amount of the *trans* isomer, since the number of metal atoms located on such surface sites of the required energy, will be minimal.

At 465K, the reaction of an equimolar mixture of H_2/C_4H_6 over Pd/silica produced both *cis* and *trans*-olefin isomers (Table 5.2.7). The amount of *cis*-2-butene detected was observed to decrease from 3.19 $x10^{-5}$ moles (pulse 1) to 1.88 $x10^{-5}$ moles (pulse 6). From pulse seven onward, the amount of *cis*-olefin formed tended to increase (3.26 $x10^{-5}$ moles [pulse 10]).

Since the activity of the catalyst for hydrogenation was found to decrease to a limiting value (60% [pulse 10]), we can assume that the initial decrease in the *cis*-olefin yield was a result of these sites being poisoned by carbonaceous residues. This is corroborated by the carbon retention data, which shows the accumulation of carbon at the surface.

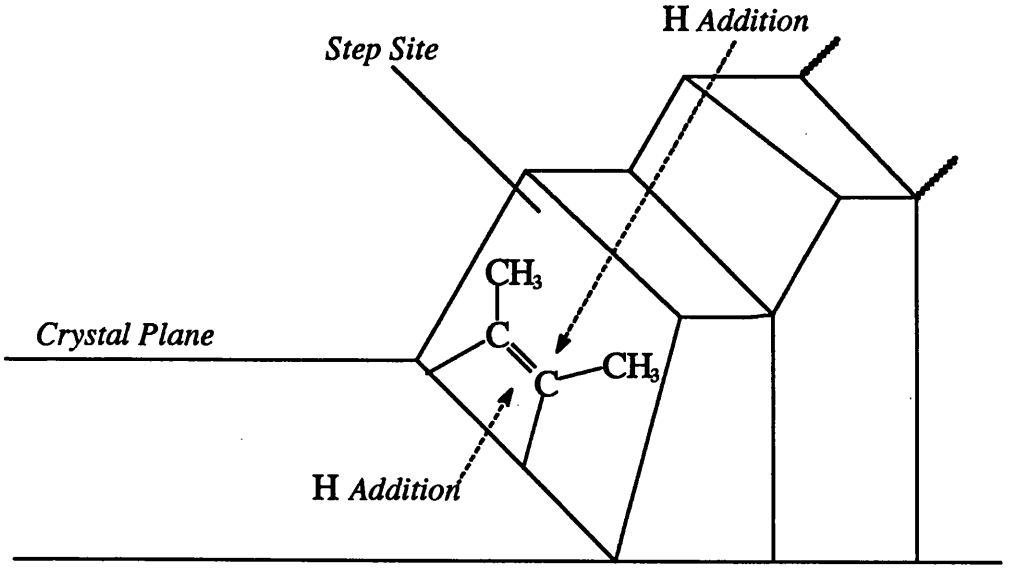

Figure 6.1.5 : *Possible Trans-2-Butene Formation Mechanism*

From pulse seven onward, where the *cis*-olefin yield increased, the degree of carbon laydown tended to decrease. Therefore, since the conversion of 2-butyne was constant, we can attribute the decrease in carbon deposition to a slow supply of hydrogen to the dissociatively adsorbed 2-butyne sites which produce hydrocarbonaceous residues.

The reaction of an equimolar mixture of H_2/C_4H_6 over Pd/silica at 373K again showed signs of catalyst deactivation (Table 5.2.9). However, at this temperature, the amount of detected *cis*-2-butene was unaltered over ten pulses. The conversion of 2-butyne decreased before finally increasing in the later pulses, at which point all the acetylene was converted. The retention of carbon by the catalyst also fluctuated, with the amount retained at the surface decreasing (3.84×10^{19} atoms $\rightarrow$ 2.4×10^{19} atoms over eight pulses) then increasing (4.76×10^{19} atoms [pulse 9]). The hydrogenation of 2-butyne to produce *cis*-2-butene occurs in parallel with this carbon deposition, with (i) hydrogenation of the associatively adsorbed acetylene and (ii) hydrogenation of the surface retained carbonaceous residues determined by the availability of hydrogen. Therefore, the initial decrease in the catalysts activity for 2-butyne conversion can be attributed to a greater rate of formation of carbonaceous residues at the surface, thus reducing the number of *cis*-2-butene formation sites. The increase in the amount of *cis*-2-butene produced in pulses nine and ten, although small, may be due to a greater rate of hydrogenation of the di-π-adsorbed butyne species as opposed to the carbonaceous residues. This may be a reflection of the greater propensity of the surface for non-dissociative adsorption of the 2-butyne molecule, a phenomenon which could be related to a surface with a reduced number of bare metal sites.

At 330K, the reaction of an equimolar mixture of H_2/C_4H_6 over Pd/silica produced no hydrogenation products. These pulse reactions showed no trend in

the conversion of 2-butyne with increased pulsing. The lack of hydrogenation activity at this intermediate temperature suggests :

(i) At ambient temperature the hydrogenation of 2-butyne to yield *cis*-2-butene proceeds via an associatively adsorbed acetylenic species

(ii) At high temperatures the hydrogenation of 2-butyne to form *cis*-2-butene proceeds with an associatively adsorbed species adsorbed on a surface carbonaceous overlayer (formed from initial dissociative adsorption of the acetylene), with the latter acting as a hydrogen transfer medium

(iii) Therefore, at 330K, we can propose that both low and high temperature reaction pathways are subject to poisoning through carbon deposition

At ambient temperature (298K), the reaction of equimolar H_2/C_4H_6 over the above catalyst displayed complete conversion of the acetylene over nine pulses (Table 5.3.2). The effect of carbon deposition is apparent in pulse ten, at which point 2-butyne conversion decreased by approximately 30%, with the decreasing yield of *cis*-2-butene also attributable to the poisoning properties of such surface carbonaceous overlayers.

The reaction of 2-butyne with excess hydrogen at 465K over Pd/silica, produced both *n*-butane and methane, with all acetylene passed over the catalyst converted to either product(s) or carbonaceous residues over thirty pulses (Table 5.2.8). The elution of both hydrogenation products was accompanied by continual carbon deposition which decreased (2.60×10^{19} atoms [pulse1] $\rightarrow$ 1.57×10^{19} atoms [pulse 30]) with increased pulsing. Taking each hydrogenation

product separately, let us first consider the mechanism for *n*-butane formation. One possible mechanism for the hydrogenation of 2-butyne to produce the corresponding alkane, will proceed with the acetylene adsorbed as shown in Figure 6.1.6. The addition of adsorbed hydrogen to this species will give rise to a surface bound olefin, which itself will undergo reduction, to yield the alkane. Therefore, the hydrogenation of 2-butyne over silica-supported palladium in excess hydrogen can be postulated to proceed by a Langmuir-Hinshelwood mechanism, with the sequential addition of adsorbed hydrogen atoms to the unsaturated hydrocarbon.

Over Pd/silica the extent of methane production was quite marked at 465K, and was found to remain relatively constant over thirty pulses. Therefore, since the formation of both *n*-butane and methane was coupled with continued carbon laydown, we can conclude that there where bare metal sites at the surface which permitted hydrogenolysis. The hydrogenation reaction shown below can be envisaged as occurring on either an exposed or carbon covered surface. Similar conclusions were reported by Maetz and Touroude[57], for the hydrogenation of 1-butyne over palladium and platinum catalysts. In this study the existence of compact overlayers existing on high co-ordination sites proved incapable of dissociating molecular hydrogen, while the low co-ordination sites (top, edge and corner atoms) were available for the hydrogenation reactions.

It may therefore be concluded that the increased surface hydrogen coverage favours the formation of the saturated product. The complete activity of this catalyst for 2-butyne conversion coupled with substantial carbonaceous overlayer formation, indicates that the hydrogenation of 2-butyne to *n*-butane and methane is a consequence of the catalysts ability to chemisorb the acetylene as either an associative or dissociative entity. The fact that no carbon was removed from the surface suggests however, that the supply of hydrogen to the

carbonaceous residue sites is minimal. Under these circumstances, the rate of hydrogen supply to the alkane precursor sites will predominate.

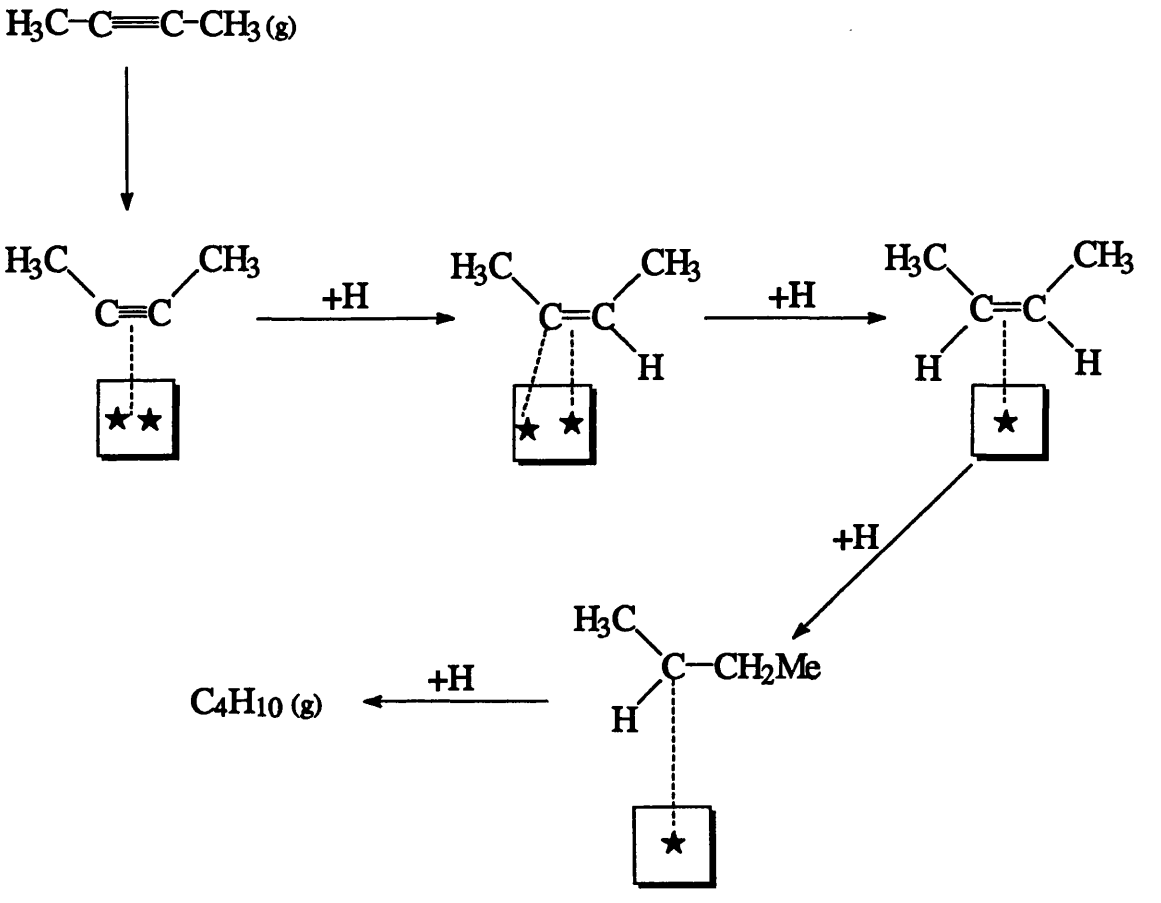

Figure 6.1.6 : *Possible Butane Formation Mechanism*

At lower temperatures (373K), 2-butyne hydrogenation over Pd/silica using excess hydrogen produced only *n*-butane and surface hydrocarbonaceous overlayers. Therefore, we can postulate that the formation of the alkane will commence via an associatively adsorbed species (as shown in Figure 6.1.6), which in the presence of high coverages of hydrogen yields the saturated product.

In these reactions, the degree of carbon laydown was less (Table 5.3.0), and indeed, in several pulses, carbon was removed from the surface. Clearly the residues formed at this temperature are prone to hydrogenation, which could explain the slight oscillations in the *n*-butane yield, with both the alkane and carbonaceous residues competing for hydrogen supply.

Over alumina-supported palladium, the reaction of an equimolar reactant mixture produced only *cis*-2-butene at 373K. In these reactions, all 2-butyne passed over the catalyst was converted to the olefin and surface carbonaceous residues. This conversion of 2-butyne was maintained over a series of ten pulses (Table 5.3.3). The ability of the substrate to produce carbonaceous residues fluctuated with increasing reaction. The fact that the amount of olefin formed decreased, suggests that either the concentration of surface sites for olefin production were reduced, or that the rate of hydrogen supply to these sites was low.

At 298K, hydrogenation of 2-butyne using an equimolar reactant mixture produced only *cis*-2-butene and unconverted acetylene (Table 5.3.5). Pd/alumina was found to operate within a steady state regime with respect to 2-butyne conversion, with the amount of *cis*-2-butene formed tending to decrease with increasing number of pulses. At this temperature, the amount of retained carbon was observed to increase suggesting an increase in the rate of dissociative adsorption of the acetylene. Therefore, since the decreasing yield of the *cis*-olefin isomer is accompanied by increased carbonaceous overlayer formation, we can propose that as the reaction progresses, the rate of hydrogen supply to the olefin formation sites (associatively adsorbed 2-butyne) is reduced. This can be attributed to the low availabilty of dissociated hydrogen atoms at the catalyst surface. From the carbon mass balance (Figure 5.4.9) it can be seen that in pulse

two the removal of surface carbonaceous residues occurs. This may well be a result of an increase in the supply of hydrogen to those sites which initiate dissociative adsorption. One possibility is that in pulse one, dissociative adsorption of 2-butyne occurs to yield a dehydrogenation product, such as C_4H_5 (shown in Figure 6.1.7). This species could then undergo hydrogenation in pulse two and desorb as 2-butyne, thus explaining the negative Δcarbon value. Another possible explanation for this observation is that the acetylene is adsorbed at a surface site which is inactive for hydrogenation, and is desorbed in a later pulse.

Using excess hydrogen, the hydrogenation of 2-butyne over Pd/alumina produced only *n*-butane and surface carbonaceous residues at 373K (Table 5.3.4). The yield of the alkane varied with pulsing, although conversion of the acetylene was maintained at 100% over thirty pulses. The production of surface carbonaceous overlayers oscillated from pulse one to twenty, with subsequent pulses being retained by the catalyst (Figure 5.4.7). Again the fluctuations in the extent of alkane and carbonaceous overlayer formation suggests that some type of competition for hydrogen between the associative and dissociative acetylene states exists. The ability of previously retained overlayers to undergo hydrogenation (reflected in negative Δcarbon values) may be an indication of the type of species formed when 2-butyne is dissociatively adsorbed on the surface. Clearly the decrease in the amount of carbon retained by the catalyst, coupled with the increasing *n*-butane yield suggests that the initial state of the surface residue is that of a dehydrogenation product. This species would undergo hydrogenation to produce the alkane. From pulse twenty-one onwards, where there is effectively no hydrogenation of the residues, it is the hydrogenation of associatively adsorbed 2-butyne which predominates. This suggests that bare metal sites must be available at the surface in order to dissociate molecular hydrogen and activate the resultant hydrogen atoms.

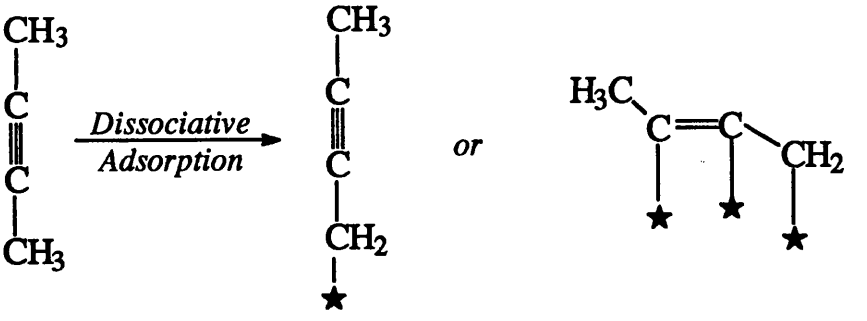

Figure 6.1.7 : *Possible Dehydrogenation Products of 2-Butyne*

At 298K, the hydrogenation of 2-butyne in excess hydrogen produced both *n*-butane and methane (Table 5.3.6). In these reactions, the yield of methane was relatively small, with the major product being the C-4 alkane. The most interesting feature of these reactions lies in the seemingly constant production of carbonaceous residues at the surface (Figure 5.5.2). However, this trend may be the result of the simultaneous removal of carbon as methane, and the continual dissociative adsorption of the acetylene. Therefore, one possibility is that the near constant carbon deposition trend may be masking these two competing reactions.

5.2.3 The Reaction of 2-Butyne with Hydrogen over Supported Platinum

The hydrogenation of 2-butyne over silica-supported platinum using an equimolar ratio of H_2/C_4H_6 produced both isomers of 2-butene at 465K (Table 5.3.7). As with the palladium-catalysed reactions, the formation of the *trans* isomer was minimal, with *cis*-2-butene constituting the major fraction of eluted

products. With increased number of pulses, the yield of this *cis* isomer and the conversion of 2-butyne were observed to decrease. Both phenomena can be attributed to a poisoning process, whereby the surface sites for both olefin production and butyne conversion (to carbonaceous residues) are reduced in number. The amount of carbon retained by this catalyst was found to increase from pulse one (0.83 $x10^{19}$ atoms) to three (2.71 $x10^{19}$ atoms), at which point all subsequent pulses removed surface carbon species. Therefore, we can state that the initial increase in carbonaceous residue formation is responsible for the decrease in the *cis*-olefin yield. The ensuing decrease in retained carbon, coupled with the deactivation of the substrate indicates that the carbonaceous residues formed originate from the adsorbed acetylene. Indeed, the trend in both the carbon deposition data and the amount of eluted acetylene suggests that this carbonaceous species is a 2-butyne derivative which is removeable from the surface by hydrogenation.

When excess hydrogen was used in the reaction mixture, Pt/silica produced both isomers of 2-butene (Table 5.3.8), and the conversion of the acetylene was maintained at 100% over thirty pulses. The amount of *trans*-2-butene detected was again small (0.55 $x10^{-5}$ moles $\rightarrow$ 0.24 $x10^{-5}$ moles) and decreased to zero after three pulses. The yield of the *cis* isomer was found to increase with increasing number of pulses (Figure 5.5.6). Similar to the other 2-butyne hydrogenation reactions performed with high coverages of hydrogen, it seems that the nature of the adsorbed acetylenic species is sensitive to the surface hydrogen concentration. However, since the existence of a higher concentration of hydrogen atoms does not produce the saturated hydrocarbon, we must consider the likely reasons for this high catalyst selectivity.

First, in considering the active surface sites, we must consider the effect of the high metal dispersion on possible reaction pathways. The existence of a large

number of exposed metal atoms at the surface of this catalyst, suggests that there is a greater possibility of metal atoms being located in low co-ordination sites. Clearly the adsorption of 2-butyne at such sites would be statistically less likely than adsorption on the more densely packed crystal planes, and so the residence time of the acetylene at the surface would be decreased. In these circumstances, the desorption of the partially hydrogenated product would occur before complete saturation. However, in view of the high turnover of 2-butyne, we can assume that such sites are minimal compared to the number of exposed metal atoms on the common crystal planes, such as the (111) and (100) faces.

A second possibility lies in the mode of 2-butyne adsorption at the surface. Since no alkane was observed we can conclude that the adsorption of 2-butyne on Pt/silica will proceed as either an associative *or* dissociative adsorbed entity. Hydrogenation of the former will proceed as detailed earlier (Section 5.2.2). In the case of the dissociatvely adsorbed acetylene we can propose that this species must retain the overall integrity of the reactant hydrocarbon such that hydrogenation will not affect the overall stereochemistry of the molecule. This route to *cis*-2-butene will become more feasible if the inital dissociative adsorption of 2-butyne occurs via (C-H) bond scission, as opposed to (C-C) bond breaking. Since (C-C) bond scission is an initial requirement for the formation of surface carbon, an increase in the amount of carbon deposited at the surface would be evidence for this reaction. However, since the carbon mass balance data indicates that almost all pulses remove carbon (deposited in initial pulses), it seems that the (C-H) bond breaking model is more likely.

In conclusion we can state that either (i) the hydrogenation occurs on crystal defect sites or (ii) the products are governed by the adsorption of the acetylene as either an associative *or* dissociative species.

At 373K, the reaction of an equimolar H_2/C_4H_6 mixture over Pt/silica was also 100% selective for the production of the *cis*-olefin isomer (Table 5.3.9). The amount of olefin formed was observed to change (Figure 5.5.8), with the general trend indicating a decrease in the amount of eluted olefin with increased number of pulses. However, in pulses nine and ten, the olefin yield was found to increase again. The activity of the catalyst for 2-butyne conversion also decreased with increasing reaction, with the amount of unreacted 2-butyne increasing sharply in pulse five. From this we can conclude that the formation of surface carbonaceous overlayers is important in the deactivation process. The increase in the olefin yield in pulses nine and ten must also be related to the deposition of carbon. From pulse six, the retention of carbon is either negative in value (-1.43×10^{19} atoms) or slightly positive (0.54×10^{19} atoms). Pulses nine and ten show significant carbon loss from the catalyst surface, suggesting that these species are, as detailed earlier (excess hydrogen; 465K), susceptible to hydrogenation and constitute a fraction of the detected *cis*-2-butene product.

At 373K, the hydrogenation of 2-butyne in excess hydrogen over Pt/silica produced only *cis*-2-butene (Table 5.4.0). However, there appeared to be oscillations in both the olefin yield and the extent of carbon retention at the surface. This behaviour may be directly related to the availability of hydrogen at the surface. With a high concentration of surface hydrogen it is reasonable to assume that the fluctuations in both the carbonaceous residue formation and the olefin yield are the result of a competition for hydrogen. Such a process will be governed by the rate of hydrogenation of the relevant adsorbed species. Since the catalyst maintains 100% conversion of the acetylene in each pulse, with only carbon remaining, we can conclude that the adsorption of 2-butyne in each successive pulse will be altered, since the availability of suitable adsorption sites will be changed by this carbon laydown. This carbon may well have the ability to

perturb the electronic nature (as well as geometric arrangement) of the acetylene, such that the availability of hydrogen at the olefin formation sites changes.

Hydrogenation of 2-butyne over alumina-supported platinum at 465K, produced both olefin isomers, when an equimolar ratio of H_2/C_4H_6 was employed (Table 5.4.1). The yield of *cis*-2-butene decreased over ten pulses (1.19×10^{-5} moles [pulse 10]) with the corresponding *trans* isomer yield observed to increase to a limiting value (0.50×10^{-5} moles [pulse 10]). The retention of carbon by the catalyst decreased to a negative minimum (-0.73×10^{19} atoms [pulse 4]; C_{total} : 5.24×10^{19} atoms [pulse 4]), before increasing in subsequent pulses. The fluctuations in the carbon retention values suggests that these residues are themselves prone to hydrogenation. Therefore, we can conclude that the decrease in retained carbon is indicative of a greater availability of hydrogen, with the subsequent increase in surface retention reflecting either (i) an increase in the rate of dissociative acetylene adsorption or (ii) the lack or slow supply of hydrogen to these sites.

Using an excess of hydrogen, Pt/alumina produced both *n*-butane and methane at 465K (Table 5.4.2). As with all other reactions performed in excess hydrogen, 100% conversion of the acetylene was maintained over thirty pulses. The yield of *n*-butane increased (1.09×10^{-5} moles $\rightarrow$ 2.01×10^{-5} moles over 30 pulses) until a steady state was achieved with respect to alkane production. Methane production was observed to fluctuate over the first ten pulses before decreasing to zero in pulse eleven. This behaviour can be attributed to the accessibility of bare metal sites at the surface. In order for (C-C) bond breaking to occur, the initial requirement is the adsorption of 2-butyne at a bare metal site(s) which initiate dissociative adsorption (see Section 5.2.1). If these sites are blocked by carbonaceous residues then this bond cleaving process will be limited. Indeed, the extent of the metals influence on the acetylene will decrease as a

function of increased acetylene distance from the surface. The relatively low quantities of carbon retained by the catalyst in these reactions may well be reflecting (i) the ease of hydrogenation of such residues or (ii) a decrease in the number of exposed metal sites for (C-C) bond scission.

Over Pt/alumina, the reaction of an equimolar ratio of H_2/C_4H_6 at 373K produced only *cis*-2-butene and unconverted 2-butyne (Table 5.4.3). The initially high catalyst activity for acetylene conversion (100%) was observed to decrease with increasing number of pulses (86% [pulse 4]), indicating deactivation through carbon laydown. The *cis*-olefin yield decreased initially before reaching a limiting value. Carbon retention increased with decreasing olefin yield and *vice versa*, suggesting that the number of active hydrogenation sites was reduced through carbon deposition, resulting in the attainment of a steady concentration of olefin formation sites.

At 373K, the reaction of 2-butyne with excess hydrogen produced *n*-butane, with 100% conversion of the acetylene (Table 5.4.4). The amount of alkane detected oscillated from pulse to pulse, with similar behaviour observed in the carbon retention data. Similar to the other reactions where oscillatory behaviour was observed, we can attribute this to the supply of hydrogen to the acetylene adsorption sites. With the surface effectively changing with each pulse, the supply of hydrogen atoms to the unsaturated hydrocarbon will vary, such that either the associatively adsorbed states (alkane precursor) or the dissociatively adsorbed states (carbonaceous residue precursor) will predominate.

5.2.4 Infra-Red Study of 2-Butyne Adsorption on Silica-Supported Palladium under Hydrogenation Conditions.

The infra-red spectrum of 2-butyne (Figure 5.7.4) shows significant intensity in the (C-H) stretching region (2927 and 2868 cm^{-1}) which is characteristic of the methyl substituents of the hydrocarbon. Two intense (C-H) deformation modes are observed at 1452 cm^{-1} and 1387 cm^{-1}, with the latter found as a shoulder on the more intense 1452 cm^{-1} band. An overtone of the 1387 cm^{-1} band is also observed at 2742 cm^{-1}.

Adsorption of 2-butyne on silica-supported palladium results in a slight shift in the frequencies of the gas IR bands, as shown in Table 5.4.8. This is indicative of weak adsorption of the acetylene at the surface. Similar to the spectrum of 2-butyne, this spectrum exhibits similar bands in the (C-H) stretching region which is evidence for the retention of the integrity of the methyl groups upon adsorption. The high frequency region contains a band at 2757 cm^{-1} which can be attributed to the overtone of the symmetric deformation mode of the methyl groups. Evidence for the assignment of this band was corroborated by the existence of the corresponding fundamental vibration, found at 1375 cm^{-1}. However, our ability to observe the asymmetric CH_3 deformation mode was hindered by the poor signal to noise ratio in this region due to moisture detection. Band identification in this region is further complicated, due to the silica support contributing to the absorption of infra-red radiation, hence, weakening any existing signal(s).

The inherent weakness of this asymmetric deformation band was verified by Chesters *et al*[26] in a publication on the results of a transmission infra-red study for *cis*-2-butene adsorption on Pt/SiO_2. Although present, and quoted at 1450 cm^{-1}, this band had a small peak height compared to its symmetric counterpart, and

was also subject to broadening. It is not possible to ascertain if this feature is present in our study due to problems with the flushing of the sample compartment, which resulted in this spectral region being partially obscured by atmospheric moisture.

Table 5.4.8 : *Relative Shifts in Dominant IR Bands Upon Adsorption*

2-Butyne $_{(ads)}$	2-Butyne $_{(g)}$	ΔFrequency / cm^{-1} *[Adsorption-Gas Phase]*	Assignment
2933	2927	6	$\upsilon CH_{3(asym)}$
2870	2868	2	$\upsilon CH_{3(sym)}$
2757	2742	15	$2\delta CH_{3(asym)}$
1375	1387	-12	$\delta CH_{3(sym)}$

From the data available to Chesters' group[26], it was concluded that the adsorption of *cis*-2-butene on Pt/SiO_2 produced a 2,3-di-σ/π butyne species via surface dehydrogenation. This entity was postulated as being coordinated on triangular sites with π bonding to the third platinum atom, as shown in Figure 6.1.8. In view of our data, and most importantly the identification of the 1375 cm^{-1} deformation band, we can propose that the chemisorption of 2-butyne on Pd/SiO_2 will occur similarly. The hydrogenation of this species to form *cis*-2-butene will proceed as detailed in Section 5.2.2.

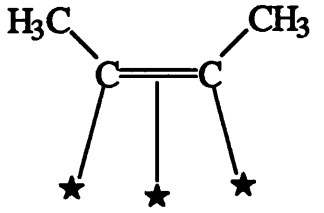

Figure 6.1.8 : *2,3-di-σ/π Butyne Species*

A second important feature of the DRIFTS spectra (Figure 5.7.5) was the ease of removal of the adsorbed hydrocarbon from the surface, suggesting that the adsorbate is not permanently retained at the surface, and may involve weak metal-acetylene bonds. This latter statement is consistent with the small frequency shifts observed on moving from the gaseous to adsorbed state. This was seen in both the DRIFTS and transmission experiments, and suggests that the species observed may be an intermediate in the hydrogenation process. This is corroborated by the results of 2-butyne hydrogenation reactions over Pd/silica. Clearly, strong adsorption of the acetylene will be a prerequisite to the formation of hydrocarbonaceous residues, which suggests that this relatively weakly co-ordinated molecule is indeed active in the hydrogenation step. The propensity of this catalyst to form surface residues would also explain the inability of the used catalyst to chemisorb CO, since all previously available coordination sites would be subject to carbon laydown.

5.2.5 Carbonaceous Residue Formation on Palladium and Platinum Surfaces

The hydrogenation of both propyne and 2-butyne gave rise to the formation of surface carbonaceous residues, which had a marked effect on both the product selectivities and the catalyst lifetime.

The first important feature of these surface residues is their ability to act as hydrogen transfer species[62]. The hydrogenation reactions of propyne clearly show the beneficial effects associated with hydrogen rich carbonaceous residues, which is their ability to supply hydrogen to associatively adsorbed acetylenic species. This behaviour is best summarised in terms of the initial chemisorption of the acetylene on the carbon covered surface (formed by dissociative adsorption of reactant hydrocarbon). The existence of a number of exposed metal atoms will be required to effect the dissociation of molecular hydrogen to produce active hydrogen atoms. These dissociated atoms can be considered to then traverse the carbonaceous overlayer until they encounter an acetylene molecule with which to react.

The precise mechanism for this hydrogen supply is not fully understood, although similar types of hydrogen transfer reactions have been documented in organometallic complexes. This process is termed α-elimination[79] and involves the transfer of one or more hydrogen atom from one organic molecule to another, resulting in the displacement of a suitable leaving group. However, one complication in attempting to correlate the α-elimination process with hydrogen transfer at surfaces lies in the electronic and geometric requirements of the former process. First, α-elimination is generally considered to proceed in high oxidation state metal complexes which contain vacant d-orbitals. The second requirement is that steric crowding within the organometallic should favour expulsion of a

suitable leaving group. A typical example of this reaction is shown in Figure 6.1.9, which proceeds by hydrogen transfer from the neopentyl group to the benzyl functionality, resulting in the displacement of toluene. It is believed that the α-H which undergoes transfer is activated by attraction to the metal centre.

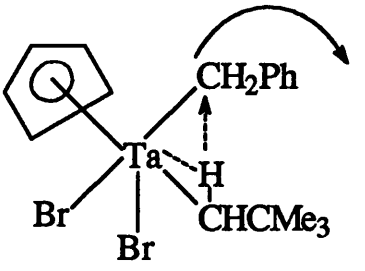

Figure 6.1.9 : *α-Elimination Process*

Therefore, in order to correlate the α-elimination process with the hydrogen transfer capability of surface hydrocarbonaceous residues, we must attempt to fulfil the overall requirements of the elimination reaction at a surface. First, the necessity of a high oxidation state metal in the organometallic complex can be related to the propensity of the metal surface to form new chemical bonds. This can be summarised in terms of the desire of the orbitals on the free metal surface to form as many bonds as possible with chemisorbed species in order to lower its surface free energy. Thus, the desire of the high oxidation state metal to undergo electron reduction can be related to the "electrophilic" nature of surface metal atoms toward electron donating adsorbates.

The second requirement of the α-elimination process is geometric in origin. This can be related to the geometric and thermodynamic requirements of surface chemisorption and desorption. As detailed earlier, the formation of

carbonaceous residues at a catalytic surface results in a reduction in the number of exposed metal atoms. In the hydrogenation reactions of propyne and 2-butyne, the quantity of carbon retained at the surface was large. One possibility is that the retained carbonaceous species are located on the support material[80]. The second scenario may involve the location of surface carbonaceous species, which are acetylenic in origin, near the active metal sites, which undergo a surface polymerisation reaction[49] to produce oligomeric species. Another factor which must be taken into consideration is the thermodynamic stabilities of the various adsorbed species at the surface. When considering the possibility of "leaving groups" we must take into account the relative heats of adsorption of the reactant and product hydrocarbons. Clearly, the hydrogenation of the acetylenic precursor to produce the product olefin or alkane (via hydrocarbonaceous overlayers) will favour the desorption of either the alkane or the olefin over the acetylene. Under these circumstances, the product hydrocarbons can be considered to act as better leaving groups than the acetylene. Therefore, taking all of these factors into consideration, the catalyst surface may be considered to mirror the organometallic complex, with the possibility of hydrogen transfer from hydrocarbonaceous residues proceeding by the α-elimination process not infeasible.

The second, detrimental feature of surface carbonaceous residue formation is its role in the deactivation process. Carbon deposited at the surface can partially or wholly obscure the metal sites so as to prevent the chemisorption of either or both reactants. Therefore, in the case of partial poisoning of the metal sites, the build up of surface carbon can be considered to alter product selectivities, whilst complete poisoning is generally thought of as involving a diffusion inhibition mechanism, such as pore blocking.

In propyne hydrogenation, the continual formation of surface carbonaceous residues resulted in a reduced turnover of the acetylene with

increasing reaction. Clearly, this phenomenon can be attributed to a site blocking process, whereby the number of active hydrogenation sites is reduced.

However, as well as considering the trend of the carbon laydown, we must also take into consideration the degree of carbon retention on each of these catalytic surfaces. Quantitative carbon mass balance information indicates that the hydrogenation reactions of propyne and 2-butyne proceeded with each catalyst retaining large quantities of carbonaceous deposits. Therefore, in view of the fact that hydrogenolysis occurred in the presence of these deposits, we must conclude that there are bare metal sites at the surface to initiate such bond breaking. Taking into consideration these observations, we can propose that the active surface during these processes may be similar to that described by Somorjai *et al*[81] for platinum reforming catalysts. In this model, shown in Figure 6.2.0, the carbonaceous deposits are always present at the surface, with their structure varying from two to three-dimensional (grow in height), with increasing temperature. One of the most significant components of this model is the existence of uncovered metal sites, upon which both hydrogen atomisation and hydrogenolysis can occur. Somorjai also postulated a model involving surface diffusion of these residues. In this process it is believed that those metal sites which are uncovered will chemisorb the reactant molecule, which subsequently compress the carbonaceous deposits by some type of surface diffusion. This therefore frees up the active metal site upon which the reaction occurs. Upon desorption of the product, the carbonaceous residues will diffuse back to their original positions, until the process is repeated by the adsorption of another reactant molecule.

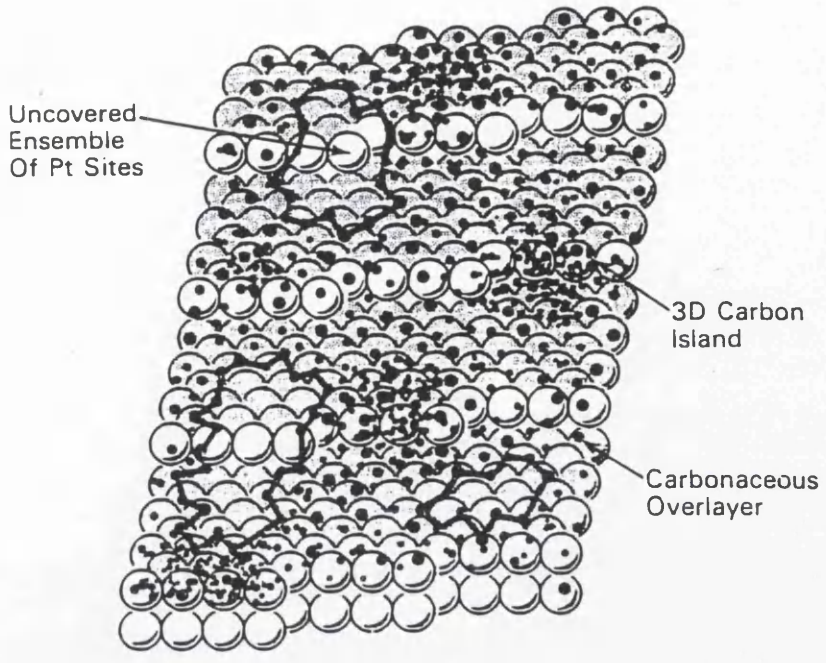

Figure 6.2.0 : *Carbonaceous Overlayers on Platinum Surface*

Therefore, for the reactions of propyne and hydrogen over supported palladium and platinum where it was found that the activity of the catalysts for propyne conversion decreased with increasing carbon deposition, we can conclude that the rate of surface diffusion of the carbonaceous deposits must also have decreased. In view of the fact that these residues may well be oligomeric, it seems plausible that as more are produced, the ease of compression of these oligomers to free up the metal sites will become more difficult.

In the case of the di-substituted acetylene, 2-butyne, the deactivation of the substrate was only observed in those reactions where the surface hydrogen coverage was low. Similar to the conclusion of Somorjai[82], this seems to indicate that the carbonaceous residues participated in the reactions by hydrogen transfer, by providing sites for rearrangement and desorption.

With higher coverages of hydrogen, the hydrogenation reactions of 2-butyne exhibited no signs of catalyst deactivation with continual carbon deposition. This suggests that either (i) the compression of these deposits

occurred readily or (ii) that the hydrogen storage capacity of these residues was such that the reaction and subsequent desorption of the acetylene was feasible. With reference to the first suggestion, it should be noted that the progress of surface chain growth in C-3 oligomers will be hindered by steric constraints. In the case of the di-substituted acetylene, 2-butyne, this same argument can also be applied, with the existence of both substituent methyl groups preventing extensive chain growth. In these circumstances, the existence of only small carbon containing residues would make compression easier, thus explaining the consistently high turnover of 2-butyne to product(s).

5.3.1 Phenylacetylene and Styrene Hydrogenation - Preface

Similar to the hydrogenation of propyne, the scheme shown in Figure 6.2.1 will be used as a reference for this section, and includes the possible reaction pathways to the phenylacetylene hydrogenation products.

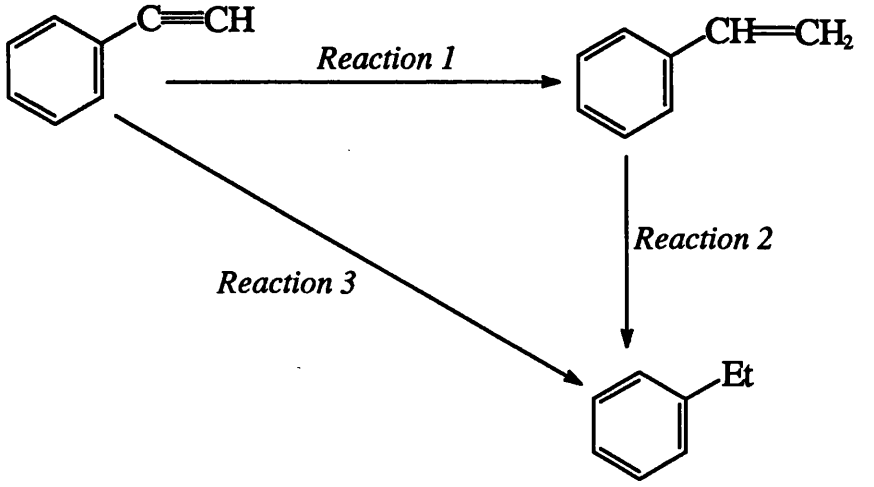

Figure 6.2.1 : *General Hydrogenation Scheme for Phenylacetylene*

5.3.2 The Liquid Phase Hydrogenation of Phenylacetylene and Styrene over Supported-Palladium

When phenylacetylene was hydrogenated in an excess of hydrogen, over silica-supported palladium, the reaction produced both styrene and ethylbenzene, with complete removal of the acetylene. On complete consumption of phenylacetylene, the hydrogenation of styrene to ethylbenzene predominated. In view of this it is reasonable to propose that the initial adsorption and hydrogenation of phenylacetylene to produce both the olefin and alkane occurs simultaneously. On removal of the acetylene, the adsorption and hydrogenation of styrene to ethylbenzene will be favoured. Therefore in relation to the general reaction scheme, we can state that:

(i) *Reaction 1* and *Reaction 3* pathways exist in the presence of the acetylene
(ii) *Reaction 2* is favoured in the absence of the acetylene
(iii) *Reaction 2* will probably be non-existent or minimal in presence of the acetylene

In the case of styrene hydrogenation, the rate of olefin consumption was less than that observed for phenylacetylene, indicating the catalysts greater proficiency for phenylacetylene hydrogenation. In view of this observation, we can propose that in the reaction of phenylacetylene and hydrogen over Pd/silica, the acetylene will be, as stated above, the favoured adsorbate, producing both the olefin and the alkane simultaneously.

Co-hydrogenation experiments performed using an equimolar ratio of phenylacetylene/styrene showed that the presence of the olefin enhanced the

catalytic hydrogenation of phenylacetylene. In the early stages of the reaction, the hydrogenation of phenylacetylene/styrene produced both styrene and ethylbenzene. Similar to phenylacetylene hydrogenation, it was only on the removal of all of the acetylene from the system that the adsorption of styrene and its subsequent hydrogenation to ethylbenzene occurred to an appreciable extent.

As expected, the hydrogenation of styrene obeyed a simple first order mechanism. In the hydrogenation of phenylacetylene, the existence of two hydrogenation products coupled with the available pathways for the reactions, made the kinetics more complicated. Therefore, to obtain information regarding the competitive adsorption of the reactants, it was necessary to examine the product distribution curves for each reaction.

Co-adsorption experiments performed by Jackson and Shaw[83] on phenylacetylene/styrene over Pd/carbon produced results indicative of equal adsorption of the olefin and the acetylene. This conclusion was reached since the rate of phenylacetylene consumption (from phenylacetylene hydrogenation only) was observed to halve when an equal amount of styrene was added to the reactant mixture. Therefore, since the rate of phenylacetylene removal was slightly greater in the presence of styrene, we can propose that, although evident, the competition for surface sites between the acetylene and the olefin was minimal. Therefore, with reference to the hydrogenation of phenylacetylene and styrene, the following conclusions can be drawn :

i) Phenylacetylene hydrogenation produced both styrene and ethylbenzene, with the rate of styrene formation greater than that of ethylbenzene

ii) Styrene hydrogenation showed that silica-supported palladium was more efficient for hydrogenation of the acetylene than the olefin

iii) In the co-hydrogenation experiments, the presence of styrene accelerated the removal of phenylacetylene. Under these circumstances, the styrene molecule can be considered to act as a promoter for the hydrogenation of phenylacetylene.

The rate of styrene formation was lower on changing from phenylacetylene to the co-hydrogenation mixture, with the corresponding rate of ethylbenzene formation found to have increased. Therefore, with reference to scheme 6.2.1, we can propose that, in the presence of styrene:

(i) *Reaction 1* is less favourable
(ii) The rate of *Reaction 3* is increased cf. phenylacetylene hydrogenation
(iii) *Reaction 2* is favoured in the absence of the acetylene

Since the addition of styrene to a phenylacetylene hydrogenation mixture results in an increase in the rate of ethylbenzene production, we can propose the following :

(i) Phenylacetylene and styrene adsorbed at different surface sites
(ii) Hydrogenation of styrene (although minimal) occurs independently of phenylacetylene hydrogenation, thus explaining the increased amount of ethylbenzene formed during the reaction

Similar to the conclusions of Al-Ammar *et al*[84], the co-adsorption of both the olefin and the acetylene in these reactions can be considered to have an effect on the amount of available hydrogen at the surface. Therefore, with the rate of

phenylacetylene hydrogenation to styrene observed to have decreased, we can propose that co-adsorption of the olefin has acted to reduce the supply of hydrogen to the olefin formation sites.

Over alumina-supported palladium, the hydrogenation of phenylacetylene produced both styrene and ethylbenzene. However, the rate of acetylene consumption was markedly reduced compared to that observed in the Pd/silica reaction. Similar to Pd/silica, the loss of phenylacetylene was accompanied by an increase in ethylbenzene formation, formed by hydrogenation of styrene. In the initial stages of the reaction, when phenylacetylene is present, the rate of styrene formation was found to be greater than that of ethylbenzene, thus indicating the propensity of the system to favour *Reaction 1*.

The hydrogenation of styrene exhibited similar changes in product distributions as were found using Pd/silica. However, over Pd/alumina the hydrogenation of styrene to ethylbenzene reached completion more rapidly, suggesting that this substrate was slightly more active for styrene hydrogenation than Pd/silica. These results are in good agreement with the work of Carturan[85] who reported the tendency of palladium catalysts with low dispersions to favour alkane formation. Wells[86] however, suggested that the formation of the active β-Pd-hydride phase occurred more readily on larger metal particles. He states that it is the hydride phase which retains the olefin at the surface long enough for it to react to yield the alkane. Of the two palladium catalysts used in this study, the opposite was found to be true, with Pd/alumina (dispersion 22% c.f. Pd/silica 10%) found to be slightly more active for styrene hydrogenation than the silica-supported catalyst.

The co-hydrogenation experiment over alumina-supported palladium proceeded to yield both the olefin and the alkane simultaneously. Therefore, we

can state that the hydrogenation of the acetylene to form the olefin can occur in the presence of the olefin itself. The rate of ethylbenzene production was found to be slightly greater than that observed in the acetylene hydrogenation experiments. Therefore, since the enhancement in alkane production is coupled with an increase in the yield of styrene, we can propose that either :

(i) The formation of ethylbenzene occurs via phenylacetylene and/or styrene hydrogenation,

with a compensation effect required, such that

(ii) All olefin removed as the alkane would be replenished by acetylene hydrogenation (rate $_{Reaction\ 1}$ > rate $_{Reaction\ 2}$), thus, maintaining the increasing olefin yield.

With reference to the co-adsorption experiments performed using silica-supported palladium, the hydrogenation of phenylacetylene/styrene over Pd/alumina can be considered to follow the same mechanism. Therefore, in conclusion, when an equal quantity of phenylacetylene/styrene is hydrogenated over Pd/alumina, both hydrocarbons will be chemisorbed and hydrogenated independently of each other, with the hydrogenation of styrene to ethylbenzene constituting a small fraction of the increased ethylbenzene yield.

5.3.3 The Liquid Phase Hydrogenation of Phenylacetylene and Styrene over Supported-Platinum

In contrast to the reactions of supported-palladium, the hydrogenation of phenylacetylene over silica-supported platinum exhibited relatively low activity. The reaction produced both styrene and ethylbenzene, with the yield of alkane reaching a maximum of only 10%, and the rate of phenylacetylene consumption far less than in the palladium-catalysed reactions. However, over Pt/silica the rate of styrene formation was approximately double that found for ethylbenzene, suggesting that *Reaction 1* was favoured over this catalyst.

In the reaction between styrene and hydrogen over silica-supported platinum, conversion of the olefin was virtually non-existent, with the maximum yield of ethylbenzene reaching only 10%. The difference in reaction conditions (compared to the phenylacetylene hydrogenation reactions) may well have contributed to this result, since both the reaction temperature and catalyst weight were lowered.

The reaction of hydrogen and an equimolar phenylacetylene/styrene mixture over the above catalyst again displayed low activity. Similar to the supported-palladium catalysts, both styrene and ethylbenzene were produced, although the quantities observed were much smaller with the platinum catalysts.

Alumina-supported platinum produced both styrene and ethylbenzene during the hydrogenation of phenylacetylene. However, the rate of phenylacetylene consumption was again less than in the palladium experiments. The rate of ethylbenzene formation was similar in magnitude to that observed over palladium. The major difference between both supported-platinum catalysts was in the rate of styrene hydrogenation. Over Pt/silica this rate was approximately 1.5 times greater, with the final reaction liquor consisting of 65%

styrene (Pt/alumina : 40% styrene), thus, indicating that the highly dispersed Pt/silica catalyst is more proficient for the adsorption and hydrogenation of the olefin than the alumina-supported catalyst. This observation may be reflecting a greater turnover frequency of the olefin on the silica-supported catalyst, or merely the ability of the smaller metal particles to attract the olefinic bond to the surface for reaction.

For the co-hydrogenation experiment, the amount of styrene remained relatively constant, with the phenylacetylene concentration observed to decrease with increasing reaction. This would imply that the formation of ethylbenzene from direct hydrogenation of phenylacetylene was feasible (*Reaction 3*). This statement is supported by the increased amount of ethylbenzene produced. The presence of styrene in equal concentration to the acetylene reduces the rate of both phenylacetylene loss and ethylbenzene formation.

Clearly, supported-platinum catalysts are not as efficient as supported-palladium for the hydrogenation of either phenylacetylene or styrene in the liquid phase. By comparing the rate coefficients for both palladium and platinum in the hydrogenation of styrene, it can be seen that those rates determined for the platinum-catalysed reactions are inherently smaller. This may in part be a result of the susceptibility of platinum catalysts to re-oxidise when exposed to low concentrations of oxygen from the atmosphere.

5.3.4 The Gas Phase Hydrogenation of Phenylacetylene and Styrene over Supported-Palladium

The hydrogenation of phenylacetylene over silica-supported palladium showed no selectivity toward the formation of styrene, producing only

ethylbenzene. The amount of ethylbenzene produced was found to increase with increasing time on-line, until a steady state was attained. This lack of catalyst selectivity may be attributed to two factors. First, the use of hydrogen gas as the flow gas in the system undoubtedly favoured the formation of the alkane. Second, the use of a relatively high reaction temperature would favour phenylacetylene desorption. These conditions would favour the relatively weak adsorption of the acetylene in an atmosphere of reducing gas which would almost certainly yield the alkane.

Increasing the weight of catalyst resulted in a more rapid attainment of steady state behaviour with respect to the rate of ethybenzene formation, with the hydrogenation of phenylacetylene over 50mg of Pd/silica giving complete conversion of the acetylene and a constant yield of alkane.

In sharp contrast to phenylacetylene hydrogenation, the reaction of hydrogen and styrene over silica-supported palladium resulted in a decrease in the conversion of styrene with increased time on-line. The initial distribution of products in this reaction were found to change from [90% styrene, 10% ethylbenzene] to 100% styrene over a one hour period. This decrease in catalyst activity may be reflecting the deactivation of the substrate, perhaps through carbon deposition.

Similar to the hydrogenation of phenylacetylene over Pd/silica, alumina-supported palladium yielded no styrene during phenylacetylene hydrogenation. The conversion of phenylacetylene was observed to increase until a steady state was reached. The distribution of products did not change over the course of the analysis. Therefore, for the same weight of catalyst, the turnover of phenylacetylene to ethylbenzene over Pd/alumina was much lower than that observed using Pd/silica. Doubling the weight of catalyst resulted in complete

conversion of the acetylene, with the yield of alkane found to increase until a steady state, with respect to alkane production was achieved.

Styrene hydrogenation over the above catalyst showed no indications of catalyst deactivation, with low conversions of styrene maintained throughout the course of the analysis. The yield of both unconverted styrene and ethylbenzene was constant also.

Therefore, in view of the above results, we can state that Pd/silica is more active than Pd/alumina for phenylacetylene hydrogenation in the gas phase. This may in part be a result of a particle size effect, since the mean particle diameters of the palladium crystallites in Pd/silica are approximately double that found in Pd/alumina. Another possibility which cannot be overlooked is the role of "spillover" hydrogen (from metal to support) on the reaction chemistry. It is well documented that silica supports have the ability to undergo rapid exchange between spiltover hydrogen and the silanol groups associated with the support[87]. Therefore, the differences in the activities of both Pd/silica and Pd/alumina may be a reflection of the active role of "spillover" hydrogen in phenylacetylene hydrogenation.

The results of the gas phase hydrogenation of styrene showed that both palladium catalysts were relatively inefficient for hydrogenation. The possible deactivation trend in the case of Pd/silica may be due to the ease of carbon residue formation on large metal particles. The low conversions over both catalysts can be attributed to a weak interaction between the adsorbate and catalyst, with the thermodynamics of styrene chemisorption, although favourable, less so than those of phenylacetylene. That coupled with the reaction conditions (high temperature, neat hydrogen flow) will result in the removal of any weakly chemisorbed styrene molecules from the surface.

In view of the styrene results, the reaction between phenylacetylene and hydrogen over supported palladium in the gas phase can be envisaged as occurring via *Reaction 3* (Figure 6.2.1).

5.3.5 The Gas Phase Hydrogenation of Phenylacetylene and Styrene over Supported-Platinum

The hydrogenation of phenylacetylene over silica-supported platinum produced ethylbenzene as the sole product. The yield of both ethylbenzene and unreacted phenylacetylene remained constant, with the conversion of phenylacetylene maintained at 70%. However, in the hydrogenation of styrene the conversion of the olefin was maintained at 100%.

Alumina-supported platinum catalysed the hydrogenation of phenylacetylene to form ethylbenzene. The activity of the catalyst decreased with increasing reaction, until a steady state was reached. Over the course of the reaction the yield of alkane decreased. The hydrogenation of styrene, catalysed by Pt/alumina, gave complete removal of the olefin, with the amount of ethylbenzene produced unaltered over the course of the analysis.

5.3.6 Mechanism for Phenylacetylene Hydrogenation to Ethylbenzene

The hydrogenation of the mono-substituted acetylene, phenylacetylene, to yield ethylbenzene may be postulated to proceed via either :

(i) Associative adsorption of the acetylene to produce an adsorbed species analagous to that postulated for propyne (Section 5.1.5)

(ii) Dissociative adsorption to produce a σ-bonded species (as detailed for propylidyne formation in Section 5.1.2) which could undergo complete reduction to yield the corresponding alkane. This initial mode of adsorption would allow the phenyl ring to adopt a position away from the surface, thus preventing any interaction between the rings π-system and the surface

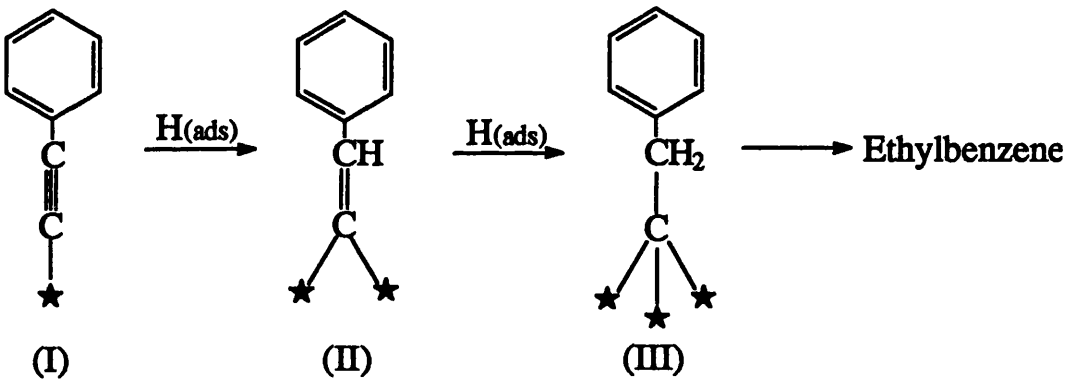

Figure 6.2.2 : *Dissociative Adsorption of Phenylacetylene to Form Ethylbenzene*

5.3.7 Gas Phase Hydrogenation of Phenylacetylene and Styrene - Conclusions

In the gas phase hydrogenation of phenylacetylene, none of the catalysts exhibited any selectivity towards the formation of styrene. Over Pd/silica, the hydrogenation of the acetylene may be envisaged as occurring via a one surface

visit mechanism, since the corresponding hydrogenation reaction for styrene exhibited low catalyst activity. In view of this latter observation, the likelihood of ethylbenzene formation proceeding via the olefin, is minimal.

Thus, the difference between silica- and alumina-supported palladium for phenylacetylene hydrogenation may be the result of :

(i) A particle size effect

(ii) The active role of "spillover" hydrogen

The activity of silica supports in hydrogenation reactions has been reported by Lenz and Conner[88], when the support materials were pretreated at high temperatures with pressures of hydrogen. This may be applicable to the phenylacetylene hydrogenation experiments, and is a possible explanation for the higher hydrogenation activity observed using the silica-supported catalyst.

The low conversions of styrene for both palladium-catalysed reactions may be the result of the high reaction temperature. Wells [86] reported that the existence of the β-Pd-H phase made olefin hydrogenation to the alkane possible. Therefore, in view of our results we can state that either (i) the β-Pd-H phase was subject to some kind of decomposition and thus, played no part in the hydrogenation, or that (ii) the initial weak adsorption of the olefin (and hence, short residence time) prevented the hydride phase from becoming involved.

The hydrogenation of phenylacetylene over Pt/alumina showed signs of catalyst deactivation. This suggests that as the reaction progressed, the number of active sites decreased which may be a result of surface poisoning, a phenomenon not observed over highly-dispersed Pt/silica.

5.4 Overall Conclusions - Effect of Substitution - Geometric or Electronic?

In order to conclude this section of work it is necessary to consider the effect of substitution on the mode and strength of the acetylenes adsorption at the active surface. Therefore, to correlate the results detailed earlier with this substitution, it is imperative that the nature of the triple bond is fully understood as the various substituent groups are replaced.

The hydrogenation reactions of propyne and 2-butyne show that the methyl mono- and di-substituted acetylenes are more prone to hydrocarbonaceous overlayer formation than the phenyl-substituted acetylene, and hence, exhibit a greater degree of deactivation. The precise nature of these surface retained species is not known, although radiotracer experiments reported by Webb *et al*[89,90] on ethene adsorption provided an informative insight into such surface residues. This study showed evidence for the retention of hydrocarbonaceous species from the formation of multiply bonded hydrogen-deficient surface residues, as shown in Figure 6.2.3.

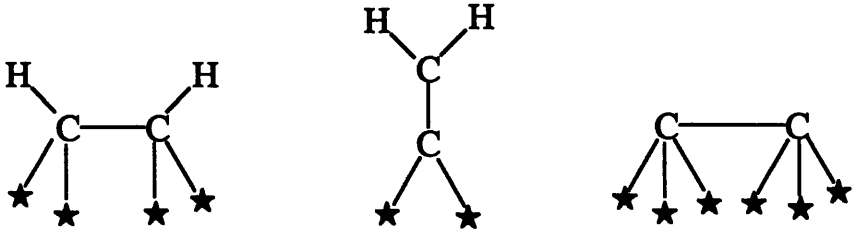

Figure 6.2.3 : *Precursors to Hydrocarbonaceous Overlayers from the Dissociative Adsorption of Ethene*

In the case of ethyne itself, the degree of surface retention is far greater than that observed for ethene, and may well be reflecting the ability of the acetylene to undergo surface polymerisation[91]. Therefore, in view of the results obtained in this study, the involvement of a geometric factor must be considered.

In order for both propyne and 2-butyne to produce surface hydrocarbonaceous species, the acetylenic molecules must first undergo chemical adsorption at the surface, such that species analogous to those in Fig 6.2.3 can form. The formation of any hydrocarbonaceous overlayer precursor will occur only if the adsorption strength of the acetylene is great enough to permit appreciable retention before the reaction and subsequent desorption of the product. Therefore, in the case of phenylacetylene adsorption, the substituent phenyl ring will orientate itself away from the active surface effectively relieving any steric hindrance experienced by the phenyl ring from the surface metal atoms. In the case of the methyl substituted acetylenes, the involvement of a geometric factor will be less complicated, thus, easing the route to hydrocarbonaceous overlayer formation.

The second parameter which must be considered in relation to the ease of hydrocarbonaceous overlayer formation is electronic in origin. It is well documented that acetylenic hydrocarbons exhibit an unpredictably high degree of shielding, which can be attributed to the circulation of electrons at the carbon atoms. However, this shielding, although present in substituted acetylenes, varies with the substituent group. Table 5.4.9 shows the ^{13}C nmr chemical shifts for the acetylenic carbon atoms of various acetylenes. It is obvious that the replacement of one hydrogen atom in propyne with a methyl group results in an increase in the chemical shift of the substituted carbon atom. This change is indicative of the deshielding of the acetylenic carbon, and can be related to the inductive effect associated with the methyl group. Essentially, this substituent has the ability to

donate electron density into the acetylenic bond. More specifically, this electron density is pushed into the π-antibonding orbitals of the bond resulting in the carbon atoms moving from sp to near sp^2 hybridisation. Therefore, the triple bond becomes weaker, with the bond order increasing to between one and two, such that the carbon atoms have some sp^2 character.

Table 5.4.9 : *^{13}C nmr Chemical Shifts of Substituted Acetylenes*

Acetylene Molecule	Substituted C atom / δ (ppm)
Propyne	66.9
2-Butyne	73.9
Phenylacetylene	83.3

Similarly for 2-butyne, the existence of two methyl substituents produces a slight increase in the chemical shift values of the substituted carbon atoms. In the case of the phenyl substituted acetylene, this change is more pronounced with the aromatic ring donating more electron density to the triple bond than the methyl substituent(s). Therefore, in view of this we can conclude that, similar to the argument invoked for the geometry factor, the strength of the acetylenes adsorption will play a key role in determining the extent of hydrocarbonaceous overlayer formation. Clearly the replacement of the substituent group has a marked effect on the electron donating capacity of the triple bond towards the surface, and from the ^{13}C nmr data shown, we can conclude that the heats of adsorption (ΔH_a) of the various acetylenes will follow the trend :

Phenylacetylene < 2-Butyne < Propyne

Therefore, the likelihood of hydrocarbonaceous overlayer formation occurring in the hydrogenation of phenylacetylene will be less than that of either propyne or 2-butyne, as was observed in this study. In conclusion, we can state that the role of the substituent group is crucial to the chemistry of the acetylene and its propensity to yield surface hydrocarbonaceous overlayers.

References

1. Z. Knor, in "Catalysis, Science and Technology", eds. J.R. Anderson and H. Boudart, Springer-Verlag, Berlin, (1982) Vol. 3, p231.
2. K.R. Christmann, in "Hydrogen Effects in Catalysis", eds. Z. Paal and P.G. Menon, Marcel Dekker, NY, (1988) Chapter 1, p3.
3. S.Tsuchiya, Y. Amenomiya and R.J. Cvetanovic, J. Catal., **9**, (1970), 245.
4. B. Lang, R.W. Joyner and G.A. Somorjai, Surf. Science, **30**, (1972), 454.
5. M.A. Morris, M. Bowker and D.A. King, in "Simple Processes at the Gas-Solid Interface", Comprehensive Chemical Kinetics Series, eds. C.H. Bamford, C.F.H. Tipper and R.G. Compton, Elsevier, (1984) Chapter 1, Vol. 19.
6. G.J. Den Otter and F.M. Dautzenberg, J. Catal., **53**, (1978), 116-125.
7. A. Frennet and P.B. Wells, Appl. Catal., **18**, (1985), 243-257.
8. R.W. Joyner and P. Meehan, Vacuum, **33**, (1983), 691.
9. M.A. Chesters, K.J. Packer, D.Lennon and H.E. Viner, J. Chem. Soc. Farad. Trans., **91**(14), (1995), 2191-2201.
10. P.M. Maitlis, "The Organic Chemistry of Palladium", Metal Complexes, (1971), Academic Press, NY Vol.1.
11. B. Sen and M.A. Vannice, J. Catal., **101**, (1986), 517.
12. P. Chou and M.A. Vannice, J. Catal., **104**, (1987), 1.
13. B. Sen and M.A. Vannice, J. Catal., **130**, (1991), 9.
14. A. Guerrero, M. Reading, Y. Grillet. J. Rouguerol, J.P. Boitiaux and J. Cosyns, Z. Phys. D-Atoms, Molecules and Clusters, **12**, (1989), 583.
15. J.G. Ulan, W.F. Maier and D.A. Smith, J. Org. Chem., **52**, (1987), 3132-3142.
16. A.A. Chen, A.J. Benesi and M.A. Vannice, J. Catal., **119**, (1989), 14-32.
17. M. Boudart and H.S. Hwang, J. Catal., **39**, (1975), 44.

18. P.C. Aben, J. Catal., **10**, (1968), 224.

19. G.C. Bond, "Catalysis by Metals", Academic Press, NY (1962).

20. B.A. Morrow and N. Sheppard, J. Phys. Chem., **70**, (1966), 2406.

21. B.A. Morrow and N. Sheppard, Proc. Roy. Soc., **A311**, (1969), 391.

22. J.D. Prentice, A. Lesuinas and N. Sheppard, J. Chem. Soc., Chem. Comm., (1976), 76.

23. N. Sheppard, D.H. Clenery, D.H. Lesuinas, J.D. Prentice, H.A. Pearse and M. Primet, in "Proc. 12th Eur. Congr. Mol. Spectroscop.", eds. M. Grossmann, S.G. Ellcomoss and J. Rimgessen, Elsevier, Amsterdam (1976), p.345.

24. L.H. Little, in "Infra-Red Spectra of Adsorbed Species", Academic Press, London (1966), p.111.

25. N. Sheppard and G. Shahid, Spectrochemica Acta, Vol. 46A, no. 6, (1990), 999-1010.

26. M.A. Chesters, C. De La Cruz, P. Gardner, E.M. McCash, P. Pudney, G. Shahid and N. Sheppard, J. Chem. Soc. Farad. Trans., **86**(15), (1990), 2757-2763.

27. S.D. Jackson, N.J. Casey and I.J. Huntington, Catalyst Deactivation, **88**, (1994), 313-318.

28. N.R. Avery and N. Sheppard, Surf. Science, **169**, (1986), L367-L373.

29. N. Sheppard and J.N. Ward, J. Catal., **15**, (1969), 50.

30. J. Sheridan, J. Chem. Soc., **301**, (1945), 133.

31. E.F.G. Herrington, Trans. Farad. Soc., **37**, (1941), 361.

32. G.C. Bond, Catalysis, **3**, (1954), 109, references therein.

33. D.W. McKee, J. Am. Chem. Soc., **84**, (1962), 1109.

34. G.I. Jenkins and E.K. Rideal, J. Chem. Soc., (1955), 2490.

35. L.L. Kesmodel, P.C. Stair, R.C. Baetzold and G.A. Somorjai, Phys. Rev. Letters, **36**, (1976), 1316.

36. J.J. Rooney, F.G. Gault and C.Kemball, J. Catal., **1**, (1962), 255.

37. J.J. Rooney, J. Catal., **2**, (1963), 53.

38. J.J. Rooney and G. Webb, J. Catal., **3**, (1964), 488.

39. M. Derrien, in "Catalytic Hydrogenation", ed. L. Cerveny, Elsevier, Amsterdam, (1986) p.613.

40. H. Lindlar and R. Dubuis, Org. Synthesis, **46**, (1966), 89.

41. S. Siegel, Adv. Catal., **16**, (1966), 160.

42. A.S. Al-Ammar and G. Webb, J. Chem. Soc. Faraday (I), **75**, (1979), 1900.

43. S. Asplund. C. Fornell, A. Holmgren and S. Irandoust, Cat. Today, **24**, (1995), 181-187.

44. S. Asplund, J. Catal., **158**, (1996), 267-278.

45. J.U. Reid, S.J. Thomson and G. Webb, J. Catal., **30**, (1973), 378-386.

46. J.U. Reid, S.J. Thomson and G. Webb, J. Catal., **30**, (1973), 372-377.

47. C.M. Pradier, M. Mazina, Y. Berthier and J. Oudar, J. Mol. Catal., **89**, (1994), 211-220.

48. J.M. Moses, A.H. Weiss, K. Matusek and L. Guczi, J. Catal., **86**, (1984), 417-426.

49. G.C. Bond and J. Sheridan, Trans. Farad. Soc., **48**, (1952), 651.

50. R.S. Mann and K.C. Khulbe, J. Phys. Chem., **73**, (1969), 2104.

51. G.C. Bond and P.B. Wells, J. Catal., **4**, (1965), 211.

52. S.D. Jackson and G. Kelly, J. Mol. Catal., **87**, (1994), 275-286.

53. S.D. Jackson and N.J. Casey, J. Chem. Soc. Farad. Trans., **91**(18), (1995), 3269-3274.

54. G. Webb, S.J. Thomson and N.C. Kuhnen, J. Chem. Soc. Farad. Trans. (I), **79**, (1983), 2195.

55. R.J. Koestner, J.C. Frost, P.C. Stair, M.A. Van Hore, Surf. Science, **116**, (1982), 85.

56. G. Webb, in "Comprehensive Chemical Kinetics", ed. C.H. Bamford and C.E. Tipper, Elsevier, Amsterdam, (1978), Vol.20, p.1.

57. Ph. Maetz and R. Touroude, J. Mol. Catal., **91**, (1994), 259-275.

58. J.P. Boutiaux, J. Cosyns and E. Robert, Appl. Catal., **35**, (1987), 193-209.

59. W.M. Hamilton and R.L. Burwell, Proc. 2nd Intern. Congr. Catal., Paris, (1960), p.987; (1961), technip, Paris.

60. E.F. Meyer and R.L. Burwell, J. Am. Chem. Soc., **85**, (1963), 2877.

61. G. Webb and P.B. Wells, Trans. Farad. Soc., Vol.61, (1965), 1232.

62. G. Webb and S.J. Thomson, J. Chem. Soc. Chem. Comm., (1976), 526.

63. O. Beeck, Discuss. Farad. Soc., **8**, (1950), 118.

64. R. Dus, Surf. Science, **50**, (1975), 241.

65. A.S. Al-Ammar, S.J. Thomson and G. Webb, J. Chem. Soc. Chem. Comm., (1977), 323.

66. A.S. Al-Ammar and G. Webb, J. Chem. Soc. Farad. Trans.(I), **74**, (1978), 195.

67. A.S. Al-Ammar and G. Webb, J. Chem. Soc. Farad. Trans.(I), **74**, (1978), 657.

68. N. Sheppard, Discuss. Farad. Soc., **41**, (1966), 177.

69. G.A. Somorjai and F. Zaera, J. Phys. Chem., **86**, (1982), 3070.

70. G.A. Somorjai and D.W. Blakely, Nature, **258**, (1975), 580

71. M. Salmeron and G.A. Somorjai, J. Phys. Chem., **86**, (1982), 341.

72. M. Primet, M. El Azhar, R. Frety and M. Guenin, Appl. Catal., **59**, (1990), 153-163.

73. H.L. Gruber, J. Phys. Chem., **66**, (1962), 48.

74. S.D. Jackson, J. Willis, G.D. McLellan, M.B.T. Keegan, R.B. Moyes, S. Simpson, G. Webb, P.B. Wells and R. Whyman, J. Catal., **139**, (1993), 191-206

75. P.R. Hartley, "The Chemistry of Palladium and Platinum", Applied Science Publishers Ltd., (1973), Ch.9, p.244-245

76. G.C. Bond and V. Ponec, "Catalysis by Metals and Alloys", Studies in Surf. Science and Catalysis, Elsevier, (1995), Vol.95, Ch.11, p.497-498.

77. G.C. Bond and V. Ponec, in "Catalysis by Metals and Alloys", Studies in Surf. Science and Catalysis, Elsevier, (1995),Vol.95, Ch.11, p.496

78. G. Webb, Ph.D Thesis, University of Hull, (1963)

79. R.J. Cross, in "The Chemistry of the Metal-Carbon Bond", Vol.2, (1985), Ed. F.R. Hartley and S. Patai, Wiley and Sons Ltd

80. R.A. Carbrol and A. Oberlin, J. Catal., **89**, (1984), 256

81. G.A. Somorjai, S.M. Davis and F. Zaera, J. Catal., **77**, (1982), 439-459

82. G.A. Somorjai, "Introduction to Surface Science and Catalysis", Wiley-Interscience Publication, (1994), Ch.7, p.507

83. S.D. Jackson and L.A. Shaw, Appl. Catal., (A)-General, Vol. 134, no.1, (1996), p.91-99

84. A.S. Al-Ammar, Ph.D Thesis, University of Glasgow, (1977)

85. G. Carturan, G. Facchin, G. Cocco, S. Enzo and G. Navazio, J. Catal., **76**, (1982), 405-417

86. P.B. Wells, J. Catal., **52**, (1978), 498

87. J.F. Cevallos Candau and W.C. Conner, J. Catal., **106**, (1987), 378-385

88. D.H. Lenz and W.C. Conner, J. Catal., **112**, (1988), 116-125

89. G. Webb, G. Taylor and S.J. Thomson, J. Catal., **12**, (1968), 150

90. G. Webb, G. Taylor and S.J. Thomson, J. Catal., **12**, (1968), 191

91. L.H. Little, N. Sheppard and D.J.C. Yates, Proc. Roy. Soc. (1960), **A249**, 242